THE ROLE OF microRNA-194 AND microRNA-375 IN PROSTATE CANCER METASTASIS

by

Rajdeep Das (MBBS, MSCP)

A thesis submitted to the University of Adelaide in the fulfilment of the requirements for the degree of

Doctor of Philosophy
Medicine

Dame Roma Mitchell Cancer Research Laboratories
Faculty of Health Sciences
School of Medicine
The University of Adelaide

August 2016

Table of contents

Abstract

Prostate cancer (PCa) is a major public health problem worldwide. In Australia, it is the most common non-dermatological cancer and second leading cause of cancer related death in men. The risk of being diagnosed with PCa increases with age, and 1 in 6 men are estimated to be affected in their lifetime. Given that Australia has an ageing population, it is projected that the number of men living with PCa will increase from 120,000 to 267,000 by 2017. While significant advances have been made in the treatment of localised, organ-confined prostate tumours, the disease becomes incurable once it has metastasized. Thus, identifying mechanisms that contribute to PCa spread is an urgent requirement.

A considerable body of research has demonstrated that aberrant expression of microRNAs (miRs), a class of small non-coding regulatory RNAs, can be an important factor in prostate cancer metastasis. Previous studies in our laboratory identified serum miR-194 and miR-375 as novel markers of disease progression in men with PCa. However, whether these two miRNAs play a direct role in the biology of prostate tumors is unknown. My PhD aimed to assess the role of miR-194 and miR-375 in PCa progression and metastasis.

My work demonstrated that miR-194 enhanced pro-metastatic features of PCa cells, including migration, invasion and epithelial mesenchymal transition (EMT), *in vitro* and also augmented metastasis *in vivo*. I identified and validated SOCS2 as a novel, direct and biologically relevant target of miR-194. My research supports a model whereby targeting of SOCS2 by miR-194 leads to activation of the JAK2/STAT3 and ERK1/2 signalling pathways, two key pathways involved in promoting PCa metastasis. Further, I have demonstrated that miR-194 is regulated by GATA2, an oncogenic transcription factor in PCa.

On the other hand, my work demonstrated that miR-375 is a potent tumour suppressor miRNA, as it can inhibit EMT, invasion and growth of prostate cancer cells. I identified YAP1, a transcriptional coactivator and a potent oncogene, as a direct and biological relevant target of miR-375. Additionally, I demonstrated that miR-375 was under the direct transcriptional control of EMT-promoting factor, ZEB1.

Collectively, these findings provide greater understanding of the role of miR-194 and miR-375 in prostate cancer metastasis. This information could inform the potential application of these miRNAs as biomarkers, and could lead to efforts to target miR-194 to prevent prostate cancer metastasis.

Declaration

I, Rajdeep Das certify that this work contains no material which has been accepted for the award of any other degree or diploma in my name, in any university or other tertiary institution and, to the best of my knowledge and belief, contains no material previously published or written by another person, except where due reference has been made in the text. In addition, I certify that no part of this work will, in the future, be used in a submission in my name, for any other degree or diploma in any university or other tertiary institution without the prior approval of the University of Adelaide and where applicable, any partner institution responsible for the joint-award of this degree

I give consent to this copy of my thesis when deposited in the University Library, being made available for loan and photocopying, subject to the provisions of the Copyright Act 1968.

I acknowledge that copyright of published works contained within this thesis resides with the copyright holder(s) of those works.

I also give permission for the digital version of my thesis to be made available on the web, via the University's digital research repository, the Library Search and also through web search engines, unless permission has been granted by the University to restrict access for a period of time

Rajdeep Das

August 2016

Acknowledgement

I would like to express my sincere gratitude to my principal supervisor Dr Luke Selth for the continuous support during the PhD studies, for his patience, motivation, and immense knowledge. His guidance helped me in all the time of research and writing of this thesis. I could not have imagined having a better supervisor for my PhD study.

Besides Dr Selth, I would like to acknowledge Assoc. Prof Lisa Butler and Dr Philip Gregory, my co-supervisors, for their insightful comments and encouragement, but also for the hard question which encouraged me to widen my research from various perspectives.

My sincere appreciation goes to Prof Wayne Tilley, who provided me an opportunity to join his team, and gave access to the DRMCR laboratories and other research facilities. Without his precious support it would not be possible to conduct this research.

I also thank my laboratory colleagues for the stimulating discussions, for the sleepless nights we were working together before deadlines, and for all the fun we have had in the last four years.

Last but not the least, I would like to thank my family: my parents and my brother for supporting me spiritually throughout the PhD and my life in general.

CHAPTER 1: GENERAL INTRODUCTION

1.1. Anatomy and physiology of the prostate gland

The prostate gland is a small, rounded organ with a diameter of approximately 4 cm. It is positioned immediately below the urinary bladder, where it encircles the proximal portion of the urethra. The prostate consists of glands, smooth muscles and connective tissue and is enclosed by a fibrous capsule-like structure. The glandular ducts open up into urethra. The human prostate can be classified by two different systems; zones or lobes (Figure 1.1). The zonal classification is used more in pathology; classifying the prostate into four different regions – the peripheral, central, transition and the anterior-fibromuscular zone (McNeal 1981). The peripheral zone (PZ), where the majority of prostate cancers originate, forms about 75% of the prostate and surrounds the urethra (McNeal, et al. 1988). The central zone (CZ) surrounds the ejaculatory ducts and forms 25% of the prostate. Only 2.5% of prostatic cancers arise in this region, however the cancers that do develop here are more aggressive (Cohen, et al. 2008). The transition zone (TZ) accounts for around 20% of prostatic cancers and surrounds the proximal urethra (Vargas, et al. 2012). The TZ grows larger over time; benign prostatic enlargement originates in this region. The final region, the anterior fibro-muscular zone, consists of muscle and fibrous tissue only. The lobe classification system also divides the prostate into four different regions, the anterior lobe (roughly the same as the TZ), posterior lobe (comparable to the PZ), lateral lobes (spans all zones) and the median or middle lobe (CZ). This classification is usually used when describing the anatomy of the prostate.

1.2. Morphology of the prostate gland

The glandular ducts are lined by a prostatic epithelium where three distinct cell types can be distinguished; luminal cells, basal cells and neuroendocrine cells (Figure 1.2). The predominant cell type is the secretory luminal cell. Luminal cells are terminally differentiated and characterised by the expression of the androgen receptor (AR) (Sar, et al. 1990). They produce PSA and prostatic acid phosphatase (PAP) and they are dependent on androgens for survival (Kyprianou and Isaacs 1988). The basal cells are relatively undifferentiated, express low levels of AR (Bonkhoff and Remberger 1993), are not dependent on androgens for survival (Kyprianou and Isaacs 1988; Sar et al. 1990) and lack secretory function and expression of PSA. Although their function is not fully understood, it is believed that a subset of the basal cells function as stem cells in the prostate (Isaacs

1999). It has been suggested that the androgen-independent (AI) prostate stem cells give rise to a population of androgen responsive transit amplifying cells that in turn can amplify the number of luminal cells (Collins and Maitland 2006; Isaacs 1999; Maitland, et al. 2006). The characteristics of the transit amplifying cells are proposed to be intermediate between basal cells and luminal cells. Finally, the third prostatic epithelial cell type is the neuroendocrine cell, which are terminally differentiated and androgen-insensitive cells dispersed throughout the basal cell layer. They contain serotonin and thyroid-stimulating hormone that support the growth of the luminal cells (Bonkhoff, et al. 1995). The stroma is composed of smooth muscle cells, endothelial cells, nerves, fibroblasts, dendritic cells and infiltrating immune cells. The fibroblastic stromal cells express AR and are androgen responsive (Loda, et al. 1994; Prins, et al. 1991). They produce growth factors for the epithelial cells in an androgen-dependent (AD) manner (Culig, et al. 1996) and the crosstalk between the stroma and epithelium is an important regulator of prostate growth and differentiation (Chung 1995).

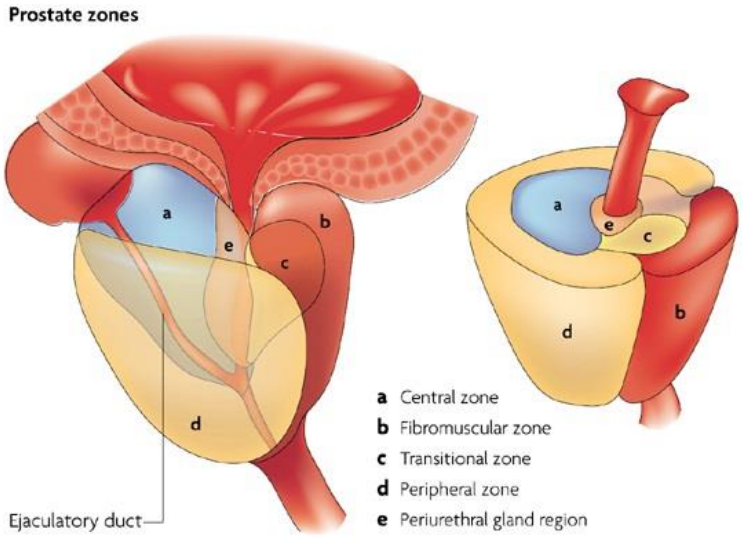

Figure 1.1: Prostate anatomy [figure adapted from (De Marzo, et al. 2007)]

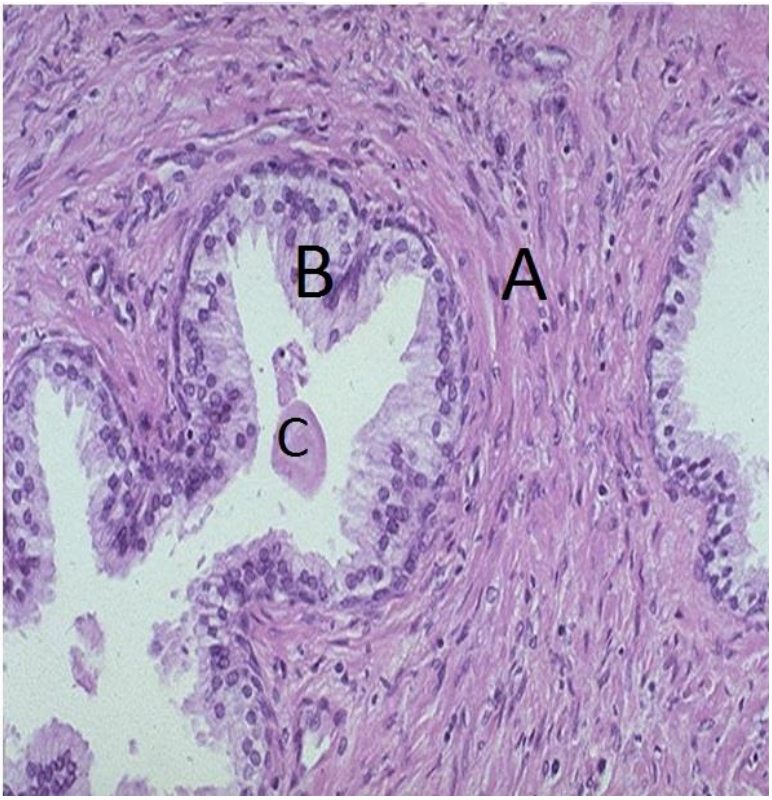

Figure 1.2: Normal histology of prostate (A- fibromuscular stroma; B- two epithelial layers and C - secretions [http://www.pathologyoutlines.com/topic/prostatehistology.html – accessed on 02/08/16]

1.3. Function of the prostate gland

The primary function of the prostate gland is to store part of seminal fluid and assist ejaculation during sexual activity. The smooth muscles in the prostate help to expel semen during ejaculation. The slightly alkaline fluid produced by the prostate makes up 25% of seminal fluid and allows sperm motility and viability. The vaginal tract is acidic therefore the alkalinity of the semen neutralizes the environment to allow the sperm to stay viable. A major constituent of prostatic secretion is prostate specific antigen (PSA), along with citrate (18.7 mg/ml), zinc (488 μg/ml), spermine (243 mg/ml) and cholesterol (78 mg/ml) (Kumar and Majumder 1995)

1.4. Regulation of the prostate gland:

Development and growth of the prostate gland is highly dependent on androgens. The production of androgens is regulated from the hypothalamus by secretion of gonadotropin-releasing hormone (GnRH), which acts on the pituitary gland (Obeid, et al. 2016; Verze, et al. 2016). The pituitary responds with secretion of luteinizing hormone (LH), which thereafter induces the secretion of testosterone from the Leydig cells of the testis (Obeid et al. 2016; Verze et al. 2016). In addition, the hypothalamus release corticotropin-releasing hormone (CRH) that induces the secretion of adrenocorticotropic hormone (ACTH) from the pituitary gland. ACTH influences the adrenal glands to produce testosterone and other weak androgens, for example adrenostenediol (Obeid et al. 2016; Verze et al. 2016). Of the circulating testosterone, 95% originates from the testis and the remaining 5% originates from the adrenal glands (Figure 1.3).

Circulating testosterone diffuses into the epithelial and stromal cells of the prostate where it is converted by the enzyme 5α-reductase into dihydrotestosterone (DHT). Both testosterone and DHT can bind the AR, but DHT has a stronger binding affinity and is more potent (Krieg, et al. 1995). Ligand-free AR in the cytosol is bound to heat-shock proteins (Hsp-70 and Hsp-90) that stabilize the receptor and protects it from degradation. Androgen binding to the receptor induces a conformational change that results in dissociation of the Hsp proteins. Two copies of AR with bound ligand then form a homodimer that is stabilized by phosphorylation and transported into the nucleus. Inside the nucleus, the complex binds to specific DNA sites termed androgen response elements

(AREs) and regulates transcription of genes regulating growth, differentiation and survival.

1.5. Effects of androgen deprivation

The normal prostate gland needs androgens for survival. Androgen withdrawal results in loss of secretory function, decreased cell proliferation and a rapid reduction in glandular size, which is caused by a widespread apoptosis among the epithelial cells (Medh and Thompson 2000). It was for a long time assumed that castration-induced epithelial cell death was mediated by decreased AR signalling in the epithelial cells. However, recent studies indicate that it is in fact the stroma that regulates the major effects observed in the epithelium (Kurita, et al. 2001; Leach, et al. 2015). In addition, the prostate epithelial cell death is preceded by a major reduction in blood flow and by apoptosis of the endothelial cells (Lissbrant, et al. 2001; Wikstrom, et al. 2002). Castration-induced prostate involution is therefore partly caused by insufficient blood flow.

1.6. Prostate cancer

Prostate cancer (PCa) is the most common non-dermatological malignancy and the sixth most common cause of death from cancer in men worldwide (Miller, et al. 2016; Siegel, et al. 2016). PCa is diagnosed either as a localized or metastatic disease. In general, localized prostate cancers are asymptomatic and are diagnosed by measuring the serum levels of prostate-specific antigen (PSA), an androgen regulated serine protease, in combination with digital rectal examination (DRE) (Chou, et al. 2011b; Heidenreich, et al. 2011b). Definitive diagnosis subsequently requires transrectal ultrasound (TRUS) followed by biopsy (transrectal or transperineal) (Heidenreich, et al. 2011a; Heidenreich et al. 2011b).

The biopsy also permits grading/staging of the disease. The Gleason scoring system is a well-established predictor of pathological stage and oncological outcomes for men with prostate cancer (Pierorazio, et al. 2013). Primarily, this architectural scoring system helps to characterize well-differentiated cells (cells look almost like normal cells) from poorly-differentiated cells (cells which are irregular, distorted, and look less like normal cells). A detailed Gleason's pattern scale is shown in figure 1.4. The scoring system (ranging from 2 to 10) is used to grade the prostate tissue and is currently the best measure of a particular tumour's probability of metastasising (Shah 2009). An overall score comprising the most prevalent pattern and the second most prevalent pattern (primary + secondary pattern) is termed the Gleason grade (Shah 2009). Following assessment of the tumour by pathologic

system, tests including radionucleotide bone scan / bone mineral density (BMD) scan, pelvic lymphadenectomy and/or seminal vesical biopsy can also be recommended for more detailed staging of the disease (Brawer 2006; Shah 2009). A detail of anatomic staging/prognostic groups with definitions of primary tumour (from clinical as well as pathological view), regional lymph nodes (both clinical and pathological view) and distant metastasis is shown in Table 1 (Adapted from American Joint Committee on Cancer (AJCC) guidelines, 7th edition. 2010).

Currently, there are various therapeutic approaches towards the disease. The approaches include watchful waiting/ active surveillance for stage I, radical prostatectomy and/or radiation therapy (external beam or brachytherapy) for stage II, radiation with androgen deprivation therapy (ADT) for stage III and ADT for stage IV (Heidenreich et al. 2011a; Mottet, et al. 2011). However, PCa treatment is highly personalized as the disease varies from person to person.

In metastatic PCa, ADT is the primary treatment of choice. ADT consists of surgical (orchitectomy; removal of testicles) or medical castration (with gonadotropin releasing hormone (GnRH) agonist)(Haseen, et al. 2010) either alone or in combination with anti-androgen (Taylor, et al. 2009). This therapy is effective because androgens are critical for the development and growth of both normal and malignant prostate cells (Heinlein and Chang 2004; Yang, et al. 2005). However, ADT may also be used when the disease is localized (within the prostate) if it is a high risk tumour or surgery/radiotherapy are not the best options because of the health of the patient (Brawer 2006; Kohli and Tindall 2010; Taylor et al. 2009). Moreover, the invasiveness of surgery makes them unacceptable options for many men with localized disease (Potosky, et al. 2002). Despite almost all patients achieving remission following ADT, the disease inevitably progresses at a median of 2–3 years to an incurable form referred to as castration resistant prostate cancer (CRPC) (Karantanos, et al. 2013; Kohli and Tindall 2010). CRPC is associated with poor prognosis and shortens the survival time to 16 – 18 months on average (Attar, et al. 2009; Harris, et al. 2009; Sun, et al. 2010).

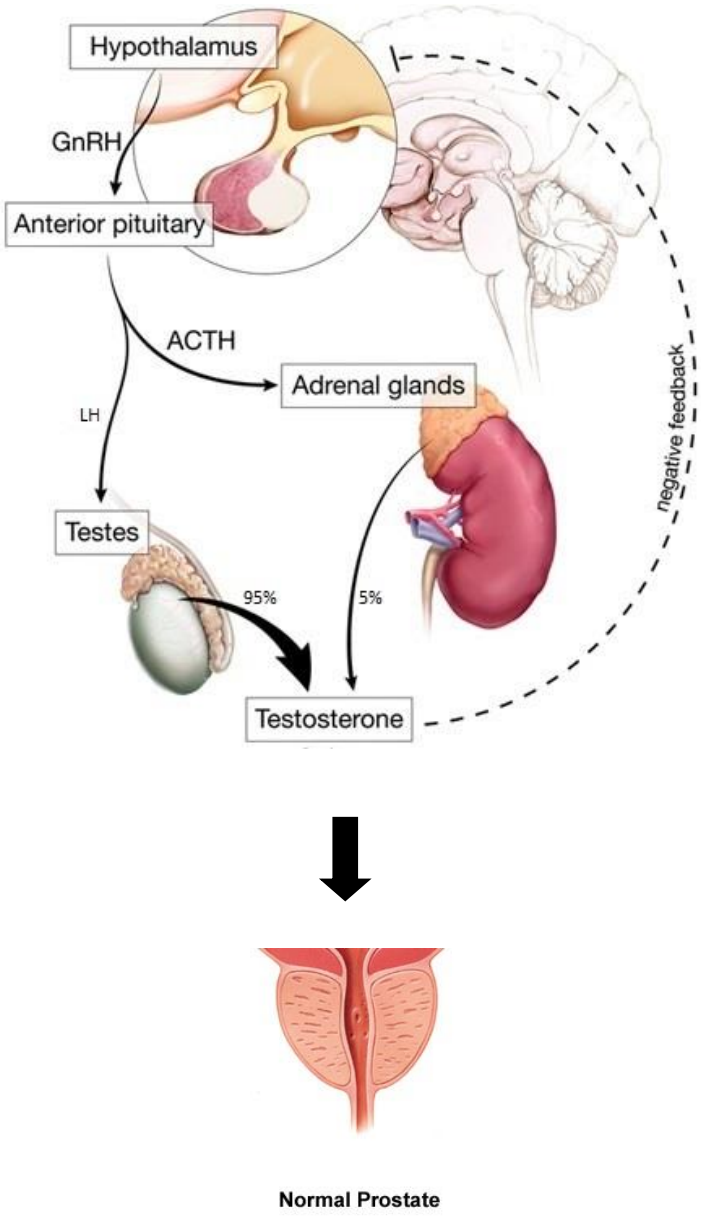

Figure 1.3: The production of testosterone is under the superior control of the hypothalamus and the pituitary gland. The hypothalamus secretes GnRH that influences the pituitary to produce LH and ACTH, respectively. LH influences the testis to produce testosterone and ACTH regulates the production of testosterone and other weak androgens from the adrenal glands. The majority of the testosterone originates from the testis. GnRH = gonadotropin-releasing hormone; LH = luteinizing hormone; ACTH = adrenocorticotropic hormone [Image adapted from http://thepainsource.com/ (accessed on 27/03/2016)]

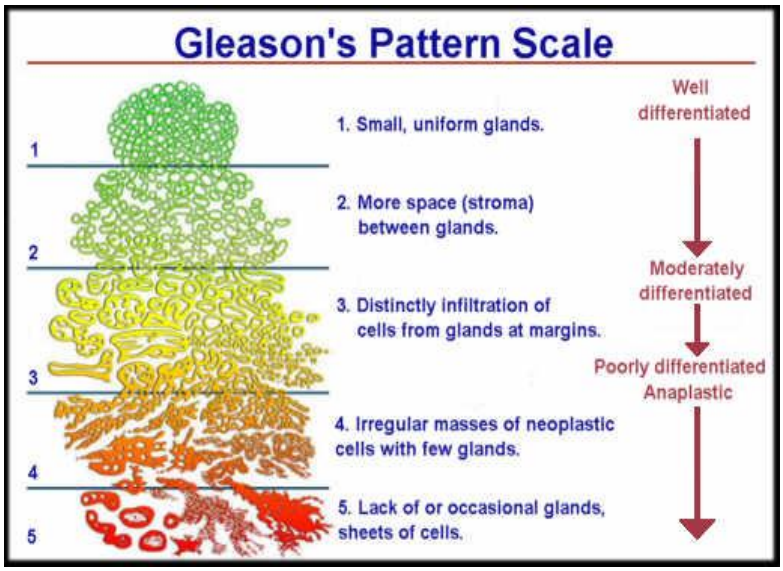

Figure 1.4: Showing detail Gleason's pattern scale (Gordetsky and Epstein 2016; Maygarden and Pruthi 2005).

Table 1: Anatomic staging of prostate cancer (Cancer 2010)

ANATOMIC STAGE/PROGNOSTIC GROUPS[6]					
Group	T	N	M	PSA	Gleason
I	T1a–c	N0	M0	PSA <10	Gleason ≤6
	T2a	N0	M0	PSA <10	Gleason ≤6
	T1–2a	N0	M0	PSA X	Gleason X
IIA	T1a–c	N0	M0	PSA <20	Gleason 7
	T1a–c	N0	M0	PSA ≥10<20	Gleason ≤6
	T2a	N0	M0	PSA ≥10<20	Gleason ≤6
	T2a	N0	M0	PSA <20	Gleason 7
	T2b	N0	M0	PSA <20	Gleason ≤7
	T2b	N0	M0	PSA X	Gleason X
IIB	T2c	N0	M0	Any PSA	Any Gleason
	T1–2	N0	M0	PSA ≥20	Any Gleason
	T1–2	N0	M0	Any PSA	Gleason ≥8
III	T3a–b	N0	M0	Any PSA	Any Gleason
IV	T4	N0	M0	Any PSA	Any Gleason
	Any T	N1	M0	Any PSA	Any Gleason
	Any T	Any N	M1	Any PSA	Any Gleason

Definitions

Primary Tumor (T)

CLINICAL

- TX Primary tumor cannot be assessed
- T0 No evidence of primary tumor
- T1 Clinically inapparent tumor neither palpable nor visible by imaging
- T1a Tumor incidental histologic finding in 5% or less of tissue resected
- T1b Tumor incidental histologic finding in more than 5% of tissue resected
- T1c Tumor identified by needle biopsy (for example, because of elevated PSA)
- T2 Tumor confined within prostate[1]
- T2a Tumor involves one-half of one lobe or less
- T2b Tumor involves more than one-half of one lobe but not both lobes
- T2c Tumor involves both lobes
- T3 Tumor extends through the prostate capsule[2]
- T3a Extracapsular extension (unilateral or bilateral)
- T3b Tumor invades seminal vesicle(s)
- T4 Tumor is fixed or invades adjacent structures other than seminal vesicles, such as external sphincter, rectum, bladder, levator muscles, and/or pelvic wall (Figure A)

Pathologic (pT)[3]

- pT2 Organ confined
- pT2a Unilateral, one-half of one side or less
- pT2b Unilateral, involving more than one-half of side but not both sides
- pT2c Bilateral disease
- pT3 Extraprostatic extension
- pT3a Extraprostatic extension or microscopic invasion of bladder neck[4]
- pT3b Seminal vesicle invasion
- pT4 Invasion of rectum, levator muscles, and/or pelvic wall

Regional Lymph Nodes (N)

CLINICAL

- NX Regional lymph nodes were not assessed
- N0 No regional lymph node metastasis
- N1 Metastasis in regional lymph node(s)

PATHOLOGIC

- pNX Regional nodes not sampled
- pN0 No positive regional nodes
- pN1 Metastases in regional node(s)

Distant Metastasis (M)[5]

- M0 No distant metastasis
- M1 Distant metastasis
- M1a Nonregional lymph node(s)
- M1b Bone(s)
- M1c Other site(s) with or without bone disease

1.7. Metastasis

Metastasis is a complex series of events in which cancer cells leave their original niche and move to a distant part of the body (Nguyen and Massague 2007). On leaving the primary site, these malignant cells are exposed to an unfavourable surrounding which is different from their original microenvironment and most of them cannot survive this stress (Chaffer and Weinberg 2011; Nguyen and Massague 2007). However, tumours have the capacity to generate cells with characteristics that are competent to withstand the incompatible environment (Nguyen and Massague 2007). Such characteristics include an extensive invasive capacity, an ability to detach and translocate to distant tissue and capacity to evade microenviromental constraints (Gupta and Massague 2006; Nguyen and Massague 2007).

Metastasis dissemination of tumour cells can be divided into several key steps (Figure 1.5) (Chaffer and Weinberg 2011; Gupta and Massague 2006; Nguyen, et al. 2009; Nguyen and Massague 2007; Steeg 2006). First, cancer cells acquire an invasive phenotype that allows penetration of the surrounding stroma. Next, the cells enter the bloodstream through the microvasculature of the lymphatic system (intravasation). Circulating tumour cells that evade detachment triggered cell death (anoikis) display properties of anchorage independent survival. Some of these cells can then exit the circulation (extravasation) which occurs either by vascular remodeling events that facilitate transmigration or subsequent disruption of capillaries by expanding tumour emboli. After invading the parenchyma of the target organ, the cancer cells must adapt to the foreign microenvironment, continue proliferating and evade the immune response of the organ. For cells that achieve this, formation of a secondary tumour (colonization) can take place either by immediate proliferative growth following extravasation or after a sustained period of micro-metastatic latency.

Metastasis of prostate cancer primarily occurs to bone (Edlund, et al. 2004). PCa metastasis to bone is facilitated by three important factors (Edlund et al. 2004; Kim, et al. 2005; Podgorski, et al. 2005). First, bones provide a suitable environment for the cancer cells due to their high vascularity. Second, prostate tumour cells produce adhesive molecules that bind them to marrow stromal cells and bone matrix. These adhesive interactions cause the malignant cells to increase the production of angiogenic factors and bone-resorbing factors that further enhance tumour growth in bone. Third, bone is also a large repository for immobilized growth factors, which are released and activated during

bone resorption and thus provide a fertile ground for prostate tumour cells to grow (Roodman 2004).

1.8. Epithelial mesenchymal plasticity (EMP) during development:

Epithelia are sheets of polarised cells lining the flat surfaces and cavities in the body (Shook and Keller 2003). Of the four basic types of tissue found in human body (connective, epithelial, muscle, nervous), epithelial tissues are the most abundant (Shook and Keller 2003). They are defined by their attachment to an underlying basement membrane and by cell-cell adhesions (Figure 1.6) (Shook and Keller 2003). During embryonic development, the cells need to proliferate but due to the rigid structure of an epithelium, the cells are restricted in their movements. So, in order to proliferate, the epithelial cells are internalized to give rise to mesodermal tissue. This cellular program is called epithelial-to-mesenchymal cell transition (EMT), which is a rapid and reversible biological process that enables an epithelial cell to undergo multiple biochemical changes to a mesenchymal phenotype (Hugo, et al. 2007; Kalluri and Weinberg 2009; Klymkowsky and Savagner 2009). Mesenchymal cells generally maintain fewer and less permanent contacts with adjacent cells and are motile and invasive (Hay 2005; Micalizzi and Ford 2009) (Lim and Thiery 2012).

The molecular processes underlying EMT include activation of transcription factors, expression of cell surface proteins such as β4 integrins, α5β1 integrin, and αVβ6 integrin and production of extracellular matrix (ECM) degrading enzymes (Kalluri and Neilson 2003; Kalluri and Weinberg 2009). However, the core component of an EMT is abatement of cell to cell adherence which is largely due to a decrease in the cell adhesion molecules, such as E-cadherin, occludins and claudins (Hugo et al. 2007; Kalluri and Weinberg 2009).

The reverse process, termed mesenchymal-epithelial transition (MET) (Yang, et al. 2004) (Hugo et al. 2007; Kalluri and Weinberg 2009), also takes place during development. During MET the motile and multipolar mesenchymal cells transform to an even array of polarised cells (Kalluri and Weinberg 2009). In contrast to the developmental EMT, less is known about MET. The best-studied MET event during embryogenesis is the formation of the nephron epithelium in the developing kidney (Davies 1996; Hugo et al. 2007). During this process, nephric mesenchymal cells aggregate around individual branches of the ureteral bud, begin to express laminin, polarize, and eventually develop cell-cell adhesions

and differentiate into epithelial cells that form kidney tubules. This dynamic phenotypic epithelial-mesenchymal plasticity (EMP) is tightly regulated in different tissues and occurs throughout the developmental stages. (Biamonti, et al. 2012).

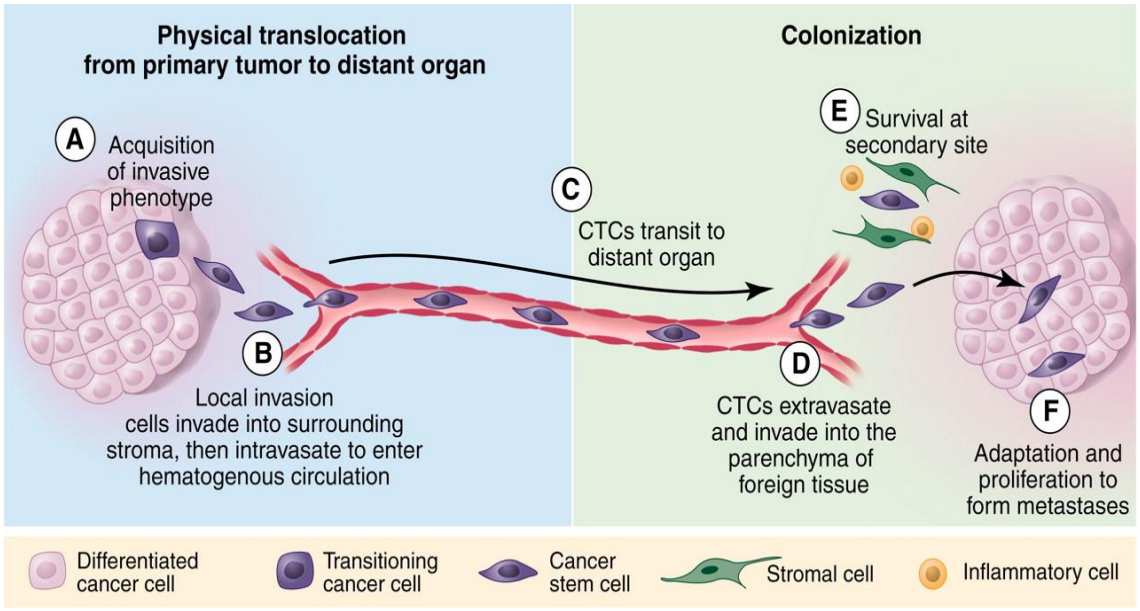

Figure 1.5: The metastatic cascade (Chaffer and Weinberg 2011)

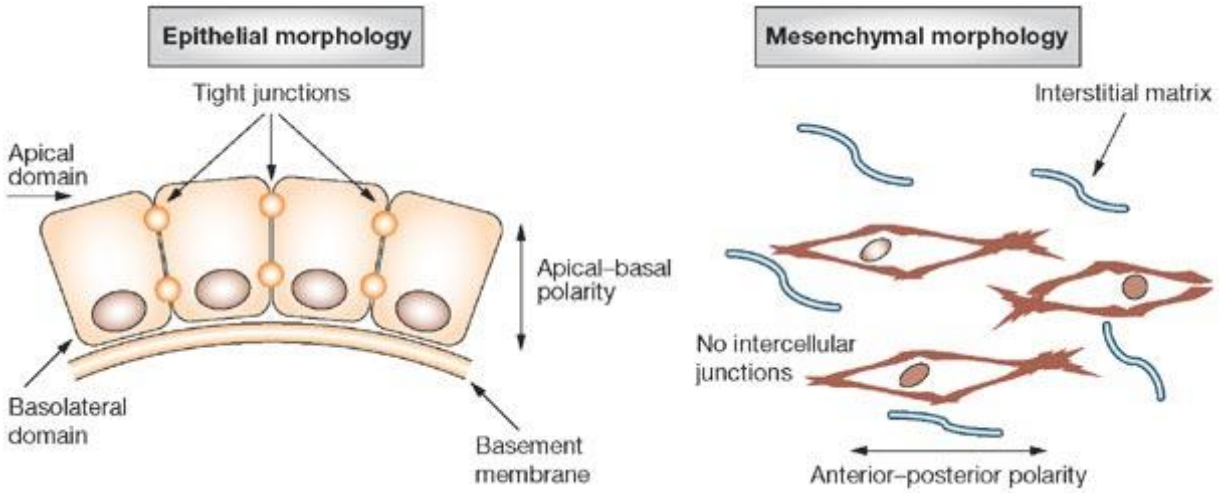

Figure 1.6: Morphologic characteristics of epithelial and mesenchymal cells (Turley, et al. 2008)

1.9. EMP and prostate cancer:

This section of general introduction was published as a review article.

Publication:

Epithelial plasticity in prostate cancer: principles and clinical perspectives. *Trends Mol Med* 2014;**20**: 643–651.

Rajdeep Das, Philip A Gregory, Bret G Hollier, Wayne D Tilley, Luke A Selth.

http://www.cell.com/trends/molecular-medicine/fulltext/S1471-4914(14)00141-5

Review

CellPress

Epithelial plasticity in prostate cancer: principles and clinical perspectives

Rajdeep Das[1,2,3*], Philip A. Gregory[3,4*], Brett G. Hollier[5], Wayne D. Tilley[1,2,3], and Luke A. Selth[1,2,3]

[1] Dame Roma Mitchell Cancer Research Laboratories and Adelaide Prostate Cancer Research Centre, The University of Adelaide, South Australia, Australia
[2] Freemasons Foundation Centre for Men's Health, The University of Adelaide, South Australia, Australia
[3] Discipline of Medicine, The University of Adelaide, South Australia, Australia
[4] Division of Human Immunology, Centre for Cancer Biology, University of South Australia and SA Pathology, South Australia, Australia
[5] Institute of Health and Biomedical Innovation, Australian Prostate Cancer Research Centre – Queensland, Princess Alexandra Hospital, Queensland University of Technology, Queensland, Australia

Statement of Authorship

Title of Paper	Epithelial plasticity in prostate cancer: principles and clinical perspectives
Publication Status	☑ Published ☐ Accepted for Publication ☐ Submitted for Publication ☐ Unpublished and Unsubmitted w ork w ritten in manuscript style
Publication Details	Epithelial plasticity in prostate cancer: principles and clinical perspectives. **Rajdeep Das**, Philip A. Gregory, Brett G. Hollier, Wayne D. Tilley, Luke A. Selth. Trends Molecular Medicine. 2014 Nov;20(11):643-51. doi:10.1016/j.molmed.2014.09.004.

Principal Author

Name of Principal Author (Candidate)	Rajdeep Das		
Contribution to the Paper	With Dr Selth (corresponding author), I conceptualized the manuscript, did an extensive literature search and wrote the manuscript		
Overall percentage (%)	50%		
Certification:	This is a review of literature that I wrote during the period of my Higher Degree by Research candidature and is not subject to any obligations or contractual agreements with a third party that would constrain its inclusion in this thesis. I am the primary author of this paper.		
Signature		Date	27/07/2016

Co-Author Contributions

By signing the Statement of Authorship, each author certifies that:

i. the candidate's stated contribution to the publication is accurate (as detailed above);

ii. permission is granted for the candidate in include the publication in the thesis; and

iii. the sum of all co-author contributions is equal to 100% less the candidate's stated contribution.

Name of Co-Author	Philip A. Gregory		
Contribution to the Paper	Helped in manuscript writing, editing and evaluation		
Signature		Date	27/07/2016

Name of Co-Author	Brett G. Hollier		
Contribution to the Paper	Helped in manuscript editing and evaluation		
Signature		Date	27-7-2016

Name of Co-Author	Wayne D. Tilley		
Contribution to the Paper	Helped in manuscript editing and evaluation		
Signature		Date	27-7-2016

Name of Co-Author	Luke A Selth		
Contribution to the Paper	Supervised development of work; conceptualized the manuscript; co-wrote the manuscript; and helped in manuscript editing and evaluation		
Signature		Date	27/07/2016

Continuation of section 1.9: EMP and prostate cancer:

Over the past decade, the capacity of cancer cells to oscillate between epithelial and mesenchymal phenotypes, termed epithelial plasticity (EP), has been demonstrated to play a critical role in metastasis. This phenomenon may be particularly important for prostate cancer (PC) progression, since recent studies have revealed interplay between EP and signaling by the androgen receptor (AR) oncoprotein. Moreover, EP appears to play a role in dictating the response to therapies for metastatic PC. This review will evaluate preclinical and clinical evidence for the relevance of EP in PC progression and consider the potential of targeting and measuring EP as a means to treat and manage lethal forms of the disease.

Prostate cancer: a major health problem

PC is the second most common solid tumor in men worldwide and a leading cause of cancer-related death [1]. More than 90% of PC-associated mortality is caused by metastasis, which occurs primarily to the bones and lymph nodes, although visceral metastases in liver and lungs, amongst other sites, are also common [2]. The mainstay treatment for men with metastatic PC is androgen deprivation therapy (ADT). ADT exploits the fact that normal and malignant prostate cells require androgens [i.e., testosterone and 5α-dihydrotestosterone (DHT)], which signal through the AR, for growth and survival. ADT typically involves chemical castration to markedly reduce the levels of circulating androgens; this can be combined with AR antagonists. While most men initially respond to ADT, disease progression invariably occurs after a median delay of 18–24 months [3]. Cancer that has progressed following failure of ADT is referred to as castration-resistant PC (CRPC). CRPC is treated with chemotherapy and/or new generation androgen signaling inhibitors (e.g., abiraterone acetate, which inhibits androgen biosynthesis, and enzalutamide, a potent AR antagonist), the latter reflecting the continued reliance of CRPC tumors on AR signaling. However, these treatments only provide marginal survival benefits and palliation, and patients generally die within 2 years [4]. Therefore, novel therapies for CRPC, including those that would prevent and/or inhibit PC metastasis, are urgently required.

Epithelial plasticity and metastasis

Metastasis of carcinomas (epithelial-derived cancers) encompasses a complex series of events whereby epithelial tumor cells invade the surrounding stroma, enter blood or lymphatic circulation, disseminate to distant anatomic sites, exit the vasculature, and colonize a secondary location through metastatic outgrowth. Over the past decade, epithelial–mesenchymal transition (EMT) has been demonstrated to play a critical role in certain phases of this process [5]. EMT is a normal physiological process whereby sessile epithelial cells lose adhesion and detach from tight junctions, change shape and polarity, and become more migratory and invasive, and it plays a fundamental role during wound healing and morphogenesis. At a molecular level, EMT is associated with loss of epithelial factors, such as E-cadherin, epithelial cell adhesion molecule (EpCAM), zona occludens protein-1 (ZO-1), some cytokeratins (CKs) and miR-200 family members, and gain of mesenchymal factors, such as vimentin, fibronectin, and N-cadherin. Cancer cells hijack EMT to facilitate escape from the primary tumor, migration and invasion into the stroma,

and entry/exit from the bloodstream [6]. In tumors, EMT is thought to be primarily triggered by soluble factors secreted from the surrounding stroma and other infiltrating immune cells that impinge on tumor cell signaling pathways, including transforming growth factor-β (TGF-β), Wnt/β-catenin, fibroblast growth factor (FGF), epidermal growth factor (EGF), and Notch, which in turn converge on central transcriptional mediators of the EMT program, for example, members of the Snail, Twist, and zinc finger E-box-binding homeobox (ZEB) families. These EMT transcription factors (EMT-TFs) orchestrate the aforementioned molecular alterations and subsequent underlying changes in cell state [6]. Tumor cells that have undergone an EMT often exhibit other properties that facilitate metastasis and survival within circulation, including suppression of senescence, apoptosis, and anoikis [6].

The role of EMT in cancer metastasis had previously been called into question by the observation that many metastases possess features of the primary tumor, including the expression of epithelial markers (e.g., E-cadherin) [7]. This was clearly inconsistent with the expectation that changes in gene expression associated with EMT would be enriched in metastases. However, this expectation relied on the hypothesis that EMT produced a permanent phenotypic change, whereas it is now clear that cells are capable of reverting back to epithelial phenotypes. This so-called mesenchymal–epithelial transition (MET) would be expected to facilitate the growth of disseminated tumor cells (DTCs) or micrometastases into clinically-relevant metastases, since re-differentiation to an epithelial state is associated with restoration of proliferative capacity [8]. There is now compelling evidence supporting a critical role for MET in metastatic colonization of secondary sites [9, 10, 11, 12, 13, 14].

In this review, the term EP will be used to describe reversible transitions between epithelial and mesenchymal states (i.e., EMT and MET). Such plasticity is linked to the frequent appearance of stem cell-like properties during cancer progression [15, 16, 17, 18], a concept that will be addressed further later in the review.

Epithelial plasticity and prostate cancer progression

Visualizing EP during cancer progression is inherently difficult because of its transient nature, heterogeneity in tumor cell populations, the scarcity of metastatic tissue cohorts, and the lack of robust EP biomarkers. Nevertheless, the importance of EP during PC progression is now well accepted. Important findings that have led to this realization

include, among others: evidence for EMT in circulating tumor cells (CTCs) [19, 20, 21, 22]; altered expression of epithelial/mesenchymal markers and EMT-TFs in primary tumors compared to normal tissues [23], including specific changes at the invasive front [24]; and altered expression of epithelial/mesenchymal markers and EMT-TFs in response to ADT and chemotherapy ([25, 26, 27], and see below). As is evident from these examples, the preponderance of work in this field has substantiated the role of EMT during disease progression (for excellent recent reviews, see [28, 29]). In this section of the review, the focus will be on more recent evidence implicating the reverse process, MET, in PC metastasis and the generation of tumor initiating cells.

Cell line models have afforded extensive and diverse evidence for MET during PC progression. An early study analyzing mesenchymal AT3 cell xenografts in Copenhagen rats found that tumors and lung metastases gained expression of E-cadherin and ZO-1 expression and lost expression of vimentin [30]. Interestingly, in both the primary tumors and the metastases, the cells that had undergone an apparent MET clustered in proximity to stromal components, highlighting potential interplay with microenvironmental cues. Further supporting this concept, DU145 cells co-cultured with hepatocytes exhibited upregulation of E-cadherin and increased chemoresistance [31], while ARCaP$_M$ mesenchymal PC cells gained E-cadherin and lost N-cadherin when grown in the presence of bone marrow stromal cells [32]. The most direct evidence for MET influencing metastasis was provided by a recent study in which repeated rounds of lymph node metastatic selection from mice bearing orthotopic DU145 tumors resulted in cells that had gained epithelial and lost mesenchymal features [9]. This elegant *in vivo* cycling strategy not only provided evidence for spontaneous MET during colonization of lymph nodes but also facilitated the identification of a novel MET-suppressing miRNA, miR-424.

Support for MET in PC progression is further yielded by clinical studies of CTCs and circulating biomarkers. CTCs from 10 patients with metastatic CRPC were found to coexpress vimentin and epithelial CKs in all cases, while other combinations of mixed epithelial/mesenchymal marker expression were also evident [19]. Interestingly, this same study examined bone metastasis biopsies from two of the patients and observed loss of vimentin expression in the CK-positive tumor foci, providing evidence for an MET during metastatic colonization. Studies aimed at assessing the biomarker potential of circulating miRNAs have revealed that serum levels of epithelial miRNAs, including miR-194, miR-

200 family, and miR-375, are associated with metastatic PC and/or predict disease progression following surgery for localized disease [33, 34, 35, 36]. Interestingly, circulating levels of many of the same miRNAs are prognostic and correlated with CTCs in breast cancer [37]. The frequent elevation of epithelial miRNAs in circulation may reflect upregulation of these factors, and consequent MET, in CTCs/DTCs to enable efficient metastatic colonization. Supporting this concept, miR-194 is expressed at higher levels in metastases compared to primary tumors [34] and is upregulated following lymph node colonization and MET of DU145 cells [9].

The emerging link between epithelial identity and stem-ness further supports the role of MET in PC metastasis. The notion that EP fuels the generation of cancer stem cells (CSCs) has long been established, with the majority of research indicating that stem-ness is generally associated with EMT and mesenchymal features [38]. Recent findings in PC models indicate that the opposite can also be true. For example, Celia-Terrassa and colleagues found that an epithelial derivative of the PC3 model possessed considerably greater metastatic capacity than its mesenchymal counterpart following orthotopic tumor cell implantation, despite the latter being more migratory and invasive *in vitro* [10]. Indeed, the epithelial PC3 subtype exhibited enhanced self-renewal, pluripotency, and capacity to grow under attachment-independent conditions, leading the authors to speculate that CSCs and/or tumor initiating cells (TICs) are enriched in this cell population. A similar study demonstrated that E-cadherin-positive but not E-cadherin-negative PC3 and DU145 cells expressed the stem-ness markers SRY (sex determining region Y)-box2 (SOX2), octamer-binding transcription factor (OCT) 3/4, and Nanog and were more tumorigenic [39]. Additionally, the tumorigenicity of chemo-resistant DU145 cells was enhanced after treatment with 5′-aza-deoxycytidine, which led to increased expression of E-cadherin and CD44 [40]. A connection between epithelial identity and stem-ness has also been demonstrated in other cancer models and in normal physiology: for example, loss of the paired related homeobox 1 (Prrx1) transcription factor in the mesenchymal BT-549 breast cancer line is accompanied by acquisition of MET and CSC features [12], an MET is required for the cellular reprogramming required to induce pluripotent stem cells [41], while mouse embryonic stem cells display both stem and epithelial properties [42].

Although these observations appear to challenge the notion that EMT is coupled to stem-ness, a more accurate interpretation is that they indicate that stem-ness, plasticity, and

tumorigenicity are associated with partial rather than complete changes in cell state [43]. This concept is described in more detail in Box 1. In short, the abundant evidence coupling EMT to stem-ness and the more recent studies coupling MET/epithelial-ness to stem-ness are less likely to be contradictory than reflective of experimentation that captures transitional rather than absolute phenotypes. One other important factor that complicates such observations is the ability of distinct populations of epithelial-like and mesenchymal-like cells to cooperate during migration, invasion, and metastasis; moreover, such interactions between the different cell types can also influence the phenotype of the other [10].

While the aforementioned studies provide compelling evidence for MET in PC metastasis, it is important to bear in mind that they all utilized static measurements, which only provide information on the specific stage at which the tissues or cells were harvested. Tools enabling temporal delineation of EP (see, for example, [12, 13]) that could, for instance, be used to demonstrate directly the role of MET in metastatic colonization are now critical to advance this field.

Interactions between epithelial plasticity and prostate cancer treatment response

Interaction of androgen receptor signalling with epithelial plasticity: implications for androgen deprivation therapy

Androgen signaling through the AR not only regulates prostate growth but is integral for maintaining the structure, function, and differentiation status of prostatic epithelium [44]. It was therefore somewhat unexpected that the earliest studies examining the interplay between AR signaling and EP reported that AR/androgens could stimulate transition to cells possessing mesenchymal features. For example, AR activity was positively correlated with the invasive capacity of androgen-dependent MDA PC 2b cells [45]. More recently, AR has been reported to stimulate expression of *ZEB1* by binding to two androgen response elements (AREs) in the promoter, although these experiments were performed in a PC3 derivative stably expressing AR and could not be confirmed in the more relevant AR-positive model, LNCaP [46]. AR can also upregulate the expression of Slug, and Slug interacts directly with AR to coactivate gene expression and facilitate castration resistance both *in vitro* and *in vivo* [47, 48]. Interestingly, there is evidence that both the Slug/AR and ZEB1/AR associations are conserved in other tissues, since Slug is also induced by androgens in bladder cancer cells via activation of Wnt/β-catenin

signaling, resulting in EMT and enhanced metastasis of xenografts [49], while AR can induce ZEB1 in triple-negative breast cancer cell lines [50].

In contrast to the studies described above, an emerging paradigm purports that inhibiting androgen signaling results in EMT. ADT in patients increased the expression of N-cadherin [25] and cadherin-11 [51]. Sun and colleagues demonstrated that castrate normal mouse prostate tissue and human LuCaP35 prostate tumor explants displayed a more mesenchymal phenotype, and stem cell-like features, compared with non-castrate tissues [52]. Importantly, these findings were partially validated by analysis of microarray data from an ADT-treated patient cohort. This same study elucidated a bidirectional negative feedback loop between AR and Zeb1, revealing a potential mechanistic explanation for ADT-mediated EMT. A more recent paper reported that small interfering RNA (siRNA)-mediated suppression of AR activity enhanced PC cell migration/invasion and EMT via chemokine ligand 2 (CCL2)-dependent activation of signal transducer and activator of transcription 3 (STAT3) and macrophage recruitment [53]. CCL2 was associated with poor prognosis in clinical samples, providing clinical support for this pathway. The link between loss of AR activity, STAT3 signaling, and EP was later validated by the observation that loss of AR expression resulted in STAT3 activation and the expansion of a CSC-like population [54]. Indeed, elevated stem-like cell markers occurred concurrently with high STAT3 activity and low AR expression in human prostate tumors. Other work has found that AR can antagonize protein kinase C/Twist1, β-catenin, and TGF-β/Smad3 signaling pathways in PC [55, 56, 57, 58]. Mechanistically, the inverse relationship between AR and Twist1 may be explained by the observation that Twist1 is transcriptionally repressed by NKX3-1, an androgen-regulated homeobox transcription factor [59]. To summarize, AR signaling appears to actively inhibit numerous EMT-promoting pathways/factors, and ADT can relieve this inhibition.

Context-dependency of interplay between androgen signaling and epithelial plasticity

The reasons underlying apparently contradictory findings in relation to interplay between androgen signaling and EP remain to be fully elucidated. We favor the view that the canonical androgen signaling system, such as that found in normal prostatic epithelium or some treatment-naïve tumors, will generally maintain epithelial differentiation and inhibit EMT/EP (Figure 1). By contrast, aberrant androgen signaling found in some tumors *de novo*, and enriched for during adaptive responses to therapy and in treatment-resistant cells (i.e., CRPC), can promote EMT/EP (Figure 1). One pertinent illustration of this

concept is provided by constitutively active AR splice variants (ARVs), which lack the ligand binding domain and can therefore signal in the absence of androgen. ARVs are upregulated in response to ADT and can be highly expressed in CRPC samples [60]. Accumulating evidence suggests that ARV signaling is distinct from that of the canonical AR, and may stimulate EMT. For example, overexpression of the constitutively active AR-V7 variant in LNCaP cells caused induction of N-cadherin, vimentin, Snail, and Zeb1 [61]. A transgenic mouse model expressing the ARv657es variant specifically in prostatic epithelium developed tumors characterized by elevated levels of vimentin and Twist and enhanced Wnt/β-catenin signaling [62], while an equivalent AR-V7 transgenic mouse developed prostatic intraepithelial neoplasia, a precursor of malignancy, that exhibited an EMT phenotype [63]. The transmembrane protease serine 2 (TMPRSS2):ERG fusion protein likely represents another mechanism by which malignancy distorts the relationship between AR signaling and EP. Fusions between the AR-regulated*TMPRSS2* gene and *ETS-related gene* (*ERG*) are found in approximately 50% of PCs and are associated with poor prognosis [64]. TMPRSS2:ERG appears to have a diverse and potent role in driving EMT: it can upregulate Frizzled4 (FZD4) and thereby augment the Wnt signaling pathway, bind to and activate the *ZEB1*promoter, positively regulate integrin-linked kinase and its downstream effectors Snail and lymphoid enhancer-binding factor 1 (LEF-1), and directly repress transcription of the EMT-suppressing miRNA, miR-200c [64, 65, 66, 67]. Other mechanisms by which malignancy could convert androgen signaling from pro-differentiation to pro-EP include loss of forkhead box protein A1 (FoxA1), a pioneer transcription factor that constrains the AR cistrome to promote growth and epithelial identity [48], and AR-independent androgen activity or non-genomic AR activity that converges on the β-catenin signaling pathway [68].

While we believe that a model whereby aberrant AR signaling can enhance EP is sound (Figure 1), it must be noted that prostate specific antigen (PSA) remains a useful indicator of treatment response and disease progression in metastatic PC and CRPC [69]. PSA is an AR-regulated protease and a prostate epithelial marker. This indicates that aberrant AR signaling in advanced disease would still, in the majority of cases, maintain epithelial transcriptional programming even if it concomitantly enhances EP. In other words, modulation of the AR signaling system in response to malignancy and selective pressures imposed by therapy will skew the pro-differentiation versus pro-EP equilibrium but is not expected to cause complete phenotypic transitions (see the legend for Figure 1 for more

detail). A consequence of this is that tumor cells with AR-driven EP would likely possess both epithelial and mesenchymal attributes, potentially conferring the highest metastatic capacity (Box 1).

In short, the complexity of the interplay between AR signaling and EP is likely dictated by the status quo of AR signaling in the tumor (or particular cancer model) and is therefore highly context dependent. The crosstalk between AR and other signaling pathways such as Wnt, TGF-β, Src kinase, and Akt/mammalian target of rapamycin (mTOR), in some cases independent of androgen, adds another level of convolution. Another noteworthy implication of these concepts is that observations regarding EP made using cell line models, many of which are derived from metastases and represent aggressive, abnormal forms of the disease with aberrant (or indeed absent) AR signaling, necessitate careful interpretation. Contradictory findings in the literature could reflect laboratory-specific cell lineages and/or subtly different experimental conditions.

Interaction of epithelial plasticity with chemo- and radio-therapy of prostate cancer

The most common chemotherapy for PC is docetaxel, an antimitotic microtubule-stabilizing agent (taxane). However, approximately half of patients do not respond to docetaxel (i.e., exhibit *de novo* resistance) and all men ultimately develop resistance. The development of resistance to chemotherapy has been linked to acquisition of EP in both PC model systems and patient samples. For example, docetaxel-resistant DU145 and 22Rv1 cells lose expression of the epithelial differentiation markers CK18, CK19, and PSA [27]. In these model systems grown *in vitro* and as xenografts, docetaxel resistance was suppressed by treatment with agents that target the EMT/stem-promoting NOTCH and Hedgehog pathways. Importantly, the loss of CK18/19 was recapitulated in docetaxel-treated patient metastases and associated with clinical aggressiveness and poor prognosis. Other studies have found that high-risk prostate tumors treated with neoadjuvant chemotherapy exhibit gene and protein expression alterations indicative of EMT [70, 71]. Indeed, loss of E-cadherin was associated with both treatment and the onset of resistance [71]. Importantly, *ZEB1* siRNA knockdown could partially overcome the drug-resistant EMT phenotype in docetaxel-resistant PC3 and DU145 derivatives, providing direct evidence for a link between mesenchymal characteristics and chemoresistance [70]. Paclitaxel is another taxane that has been trialed as a treatment for CRPC, but is not in current clinical use. Similar to findings from preclinical studies of docetaxel, the acquisition of paclitaxel resistance in PC cells was associated with enhanced migratory,

invasive, colony-forming, and tumorigenic capacity, upregulation of mesenchymal factors (ZEB1, vimentin, and Snail), and loss of E-cadherin and keratins [72].

Radiotherapy is a common treatment for localized PC, particularly in men with higher risk disease, but up to a third of patients experience disease recurrence. Of note, radiotherapy is often used in combination with ADT, complicating any associations with EP that are identified. Nevertheless, data from cell line models provides evidence linking radio-resistance to enhanced EP. For example, a recent study generated three radio-resistant PC cell lines based on the PC3, DU145, and LNCaP models and demonstrated that resistance was associated with enhanced colony formation, invasion, and spheroid formation capabilities and elevated expression of mesenchymal and stem-ness markers [73]. More evidence linking EP to the cellular response to radiation therapy was provided by studies of the ARCaP PC model [32]. An epithelial subtype of ARCaP ($ARCaP_E$) was more sensitive to radiation than its mesenchymal counterpart ($ARCaP_M$) and, interestingly, co-culture of $ARCaP_E$ but not $ARCaP_M$ cells with stromal cells enhanced radio-resistance. Treatment of ARCaP:bone stroma co-cultures with an E-cadherin blocking antibody or a pan-integrin blocking antibody increased cancer cell radiation sensitivity, suggesting that stroma-induced radiation resistance can be mediated through E-cadherin and integrin signaling in epithelial and mesenchymal cells. Collectively, these results demonstrate that both mesenchymal phenotypes and re-epithelialization events are associated with radio-resistance in the ARCaP model. While this appears somewhat paradoxical, it is consistent with the emerging concept that the tumor microenvironment plays a critical role in EP and treatment response.

A possible mechanistic explanation for the association between EMT and both chemo- and radio-resistance is that the DNA damage response triggered by these therapies causes stromal cells to secrete WNT16B, which can activate EMT in neighboring cancer cells through the nuclear factor-κB (NF-κB) pathway [74]. Stromal WNT16B is associated with poor outcomes in PC and treatment resistance in PC and is also elevated in breast and ovarian tissues following chemotherapy, highlighting the potential importance of this mechanism.

Summary of the interplay between treatments for advanced prostate cancer and epithelial plasticity

The current body of evidence indicates that acquisition of EP is a common outcome of treatments for advanced PC and may drive therapeutic resistance. Enhanced EP, particularly when it results in tumor cells occupying transitional states along the epithelial–mesenchymal spectrum, is often associated with the emergence of tumor-initiating and stem-like features (Box 1). It follows then that the changes in EP are not only a consequence but also a cause of treatment resistance. Therefore, co-targeting EP may increase therapeutic efficacy of ADT, chemotherapy, and radiotherapy. A summary of associations between PC treatment resistance mechanisms and EP is provided in Table 1.

Another important implication from these observations is the potential for cross-resistance mediated through EP-related mechanisms. The phenomenon of cross-resistance between ADT and chemotherapy is becoming increasingly clinically relevant [75]. While changes to the AR signaling pathway during treatment are generally considered to be the most important driver of such cross-resistance, enhanced EP may also partly explain this phenomenon.

Targeting and measuring epithelial plasticity to improve patient outcomes

Targeting AR signaling remains the focus of therapeutic strategies for advanced PC, which is justified given the success of newer agents such as enzalutamide and abiraterone. Despite these advancements, many patients do not respond to further targeting of AR signaling and none are cured. This likely reflects the heterogeneity of lethal prostate tumors, which are frequently characterized by a mixed population of AR-positive and AR-negative cells [2]. Notably, PC stem cells are likely to be AR-negative [76]. These observations support the idea of co-targeting EP and associated stem-ness as a means to suppress metastasis and CRPC. An exciting preclinical study found that monoclonal antibodies targeting N-cadherin could suppress CRPC xenograft growth and metastasis [26]. More recent work has demonstrated the therapeutic potential of inhibiting β2-microglobulin (β2-M), a soluble signaling molecule that promotes EMT, using an anti-β2-M monoclonal antibody [77]. However, targeting ‘pure’ mesenchymal factors such as N-cadherin or EMT-inducing factors such as β2-M might be counter-productive in patients who have DTCs, CTCs, or dormant micrometastases at the time of treatment, since promoting reversion of such cells to an epithelial state could reactivate proliferation and facilitate the formation of clinically-relevant metastasis. This may be particularly relevant in PC, since malignant cells likely disseminate early from the primary tumor [78].

Therefore, a more optimal strategy may be to target stem-ness factors that are coexpressed in epithelial and mesenchymal cell fractions. Indeed, agents that can inhibit Hedgehog, NOTCH, and TGF-β signaling are being intensively investigated (e.g., [27, 79]). Targeting stem-ness may be particularly relevant in PC subtypes that have lost expression of the AR, such as neuroendocrine (NE) tumors. The relationship between NE differentiation, EP, and stem-ness is discussed in more detail in Box 2.

In addition to being a therapeutic target, EP could be a clinically useful biomarker of PC progression. PC CTCs are characterized by mixed epithelial/mesenchymal populations and stem-ness markers [19, 20, 21, 22], and it is expected that future studies will discover correlates of specific CTC plasticity states with clinical outcomes, as has been observed in colorectal cancer [80]. In this respect, combining measurements of EP and AR signaling markers could potentially improve predictive power [81].

Concluding remarks and future perspectives

Despite the recent advances in the treatment of advanced PC, metastatic disease is incurable and a major cause of cancer mortality in men. EP, encompassing both EMT and MET, has emerged as a critical factor in PC metastasis. Of note, compared to earlier therapies, the newer, more potent drugs for advanced disease may enhance the plasticity of tumor cells, exacerbating the importance of EP in PC progression. Reciprocally, EP appears to be an important feedback therapy resistance mechanism. Future studies should focus on achieving a better understanding of the pathobiology of EP (Box 3). We believe some productive avenues of research to achieve this are: (i) measuring how AR signaling is altered in response to EMT and enhanced plasticity in general, to define the context-dependent relationship between these two processes; (ii) elucidating the 'EP-ome' in diverse PC models; (iii) accurately measuring, in large clinical cohorts including CTCs, the impact of treatment on EP (and vice versa); (iv) using data from the preceding aim, deciphering the clinical importance of MET in the later phases of metastasis and CRPC; (v) expanding the examination of EP-targeted therapeutics in relevant preclinical models; and (vi) identifying stem-ness markers that are associated with both epithelial and mesenchymal states as possibly therapeutic avenues for exploitation. Collectively, such research will lead to new drugs that could be applied in combination with current therapies to prevent or restrict metastasis, and yield improved strategies to monitor PC progression, with accompanying improvements in outcomes.

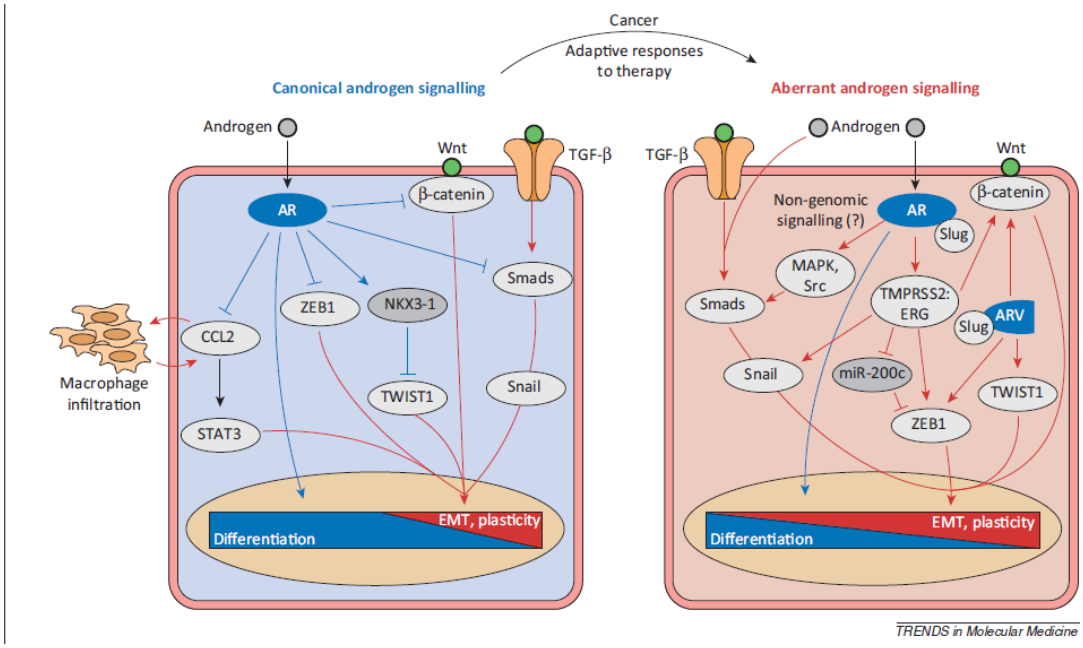

Figure 1: Interplay between androgen receptor (AR) signaling and epithelial plasticity (EP). The left cell highlights mechanisms by which canonical AR signaling can suppress transcriptional programs mediating epithelial–mesenchymal transition (EMT) and plasticity (depicted by a box within the white nucleus), whereas the right cell highlights mechanisms by which aberrant AR signaling can promote such programs. Some of the mechanisms underlying aberrant androgen signaling are intrinsic to AR (e.g., the emergence of constitutively-active AR splice variants, non-genomic AR signaling), whereas others are a consequence of different factors that are altered in the malignant and/or therapy-resistant phenotype [e.g., TMPRSS2:ERG (*ETS-related gene*) gene fusions]. Note that in the majority of cases, canonical androgen signaling is still active in cancer and therapy-resistant cells; likewise, aberrant androgen signaling can occur in normal epithelial cells. However, the pro-differentiation versus pro-EMT/plasticity equilibrium is skewed in tumors, particularly following treatment. Thus, pathways shown in the left cell would be enriched in normal prostatic epithelial cells, whereas pathways in the right cell would be enriched in cancer and in response to selective pressures imposed by therapies such as ADT. Not all pathways discussed in the manuscript are shown in this figure.

Box 1. Epithelial plasticity: many roads to metastasis?

EP describes a reversible transition of cells between epithelial and mesenchymal states. As metastases often resemble the primary tumor in morphology, EP provides a conceptual framework whereby cells can activate, under the appropriate circumstances, the necessary capabilities required to complete the metastatic cascade. These properties include the ability to invade, survive, successfully seed, and revert to a proliferative state in a foreign environment [82]. The concept of EP has been expanded in recent years with the recognition that cancer cells may undergo partial EMT or MET, and in fact that resulting 'quasi' states may be advantageous to metastatic progression (Figure I). Indeed, cells that have transited fully towards a mesenchymal state are thought to have lost the plasticity required for metastasis formation [13]. Moreover, partial EMT and the resultant quasi-mesenchymal phenotype is often associated with acquisition of stem-ness properties [15]. Such cells have been referred to as 'migrating cancer stem cells' [82] and generally possess increased tumor initiation and self-renewal capacity. However, despite the numerous examples showing that mesenchymal and stem-like features are associated with enhanced metastasis, recent exceptions where epithelial (or quasi-epithelial) cells possess stem-like properties have also been observed [10,12] (Figure I). In reality, a heterogeneity of cellular states exists within a primary tumor, with interactions between different cell types likely impinging on the action of the other (e.g., [10,14]). It is also important to note that undifferentiated metastasis can form in the absence of EP, and that this may be driven more by genetic influences [83]. Undifferentiated metastases may reflect situations where the primary tumor has disseminated early and subsequent primary tumor and metastases progression occur along parallel paths (the 'parallel progression' concept) [84].

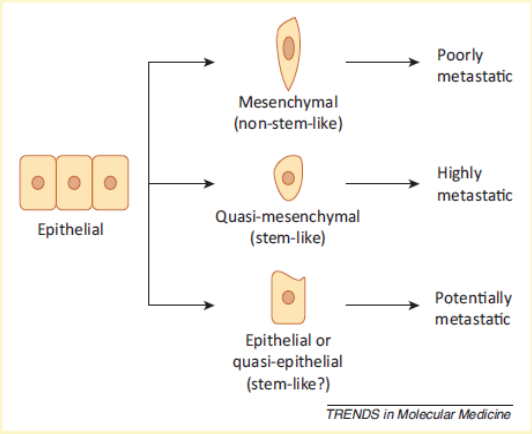

Figure I. Epithelial plasticity in metastasis. A schematic of possible transition routes of epithelial tumor cells to de-differentiated progeny with varying metastatic capacities. Cells that are quasi-mesenchymal or quasi-epithelial can attain stem-like characteristics, which are thought to enhance metastatic progression. Fully mesenchymal cells lack plasticity and therefore appear to have a poor ability to adapt and proliferate at secondary sites, limiting their metastatic potential.

Box 2. The relationship between neuroendocrine differentiation and epithelial plasticity in prostate cancer

NE cells are a minor population in the epithelial compartment of normal prostate glands, widely interspersed amongst the basal and luminal cells. The clinical or pathological definition of neuroendocrine differentiation (NED) is vague, but it is often defined histologically as the presence of AR/PSA-negative cells that express one or more NE-derived peptides such as chromogranin A, synaptophysin, and/or neuron-specific enolase [86]. Although an extremely small proportion of PC patients can present with overt *de novo* NE tumors, NED occurs much more commonly in response to treatment [87]. Indeed, approximately 50% of patients with CRPC have evidence of NED, which is associated with metastasis to viscera and a poor prognosis [88].

Emerging evidence suggests that the development of NED is associated with acquisition of EP and stem-ness. Data from cell lines and mouse models indicates that the Wnt/TGF-β and Hedgehog signaling pathways play an important role in NED [86,88], while overexpression of the Snail EMT-TF in LNCaP cells resulted in the development of NE features [89]. Another study isolated a population of CSCs from the DU145 model and found that they were highly tumorigenic, with the resultant tumors characterized by a high density of NE cells and an EMT phenotype [90]. Two studies utilizing patient samples support the aforementioned preclinical findings. First, quantitative RT-PCR (qRT-PCR) and immunohistochemical analysis of primary prostate tumors identified a rare population of CSCs that coexpressed the stem-ness marker Oct4A and the NE markers chromogranin A and synaptophysin [91]. Second, transcriptomic profiling of primary and metastatic neuroendocrine PC identified frequent overexpression and gene amplification of *AURKA* (Aurora kinase A) [92], which can promote EMT and stem-ness in other cancer types. Collectively, these observations provide evidence for intimate connections between EP, stem-ness, and NED in PC. Neuroendocrine PC is predicted to occur more frequently in response to the next generation of potent AR-targeted agents (e.g., abiraterone acetate, enzalutamide) [86]; therefore, elucidating the molecular mechanisms underlying these connections is an increasingly pressing clinical issue.

Box 3. Outstanding questions

- In what contexts does AR signaling enhance or suppress EP?
- How common is EMT (or partial EMT) in response to ADT? Are there common drivers of ADT-associated EP that could be targeted?
- Is EP a cause or consequence of resistance to ADT, chemotherapy, and radiotherapy?
- To prevent or suppress PC metastasis, is it best to target epithelial factors, mesenchymal factors, stem-ness factors, or a combination thereof?
- Could measurements of EP in CTCs be used as markers of clinical outcome and/or AR signaling status?
- How frequently does metastasis of PC occur in the absence of EP? How important are other phenomena, such as basal epithelial cell extrusion [93] or 'parallel progression' [84], for tumor cell dissemination?

Table 1. Evidence for associations between treatment resistance mechanisms in prostate cancer and epithelial plasticity[a]

Resistance mechanism	Associated therapy	Interplay with EP	Refs
AR amplification and overexpression	ADT, CT, RT	AR maintains epithelial differentiation and suppresses EMT in a context-dependent manner	[52–57]
		AR promotes EMT in a context-dependent manner	[47,48]
Expression of constitutively active AR splice variants	ADT	AR-V7 and ARv567es directly promote EMT	[61–63]
AR cofactor perturbation (co-activator gain, co-repressor loss/suppression)	ADT	Slug acts as a co-activator of AR in CRPC	[47]
Non-genomic signaling of AR through Src/MAPK/ERK pathway	ADT	MAPK and Src activation can promote EMT	[68]
Activation of the PI3K/Akt/mTOR pathway	ADT, RT	PI3K/Akt/mTOR promotes EMT	[73]
Activation of Notch/Hedgehog signaling	CT	Notch/Hedgehog signaling promotes EMT and stem-ness	[16,27]
Activation of WNT/β-catenin signaling pathway	ADT, CT, RT	WNT16B can activate EMT	[52,74]
c-Myc amplification and overexpression	ADT	c-Myc can promote EMT	[85]

[a]Abbreviations: ADT, androgen deprivation therapy; AR, androgen receptor; CRPC, castration-resistant prostate cancer; CT, chemotherapy; EMT, epithelial–mesenchymal transition; RT, radiotherapy.

Concluding remarks and future perspectives

Despite the recent advances in the treatment of advanced PC, metastatic disease is incurable and a major cause of cancer mortality in men. EP, encompassing both EMT and MET, has emerged as a critical factor in PC metastasis.

References

1 Siegel, R. *et al.* (2012) Cancer statistics, 2012. *CA* 62, 10–29
2 Shah, R.B. *et al.* (2004) Androgen-independent prostate cancer is a heterogeneous group of diseases: lessons from a rapid autopsy program. *Cancer Res.* 64, 9209–9216
3 Asmane, I. *et al.* (2011) New strategies for medical management of castration-resistant prostate cancer. *Oncology* 80, 1–11

4 Rescigno, P. *et al.* (2012) New perspectives in the therapy of castration resistant prostate cancer. *Curr. Drug Targets* 13, 1676–1686
5 Kalluri, R. and Weinberg, R.A. (2009) The basics of epithelial-mesenchymal transition. *J. Clin. Invest.* 119, 1420–1428
6 De Craene, B. and Berx, G. (2013) Regulatory networks defining EMT during cancer initiation and progression. *Nat. Rev. Cancer* 13, 97–110
7 Rubin, M.A. *et al.* (2001) E-cadherin expression in prostate cancer: a broad survey using high-density tissue microarray technology. *Hum. Pathol.* 32, 690–697
8 Nieto, M.A. (2013) Epithelial plasticity: a common theme in embryonic and cancer cells. *Science* 342, 1234850 http://dx.doi.org/10.1126/science.1234850
9 Banyard, J. *et al.* (2013) Regulation of epithelial plasticity by miR-424 and miR-200 in a new prostate cancer metastasis model. *Sci. Rep.* 3, 3151 http://dx.doi.org/10.1038/srep03151
10 Celia-Terrassa, T. *et al.* (2012) Epithelial-mesenchymal transition can suppress major attributes of human epithelial tumor-initiating cells. *J. Clin. Invest.* 122, 1849–1868
11 Korpal, M. *et al.* (2011) Direct targeting of Sec23a by miR-200s influences cancer cell secretome and promotes metastatic colonization. *Nat. Med.* 17, 1101–1108
12 Ocana, O.H. *et al.* (2012) Metastatic colonization requires the repression of the epithelial-mesenchymal transition inducer Prrx1. *Cancer Cell* 22, 709–724
13 Tsai, J.H. *et al.* (2012) Spatiotemporal regulation of epithelial-mesenchymal transition is essential for squamous cell carcinoma metastasis. *Cancer Cell* 22, 725–736
14 Tsuji, T. *et al.* (2008) Epithelial-mesenchymal transition induced by growth suppressor p12CDK2-AP1 promotes tumor cell local invasion but suppresses distant colony growth. *Cancer Res.* 68, 10377–10386
15 Mani, S.A. *et al.* (2008) The epithelial-mesenchymal transition generates cells with properties of stem cells. *Cell* 133, 704–715
16 Kong, D. *et al.* (2010) Epithelial to mesenchymal transition is mechanistically linked with stem cell signatures in prostate cancer cells. *PLoS ONE* 5, e12445
17 Albino, D. *et al.* (2012) ESE3/EHF controls epithelial cell differentiation and its loss leads to prostate tumors with mesenchymal and stem-like features. *Cancer Res.* 72, 2889–2900
18 Giannoni, E. *et al.* (2010) Reciprocal activation of prostate cancer cells and cancer-associated fibroblasts stimulates epithelial-mesenchymal transition and cancer stemness. *Cancer Res.* 70, 6945–6956
19 Armstrong, A.J. *et al.* (2011) Circulating tumor cells from patients with advanced prostate and breast cancer display both epithelial and mesenchymal markers. *Mol. Cancer Res.* 9, 997–1007
20 Chen, C.L. *et al.* (2013) Single-cell analysis of circulating tumor cells identifies cumulative expression patterns of EMT-related genes in metastatic prostate cancer. *Prostate* 73, 813–826
21 Friedlander, T.W. *et al.* (2014) Detection and characterization of invasive circulating tumor cells derived from men with metastatic castration-resistant prostate cancer. *Int. J. Cancer* 134, 2284–2293
22 Gorges, T.M. *et al.* (2012) Circulating tumour cells escape from EpCAM-based detection due to epithelial-to-mesenchymal transition. *BMC Cancer* 12, 1–13
23 Gravdal, K. *et al.* (2007) A switch from E-cadherin to N-cadherin expression indicates epithelial to mesenchymal transition and is of strong and independent importance for the progress of prostate cancer. *Clin. Cancer Res.* 13, 7003–7011
24 Sethi, S. *et al.* (2010) Molecular signature of epithelial-mesenchymal transition (EMT) in human prostate cancer bone metastasis. *Am. J. Transl. Res.* 3, 90–99
25 Jennbacken, K. *et al.* (2010) N-cadherin increases after androgen deprivation and is associated with metastasis in prostate cancer. *Endocr. Relat. Cancer* 17, 469–479
26 Tanaka, H. *et al.* (2010) Monoclonal antibody targeting of N-cadherin inhibits prostate cancer growth, metastasis and castration resistance. *Nat. Med.* 16, 1414–1420
27 Domingo-Domenech, J. *et al.* (2012) Suppression of acquired docetaxel resistance in prostate cancer through depletion of notch- and hedgehog-dependent tumor-initiating cells. *Cancer Cell* 22, 373–388
28 Bitting, R.L. *et al.* (2014) The role of epithelial plasticity in prostate cancer dissemination and treatment resistance. *Cancer Metastasis Rev.* 33, 441–468
29 Li, P. *et al.* (2014) Contributions of epithelial-mesenchymal transition and cancer stem cells to the development of castration resistance of prostate cancer. *Mol. Cancer* 13, 55
30 Oltean, S. *et al.* (2006) Alternative inclusion of fibroblast growth factor receptor 2 exon IIIc in Dunning prostate tumors reveals unexpected epithelial mesenchymal plasticity. *Proc. Natl. Acad. Sci. U.S.A.* 103, 14116–14121
31 Chao, Y. *et al.* (2012) Hepatocyte induced re-expression of E-cadherin in breast and prostate cancer cells increases chemoresistance. *Clin. Exp. Metastasis* 29, 39–50
32 Josson, S. *et al.* (2010) Tumor-stromal interactions influence radiation sensitivity in epithelial- versus mesenchymal-like prostate cancer cells. *J. Oncol.* http://dx.doi.org/10.1155/2010/232831
33 Brase, J.C. *et al.* (2011) Circulating miRNAs are correlated with tumor progression in prostate cancer. *Int. J. Cancer* 128, 608–616
34 Selth, L.A. *et al.* (2013) Circulating microRNAs predict biochemical recurrence in prostate cancer patients. *Br. J. Cancer* 109, 641–650
35 Bryant, R.J. *et al.* (2012) Changes in circulating microRNA levels associated with prostate cancer. *Br. J. Cancer* 106, 768–774
36 Selth, L.A. *et al.* (2012) Discovery of circulating microRNAs associated with human prostate cancer using a mouse model of disease. *Int. J. Cancer* 131, 652–661
37 Madhavan, D. *et al.* (2012) Circulating miRNAs as surrogate markers for circulating tumor cells and prognostic markers in metastatic breast cancer. *Clin. Cancer Res.* 18, 5972–5982
38 Pattabiraman, D.R. and Weinberg, R.A. (2014) Tackling the cancer stem cells – what challenges do they pose? *Nat. Rev. Drug Discov.* 13, 497–512
39 Bae, K.M. *et al.* (2010) Expression of pluripotent stem cell reprogramming factors by prostate tumor initiating cells. *J. Urol.* 183, 2045–2053
40 Yan, H. *et al.* (2011) Drug-tolerant cancer cells show reduced tumor-initiating capacity: depletion of CD44 cells and evidence for epigenetic mechanisms. *PLoS ONE* 6, e24397
41 Li, R. *et al.* (2010) A mesenchymal-to-epithelial transition initiates and is required for the nuclear reprogramming of mouse fibroblasts. *Cell Stem Cell* 7, 51–63
42 Redmer, T. *et al.* (2011) E-cadherin is crucial for embryonic stem cell pluripotency and can replace OCT4 during somatic cell reprogramming. *EMBO Rep.* 12, 720–726
43 Shamir, E.R. *et al.* (2014) Twist1-induced dissemination preserves epithelial identity and requires E-cadherin. *J. Cell Biol.* 204, 839–856
44 Murashima, A. *et al.* (2014) Androgens and mammalian male reproductive tract development. *Biochim. Biophys. Acta* http://dx.doi.org/10.1016/j.bbagrm.2014.05.020
45 Hara, T. *et al.* (2008) Androgen receptor and invasion in prostate cancer. *Cancer Res.* 68, 1128–1135
46 Anose, B.M. and Sanders, M.M. (2011) Androgen receptor regulates transcription of the ZEB1 transcription factor. *Int. J. Endocrinol.* 2011, 10
47 Wu, K. *et al.* (2012) Slug, a unique androgen-regulated transcription factor, coordinates androgen receptor to facilitate castration resistance in prostate cancer. *Mol. Endocrinol.* 26, 1496–1507
48 Jin, H.J. *et al.* (2013) Androgen receptor-independent function of FoxA1 in prostate cancer metastasis. *Cancer Res.* 73, 3725–3736
49 Jing, Y. *et al.* (2014) Activated androgen receptor promotes bladder cancer metastasis via Slug mediated epithelial-mesenchymal transition. *Cancer Lett.* 348, 135–145
50 Graham, T.R. *et al.* (2010) Reciprocal regulation of ZEB1 and AR in triple negative breast cancer cells. *Breast Cancer Res. Treat.* 123, 139–147
51 Lee, Y.C. *et al.* (2010) Androgen depletion up-regulates cadherin-11 expression in prostate cancer. *J. Pathol.* 221, 68–76
52 Sun, Y. *et al.* (2012) Androgen deprivation causes epithelial-mesenchymal transition in the prostate: implications for androgen-deprivation therapy. *Cancer Res.* 72, 527–536
53 Izumi, K. *et al.* (2013) Targeting the androgen receptor with siRNA promotes prostate cancer metastasis through enhanced macrophage recruitment via CCL2/CCR2-induced STAT3 activation. *EMBO Mol. Med.* 5, 1383–1401
54 Schroeder, A. *et al.* (2014) Loss of androgen receptor expression promotes a stem-like cell phenotype in prostate cancer through STAT3 signaling. *Cancer Res.* 74, 1227–1237

55 Wan, X. *et al.* (2012) Activation of beta-catenin signaling in androgen receptor-negative prostate cancer cells. *Clin. Cancer Res.* 18, 726–736
56 Song, K. *et al.* (2010) DHT selectively reverses Smad3-mediated/TGF-beta-induced responses through transcriptional down-regulation of Smad3 in prostate epithelial cells. *Mol. Endocrinol.* 24, 2019–2029
57 Shiota, M. *et al.* (2014) Inhibition of protein kinase C/Twist1 signaling augments anticancer effects of androgen deprivation and enzalutamide in prostate cancer. *Clin. Cancer Res.* 20, 951–961
58 Alonso-Magdalena, P. *et al.* (2009) A role for epithelial-mesenchymal transition in the etiology of benign prostatic hyperplasia. *Proc. Natl. Acad. Sci. U.S.A.* 106, 2859–2863
59 Eide, T. *et al.* (2013) TWIST1, A novel androgen-regulated gene, is a target for NKX3-1 in prostate cancer cells. *Cancer Cell Int.* 13, 4
60 Chan, S.C. and Dehm, S.M. (2014) Constitutive activity of the androgen receptor. *Adv. Pharmacol.* 70, 327–366
61 Cottard, F. *et al.* (2013) Constitutively active androgen receptor variants upregulate expression of mesenchymal markers in prostate cancer cells. *PLoS ONE* 8, e63466
62 Liu, G. *et al.* (2013) AR variant ARv567es induces carcinogenesis in a novel transgenic mouse model of prostate cancer. *Neoplasia* 15, 1009–1017
63 Sun, F. *et al.* (2014) Androgen receptor splice variant AR3 promotes prostate cancer via modulating expression of autocrine/paracrine factors. *J. Biol. Chem.* 289, 1529–1539
64 Becker-Santos, D.D. *et al.* (2012) Integrin-linked kinase as a target for ERG-mediated invasive properties in prostate cancer models. *Carcinogenesis* 33, 2558–2567
65 Gupta, S. *et al.* (2010) FZD4 as a mediator of ERG oncogene-induced WNT signaling and epithelial-to-mesenchymal transition in human prostate cancer cells. *Cancer Res.* 70, 6735–6745
66 Leshem, O. *et al.* (2011) TMPRSS2/ERG promotes epithelial to mesenchymal transition through the ZEB1/ZEB2 axis in a prostate cancer model. *PLoS ONE* 6, e21650
67 Kim, J. *et al.* (2013) TMPRSS2-ERG gene fusions induce prostate tumorigenesis by modulating microRNA miR-200c. *Oncogene* http://dx.doi.org/10.1038/onc.2013.461
68 Zhu, M.L. and Kyprianou, N. (2010) Role of androgens and the androgen receptor in epithelial-mesenchymal transition and invasion of prostate cancer cells. *FASEB J.* 24, 769–777
69 Armstrong, A.J. *et al.* (2012) Biomarkers in the management and treatment of men with metastatic castration-resistant prostate cancer. *Eur. Urol.* 61, 549–559
70 Marin-Aguilera, M. *et al.* (2014) Epithelial-to-mesenchymal transition mediates docetaxel resistance and high risk of relapse in prostate cancer. *Mol. Cancer Ther.* http://dx.doi.org/10.1158/1535-7163.MCT-13-0775
71 Puhr, M. *et al.* (2012) Epithelial-to-mesenchymal transition leads to docetaxel resistance in prostate cancer and is mediated by reduced expression of miR-200c and miR-205. *Am. J. Pathol.* 181, 2188–2201
72 Kim, J.J. *et al.* (2013) Acquisition of paclitaxel resistance is associated with a more aggressive and invasive phenotype in prostate cancer. *J. Cell. Biochem.* 114, 1286–1293
73 Chang, L. *et al.* (2013) Acquisition of epithelial-mesenchymal transition and cancer stem cell phenotypes is associated with activation of the PI3K/Akt/mTOR pathway in prostate cancer radioresistance. *Cell Death Dis.* 4, e875
74 Sun, Y. *et al.* (2012) Treatment-induced damage to the tumor microenvironment promotes prostate cancer therapy resistance through WNT16B. *Nat. Med.* 18, 1359–1368
75 Kahn, B. *et al.* (2014) Androgen receptor as a driver of therapeutic resistance in advanced prostate cancer. *Int. J. Biol. Sci.* 10, 588–595
76 Goldstein, A.S. *et al.* (2010) Identification of a cell of origin for human prostate cancer. *Science* 329, 568–571
77 Josson, S. *et al.* (2011) beta2-microglobulin induces epithelial to mesenchymal transition and confers cancer lethality and bone metastasis in human cancer cells. *Cancer Res.* 71, 2600–2610
78 Morgan, T.M. *et al.* (2009) Disseminated tumor cells in prostate cancer patients after radical prostatectomy and without evidence of disease predicts biochemical recurrence. *Clin. Cancer Res.* 15, 677–683
79 Smith, A.L. *et al.* (2012) Molecular pathways: targeting the TGF-beta pathway for cancer therapy. *Clin. Cancer Res.* 18, 4514–4521
80 Iinuma, H. *et al.* (2011) Clinical significance of circulating tumor cells, including cancer stem-like cells, in peripheral blood for recurrence and prognosis in patients with Dukes' stage B and C colorectal cancer. *J. Clin. Oncol.* 29, 1547–1555
81 Miyamoto, D.T. *et al.* (2012) Androgen receptor signaling in circulating tumor cells as a marker of hormonally responsive prostate cancer. *Cancer Discov.* 2, 995–1003
82 Brabletz, T. *et al.* (2005) Opinion: migrating cancer stem cells - an integrated concept of malignant tumour progression. *Nat. Rev. Cancer* 5, 744–749
83 Brabletz, T. (2012) To differentiate or not – routes towards metastasis. *Nat. Rev. Cancer* 12, 425–436
84 Klein, C.A. (2009) Parallel progression of primary tumours and metastases. *Nat. Rev. Cancer* 9, 302–312
85 Amatangelo, M.D. *et al.* (2012) c-Myc expression and MEK1-induced Erk2 nuclear localization are required for TGF-beta induced epithelial-mesenchymal transition and invasion in prostate cancer. *Carcinogenesis* 33, 1965–1975
86 Terry, S. and Beltran, H. (2014) The many faces of neuroendocrine differentiation in prostate cancer progression. *Front. Oncol.* 4, 60
87 Aparicio, A.M. *et al.* (2013) Platinum-based chemotherapy for variant castrate-resistant prostate cancer. *Clin. Cancer Res.* 19, 3621–3630
88 Yu, X. *et al.* (2011) Wnt/beta-catenin activation promotes prostate tumor progression in a mouse model. *Oncogene* 30, 1868–1879
89 McKeithen, D. *et al.* (2010) Snail transcription factor regulates neuroendocrine differentiation in LNCaP prostate cancer cells. *Prostate* 70, 982–992
90 Salvatori, L. *et al.* (2012) Cell-to-cell signaling influences the fate of prostate cancer stem cells and their potential to generate more aggressive tumors. *PLoS ONE* 7, e31467
91 Sotomayor, P. *et al.* (2009) Oct4A is expressed by a subpopulation of prostate neuroendocrine cells. *Prostate* 69, 401–410
92 Beltran, H. *et al.* (2011) Molecular characterization of neuroendocrine prostate cancer and identification of new drug targets. *Cancer Discov.* 1, 487–495
93 Slattum, G.M. and Rosenblatt, J. (2014) Tumour cell invasion: an emerging role for basal epithelial cell extrusion. *Nat. Rev. Cancer* 14, 495–501

1.10. MicroRNAs

MicroRNAs (miRNAs) are a large family of small (~ 21 nucleotides long) non- coding RNAs (Davis and Hata 2009; Krol, et al. 2010). They are key regulators of gene expression at the posttranscriptional level (Bartel and Chen 2004; Krol et al. 2010). Mature miRNA guides the multi-protein RNA-induced silencing complex (RISC) to silence target mRNAs that share regions of homology. This silencing occurs either by mRNA cleavage or translational repression (Figure 1.7).

In the nucleus, primary miRNAs (pri-miRNA), which can be several thousand bases long, are transcribed either by RNA polymerase II or III from independent miRNA genes or are spliced from the introns of protein coding genes (Carthew and Sontheimer 2009; Kim, et al. 2009). Following transcription, the pri-miRNA is processed by Drosha (RNAse enzyme) into a 60 – 100 nucleotide hairpin structure called precursor-miRNA (pre-miRNA). This pre-miRNA then transported from the nucleus to the cytoplasm by exportin-5 where it undergoes a second cleavage by another RNAse enzyme (Dicer). This cleavage results in a double stranded ~ 21-22 nucleotide duplex product which contains a mature miRNA guide stand and a miRNA passenger strand (miRNA: miRNA duplex). The passenger stand of miRNA is degraded while the functional stand is loaded into RISC together with Argonaute (Ago) proteins.

Experimental and computational studies have determined that a single miRNA may target several mRNAs with partial complementarity, mostly involving residues 2–8 from the 5'termini (seed region) (Bartel 2009; Hibio, et al. 2012; Selbach, et al. 2008). Furthermore, in mammals, miRNAs are anticipated to control more than 60% of human protein coding genes (Friedman, et al. 2009; Selbach et al. 2008). It is therefore not surprising that miRNAs function in all aspects of normal physiology including, organ development (Tomankova, et al. 2010), cardiovascular homeostasis (Grueter, et al. 2012), cognitive functions (Fiore, et al. 2011), cell metabolism (Dumortier, et al. 2013).

1.11. MicroRNAs and cancer

The Croce laboratory was the first to demonstrate direct evidence for involvement of miRNAs in cancer (Calin and Croce 2006). They studied a well-known chromosomal abnormality (deletion on chromosome 13) in chronic lymphocytic leukaemia (CLL) and found that this region encodes two microRNAs, miR-15a and miR-16a (Zhang, et al. 2007). Analysis of the deleted region revealed that these two miRNAs were the only genes which were lost in the majority of CLL patients. Furthermore, gene expression profiling indicated that these two miRNAs were downregulated in around 68% of patients diagnosed with CLL (Yanaihara, et al. 2006; Zhang et al. 2007). Since that seminal finding, it has been established that miRNA are deregulated in most types of cancer (Selth, et al. 2012a; Yanaihara et al. 2006; Zhang et al. 2007).

Oncogenic miRNAs, also called "oncomirs", promote tumour development by repressing the expression of tumour suppressor genes (Figure 1.8) and are frequently over-expressed

in cancer. For example, miR-17-92 cluster is commonly amplified and over-expressed in many cancers (Hayashita, et al. 2005; He, et al. 2005a) and forced overexpression of this miRNA using an animal model (transgenic mice) significantly increased the formation of lymphoid malignancies by targeting tumour suppressor genes *PTEN* and *RB2*. Other examples of oncomirs include: miR-21, which is overexpressed in breast, colon, lung and prostate cancers (Volinia, et al. 2006; Yanaihara et al. 2006) and suppresses the expression a large number of genes, including PTEN, PDCD4, TGFBR2, SPRY1, SPRY2, etc. that participate directly or indirectly in the extrinsic or intrinsic apoptosis pathways to promote tumorigenesis (Buscaglia and Li 2011); miR-155, which is up-regulated in human B-cell lymphomas (BCL) and impairs the transcriptional activity of BCL6 by targeting histone deacetylase 4 (HDAC4) (Eis, et al. 2005; He et al. 2005a; He, et al. 2005b); miR-18 and miR-224, both of which are over-expressed in hepatocellular carcinoma (HCC) and act by down-regulating connective tissue growth factor (CTGF), receptor activator nuclear factor kappa B ligand (RANKL), platelet-derived growth factor receptor precursor beta (PDGFRB) and Ras-related protein RAB-9B (Murakami, et al. 2006).

Tumour suppressor miRNAs repress the expression of oncogenes and are frequently down-regulated or lost in cancer (Figure 1.8). One of the best examples of this category is miRNA let-7. In humans, let -7 (a,b,c,d) expression was found to be lower in lung cancer patients (Takamizawa, et al. 2004; Yanaihara et al. 2006) and reduced let-7 was associated with a shorter post-operative survival rate (Takamizawa et al. 2004). Let-7 has been found to negatively regulate multiple oncogenes, such as *RAS*, *MYC*, *HMGA2*, and promoters of cell cycle progression, such as *CDC25A*, *CDK6*, and Cyclin D2 (Johnson, et al. 2007; Johnson, et al. 2005; Lee and Dutta 2007; Trang, et al. 2010). Other examples include: miR-125b in breast cancer targeting oncogenes *YES*, *ETS1*, *TEL*, and *AKT3*(Iorio, et al. 2005); miR-199 a/b-3p targeting tumour-promoting gene PAK4 in HCC (Murakami et al. 2006); miR-143 and miR-145 in colorectal cancer by targeting RAF1 kinase, G-protein γ7 (Michael, et al. 2003).

In summary, it is apparent that loss- or gain-of-function of specific miRNAs contributes to cellular transformation and tumorigenesis (Figure 1.8).

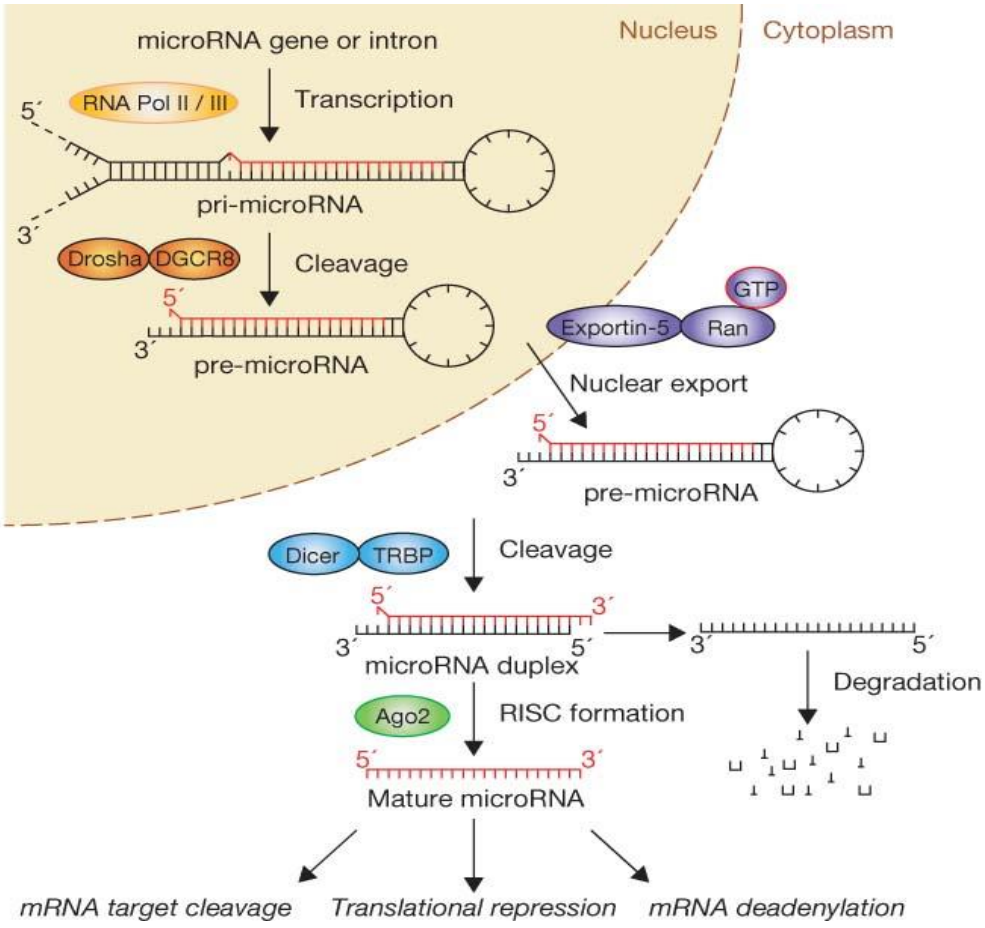

Figure 1.7: MicroRNA biogenesis (Winter, et al. 2009)

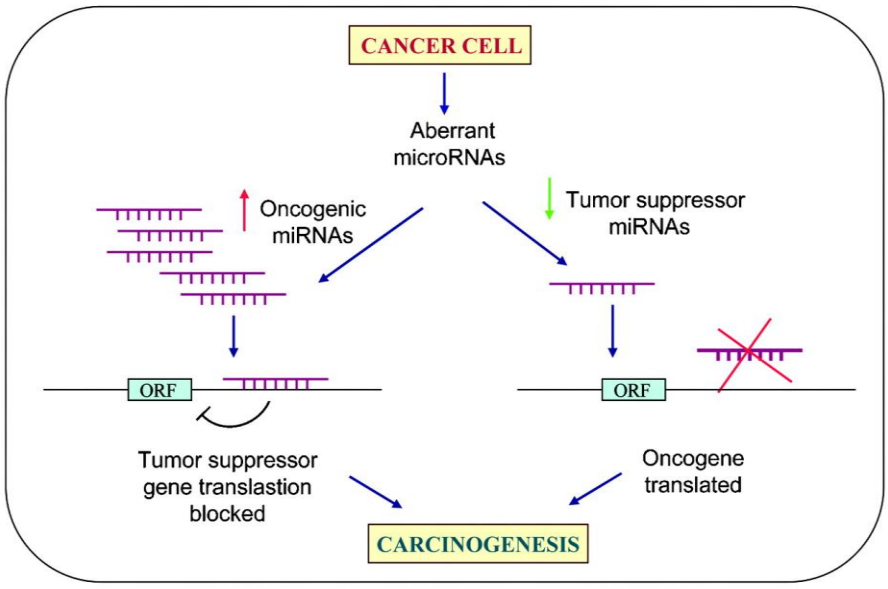

Figure 1.8: The oncogenic and tumour suppressor role of miRNAs (Paranjape, et al. 2009)

1.12. Prostate cancer-associated microRNAs and EMT

Many studies have now demonstrated that miRNA play a critical role in EMP. The miR-200 family (miR-200a, miR-200b, miR-200c, miR-141 and miR-429) is the best studied in this process (Gregory, et al. 2008; Korpal and Kang 2008; Park, et al. 2008). Korpal et al (Korpal and Kang 2008) and Hurteau et al (Hurteau, et al. 2007) first demonstrated that forced overexpression of miR-200c initiates an epithelial phenotype which leads to upregulation of E-cadherin in cell line cancer models. Gregory et al (Gregory et al. 2008) then went on to show that miR-200 family promotes epithelial phenotypes by targeting the ZEB family of transcription factors, which are potent inducers of EMT (Gregory et al. 2008; Hurteau et al. 2007; Korpal and Kang 2008).

In prostate cancer, along with the miR-200 family, miR-205 has also been studied extensively. Several studies found that miR-205 is significantly down-regulated in PCa specimens and the same was found to be true in prostatic cancer cell lines (Gandellini, et al. 2009; Gandellini, et al. 2012; Majid, et al. 2010; Porkka, et al. 2007; Schaefer, et al. 2010). Furthermore, miR-205 was found to be consistently low in patients with metastasis when compared with patients with localised tumour (primarily in the basal cells of prostate gland) (Gandellini et al. 2009; Gandellini et al. 2012; Tucci, et al. 2012). Additionally, it was found that upon ectopic expression of miR-205 in PCa cell lines (22RV1, PC3 and DU145 but not LNCaP) there was a marked increase in the level of E-cadherin protein (Gandellini et al. 2009; Hagman, et al. 2013). The miR-143/145 cluster is found to be deregulated in primary cancer in comparison with normal prostate tissue. Studies both *in vitro* and *in vivo* have reported that upregulation of miR-143 and miR-145 prevents migration and invasion of PCa cells (Peng, et al. 2011). The same study also demonstrated the capability of these miRNAs to suppress mesenchymal markers (fibronectin and vimentin) and increase E-cadherin when overexpressed in PCa cell line (PC3) (Peng et al. 2011).

1.13. Circulating miRNAs as biomarkers of PCa

The use of prostate-specific antigen (PSA) for the diagnosis of PCa is associated with several clinical issues. First, PSA lacks specificity as it is also elevated in many other conditions including benign prostatic hyperplasia (BPH), urinary retention, prostatitis, trauma, and physical manipulation. Second, PSA levels only correlate loosely with disease severity. Perhaps more important than its diagnostic inaccuracy, three large clinical trials

have revealed that PSA testing/screening is associated with a high rate of over-diagnosis and overtreatment (Andriole, et al. 2009; Chou, et al. 2011a; Schroder, et al. 2009). Clearly, one of the major requirements for prostate cancer management is to identify new biomarkers that can more accurately diagnose prostate cancer and, perhaps more importantly, distinguish slow-growing tumours from the aggressive subtypes (Andriole et al. 2009; Andriole, et al. 2012; Crawford, et al. 2011; Schroder et al. 2009)

Given that microRNAs are dysregulated in human cancers, there has been considerable interest with regards to their capability as biomarkers. Lu and colleagues (Lu, et al. 2005) were the first to demonstrate the utility of miRNA expression profiles for accurate identification of tumours of histologically uncertain cellular origin. Since that time, many groups have shown that miRNAs are powerful biomarkers for the diagnosis, prognosis and prediction of cancer (Allegra, et al. 2012; Boeri, et al. 2012; Boeri, et al. 2011; Ma, et al. 2012; Valladares-Ayerbes, et al. 2012; Wittmann and Jack 2010). Indeed, miRNAs have recently been added in the panel of molecular markers to improve diagnostic accuracy for patients with intermediate thyroid nodules and pancreatic ductal carcinoma (ASURAGEN ; MiRNATherapeutics).

A number of studies published in 2008 demonstrated the presence of miRNAs in the cell-free fraction of blood (i.e: serum and plasma) and other bodily fluids (Chim, et al. 2008; Lawrie, et al. 2008; Mitchell, et al. 2008). These studies suggested that miRNAs could be sampled in a non-invasive manner to detect and manage disease. Morever, miRNAs in human plasma are present in a remarkably stable form, protected from endogenous RNase activity (Mitchell et al. 2008).

For the past 3 years, our laboratory has been interested in identifying circulating miRNAs that could be used to better manage prostate cancer patients. In a first for this field, we demonstrated that certain circulating miRNAs were common between prostate cancer patients and a mouse model of prostate cancer, highlighting the potential of such models for the discovery of novel biomarkers (Selth, et al. 2012b). Two of these miRNAs, miR-141 and miR-375, had been identified previously as markers of metastatic prostate cancer (Brase, et al. 2011; Bryant, et al. 2012; Mo, et al. 2012). More recently, our laboratory evaluated the ability of circulating miRNAs to predict PCa progression in men treated by radical prostatectomy (RP) (Selth, et al. 2013). Analysis of a small discovery cohort found that the expression of three miRs namely, miR-141, miR-146b-3p and miR-194, were found at differential levels in men who underwent disease recurrence versus those who did

not. In a larger validation cohort, miR-146b-3p and miR-194 were positively correlated with disease progression (example shown in Figure 1.9).

1.13.1. Expression of miR-194 and miR-375 in prostate cancer

In addition to their potential utility as biomarkers, we are interested in determining whether any of these circulating miRNAs play a direct role in prostate cancer development and progression.

Based on our earlier studies, we made a short-list of four miRNAs, miR-141, miR-146b-3p, miR-194 and miR-375, for further functional analysis. MiR-141 is a member of the miR-200 family of EMT suppressors and has been extensively studied in prostate and other malignancies (Brase et al. 2011; Bryant et al. 2012; Mitchell et al. 2008; Nguyen, et al. 2013). MiR-146b-3p appears to only be a circulating marker of prostate cancer because we have demonstrated that it is not expressed in prostate tissues (Selth et al. 2013). Therefore, we have prioritised research into miR-194 and miR-375 as novel contributors to prostate cancer.

Other studies have provided further evidence for the importance of miR-375 and miR-194 in prostate cancer. MiR-375 is the most frequently over-expressed miRNA in prostate cancer, both in tumours (Szczyrba, et al. 2010) and in circulation (Sita-Lumsden, et al. 2013). Moreover, it has been associated with prognostic clinicopathological parameters of the disease (Brase et al. 2011; Bryant et al. 2012), metastasis (Selth et al. 2012b) (Figure 1.10) and biochemical recurrence (BCR) with RP (Selth et al. 2012b) (Figure 1.11).

In addition to our finding that circulating miR-194 is a marker of disease progression, this miRNA was reported to be elevated in tumours from men who experienced early BCR (within 2 years of radical prostatectomy) compared to men who did not experience BCR for $\geq$10 years after surgery (Tong, et al. 2009). Furthermore, miR-194 was found to be elevated in patients who subsequently experienced recurrence in two independent clinical cohorts (Selth et al. 2013) (Figure 1.12).

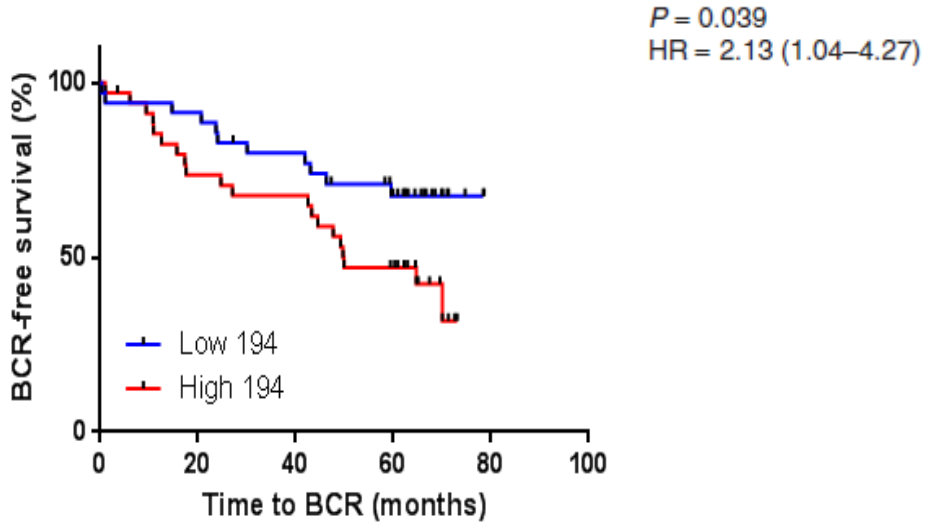

Figure 1.9: Kaplan–Meier analysis showing estimated biochemical recurrence (BCR)-free probability in patients with high (above median) or low (below median) levels of circulating miR-194 (Selth et al. 2013)

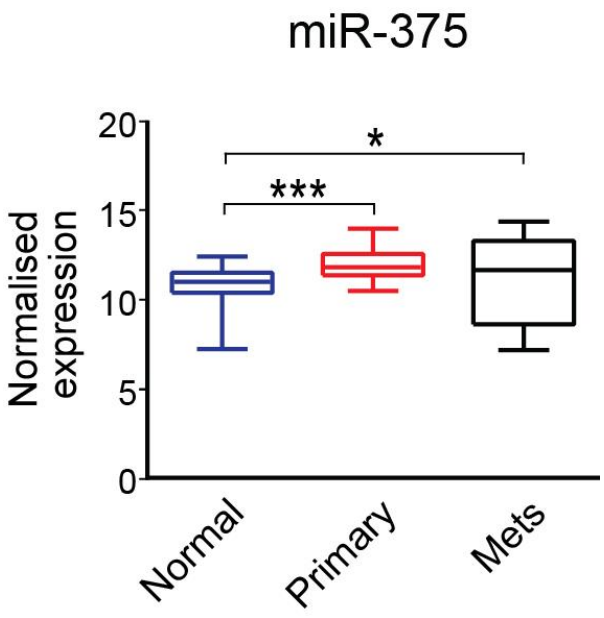

Figure 1.10: Relative expression of miR-375 in normal prostate tissue, primary prostate tumours (Primary) and metastases (Met) following analysis of MSKCC cohort (Selth et al. 2012b)

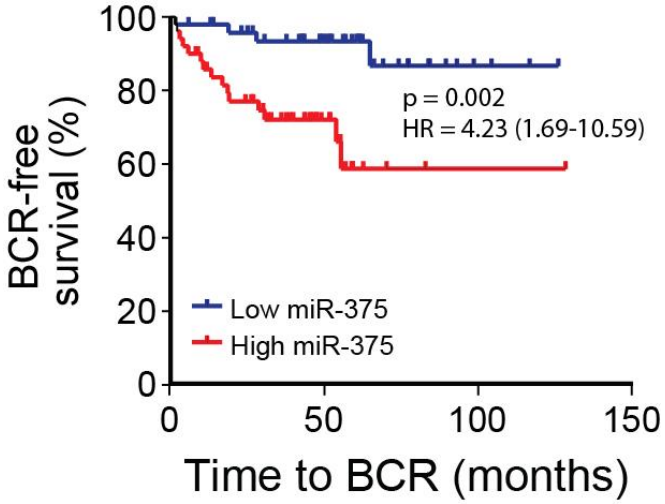

Figure 1.11: Kaplan–Meier curve showing estimated PSA recurrence-free probability in patients with high or low intra-tumoral expression of miR-375 (Selth et al. 2012b)

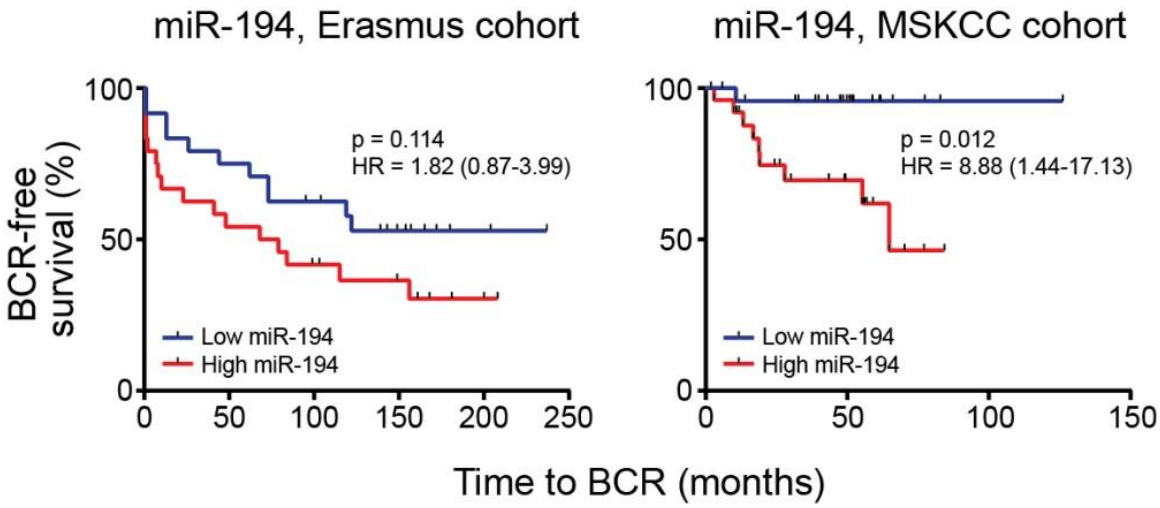

Figure 1.12: Kaplan–Meier curves showing estimated biochemical recurrence (BCR)-free probability in patients with high or low intra-tumoural expression of miR-194 in Erasmus and MSKCC cohort (Selth et al. 2013)

Both of these miRNAs have also been found to be deregulated in other malignancies. MiR-375 is down-regulated in gastric cancer (Ding, et al. 2010; Tsukamoto, et al. 2010), head and neck squamous cell carcinoma (Hui, et al. 2010), pharyngeal squamous cell carcinoma (Lajer, et al. 2011) and cervical cancer (Li, et al. 2011). Conversely, miR-375 is up-regulated in ER-alpha-positive breast cancer patients (de Souza Rocha Simonini, et al. 2010), adenocarcinoma of lung (Yu, et al. 2010) and patients with HBV-positive hepatocellular carcinoma (Li, et al. 2010). These reports suggest that the function of miR-375 may vary depending on its spatial expression and by malignancy. MiR-194 is overexpressed in oesophageal adenocarcinoma and Barret's oesophagus (Wijnhoven, et al. 2010) and pancreatic ductal adenocarcinoma (Mees, et al. 2010), but down-regulated in colon cancer (Braun, et al. 2008), colorectal cancer (Chiang, et al. 2012), nephroblastomas (mainly mixed-type) (Senanayake, et al. 2012) and liver cancer (Meng, et al. 2010).

The molecular function and targets of these miRNAs in prostate cancer are largely unknown, but recent evidence from other malignancies suggests that both may be involved in metastasis and EMP. For example, it was reported that over-expression of miR-194 reduced expression of N-cadherin and suppressed invasion and migration of the liver mesenchymal-like cancer cells both *in vitro* and *in vivo* (Meng et al. 2010). Furthermore, miR-194 was also found to reduce invasion of endometrial carcinoma cells (Dong, et al. 2011) and breast cancer cells (Le, et al. 2012) by suppressing self-renewal factor BMI-1 and cytoskeletal proteins (talin2 and profilin2), respectively. MiR-375 was shown to partially reverse EMT in MCF-7 breast cancer cells (Ward *et al*, 2013) and inhibit melanoma invasion and motility (Mazar, et al. 2011). These observations are interesting because many of the other circulating miRNAs associated with prostate cancer are also associated with epithelial phenotypes. For example, miR-141 and miR-200b target the Zeb1/2 transcription factors and thereby repress EMT (Hill, et al. 2013).

Collectively, these findings have led us to hypothesise that epithelial miRNAs may be important drivers of PCa metastasis. This is an interesting concept and contrasts with other malignancies in which epithelial miRNAs are frequently down-regulated and positively associated with good outcomes, with the thought being that they can repress EMT in the earlier stages of metastasis (Dong et al. 2011; Zhou, et al. 2012). We will investigate the molecular functions of miR-194 and miR-375 to test the hypothesis that epithelial miRNAs have roles in prostate cancer progression and metastasis, potentially by modulating the epithelial-mesenchymal plasticity of tumour cells.

1.14. Hypothesis and aims:

Preliminary data from our laboratory suggests that elevated levels of miR-375 and miR-194, both in prostate tumours and in circulation of patients, are associated with poor prognosis. Therefore, we hypothesise that these miRNAs have roles in prostate cancer progression and metastasis, potentially by modulating the epithelial-mesenchymal plasticity of tumour cells. The broad aim of the project was to understand the underlying molecular mechanism of these miRNAs in the metastatic process of prostate cancer.

The **specific aims** of this project were as follows:

Aim 1: To determine the function of miR-194 and miR-375 in prostate cancer progression and metastasis

Aim 2: To identify and validate the gene targets of miR-194 and miR-375 through which their effects on metastasis are mediated.

Aim 3: To determine the upstream regulators of miR-194 and miR-375

CHAPTER 2: MATERIALS AND METHODS

This chapter will outline the materials used and methods that have been performed in the studies reported in the Results section. Reagents listed below each method were used according to procedures outlined by the Health, Safety and Wellbeing Policy principles and relevant sections of the Work Health and Safety Act 2012.

2.1. Materials

Table 2.1: Common chemicals and reagents

Reagent	Supplier	Catalogue number
1kb DNA ladder	New England Biolabs	N3232S
100 bp DNA ladder	New England Biolabs	N3231S
Agarose, analytical grade	Sigma Aldrich	A6013
Bradford assay reagent	BioRad	500-0006
BSA (bovine serum albumin)	Sigma Aldrich	A9647
Chloroform	Sigma Aldrich	C2432
Cover slips	HD Scientific Supplies	----------
Criterion precast gel (4-12%)	BioRad	567-1084
DAPI prolong gold mount media	Molecular Probes (Life Tech)	P26935
dNTPs (deoxynucleotide triphosphates)	Promega Corporation	U1511
DMSO (dimethyl sulfoxide)	BDG Laboratory Supplies	D2650
DynaBeads	Invitrogen	112.03D
Eosin	Australian Biostain P/L	AEPA
Ethanol, general use	Chem Supply	EA061
Ethanol, molecular grade	Sigma Aldrich	E7023
FBS (fetal bovine serum)	Sigma Aldrich	12003C
Formaldehyde	Chem Supply	FA010
Haematoxylin	Australian Biostain P/L	AHLMA
Inactivation buffer (supplied	Ambion Inc.	AM1907

with Turbo free)		
iScirpt cDNA synthesis kit	BioRad	170-8891
iQ SYBR Green Supermix	BioRad	170-8885
K-SFM (Keratinocyte Serum Free Medium)	Gibco	
Lentiviral Packaging Mix (pLP1, pLP2, pVSVG)	Virapower (Invitrogen)	K4975-00
Lentiviral Transfer (Payload) Plasmid	GeneCopoeia	----------
Lipofectamine 2000	Invitrogen	11668-019
Matrigel	Corning Scientific	BD 354234
Methanol	Chem Supply	MA004
Nitrocellulose membrane (0.4 µm)	BioRad	162-0115
Nuclear free water	Ambion Inc.	AM9937
PBS (phosphate buffered saline)	Sigma Aldrich	D8537
Ponceau S	Sigma Aldrich	P3504
Propidium Iodide	Sigma Aldrich	P4864
PVDF transmembrane	Amersham	RPN303F
QIAquick Plasmid Midiprep Kit	QIAGEN	12143
QIAquick Plasmid Miniprep Kit	QIAGEN	27106
Restriction Digest enzymnes and buffer	New England Biolabs	----------
RPMI 1640 liquid media	Sigma Aldrich	R8758
SDS (sodium dodecyl sulphate)	Sigma Aldrich	75746
SDS (sodium dodecyl sulphate) TGX precast	BioRad	----------
SDS (sodium dodecyl sulphate) Criterion	BioRad	----------
siRNA SOCS2 - 1	Ambion	s16858
siRNA SOCS2 - 2	Ambion	s16859

Skim milk powder	Coles Brand	----------
Triton-X 100	Sigma Aldrich	T8787
TRIZOL Reagent	Sigma Aldrich	T9424
Trypsin EDTA solution	Sigma Aldrich	T4049
Tween 20	Sigma Aldrich	P7949
Lipofectamine RNAiMax	Thermo Fisher Scientific	13778150
Optimem	Thermo Fisher Scientific	31985070
Pre-microRNA-194 precursors	GenePharma	----------
Pre-microRNA-194 precursors (miRVana)	Ambion	MC10004
Pre-microRNA-375 precursors	GenePharma	----------
Anti-microRNA-194 inhibitors (LNA)	Exiqon	4100890-001
Anti-microRNA-375 inhibitors (LNA)	Exiqon	4101396-001
miRCURY LNA Detection probe: miR-194	Exiqon	18082-15
miRCURY LNA Detection probe: miR-375	Exiqon	38181-15
miRCURY LNA Detection probe: U6	Exiqon	99002-15

Table 2.2: Commonly Used Buffers and Media

Buffer/Medium Name	Buffer/Medium Components
EDTA 0.2 M, pH 8.0	74.45 g EDTA Volume to 800 mL with water pH 8.0 Volume to 1 L with water
EGTA 0.5 M, pH 8.0	190.175 g EGTA Volume to 800 mL with water pH 8.0 Volume to 1 L with water
KCl 1 M	7.45 g KCl Volume to 100 mL with water
LB Medium	25 g LB Broth 1 L RO H2O (Add 20 g Agar for plates)
Loading Dye (6x) for agarose gels	50 mL Glycerol 40 mL 0.5 M EDTA (pH 8.0) 0.25 g Bromophenol blue 0.25 g Xylene cyanol Volume to 100 mL with water Store at 4°C
Loading Dye (6x) for western blot	7 mL 4x Tris-Cl/SDS 3 mL Glycerol 1 g SDS 0.93 g DTT 1.2 mg Bromophenol blue Volume to 10 mL with water Store at -20°C
Ponceau S Stain	2 g Ponceau S 30 g Trichloracetic Acid 30 g Sulfosalycylic Acid Volume to 100 mL with water
RIPA Buffer	10 mM Tris 150 mM NaCl 1 mM EDTA 1% Triton X-100
Running Buffer (10x)	77.5 g Tris Base 360 g Glycine 25 g SDS 2.5 L RO H2O
TAE Buffer (50x)	242 g Tris 57.1 mL Glacial acetic acid

	100 mL 0.5 M EDTA pH 8.0 Volume to 1 L with water
TBS (10x)	151.5 g Tris 219 g NaCl Volume to 2.5 L with water pH 7.4
TBST (1x)	2.5 mL Tween20 250 mL 10x TBS 2.25 L RO H2O
Transfer Buffer (10x)	77.5 g Tris 360 g Glycine Volume to 2.5 L with water
Tris-HCl, pH 6.5, 7.5, 8.1	121.1 g Tris Volume to 800 mL with water pH to desired level with concentrated HCl Volume to 1 L with water

Table 2.3: Primers

Primer Name	**Sequence**	**Use**
GAPDH fwd	TGCACCACCAACTGCTTAGC	qRT-PCR
GAPDH rvs	GGCATGGACTGTGGTCATGAG	qRT-PCR
Fibronectin fwd	TGATCACATGGACGCCTGC	qRT-PCR
Fibronectin rvs	GAGTCAAGCCGGACACAACG	qRT-PCR
ZO-1 fwd	GCAGCTAGCCAGTGTACAGTATAC	qRT-PCR
ZO-1 rvs	GCCTCAGAAATCCAGCTTCACGAA	qRT-PCR
ZEB1 fwd	TTCAAACCATAGTGGTTGCT	qRT-PCR
ZEB1 rvs	TGGGAGATACCAAACCAACTG	qRT-PCR
ECAD fwd	CCCACCACGTACAAGGGTC	qRT-PCR
ECAD rvs	CTGGGGTATTGGGGGCATC	qRT-PCR
NCAD fwd	CAACTTGCCAGAAAACTCCAGG	qRT-PCR
NCAD rvs	ATGAAACCGGGCTATCTGCTC	qRT-PCR
VIM fwd	GAACGCCAGATGCGTGAAATG	qRT-PCR
VIM rvs	CCAGAGGGAGTGAATCCAGATTA	qRT-PCR
SNAI1 fwd	TCGCTGCCAATGCTCATC	qRT-PCR
SNAI1 rvs	GTAGAGGAGAAGGACGAAGGAG	qRT-PCR
SNAI2 fwd	ATACCACAACCAGAGATCCTCA	qRT-PCR
SNAI2 rvs	GACTCACTCGCCCCAAAGATG	qRT-PCR
SOCS2 fwd	GTCAGACAGGATGGTACTG	qRT-PCR

SOCS2 rvs	TCCAATCTGAATTTTCCGTC	qRT-PCR
SOCS2 3'UTR fwd	CCAGATACAGGGGGATACCTG	qRT-PCR
SOCS2 3'UTR rvs	TGGCAATCCTCTATTACCATGA	qRT-PCR
BCL2 fwd	GGGCATTCAGTGACCTGACA	qRT-PCR
BCL2 rvs	GCATTGTTCCCATAGAGTTC	qRT-PCR
BIRC5 fwd	CTGGCAGCCCTTTCTCAA	qRT-PCR
BIRC5 rvs	CAGCCTTCCAGCTCCTTG	qRT-PCR
BRF1 fwd	GGCATTGATGACCTGGAGAT	qRT-PCR
BRF1 rvs	ACCAGAGGCCTCAACCTTTT	qRT-PCR
CDC25A fwd	GCCTCTCGTGGCAGGGCAGTC	qRT-PCR
CDC25A rvs	CATCACCTGGCCTGAGGA ATC	qRT-PCR
ELK1 fwd	GAGCTGCCAACATTGCCAAC	qRT-PCR
ELK1 rvs	GGAGATGATGTGGCCATTGC	qRT-PCR
ELK4a fwd	CTGTTGCTCCCCTAAGTCCA	qRT-PCR
ELK4a rvs	CCAGCCCAGACAGAGTGAAT	qRT-PCR
ELK4b fwd	AGCCGAGCCCTCAGATACTA	qRT-PCR
ELK4b rvs	ACCATAAAGAGCGAGCAAGC	qRT-PCR
FSCN2 fwd	AGGCGGCCAACGAGAGGAAC	qRT-PCR
FSCN2 rvs	ACGATGATGGGGCGGTTGAT	qRT-PCR
c-MYC fwd	TCCTCGGATTCTTCTGCTCTC	qRT-PCR
c-MYC rvs	CTCTGACCTTTTGCCAGGAG	qRT-PCR
N-MYC fwd	CTGGGAACTGTGTTTGGAG	qRT-PCR
N-MYC rvs	CGACTGAGGGCTTCTTTC	qRT-PCR
GATA2 fwd	CATCAAGCCCAAGCGAAGA	qRT-PCR
GATA2 rvs	TTTGACAGCTCCTCGAAGCA	qRT-PCR
KLK3 fwd	GCCTGGATCTGAGAGAGATATCATC	ChIP qPCR
KLK3 rvs	ACACCTTTTTTTTTCTGGATTGTTG	ChIP qPCR
TMPRSS2 fwd	GGTAAACTCTCCCTGCCACA	ChIP qPCR
TMPRSS2 rvs	TACTCCAGGAAGTGGGGATG	ChIP qPCR

Table 2.4: Antibodies

Primary Antibody	**Dilution**	**Catalogue number/Supplier**
Tubulin	1:1000	Merick Millipore
E-Cadherin	1:2000	#610182, BD Biosciences
ZO-1	1:500	sc-10804, Santa Cruz
Fibronectin	1:750	#610077, BD Biosciences
N-Cadherin	1:750	sc-7939, Santa Cruz
GAPDH	1:5000	MAB374, Merck Millipore
SOCS2	1:500	# 2779, Cell Signaling
GATA2	1:500	sc-9008, Santa Cruz
Phospho ERK1/2 (Tyr)	1:500	#9101, Cell Signaling
Total – ERK1/2	1:500	#9102, Cell Signaling
Phospho STAT3 (Tyr)	1:500	#9131, Cell Signaling
Phospho STAT3 (Ser)	1:500	#9134, Cell Signaling
Total – STAT3	1:500	#9132, Cell Signaling
Total – JAK2	1:500	#3230, Cell Signaling
Total – FLT3	1:500	#3462, Cell Signaling
Secondary Antibody	**Marker**	**Catalogue number/Supplier**
Goat anti-rabbit	HRP	PO448, DAKO
Goat anti-mouse	HRP	PO161, DAKO
Goat anti-rabbit	Biotin	E0432, DAKO
Goat anti-mouse	Biotin	E0433, DAKO
ALEXA goat anti-rabbit	ALEXA 488nm	A-11034 , Thermo Fisher
ALEXA goat anti-mouse	ALEXA 594nm	A-11005, Thermo Fisher

2.2. Methods

2.2.1 Computational analysis *(in silico)*

Bioinformatic prediction of miR-194 and miR-375 targets was performed using three different freely available programs: TargetScan (http://www.targetscan.org), miRanda (http://www.microrna.org/microrna/home.do) and TargetRank (http://hollywood.mit.edu/targetrank/) (Witkos, et al. 2011). These target prediction programs uses several characteristics to determine whether a miRNA can potentially target an mRNA. The 5′ seed region of the miRNA (bases 2 to 8) must show sequence complementarity to the 3′ UTR of a target gene, and the target site within the mRNA should be conserved among different species. Therefore, we also considered the predicted targets listed initially by the programs. In addition, a thorough literature search was done to further gather evidence towards the functionality of potential miRNA targets in the metastatic process.

2.2.2 Cell Culture

2.2.2.1 *Maintaining and Passaging Cells*

The human prostate carcinoma cell lines, RWPE-1, C4-2B, 22Rv1, LNCaP, DU145 and PC-3, were obtained from the American Type Culture Collection (ATCC). Cell Bank Australia performed verification of all cell lines in 2010 and 2016 via short-tandem repeat profiling. RWPE-1 cell line was maintained in Keratinocyte-SFM media and C4-2B, 22Rv1, LNCaP and DU145 cell lines were maintained in RPMI-1640 containing 10% Fetal Bovine Serum (FBS). The PC3 cell line was maintained in RPMI-1640 containing 5% FBS. HEK293T/17 cells were obtained from ATCC and used for preparation of lentiviral constructs and were maintained in Dulbecco's Modified Eagle's Medium (DMEM) containing 10% FBS.

To prepare cells for storage in liquid nitrogen, fully confluent T75 flasks were collected using trypsin followed by centrifugation at 450 rcf for 5 min. Pellets were resuspended in 1.5 mL of cell line specific media and 1.5 mL of freezing mix (40% DMSO, 40% FBS, 20% culture media) on ice. One ml of cell:freeze mix suspension was added to each cryo-vial, labelled appropriately and placed in an isopropanol filled Mr. Frosty freezing container at -80°C. Once cells were adequately frozen they were transferred to liquid nitrogen for long term storage.

Human prostate cancer cell lines obtained from liquid nitrogen stores were thawed quickly by gentle agitation in a 37°C water bath then mixed with 9 mL cell line specific culture medium. Cells were centrifuged at 450 rcf for 5 min and pellets were resuspended in 10 mL cell line specific culture media and placed directly into a T25 flask overnight at 37°C with 5% CO_2. Cells were passaged to a T75 flask the following day and were then passaged a second time prior to use in experiments.

2.2.2.2 *MicroRNA (miR) and Short interfering RNA (siRNA) transfection*

Prostate cancer cells were grown to a density of 70 to 90% and seeded into appropriate tissue culture plates. The cells were transfected with 20 nM of pre-miR microRNA precursors or siRNA and 50 nM of anti-miR microRNA inhibitors or their appropriate negative controls using the RNAiMax transfection agent (details of the agents are in table Catalogue # 13778150). RNAiMax was diluted in Opti-MEM and was incubated 10 min at RT. The miRNA precursors and miRNA inhibitors were diluted in Opti-MEM. The transfection agent was mixed with RNA and incubated for an additional 10 min at RT. The transfection complexes were added drop-wise to the cell cultures. The cells were allowed to rest for 72 h prior to subsequent assays, except proliferation assays where the cells were counted at 24 h and 48 h post transfection. The transfection efficiency was monitored by RT-qPCR.

2.2.3 Trypan blue exclusion test of cell viability

Cell viability is calculated as the number of viable cells divided by the total number of cells within the grids on the haemocytometer. If cells take up trypan blue, they are considered non-viable. First, using a haemocytometer, the cell density of the cell line suspension was determined. Second, 20 ul of trypan blue stock solution was added to 20 ul of cell suspension and loaded on a haemocytometer to examine the cells under microscope, immediately. Finally, the number of blue stained cells and the total number of cells are counted and inserted into the following formula:

% viable cells = [1.00 – (Number of blue cells ÷ Number of total cells)] × 100

2.2.4 Western Blotting

2.2.4.1 *Preparation of Cell Lysates*

Cells were washed with 1x PBS and removed from culture plates by scraping in 100 µl RIPA lysis buffer per well of a 6-well plate. Cell lysates were centrifuged for 10 min at 10000 rcf and 4°C and supernatant containing protein was collected and stored at -80°C.

2.2.4.2 *Bradford Assay*

Total protein concentration of cell lysates was determined via Bradford assay. Microtiter plates were set up as follows in clear, untreated, flat bottomed 96 well microtiter plates with lids (Cole Parmer, Cat no: KH-01728-01). Numbers indicate µl of 1 mg/mL BSA added to each standard well and letters indicate duplicate sample wells to which 1 µl of sample was added per well. 20% Bradford reagent was added to every well to a total volume of 200 µl. The plate was mixed and incubated at RT for 5min before being read at 595 nm on a PolarStar microplate reader:

Standards in duplicate		Samples in duplicate									
0	0	a	a								
1	1	b	b								
2	2	c	c								
3	3	d	d								
4	4	e	e								
5	5										
6	6										

2.2.4.3 *Sodium Dodecyl Sulfate Polyacrylamide Gel Electrophoresis (SDS-PAGE)*

BioRad precast SDS-PAGE gels were run using 25 µg of total protein per well unless indicated otherwise. Protein lysates were mixed 5:1 with 6x load dye and heated at 95°C for 5 minutes prior to gel loading. The SDS-PAGE running apparatus was filled with 1x SDS-running buffer (BioRad). To examine fibronectin expression, protein lysates were run on 4-15% gradient gels at constant voltage (80 V) for 15 min followed by 150 V for 2 h. To detect all other proteins, lysates were run on 10% or 4 – 12% gels at constant voltage (120 V) for 90 min.

2.2.4.4 *Western Transfer and Immunoblot*

Proteins were transferred from SDS-PAGE gel to nitrocellulose membrane using a BioRad transfer apparatus (miniPROTEAN®Tetra Cell or CriterionTM Cell) filled with 1x Transfer Buffer. Transfer of proteins from SDS-PAGE gel to nitrocellulose membrane was run using a BioRad CriterionTM Blotter at constant amperage (400 mA) for 60 minutes. Nitrocellulose membranes were then blocked for 60 minutes or overnight at 4°C on a rocking tray using 3% skim milk powder or 3% Bovine Serum Albumin (BSA) dissolved in 1x TBST. Membranes were probed using primary and HRP-conjugated secondary antibodies as indicated in table 2.4. HRP-conjugates were detected using ECL solution and imaged on a BioRad Chemidoc MP imaging system and processed using Image Lab Software. Densitometry and further analysis of protein expression was determined using Image Lab Software.

2.2.5 Quantitative polymerase chain reaction (qRT-PCR)

2.2.5.1 *RNA Isolation*

PCa cell lines were plated in 6-wells plates with miRNA transfection mix at $1x10^5$ cells (C4-2B, PC3 and DU145), 1.5 x 10^5 cells (LNCaP) and 2 x 10^5 cells (22Rv1) per well in 2.5 mL of growth media as specified in section 2.2.2.1 and incubated at 37°C and 5% CO_2 for 72 h to adhere to culture plates. Cells were washed with 1x PBS and collected using 1 mL Trizol per well. Chloroform isolation and isopropanol precipitation were used to extract RNA from cell lysates. Trizol samples were mixed with 200 µl of chloroform and shaken vigorously for 15 s then left to incubate for 3 mins at RT. Samples were then centrifuged at 12000 rcf at 4°C for 15 min and the clear aqueous layer was collected,

taking care not to disrupt the interphase layer (which contains DNA). The aqueous layer was mixed with 500 µl isopropanol, mixed and incubated for 10 min at RT. RNA was pelleted by centrifugation at 12000 rcf at 4°C for 10 min, washed in 75% EtOH and resuspended and dissolved in RT-PCR grade water. RNA concentrations were determined by spectrophotometry using a Thermo Scientific NanoDrop 2000.

2.2.5.2 *DNase Treatment*

RNA samples were DNase treated using TURBO DNA-freeTM DNase Treatment kits (Ambion cat#AM1907). RNA (1 to 2 µg) was diluted in RNase free water to a total volume of 44 µl, gently mixed with 5 µl of 10xTurbo DNAse Buffer with 1 µl TURBO DNase*free* and incubated at 37°C for 30 min. 5 µl of DNase inactivation reagent was gently mixed into each sample and repeatedly mixed 2 to 3 times over an incubation period of 5 min at RT. Inactivation reagent was removed by centrifugation of samples at 10000 rcf for 1.5 min and subsequent collection of supernatant being sure not to disrupt inactivation reagent. To ensure thorough mixing, samples were incubated at 55°C for 10 min, flicking twice or thrice during this time. RNA concentrations were determined using Nanodrop.

2.2.5.3 *Reverse Transcription*

Reverse transcription of RNA samples was performed following DNase treatment using iScriptTM Reverse Transcription kits. RNA (1000 ng) was prepared in a 1:5 mix with iScript master mix, including one control containing all products except reverse transcriptase and a second control containing all products except RNA. RNA-iScript samples were incubated at RT for 5 min, 42°C for 30 min and 85°C for 5 min. Resultant cDNA samples were diluted 1:5 and stored at -20°C.

2.2.5.4 *Quantitative Reverse Transcriptase Polymerase Chain Reaction (qRT-PCR)*

RNA expression was examined via qRT-PCR using a BioRad C1000 Thermal Cycler and CFX384TM Real-Time System. RNA expression of target genes was measured and expression was expressed relative to reference genes as indicated. Samples were prepared by mixing 0.5 µl forward primer (5 pmol per µl), 0.5 µl reverse primer (5 pmol per µl), 5 µl iQ SYBR Green Supermix, 2 µl RNase free water, and 2 µl cDNA. Three biological and three technical replicates were performed for all reactions. qRT-PCR reaction followed 3 min 95°C x1 followed by 40x 15 sec 95°C, 15 sec 55°C, 30 sec 72°C and

finally 1 min 95°C x1, 1 min 55°C x1 and 70x 10 sec 60°C. Data were analysed using CFX Manager Software Version 3.0 (Bio-Rad Laboratories, Inc.).

2.2.6 Immunohistochemistry

2.2.6.1 Preparation of sections

Paraffin embedded human prostate cancer sections (3 μm) were cut using a microtome and collected on Superfrost Ultra-plus slides. Slides were placed on a heating block at 62°C for a minimum of 2 h prior to beginning the staining procedure. Slides were de-waxed in three 5 min washes of 100% xylene. Xylene was cleared by dipping slides 10 times each in 3 pots of 100% EtOH, then slides were stained for haematoxylin/eosin (H&E) or immunohistochemistry using primary antibodies directed at specific proteins of interest.

2.2.6.2 Haematoxylin and Eosin (H&E) staining

For H&E staining, slides were washed for 2 min in running tap water, stained for 4 min in 1:2 Haematoxylin then rinsed in running tap water for 2 min or until the water ran clear. Slides were differentiated with 0.3% acid alcohol by dipping into the solution twice. Slides were again rinsed in running tap water for 3 min, counterstained with Eosin for 1 min and rinsed one final time in running tap water until the water ran clear. Finally, slides were dehydrated and cleared in ethanol by dipping 10 times each in 3 separate pots followed by 3 times 5 min incubation in xylene and coverslips were sealed using DPX mounting media. Scanning of all slides was completed using a Nanozoomer digital slide scanner (Hamamatsu). Images were viewed with NDPview software.

2.2.6.3 *Immunohistochemistry*

Slides were washed twice for 3 min in PBS then endogenous peroxidase activity was blocked with 0.3% H_2O_2 for 5 min. Antigen retrieval was completed in citrate buffer (0.525 g in 250 mL RO-water, pH 6.5) using a Biocare Medical Decloaking Chamber V3.7.2.2 for 15 min at 95°C and 2.5 psi. Slides were then blocked in 5% goat serum for 30 min at RT, and incubated with primary antibody as indicated overnight at 4°C. Secondary biotinylated antibody was added to slides at a dilution of 1:400 in blocking solution for 1h at RT followed by HRP-strepdavidin at 1:500 for 1 hr at RT. Freshly mixed DAB: H_2O_2 was added to slides for exactly 6 mins. Slides were counterstained in fresh 1:5 haematoxylin for 1.5 min. Slides were dehydrated and cleared in ethanol by dipping 10

times each in 3 separate pots followed by 3 times 5 min incubation in xylene. Coverslips were sealed using DPX. Scanning of all slides was completed using a Nanozoomer digital slide scanner (Hamamatsu). Images were viewed with NDPview software.

2.2.7 Fluorescence Microscopy

Prostate cancer cells were transfected with microRNA mimic or control, as described above, plated onto chamber slides (Lab-Tek, Thermo Fisher Scientific) and stained at day 3. For E-cadherin staining, cells were fixed in 4% paraformaldehyde, permeabilized in 0.1% Triton X-100 and probed with an anti-E-cadherin antibody (1:500; BD Biosciences, 610182). To detect nuclei, cells were co-stained with 4´-6-Diamidino-2-phenylindole (DAPI; Invitrogen). For F-actin staining, fixed and permeabilized cells were incubated with rhodamine phalloidin (Invitrogen) for 10 min. Cells were observed on and pictures were taken using a confocal microscope (Leica SP5).

2.2.8 Cell migration assay

The cell migration assay or scratch wound assay is a simple and reproducible assay which is commonly used to measure the migratory ability of the cells. Briefly, following transfection with miRNA- mimics or inhibitors in a 24-wells microplate (Essen-Image Lock), cells are grown to confluence (monolayer) and then a thin "wound" is introduced by scratching with sterile pipette tips. The microplate is then placed in the Incucyte imaging system to record the migratory ability of the cells into the "wound" over a period of time. Cells at the wound edge polarise and migrate into the "wound" space (figure 2.1)

2.2.9 Cell invasion assay

Twenty-four wells culture plates were prepared by pipetting 100 µl of 1:1 Matrigel diluted in ice cold PBS into 8 µm pore 6.5 mm diameter uncoated transwells and incubating for 30 min at 37°C. Transwells were inverted and 100 µl of $5x10^5$ cells per mL cell suspension was pipetted onto the underside of each transwell filter. Transwell plates were covered with the base of their 24 well culture plate and incubated inverted for 4 h to allow cells to adhere to the transwell membrane. Transwells were then returned to their original orientation and washed twice with 1 mL serum free medium by gently dipping into culture plate wells containing medium. Transwells were left to incubate in 1 mL serum free media containing indicated treatments. 100 µl RPMI 1640 containing 10% FBS was added to each transwell on top of the matrigel layer. Plates were incubated for 5 days at 37°C and

5% CO_2. Cells were stained in culture wells filled with 1 mL PBS containing 10 µg per mL propidium iodide for 30 min at RT in the dark. Images were collected by confocal microscopy using the inverted Ziess LSM 700 or Leica SP5 microscope. Transwells were placed onto a large coverslip covered in a small amount of PBS ensuring no bubbles were present for imaging with non-immersion 20x objective. Z-stack sections of Matrigel were captured every 10µm beginning at the transwell membrane (0 µm) through the entire 100 µl (100 µm) plug. Individual z-stack sections were quantified by Image J software using analyse-measure to determine amount of PI staining in each z-stack section. Average measure of all slices from 50-90 µm was calculated and indicates proportion of cells that invaded. The details of this new method written in chapter 3.

2.2.10 Chick Chorioallantoic Membrane (CAM) Assay

Fertilised white leghorn chicken eggs were obtained from Hi-chick Gawler, South Australia. Eggs were incubated in a MultiQuip Incubator (E2) incubator at 37.3°C and 60% humidity from day 0 to day 3 of chick embryo development with twice daily rotation and humidity maintained at 60%. On day 3 of development, the incubator temperature was reduced to 37°C and small window holes were made in the eggs, to detach the CAM from the egg shell before it begins to harden. The window holes were sealed with cellophane tape and all eggs were returned to the incubator until day 11 of chick embryo development. On day 11, the indicated number of 22Rv1, LNCaP or PC3 cells were added to Matrigel at a ratio of 1:1 cell suspension to Matrigel. 30 µl drops of cell-Matrigel mix were pipetted onto parafilm and placed at 37°C for 30-60 min to harden. One Matrigel implant was placed on each chick embryo through the pre-made window. Eggs were then re-sealed and incubated for indicated number of days. The Matrigel areas of the CAMs were cut from eggs and immediately rinsed in 1xPBS and fixed in 4% paraformaldehyde for 24 h. CAMs were transferred to 70% EtOH until processing of serial sections on paraffin embedded blocks. CAM blocks were processed through a series of washing, clearing and embedding steps which included: 70% EtOH 1hr, 95% EtOH 1 h, 1st 100% EtOH 1 h, 2nd 100% EtOH 1.5 h, 3rd 100% EtOH 1.5 h, 4th 100% EtOH 2 h, 1st clearing agent [xylene] 1 h, 2nd clearing agent [xylene] 1 h, 1st wax [paraplast X-tra] at 58°C for 1 h and 2nd wax [paraplast X-tra] at 58°C for 1 h. CAMs were embedded in molten paraffin in appropriate sized molds by slicing CAM tissue in half through the centre of the matrigel and placing cut sides down while filling blocks with molten paraffin. Cassettes were placed on top of paraffin and molds were transferred to cold plate to solidify. Paraffin

embedded CAM tissues were cut at 4 μm on a microtome and collected on Superfrost Ultra-plus slides for immunohistochemistry as described in section 2.2.6.

2.2.11 In vivo assays

In the present study, we performed two different *in vivo* metastatic assays, namely experimental metastasis assay and spontaneous metastasis assay. The specific aspects of the metastatic cascade that were investigated by the experimental metastasis assay include survival in circulation and avoiding anoikis, extravasation and colonisation at a distant site and the formation of micro- and macro-metastases. The spontaneous metastatic assay further measured the ability of cancer cells to successfully invade from the primary tumour and intravasate into circulation.

2.2.11.1 Lentiviral transduction of miR-194 overexpression

Preparation of Lentiviral Plasmid

HEK293T/17 cells were seeded [1.67x105 cells per cm^2] and incubated overnight at 37°C with 5% CO_2. A DNA mix was prepared by combining a solution containing 3 packaging plasmids (pLP1, pLP2, pVSVG) with each of the lentiviral transfer (payload) plasmids. Plasmid DNA and the transfection reagent polyethylenimine (PEI) were separately diluted into sterile 0.9% NaCl to a total of 100 μL each. The DNA mix was added to PEI solution at a ratio of 3.1 μg PEI:1 μg DNA.

The DNA:PEI solution was incubated at RT for 15 min then added to HEK cell media containing 5% FBS. Following the addition of plasmid to HEK cell culture, full viral safety precautions were followed. T75 culture flasks were seeded and incubated at 37°C and 5% CO_2 for 3 days before harvesting active viral supernatant. Viral supernatant was passed through a 0.45 μm PVDF syringe filter to remove any residual cell debris then stored in sterile screw-capped 1.5 mL tubes at -80°C.

Transduction

For transduction, luciferase-tagged PC3 and LNCaP cells were seeded at $1.25x10^7$ cells per T75 flask and left overnight at 37°C with 5% CO_2 to adhere. The next day, cells were transduced with concentrated lentivirus using a MOI of 1 and 6 μg/mL (as final concentration) Polybrene (Sigma) in normal growth media. 500 μl viral supernatant was added to each well and incubated another 72 h to allow for overexpression to occur. At

this time 0.4 μg per mL (for LNCaP-luc cells) and 0.8 μg per mL (for PC3-luc cells) of puromycin was added to 2 mL of cell line specific medium and added to each well to select for cells expressing puromycin selectable overexpression plasmid and grown a further 72 h at 37°C with 5% CO_2. Cells were lysed with 100 μl RIPA buffer and protein lysates were collected and processed for western blotting.

2.2.11.2 Experimental metastasis assay/ Tail-vein assay

In this assay, intravenous (IV) injection of tumour cells was done through the lateral tail vein in immune-compromised mice. We injected PC3 cells stably transduced to express luciferase (PC3-luciferase), allowing monitoring of tumour growth and colonization using bioluminescence imaging (BLI). BLI is based on using a sensitive cooled charge-coupled device (CCD) array to detect photons emitted from luciferase expressing cells in tissues after conversion of the luciferin substrate in a reaction. The levels of miR-194 and miR-375 were modulated in the highly migratory PC3-luciferase cell lines using lentiviral based transduction, described previously. The tumour growth was monitored by taking serial images at weekly intervals post-injection.

2.2.11.3 Spontaneous metastasis assay

In this assay stable cancer cells are injected into an orthotopic tissue (i.e. grown in the correct anatomical location). In the present study luciferase-expressing PC3 line was injected directly into the prostate of immune-compromised mice. The tumour growth was then tracked over time using BLI.

2.2.12 MicroRNA *in situ* hybridization (ISH)

MicroRNA *in situ* hybridization is a technique that allows precise localization of miRNA expression in human clinical prostate tissues. In this study, we analysed tissue samples from different stages/grades of prostate cancer.

Non-mammalian hapten digoxigenin (DIG)-labeled LNA (locked nucleic acid) ISH probes was used. The microRNAs in the tissues was de-masked using Proteinase-K, which allowed the access of double-DIG-labeled LNA probes to hybridize to the microRNA sequence. Digoxigenins then recognized by a specific anti-DIG antibody that directly conjugated with the enzyme Alkaline Phosphatase (AP) (figure 2.2)

2.2.13 Plasmid isolation

Plasmids isolation from overnight cultures was performed using the QIAprep Spin Miniprep Kit according to the manufacturer's recommendations. Briefly, 2 ml of bacterial overnight cultures was centrifuged for 3 min at 6,800x g and the bacterial pellet was resuspended in 250 µl buffer P1. Subsequently, 250 µl buffer P2 was added and the suspension was mixed by inverting the tube. To stop lysis, 350 µl buffer N3 was added and the solution was centrifuged for 10 min at 12,000x g. The supernatant was purified using a spin-column according to the manufacturer's recommendations, and DNA was eluted in 40 µl H_2O.

2.2.14 Statistical analyses

All experiments were performed at least three times. Results were statistically analyzed using GraphPad Prism 6 v0008 software. Error bars represent the standard error of the mean (SEM). Scatter plots were analyzed using student's t tests which were two-tailed and unpaired, with statistical significance accepted at $p < 0.05$. Nonlinear regression (curve fit) and Pearson product moment correlation coefficient were used for correlation analysis of miR-194 and target mRNAs.

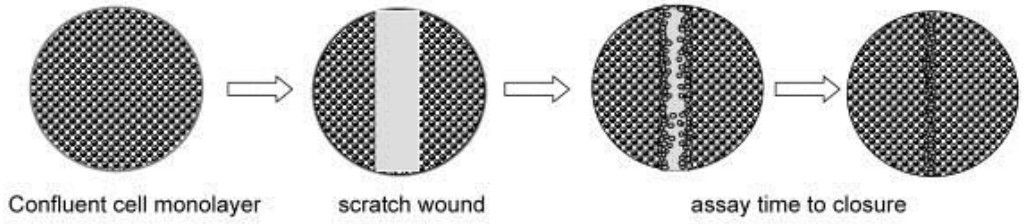

Figure 2.1: Shows a wound introduced by a scratching with pipette tips and the migratory ability of the cells at the wound edge are recorded over a period of time

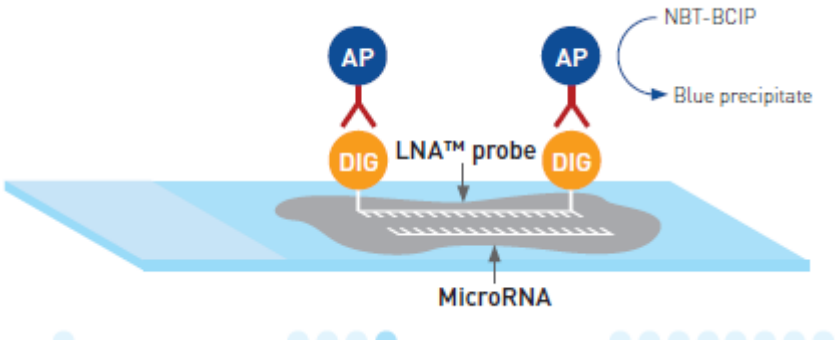

Figure 2.2: Specific anti-DIG antibody directly conjugated with the enzyme Alkaline Phosphatase (AP). AP then converts the soluble substrates 4-nitro-blue tetrazolium (NBT) and 5-bromo-4-chloro-3'-indolylphosphate (BCIP) into a water and alcohol insoluble dark-blue NBT-BCIP precipitate. [Image adapted from http://www.exiqon.com/mirna-ish-kit (accessed on 27/06/2013)]

CHAPTER 3: OPTIMISATION OF TWO METHODS FOR FUNCTIONAL AND EXPRESSION ANALYSIS OF miRNAS:
miRNA IN SITU HYBRIDIZATIO (miR-ISH) AND PROSTATE CANCER CELL INVASION ASSAYS

3.1. Introduction

3.1.1. MicroRNA in situ hybridization (miR-ISH)

Changes in specific microRNA (miRNA) expression have been shown to be associated with cancer diagnosis or outcome. In fact, it has been shown that specific miRNAs function as tumour suppressors and oncogenes in human malignancies (Bartel and Chen 2004; Esquela-Kerscher and Slack 2006; Ryan, et al. 2010). However, tissue-specific expression patterns of miRNAs in tumours remain understudied. The miRNA in situ hybridization (ISH) technology enables the determination of miRNA expression at the cellular level, and therefore addresses the question: What cell population in a tissue expresses the miRNA? A precise answer to that question is of high importance since it directs the biological interpretation for further functional studies in disease models and in molecular and cellular assays.

3.1.2. Inverse invasion assay

In pathology, invasion of carcinomas is defined as the penetration of tissue barriers, such as intrusion of tumour cells into the basement membrane and infiltration into the underlying interstitial tissues. On the other hand, invasion in experimental cell biology is defined as cell movement through a 3-dimensional (3D) matrix, which is accompanied by a restructuring of the 3D environment. In order to travel through the matrix, a cell must modify its shape and interact with the extra-cellular matrix (ECM), which on the one hand provides the cell attachment substrate and on the other represents a barrier toward the moving cell body. In cancer biology, particularly in the field of metastasis research, invasion assays are critical. Therefore, to understand the actions of miR-194 and miR-375 on prostate cancer cells, optimising an invasion assay was an important part of my PhD.

3.2. Materials and Methods

3.2.1 MiR-ISH

Tissue samples

Formalin-fixed paraffin embedded tissue samples of prostate cancer were used. The tissue blocks should not be older than a year.

LNA probes

For specific detection of miRNAs, the use of Locked Nucleic Acids (LNA), a nucleic acid analogue in which the ribose ring is locked into a C3′-endo conformation by a 2′-O, 4′-C methylene bridge, have shown great advantages in a variety of platforms, including microarray profiling (Tolstrup, et al. 2003), qPCR (Denys, et al. 2010) as well as *in situ* hybridization (Kloosterman, et al. 2006). For the studies in this thesis, double digoxigenin (DIG)-labeled miRCURY LNA microRNA detection probes (Exiqon, Denmark) were employed.

Buffers and reagents

- Proteinase-K buffer: to make 1 L of Proteinase-K buffer: add 5 ml of 1 M Tris–HCl (pH 7.4), 2 ml 0.5 M EDTA, and 0.2 ml 5 M NaCl to 900 ml Milli-Q water. Adjust volume to 1,000 ml and autoclave.
- Proteinase-K reagent: For 10 ml proteinase-K reagent with a concentration 15 µg /ml: add 7.5 ml proteinase-K stock of 20 µg /ml to 10 ml proteinase-K buffer.
- SSC buffers: to make 1 L of 5× SSC: add 250 ml 20× SSC to 750 ml Milli-Q water. To 1 L of 1× SSC: add 50 ml 20× SSC to 950 ml Milli-Q water. To make 1 L of 0.2× SSC: add 10 ml 20× SSC to 990 ml Milli-Q water. All SSC buffers should be autoclaved.
- PBS-T: to make 1 L of PBS-T: add 1 ml 0.1% Tween-20 to 1 L of PBS (pH 7.4).
- KTBT: 50 mM Tris–HCl, 150 mM NaCl, 10 mM KCl. To make 1 L of KTBT buffer: add 7.9 g Tris–HCl, 8.7 g NaCl, and 0.75 g KCl to 900 ml Milli-Q water. Adjust volume to 1000 ml. Do not adjust pH. Finally, autoclave.
- Levamisol stock: 100 mM. To prepare 100 mM stock by add 10 ml Milli-Q water to 250 mg Levamisole.

Method/steps

This method is a modified version of a published miR-ISH protocol (Jorgensen, et al. 2010):

1. Deparaffinize slides in xylene and ethanol solutions in coplin jars ending up in PBS. In parallel, prepare a water bath and SSC buffers to be heated to 55°C (the hybridization temperature).
2. Deparaffination: Place slides in Xylene for 15 min (through 2–3 times) and then hydrate through ethanol solutions at a decreasing concentrations: 99% (three times), 96% (two times), and 70% (two times) to PBS (two times). Each solution should include one 5-min incubation.
3. Apply 300 µl/slide proteinase-K reagent at 15 mg/ml directly on the slide over the tissue and incubate for 10 min at 37°C in the hybridizer.
4. Discard the proteinase-K reagent and wash twice with PBS.
5. Dehydrate slides through ethanol solutions at an increasing concentrations: 70% (two times), 96% (two times), and 99% (two times). Keep the dehydration short by one immersion. Air dry the slides on clean paper towels for approximately 15 min. In parallel, denature LNA probe at 95^0C for 4 minutes and dilute the probe in Exiqon ISH buffer. The ISH buffer should be added immediately.
6. Apply hybridization mix containing the double DIG-labeled LNA probe on each tissue section. Gently cover with cover glass. Do not seal the cover slips. Place the slides in the hybridizer and start a program hybridizing for 1 h at 55°C. The hybridization step should not exceed 2 h.
7. Carefully detach cover glass and place the slides into 5× SSC at room temperature (RT). Place slides in a staining rack.
8. The stringent washing steps are performed by placing the staining racks with slides in jars containing 5× SSC (1 × 5 min), 1× SSC (2 × 5 min), and 0.2× SSC (2 × 5 min) at the hybridization temperature (55°C) and 0.2× SSC (1 × 5 min) at RT.
9. Transfer slides to PBS-T.
10. Incubate with 200 µl blocking solution for 15 min at RT. Blocking solution: Prepare blocking solution. For 1600 µl blocking reagent, add 32 µl sheep serum (final concentration 2%).

11. Apply sheep anti-DIG-AP at 1:800 diluted in blocking solution containing 2% sheep serum and incubate for 60 min at RT (two times for 30 min). Preparation of anti-DIG reagent: for example, for 1600 µl anti-DIG reagent with a dilution of 1:800: add 2 µl sheep-anti-DIG AP conjugated to 1600 µl blocking solution
12. Wash each slide with 300 µl PBS-T two times for at least 3 min.
13. Incubate freshly prepared NBT/BCIP substrate reagent containing 0.2 mM Levamisole and incubate 300 µl for 2 h at 30°C in the incubation racks. Protect from light during development. For 10 ml AP substrate: In 10 ml Milli-Q water, add one NBT–BCIP tablet (Roche) and add 20 µl Levamisol stock to a final concentration of 0.2 mM. Keep protected from light.
14. Incubate slides with 300 µl KTBT buffer two times for 5 min.
15. Wash with Milli-Q water two times for 1 min.
16. Counter stain with Nuclear Fast Red for 1 min: 200–300 µl per slide. This is an optional step. This step is not recommended to determine miRNA that have a very low expression level. However, must be used for U6 slides.
17. Rinse the slides in tap water for 10 min.
18. Dehydrate with ethanol solutions through ethanol solutions at an increasing concentration: 70% (two times), 96% (two times), and 99% (two times). Keep the dehydration short by one immersion at a time for 1-min.
19. Mount slides directly with appropriate mounting medium. Avoid air drying sections at this step.
20. Allow overnight settlement of the precipitate and analyse results by light microscopy the subsequent day.

3.2.2. Invasion assay

Method/steps

This method is a modified version of that devised in Prof Laura Machesky's laboratory at the Beatson Institute, UK (Yu and Machesky 2012). Figures 3.1 and 3.2 show the schematic of the steps.

1. Thaw an aliquot of Matrigel slowly on ice (keep the aliquot in fridge overnight).
2. Dilute 1:1 in ice cold PBS.
3. Pipette carefully 100 µl of this into each Transwell
4. Incubate for at least 30 mins at 37^{o}C to allow the Matrigel to set.
5. During this time, prepare cell suspensions in their respective growth medium.
6. When Matrigel is set, invert the Transwells.
7. Pipette 100 µl of the cell suspension (of your desired concentration) onto the underside of the filter (which is now uppermost).
8. Cover the Transwells carefully with the base of the 24 well tissue culture plate in such a way that it contacts the droplet of cell suspension.
9. Incubate the plate (inverted), for 4 hours.
10. Turned the plate right-side-up.
11. Dip each transwell sequentially into 3 x 1 ml serum free medium to wash. Leave the Transwell in wash 3 as this serves as the well in which the assay will be incubated.
12. Pipette 100 µl of media containing FBS (which will act as chemoattractant) gently into the Transwell on top of the Matrigel/PBS.
13. Replace lid and incubate the plate at 37^{o}C for 4-5 days.

Fixation and staining inverse invasion assays

Propidium iodine staining:

1. Pipette 1 ml of methanol into each well of a 24 wells plate.
2. Place at the plate -20^{o}C for 1 hour.
3. Transfer the Transwells into the cold methanol and keep them for 20 mins.
4. Transfer directly to wells containing 1 ml propidium iodide at 10 μg/ml in PBS.
5. Incubate the Transwells for 20 mins.
6. Wash each Transwell 3 times, by placing sequentially into wells containing 1 ml PBS for 5 mins per well.

Finally, proceed to perform confocal analysis. Assays can be kept at 4^{o}C for up to 1 day prior to confocal microscopy.

3.3. Results

3.3.1. MiR-ISH

Results of miR-ISH assays are shown in chapter 4. In short, we examined the expression of miR-194 at a cellular level in a panel of primary prostate tumours. MiR-194 was primarily expressed in prostate epithelial cells, with minimal staining evident in stroma. Prostate glands with more normal architecture tended to have weaker staining, whereas higher grade foci generally exhibited stronger staining.

3.3.2. Inverse Invasion assay

Results of prostate cancer invasion assays are shown in chapter 4 and 5. Briefly, I carried out this assay on a range of prostate cancer cell lines and examined their invasive capability following modulation of miR-194 and miR-375 levels. MiR-194 was found to significantly promote invasion, whereas miR-375 inhibited invasion of prostate cancer cells. Figure 3.3 shows optical sections acquired by using confocal microscope at 10 um intervals showing invasion of cells (stained with propidium iodide) through Matrigel. Figure 3.4 shows a comparison between different prostate cancer cell lines following transient transfection of negative control mimics.

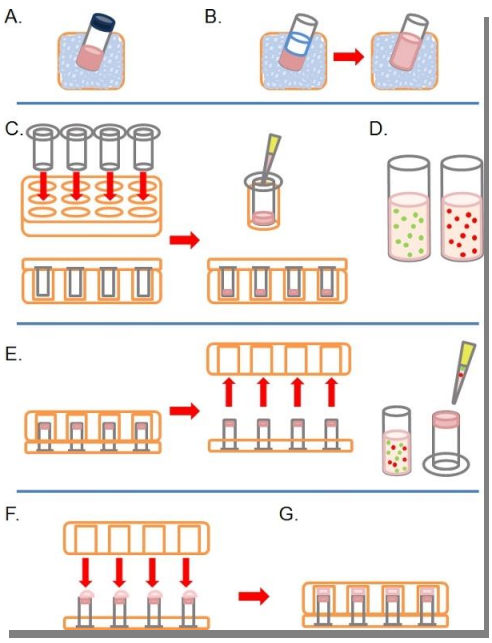

Figure 3.1: Schematic of steps involved in setting up inverse invasion assay. A) Matrigel ECM thawed on ice. B) Matrigel is diluted 1:1 with. C) Transwell inserts are placed into multiwell plates, and Matrigel pipetted into each insert. D) Cell suspensions made at desired concentration. E) Once the Matrigel has set, the plate is inverted and removed, cells are plated onto the underside filter of the Transwell inserts. F) In the inverted position, the multiwell plate is carefully placed over Transwell inserts, making contact with the cell suspension. G) Cells are allowed to adhere to the filter for 4 hours. (figure adapted from (Scott, et al. 2011))

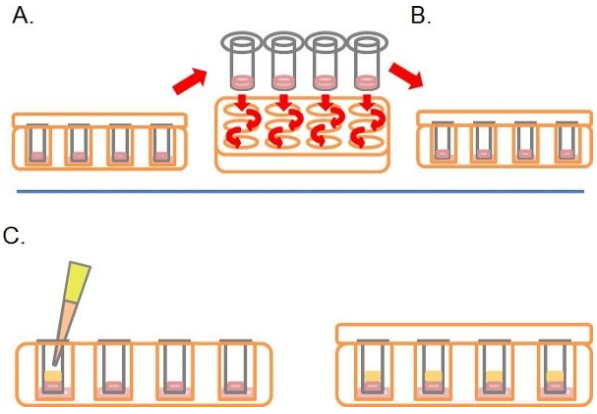

Figure 3.2: Continuation of the schematic diagram for the inverse invasion assay. A) Once cells have adhered, dip each Transwell into serum-free media twice to remove loose cells. B) Place washed Transwell into a final well containing media plus treatments as required. C) Media containing chemoattractant (e.g. 10% fetal bovine serum) as required is carefully layered onto Matrigel. (figure adapted from (Scott et al. 2011))

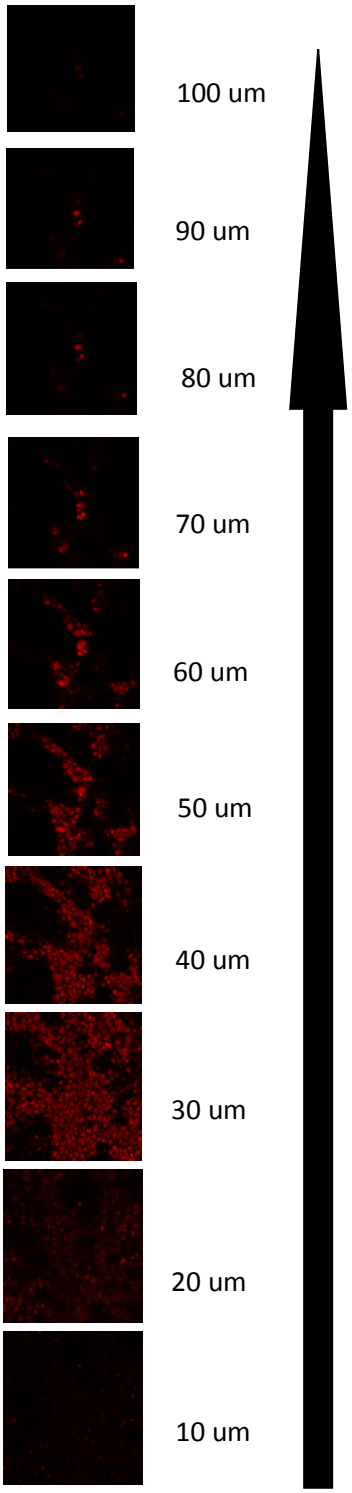

Fig. 3.3: Optical sections at 10 um intervals showing invasion through Matrigel

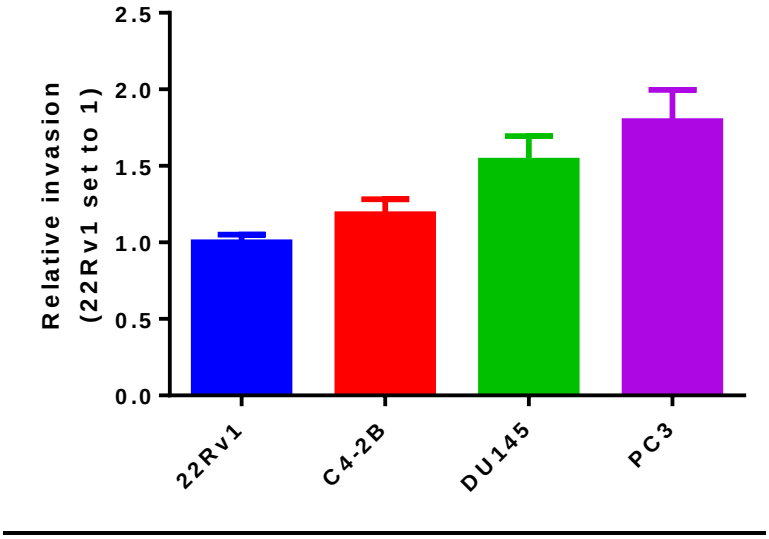

Fig. 3.4: Comparisons between different prostate cancer cells following transient transfection with negative control mimics

3.4. Discussion

3.4.1. MiR-ISH

Implementation of miRNA-ISH in a molecular biology laboratory is challenging, and the reason for frequent failure in setting up RNA-ISH technology cannot be attributed to a single process or reagent, but rather a combination of technical prerequisites. First and foremost, miRNA-ISH is designed to detect RNA, which is highly labile: thus, the laboratory should have an RNAse-free workspace and execution of all the steps must be followed in a strict RNAse-free set-up. Second, the ISH protocol contains many hands-on steps involving a variety of reagents and buffers. Each step has a risk of failure, and tissue sections can be fragile: therefore, every step should be carried out with extreme delicate attention. Finally, the miR-ISH protocol includes a number of critical steps, some of which need optimization related to the type of tissue and the detection probe used. Indeed, in the process of optimizing the miRNA-ISH technique during my PhD, I faced several challenges. More specifically, these challenges were related to the demasking and hybridization steps.

The demasking step, also known as the pre-digestion step, is based on the use of relatively non-specific tissue components like proteases (Proteinase-K). This step provides access to the miRNAs in the tissue matrix. The optimal proteinase K concentration varies, depending on the tissue type, length of fixation and size of tissue. The recommended concentration as per the manufacturer's protocol is 20 µg/ml. However, on my preliminary attempts to carry out the miRNA-ISH protocol with the above mentioned concentration, I did not get a desirable outcome. I was not able to appreciate the miRNA staining properly as I encountered an abnormal degradation of the tissues. Therefore, I decided to try a range of Proteinase-K levels, starting from as low as 5 µg/ml to 30 µg/ml. Finally, after several trials and errors, satisfactory images were obtained at a concentration of 15 µg/ml.

Similarly, the probe hybridization step is also very critical. Other than the requirement of a well-defined and stable hybridization buffer, a stable hybridization temperature and optimal probe concentration are essential. The manufacturer's protocol recommends a range of hybridization temperature (from 50^{o}C to 70^{o}C) and probe concentrations (from 1 nM to 40 nM). Similar to Proteinase-K, I tested a range of hybridization temperatures, (50^{o}C to 70^{o}C, 5^{o}C intervals) and probe concentrations (5 nM to 100 nM). The optimal

probe concentration was found to be 60 nM, concentrations below this provide a misleading faint stain. On the other hand, the optimal hybridization temperature was found to be 55^{o}C. The benefit of using hybridization temperate at 55^{o}C was twofold: a) even though the temperature is quite high for a tissue section to sustain, the glandular architecture of the prostate tissue section was well appreciated. A temperature below 55^{o}C doesn't allow the probes to hybridize properly leading to no staining at all, while a temperature above 55^{o}C distorts the cellular architecture. b) Another benefit of the hybridization temperature being set at 55^{o}C was inactivation of residual Proteinase-K from the previous step. Although the sections treated with Proteinase-K were washed with PBS prior to the hybridization step, there tended to be some carry over. Interestingly, Proteinase-K is known to be inactive at 55^{o}C or higher.

The fundamental requirement of miR-ISH is to execute the entire protocol in a strict RNase-free setup. Apart from this and the points addressed above, once the tissue sections are cut with the microtome at 5 – 6 µm thickness, leave them at 4^{o}C at least for a day and melt the paraffin on a hot-plate at 60°C for not more than 45 minutes on the same day of the ISH experiment.

3.4.2. Inverse invasion assay

Despite the availability of different assays to measure the invasive capability of cancer cells, a common problem encountered in performing invasion assay is due to different modes of cell motility. This is particularly important when a range of cancer cell lines are tested. Currently, the modes of cell motility are broadly divided into three types: a) amoeboid movement, which is characterized by cells moving as rounded, ellipsoid bodies without the involvement of focal adhesions and cell attachment (Charras and Paluch 2008; Fackler and Grosse 2008); b) mesenchymal migration, which involves strong focal attachment to the extracellular matrix, cytoskeletal contractility and elongated spindle-like cell bodies (Grinnell 2003); c) collective migration, which is characterized by the movement of a cellular cohort through the ECM with the preservation of functional cell–cell junctions (Gerharz, et al. 2007). For the studies in this thesis, mesenchymal and collective modes of motility were of particular importance. We wanted an assay which provides a 3D image and mimics the tumour microenvironment. We therefore, decided for the inverse invasion assay designed, tested and formulated by Prof Laura Machesky at the Beatson Institute, UK (Yu and Machesky 2012) and optimised the protocol for prostate cancer cell lines. Apart from the steps mentioned above in the method section, two critical

steps were to allow the invasion of prostate cancer cells to take place for at least 3 days and to perform the confocal microscopy within 24 hours after the cells were fixed and stained with propidium iodide.

CHAPTER 4: ROLE OF microRNA-194 IN PROSTATE CANCER METASTASIS

"GATA2-regulated miR-194 targets Suppressor of Cytokine Signaling 2 to promote prostate cancer metastasis"

The following chapter includes a manuscript submitted for publication to the Journal of Clinical Investigations, followed by supplementary figures and tables that make up a large portion of the work completed as a part of this PhD. A general discussion of this chapter had been included at the end.

Statement of Authorship

Title of Paper	GATA2-regulated miR-194 targets Suppressor of Cytokine Signaling 2 to promote prostate cancer metastasis
Publication Status	☐ Published ☐ Accepted for Publication ☑ Submitted for Publication ☐ Unpublished and Unsubmitted w ork w ritten in manuscript style
Publication Details	Journal of Clinical Investigation

Principal Author

Name of Principal Author (Candidate)	Rajdeep Das		
Contribution to the Paper	Carried out all experiments (cell line culture and transfection, cellular migration and invasion assays, western blots, in situ hybridization, RT-qPCR, immunofluorescence, *in vivo* assays), co-designed the study (with Dr Selth) and drafted the manuscript.		
Certification:	This paper reports on the original research that I conducted during the period of my Higher Degree by Research candidature and is not subject to any obligations or contractual agreements with a third party that would constrain its inclusion in this thesis. I am the primary author of this paper.		
Overall percentage (%)	60%		
Signature		Date	27/07/2016

Co-Author Contributions

By signing the Statement of Authorship, each author certifies that:

i. the candidate's stated contribution to the publication is accurate (as detailed above);

ii. permission is granted for the candidate in include the publication in the thesis; and

iii. the sum of all co-author contributions is equal to 100% less the candidate's stated contribution.

Name of Co-Author	Philip A. Gregory		
Contribution to the Paper	PhD project supervision; analyzed data and evaluated/edited manuscript		
Signature		Date	27/07/2016

Name of Co-Author	Rayzel Fernandes		
Contribution to the Paper	Assisted in determining the mRNA level of SOCS2 and miR-194 in patient samples and data analysis		
Signature		Date	27/07/16

Name of Co-Author	Iza Denis		
Contribution to the Paper	Assisted in whole-body imaging to monitor luciferase-expressing cells in mice		
Signature		Date	27/07/2016

Name of Co-Author	Qingqing Wang		
Contribution to the Paper	Assisted in measuring miR-194 in serum		
Signature		Date	2/8/2016.

Name of Co-Author	Scott L. Townley		
Contribution to the Paper	Assisted in RT-qPCR, Western blots and ChIP-qPCR		
Signature		Date	28/7/16

Name of Co-Author	Shuang Zhao		
Contribution to the Paper	Analysed the multi-institutional cohort data		
Signature		Date	8/8/16

Name of Co-Author	Adrienne R. Hanson		
Contribution to the Paper	Assisted in generating stable miR-194 overexpressing cell lines		
Signature		Date	27-7-16

Name of Co-Author	Marie A. Pickering		
Contribution to the Paper	Assisted in cutting formalin fixed paraffin embedded human tissue sections		
Signature		Date	27/7/16

Name of Co-Author	Heather K. Armstrong		
Contribution to the Paper	Assisted in chick chorioallantoic membrane assays		
Signature		Date	27/07/2016

Name of Co-Author	Noor A. Lokman		
Contribution to the Paper	Assisted in chick chorioallantoic membrane assays		
Signature		Date	27/07/2016

Name of Co-Author	Kim N. Chi		
Contribution to the Paper	Provided the human serum samples to determine the level of miR-194		
Signature		Date	27-JULY-2016

Name of Co-Author	Hayley S. Ramshaw		
Contribution to the Paper	Assisted with the intravenous *in vivo* assays		
Signature		Date	27/07/2016

Name of Co-Author	Elizabeth D. Williams		
Contribution to the Paper	Assisted with the intra-prostatic *in vivo* assays and evaluated/edited manuscript		
Signature		Date	10/8/2016

Name of Co-Author	Amina Zoubeidi		
Contribution to the Paper	Analyzed data and evaluated/edited manuscript		
Signature		Date	August 3rd, 2016

Name of Co-Author	Gregory J. Goodall		
Contribution to the Paper	Analyzed data and evaluated/edited manuscript		
Signature		Date	27/7/2016

Name of Co-Author	Felix Y. Feng		
Contribution to the Paper	Provided the multi-institutional cohort and helped in manuscript evaluation		
Signature		Date	July 27, 2016

Name of Co-Author	Lisa M Butler		
Contribution to the Paper	PhD project supervision; analyzed data and evaluated/edited manuscript		
Signature		Date	27/7/2016

Name of Co-Author	Wayne D Tilley		
Contribution to the Paper	PhD project supervision; analyzed data; and evaluated/edited manuscript		
Signature		Date	27/07/2016

Name of Co-Author	Luke A Selth		
Contribution to the Paper	PhD project supervision; conceived the project; helped to design the experiments, analyse data, make the figures; and co-wrote the manuscript		
Signature		Date	27/07/2016

My role in this study

I carried out all the experiments (cell line culture and transfection, cellular migration and invasion assays, western blots, in situ hybridization, RT-qPCR, immunofluorescence, *in vivo* assays), co-designed the study with my supervisors and drafted the manuscript.

Abstract

Dysregulated expression of microRNAs (miRNAs, miRs) is a hallmark of cancer. MiR-194 is elevated in prostate tumors compared to non-malignant tissues and its levels in serum are predictive of post-surgery disease recurrence, but its role in this disease is poorly understood. Here, we demonstrated that miR-194 promotes metastasis of prostate cancer. Serum levels of miR-194 are higher in men with metastatic versus localized disease, and tissue levels of miR-194 are associated with disease recurrence post-surgery and tumor aggressiveness. Over-expression of miR-194 in prostate cancer cell lines promoted migration, invasion and epithelial-mesenchymal transition *in vitro* and metastasis of xenografts *in vivo*. The ubiquitin ligase Suppressor of Cytokine Signaling 2 (SOCS2) was found to be a direct target of miR-194 in prostate cancer and a mediator of its pro-metastatic functions. Low levels of SOCS2 were strongly associated with disease recurrence and metastasis in patients, and its down-regulation augmented metastatic phenotypes. By targeting SOCS2, miR-194 de-repressed key oncogenic kinases including FLT3 and JAK2, leading to enhanced ERK and STAT3 signalling. GATA2 was found to be an upstream transcriptional regulator of miR-194 *in vitro*, a finding validated by the strong concordance between GATA2 activity and miR-194 levels in patient cohorts. Collectively, our study has elucidated a novel pro-metastatic pathway in prostate cancer with miR-194 at the nexus, providing further impetus for exploring the potential of this miRNA as a biomarker and therapeutic target.

Introduction

Prostate cancer (PCa) is the most common non-skin cancer of men and causes >300,000 deaths worldwide annually (1, 2). The predominant cause of mortality from PCa is metastasis (3, 4), which can be present at the time of diagnosis or develop after failure of primary treatment (surgery and/or radiation therapy). Therefore, both the identification of markers that accurately predict or demarcate metastatic disease at an early stage, as well as the development of strategies that effectively inhibit metastasis, would have a significant impact on patient outcomes. Both of these goals have been hindered by an imprecise understanding of the mechanisms governing dissemination of tumor cells from the prostate (5).

Metastasis of carcinomas (epithelial-derived cancers) encompasses a complex series of events whereby epithelial tumor cells invade the surrounding stroma, enter blood or lymphatic circulation, arrest at distant anatomic sites, exit the vasculature, and colonize a secondary location through metastatic outgrowth (6). Given the intricacy of the metastatic cascade, it is not surprising that many regulators of metastasis have been identified, often acting in a context-dependent manner. One such class of metastatic regulatory factors are microRNAs (miRNAs; miRs), small, non-coding RNA molecules of 21-23nt that regulate gene expression in a sequence-specific manner at both post-transcriptional and epigenetic levels (7). Aberrant miRNA expression is a common feature of many cancers, including prostate cancer (8-13), and this dysregulation can both promote and inhibit metastasis (14).

In a recent study, we identified miRNAs in the circulation that were predictive of disease recurrence following surgery for primary prostate cancer (15). The expression of one of the putative biomarkers identified in this earlier work, miR-194, was elevated in metastatic tissues, leading us to speculate that it could be a driver of prostate cancer progression. Herein, we demonstrate that miR-194 promotes prostate cancer metastasis. Mechanistically, miR-194 targets Suppressor of Cytokine Signaling 2 (SOCS2), resulting in upregulation of oncogenic and pro-metastatic STAT3 and ERK signaling pathways. Moreover, we show that miR-194 is regulated at a transcriptional level by the pro-metastatic transcription factor GATA2. Collectively, these findings elucidate a new and complete pathway driving prostate cancer metastasis.

Results

MiR-194 is a circulating marker of metastasis and a tissue marker of disease aggressiveness

In a previous study (15), we found that high levels of miR-194 in patient serum was prognostic for biochemical recurrence following radical prostatectomy. To determine whether this reflected an association between miR-194 and metastatic disease, we measured miR-194 in an independent set of serum samples obtained from patients with localized (n = 21) and metastatic (n = 18; primarily bone metastases) prostate cancer. MiR-194 levels were significantly higher in the serum of men with metastatic castration-resistant prostate cancer compared to men with localized disease (Figure 1A).

Our previous work (15) had also revealed that tumor levels of miR-194 were associated with poor outcomes, including metastasis, in two distinct cohorts from Memorial Sloan-Kettering Cancer Center (MSKCC) (16) and Erasmus Medical Center (17). To verify this finding, a larger patient dataset from The Cancer Genome Atlas (TCGA; (18)) was examined. In this cohort, miR-194 was higher in the tumors of men who subsequently experienced a new tumor event (Figure 1B) and biochemical recurrence (Figure 1C), supporting our earlier findings. Moreover, in both the TCGA and MSKCC cohorts, miR-194 expression was elevated in higher Gleason score tumors (Figure 1D).

To complement these *in silico* analyses, we undertook *in situ* hybridization (ISH) to examine miR-194 expression at a cellular level in a panel (n = 23) of primary prostate tumors. Validating the findings from the published cohorts, quantitation of staining revealed that miR-194 positivity was associated with Gleason grade (Figure 1E). MiR-194 was primarily expressed in prostate epithelial cells, with minimal staining evident in stroma (Figure 1F). Representative examples demonstrate that glands with more normal architecture tended to have weaker staining (Figure 1F, red arrows) whereas higher grade foci generally exhibited stronger staining (Figure 1F, black arrows). Collectively, these analyses of miR-194 in patient serum and tumors reveal that it is a candidate marker of disease aggressiveness, recurrence and metastasis.

MiR-194 enhances metastatic features of prostate cancer cells

Given the association between miR-194 and tumor aggressiveness, we hypothesized that it may directly enhance pro-metastatic phenotypes. To test this concept, we modulated miR-194 activity in prostate cancer cell lines by over-expression (transfection of miRNA mimics) or inhibition (transfection of LNA miRNA inhibitors) and assessed cell migration, invasion and growth. Over-expression of miR-194 caused PC3, DU145 and 22Rv1 cells to become more migratory and invasive in nature (Figures 2A-B). Conversely, suppression of endogenous miR-194 activity with an LNA inhibitor suppressed cell invasion (Figure 2C). Interestingly, concomitant with enhancing motility and invasiveness, exogenous miR-194 attenuated cancer cell growth in all models tested (Supplementary Figure 1). Epithelial-mesenchymal transition (EMT) is a fundamental aspect of morphogenesis and wound healing during which sessile epithelial cells lose cell adhesion and convert to migratory and invasive mesenchymal cells. Cancer cells can hijack this process to enable migration and invasion of tumor cells into the surrounding stroma and entry/exit from the bloodstream (19). To test whether the pro-migratory and pro-invasive activities of miR-194-were associated with EMT, expression of epithelial (E-cadherin (E-cad) and Zona occludens-1 (ZO-1)) and mesenchymal (N-cadherin (N-cad)) markers were examined by Western blotting. In both PC3 and 22Rv1 cells, delivery of miR-194 mimic resulted in changes reminiscent of EMT, namely loss of E-cad/ZO-1 and gain of N-cad/Fn (Figure 2D). Moreover, the cells lost cohesion and gained a more elongated, mesenchymal-like morphology (Figure 2E and Supplementary Figure 2). Immunofluorescence analysis validated the loss of E-cad, and staining for F-actin revealed cytoskeletal rearrangement characteristic of EMT (Figure 2E).

MiR-194 promotes prostate cancer invasion and metastasis **in vivo**

Our *in vitro* experiments indicated that miR-194 could enhance pro-metastatic features of tumor cells. We further investigated this notion using *in vivo* models of tumour invasion and metastasis. First, the pro-invasive activity of miR-194 was examined in an *ex ovo* chick chorioallantoic membrane (CAM) assays (20). Invasion of PC3 and LNCaP cells through the ectoderm into the mesoderm of the CAM was assessed after 3 days of implantation of the cancer cells and matrigel grafts on day 14 of chick embryo development by pan-cytokeratin immunohistochemistry. Following transfection of negative control LNA, both cell types invaded through the ectoderm into the mesoderm layer of the CAM, although PC3 was more aggressive (Figures 3A, 3B). Importantly,

transfection of cells with miR-194 LNA inhibitor greatly reduced the invasive capacity of both cell lines (Figures 3A, 3B). To determine if over-expression of miR-194 could enhance prostate cancer cell invasion through CAMs, we generated luciferase-tagged PC3 and LNCaP cells over-expressing miR-194, termed PC3-194 and LNCaP-194, by lentiviral transduction. These cells exhibited significantly augmented invasive capacity compared to controls (Supplementary Figure 3). Collectively, these data demonstrate a potent pro-invasive role for miR-194 in prostate cancer. Having verified the ability of miR-194 to augment prostate cancer cell invasion, we next turned to experimental metastasis assays in immunocompromised mice. The luciferase-tagged PC3-194 and control (PC3-NC) cells were injected into the tail veins of NOD/SCID mice, which were then assessed by weekly whole-animal bioluminescence imaging. In this assay, over-expression of miR-194 enhanced both the speed and extent of metastatic colonization (Figure 3C).

Tail vein assays evaluate tumor cell extravasation and metastatic colonization. To determine how over-expression of miR-194 influences spontaneous metastasis, we employed an orthotopic assay in which cells were injected directly into the prostate (i.e. intra-prostatic xenografts). Weekly monitoring of the mice revealed that tumor incidence was 77.8% for PC3-NC and 90% for PC3-194 cells, and PC3-194 tumors grew more rapidly (Figure 3D). *Ex vivo* imaging of tissues following intra-prostatic tumor growth revealed that, in 6/9 mice, PC3-194 cells spread to major visceral organs such as kidneys, lungs, livers and spleens (Figure 3E). By contrast, PC3-NC cells remained contained within the prostate in all mice (Figure 3E). The longevity of the mice post-injection further highlighted the aggressiveness of the PC3-194 cells in the orthotopic assay (Figure 3F).

SOCS2 is a clinically relevant target of miR-194

To elucidate the mechanism(s) by which miR-194 exerts its pro-metastatic effects, we identified candidate gene targets by intersecting outputs from three distinct prediction algorithms, TargetScan (21), miRanda (22) and PicTar (23) (Supplementary Figure 4). From the resultant list of 69 genes, we focused on factors that are down-regulated in prostate cancer metastases. One such gene, *Suppressor of Cytokine Signaling 2* (*SOCS2*), has a well-conserved miR-194 target site in its 3'UTR (Figure 4A). Importantly, in two distinct clinical cohorts, expression of *SOCS2* was decreased in metastatic samples (Figure 4B), as would be expected for a biologically relevant miR-194 target. Moreover, low *SOCS2* expression was associated with biochemical recurrence and metastasis in multiple

datasets: MSKCC, a large pooled multi-institutional cohort with long-term outcome data (24-29) and TCGA (Figure 4C and Supplementary Figure 5). The robust association between reduced levels of *SOCS2* and subsequent development of metastatic disease in the large multi-institutional cohort was particularly compelling in light of miR-194's pro-metastatic activity.

To validate SOCS2 as a miR-194 target, we examined its expression in response to ectopic delivery of miR-194. SOCS2 protein was decreased by transfection of miR-194 mimic and increased by miR-194 inhibition (Figures 4D-E). *SOCS2* mRNA was decreased by exogenous miR-194 (Supplementary Figure 6) but not to the same extent as SOCS2 protein, suggesting that targeting is comprised of both translational repression and transcript degradation. Down-regulation of SOCS2 by miR-194 was due to a direct miRNA:mRNA interaction, since miR-194 inhibited the expression of a luciferase reporter gene fused to a fragment of the *SOCS2* 3'UTR containing the target site (Figure 4F). Finally, confirming the potential for miR-194 targeting of SOCS2 *in vivo*, there was a negative relationship between the expression of these factors in an "in-house" cohort comprised of 44 tumor samples (Figure 4G).

Next, we assessed the relevance of SOCS2 in processes associated with miR-194-driven metastasis. Knockdown of SOCS2 (Figure 5A) recapitulated miR-194 over-expression in all phenotypes tested: specifically, down-regulation of SOCS2 reduced growth (Supplementary Figure 7) but enhanced migration (Figure 5B) and invasion (Figure 5C). To demonstrate dependence of miR-194 on SOCS2 to mediate its pro-invasive ability, we enforced expression of the *SOCS2* ORF without its 3'UTR in PC3 cells (Figure 5D). In this rescue assay, co-transfection of the *SOCS2* ORF over-expression construct (SOCS2-OE) with miR-194 significantly reversed miR-194-mediated invasion (Figure 5E). This data demonstrates that SOCS2 is a key target through which miR-194 signals to promote metastatic phenotypes in prostate cancer cells.

MiR-194-mediated suppression of SOCS2 activates STAT3 and ERK signalling pathways

SOCS2 is a member of the SOCS family of ubiquitin E3 ligases, which have pleiotropic roles in normal physiology of the immune and central nervous systems as well as in the pathophysiology of various cancers (30). In the immune system, these functions are at least partly mediated by the ability of SOCS2 to target key tyrosine kinases, such as Janus Kinase 2 (JAK2) and Fms-like tyrosine kinase 3 (FLT3), for degradation by the ubiquitin-proteasome system (30-32). Thus, we speculated that enhanced activity of JAK2- and FLT3-regulated pathways in response to loss of SOCS2 might be a mechanism by which miR-194 promotes metastasis. Indeed, total levels of both JAK2 and FLT3 were elevated in response to miR-194 over-expression and specific SOCS2 knockdown in PCa cells (Figure 6A). Moreover, miR-194 and siSOCS2 both enhanced the phosphorylation of ERK and STAT3, key downstream mediators of JAK and FLT3 signaling (Figure 6B). Activation of ERK and STAT3 pathways by miR-194 was further confirmed by measuring the expression of pro-metastatic downstream effector genes, including *BCL2*, *BIRC5*, *BRF1*, *CDC25A*, *ELK1*, *ELK4*, *FSCN2* and *MYC* (Figure 6C). All of these genes, except *BCL2*, were also positively correlated with miR-194 in clinical samples (Figure 6D and Supplementary Figure 8), suggesting that miR-194-mediated enhancement of ERK and STAT3 pathways is physiologically relevant.

If ERK and STAT3 signalling pathways are important mediators of miR-194's pro-metastatic activity, pharmacological inhibition of these pathways should reverse miR-194-driven phenotypes. To test this hypothesis, we transfected cells 22Rv1 with miR-194 in the presence and absence of an ERK1/2 inhibitor (SCH772984) or a pan-JAK inhibitor (JAK1 Inhibitor I) and measured invasion. In the presence of these drugs, the pro-invasive activity of miR-194 was completely blocked (Figure 6E).

GATA2 is an upstream regulator of miR-194

Having established key downstream mediators of miR-194 activity, we wished to identify upstream regulators that may be responsible for over-expression of this miRNA in prostate cancer. Initially, we searched for genes that were expressed concordantly with miR-194 in prostate tumors. *GATA2* was one of the most highly positively correlated genes in the TCGA cohort (Figure 7A). GATA2 is a transcription factor that plays multiple, key roles in prostate cancer growth and metastasis by modulating the AR and IGF2 signaling

pathways (33-35). Importantly, miR-194 levels were also closely associated with GATA2 activity in primary prostate tumors, as revealed by gene set enrichment analysis (GSEA) (Figure 7B).

Supporting the clinical association, knockdown of GATA2 by siRNA caused a significant reduction in miR-194 expression (Figure 7C). Interestingly, analysis of ENCODE ChIP-seq data revealed the presence of GATA2 binding sites within a few kilobases of both miR-194-encoding loci (*MIR194-1* on chromosome 1 and *MIR194-2* on chromosome 11) in the lymphoblast K562 cell line (Figure 7D). Collectively, these data indicate that GATA2 is an upstream regulator of miR-194 in prostate cancer.

Discussion

A better understanding of the mechanisms underpinning prostate cancer metastasis is vital to improve patient management and treatment. In this study, we have provided new insight into this process by identifying a new pathway influencing this process. More specifically, by targeting SOCS2, miR-194 co-ordinately stimulates multiple pro-metastatic effectors downstream of JAK2/STAT3 and FLT3/ERK. These novel mechanistic findings likely underlie the observation that miR-194 is elevated in the serum of men with metastatic disease (this study) or, as we previously showed, experience more rapid relapse following surgery (15). A model summarizing these concepts is shown in Figure 8.

Providing new insight into miR-194 in cancer is an important outcome of this study because its precise functions have been difficult to resolve, with reports of both tumour suppressive and oncogenic activity. For example, in models of gastric, colorectal, liver, kidney, breast and endometrial cancers, miR-194 has variably been shown to suppress tumor growth, invasion and metastasis, acting at least partly by driving epithelial differentiation and inhibiting EMT (36-48). By contrast, other groups have demonstrated that miR-194 can promote invasion and metastasis of pancreatic and endometrial cancer cells (49, 50) and colorectal cancer angiogenesis and growth (51), and that its expression is elevated in and during progression of oesophageal adenocarcinoma (52-55). Moreover, an elegant study using laser-captured tissues demonstrated that high expression of miR-194 at the invasive front of liver cancers was a prognostic indicator of poor recurrence-free and overall survival in colorectal liver metastases (56). Our demonstration that miR-194 promotes invasion, migration, EMT and metastasis are consistent with these latter findings. During the preparation of this manuscript, Zhang and colleagues published a

study was in which miR-194 was shown to target BMP-1 in PC3 cells, leading to decreased expression of matrix metalloproteinases 2 and 9 and subsequent suppression of invasion (57). We cannot currently explain the inconsistency between this earlier study and our current work. One explanation could simply be the known inter-laboratory heterogeneity of cancer cell lines, which can lead to variable results. In our studies, to ensure that our findings were not predicated on a single model and thus are likely to be robust, we utilized multiple cell line models and *in vivo* assays. Further research on miR-194 in prostate cancer, including identification of its complete "targetome", will undoubtedly unravel its precise role and resolve this apparent discrepancy.

The dichotomy of miR-194 action, acting as an oncomiR in some contexts and a tumor suppressor in others, is not unusual in miRNA biology. This phenomenon is underpinned by the fact that miRNA function in a particular cell or tissue is contingent on the expression of relevant gene targets in that environment. Thus, the context-dependent roles of miR-194 can be attributed to its many cancer-relevant targets, including the EMT factor N-cadherin (44, 46), the Wnt pathway receptor frizzled-6 (58), IGF1R (44), the transforming growth factor (TGF)-β pathway member activin receptor type 2B (ACVR2B) (59), the cytoskeletal protein talin2 (39), the SCF E3 ubiquitin ligase component RING box protein1 (RBX1) (37), MAP4K4 (42), the EMT-promoting transcription factor Bmi-1 (60), and the oncogenic transcription factor YAP1 (61). Here, we expand upon miR-194's target repertoire by identifying SOCS2, which we believe represents a particularly critical mediator of miR-194 action in prostate cancer. SOCS2 is a substrate-recruiting component of E3-ubiquitin ligase complexes, and its targets include factors highly relevant in pathologies such as JAK2, FLT3, IGF and growth hormone (30). By promoting degradation of these factors via the ubiquitin-proteasome pathway, SOCS2 simultaneously constrains multiple key pro-metastatic cellular pathways. Like miR-194, the function of SOCS2 in cancer is apparently complex, with reports of both oncogenic and tumor-suppressive activities (30). The same is true in prostate cancer, with recent reports producing conflicting data in relation to the function of SOCS2 (62, 63): while one study found SOCS2 to exert growth-promoting effects in prostate cancer (62), others demonstrated that SOCS2 inhibits tumor growth *in vitro* and *in vivo* and is a negative prognostic indicator post-surgery (63, 64). Our study at least partially resolves these conflicting findings by identifying a dual role for SOCS2 in prostate cancer: it is required for normal prostate cancer cell growth but acts concomitantly to inhibit metastatic

characteristics of cancer cells. Its putative role as a suppressor of metastasis is reinforced by our observation that reduced expression of this factor in large, contemporary prostate cancer cohorts is strongly associated with increased incidence of biochemical recurrence and metastasis. Moreover, we elucidated a mechanism to explain the ability of SOCS2 to curtail prostate cancer progression: by down-regulating two key kinases, FLT3 and JAK2, SOCS2 thereby inhibits key signalling pathways that are known to promote metastasis.

The relevance of a GATA2-miR-194-SOCS2 pathway in prostate cancer metastasis is supported by the known roles of GATA2, JAK2/STAT3 and MAPK/ERK signalling pathways in prostate cancer progression. GATA2 has a well-characterized function as an AR co-regulator (35, 65), but also operates independently of the AR signalling axis to promote chemoresistance and disease progression (33, 34). STAT3 acts as a key conduit in prostate cancer, integrating signals from the IL-6 cytokine and receptor tyrosine kinase pathways to drive various oncogenic processes including cell proliferation, AR activity, suppression of apoptosis and phenotypic plasticity governing EMT and cancer stem cell maintenance (66). Like STAT3, MAPK/ERK integrates multiple extrinsic signals to regulate cancer cell survival and apoptosis, amongst other functions (67). Our study provides a new link between these various signal transducers, with GATA2-regulated miR-194 at the nexus (Figure 8). Interestingly, GATA2 had previously been shown to activate multiple oncogenic kinases, including Akt and ERK, via direct regulation of the growth hormone IGF2 (34). With this in mind, we propose that miR-194 and IGF2 represent distinct downstream targets of GATA2 that nevertheless act in a complementary manner to additively enhance oncogenic signalling pathways and thereby promote prostate cancer progression. More broadly, our findings here further endorse GATA2 as a promising target in this disease (35, 68). Importantly, we believe the GATA2-miR-194 pathway may be generalizable to other tissues and malignancies, since we found evidence for a positive association between miR-194 and GATA2 signalling in breast cancer (Supplementary Figure 9).

Our interest in miR-194 arose from an earlier finding that its levels in serum/plasma, measured immediately prior to radical prostatectomy for localized prostate cancer, were predictive of recurrence after a disease-free period ranging from 1-70 months (15). In this previous study, we also noted that tissue expression of miR-194 was higher in metastatic disease, leading us to speculate that its potential as a biomarker was a consequence of its release into the blood from tumor cells with high metastatic potential and/or clinically

undetectable micro-metastases. This hypothesis is further strengthened by the work shown in this study. More specifically, using large independent clinical cohorts, we show that miR-194 levels in the primary tumor are highly prognostic for prostate cancer metastasis, and that circulating miR-194 is higher in men with metastatic compared with localized disease. Collectively, these findings support the idea that measuring circulating miR-194 could be used to detect micrometastases at the time of treatment or predict metastatic recurrence post-treatment. However, we acknowledge that the putative utility of miR-194 as a biomarker requires substantial additional validation.

In summary, our study has identified a new metastasis-promoting miRNA, miR-194, a new metastasis-suppressing factor, SOCS2, and a novel GATA2-driven pathway influencing prostate cancer metastasis. These findings have implications in terms of utilizing miR-194 as a biomarker and warrant further investigation into potential targeting of this miRNA to suppress prostate cancer progression.

MATERIALS AND METHODS

Analysis of miR-194 expression in published datasets

TCGA data was obtained from the web portal (https://tcga-data.nci.nih.gov/tcga/); miRNA expression data was obtained previously (69) whereas clinical data was downloaded on 31st October 2015. The MSKCC dataset was downloaded and processed as described previously (70).

Reagents

ERK1/2 inhibitor (SCH772984) was obtained from SelleckChem (S7101). Pan-JAK inhibitor (JAK1 Inhibitor I) was obtained from Calbiochem (420097).

Cell line culture and transfection

PC-3, DU145, 22Rv1, C4-2B and LNCaP human prostate carcinoma cells were obtained from the American Type Culture Collection. DU145, C4-2B, LNCaP and 22Rv1 cells were cultured in RPMI + 10% FBS. PC-3 cells were maintained in RPMI-1640 containing 5% FBS. All cell lines underwent verification by short-tandem repeat profiling in 2016 by CellBank Australia.

Cells were transfected with 20 nM miRNA mimics (miR-194 or negative control mimic; Shanghai GenePharma), 50 nM LNA miRNA inhibitors (miR-194 LNA inhibitor or negative control inhibitor; Exiqon), 20 nM siRNA (SOCS2 siRNA (Thermo Fisher Scientific, 4392420); GATA2 siRNA (Thermo Fisher Scientific, 1299001) or negative control siRNA; Qiagen)) using RNAiMAX transfection reagent (Life Technologies), according to the manufacturer's instructions. For plasmid transfections, cells were transfected with Lipofectamine 2000 (Life Technologies), according to the manufacturer's instructions.

MicroRNA in situ *hybridization*

In situ hybridization (ISH) was performed to determine the patterns of expression of miR-194 in human clinical PCa tissue from unmatched benign and malignant prostate tissues. ISH was performed using a locked nucleic acid (LNA)-conjugated miR-194-specific probe from Exiqon according to the manufacturer's instructions (71). Slides were examined with the aid of an Olympus BX50 microscope; 3 random fields at 60× magnification were analysed for each sample.

Growth assays

Growth curves were performed essentially as described previously (72), with some minor modifications. Briefly, cells were seeded at 2x105 (PC3) or 3x105 (22Rv1) cells/well in 6-well plates and transfected in suspension with miRNA mimic, miRNA inhibitor or siRNA as described above. Live and dead cells were subsequently quantified at the indicated time points using Trypan blue.

Cellular migration and invasion assays

In vitro scratch wound migration assays and Matrigel invasion assays in prostate cancer cell lines were conducted as described (73). For the SOCS2 rescue experiment, cells were co-transfected with miR-194 and a SOCS2 over-expression vector (Origene, SC108265).

Quantitative real-time PCR analysis of miRNA expression

Total RNA was extracted from prostate cancer cells using Trizol, essentially as described previously (74), except that the RNA was precipitated with 2.5 volume of ethanol, 10mM MgCl2, 0.1 volume of 5 M NaCl, and 20 μg of Glyco-Blue (Life Technologies) overnight at –20^{o}C. Levels of miR-194 and U6 small nuclear RNA were measured by qRT-PCR using Taqman assays, following the manufacturer's instructions (Life Technologies).

Quantitative real-time PCR analysis of mRNA expression

RNA extraction from cells, using Trizol reagent, and qRT-PCR was done as described previously (74). *GAPDH* was used for normalization of qRT-PCR data. Primer sequences are available on request.

Western blotting

Protein extraction from cells, using RIPA buffer, and Western blotting was done as described previously (74). Antibodies used in Western blotting were: E-cadherin (BD Biosciences, 610182); ERK (Cell Signaling Technology, 9102); phospho-ERK (Cell Signaling Technology, 9101); FLT3 (Cell Signaling Technology, #3462); N-cadherin (Santa Cruz Biotechnology, sc-7939); SOCS2 (Cell Signaling Technology, 2779); STAT3 (Cell Signaling Technology, 9132); phospho-STAT3 (Ser727; Cell Signaling Technology, 9134); ZO-1 (Santa Cruz, sc-10804); GAPDH (Millipore, MAB374).

Immunofluorescence

22Rv1 cells were transfected with miR-194 mimic or control, as described above, plated onto chamber slides (Lab-Tek, Thermo Fisher Scientific) and stained at day 3. For E-cadherin staining, cells were fixed in 4% paraformaldehyde, permeabilized in 0.1% Triton X-100 and probed with an anti-E-cadherin antibody (1:500; BD Biosciences, 610182). To detect nuclei, cells were co-stained with 4´-6-Diamidino-2-phenylindole (DAPI; Invitrogen). For F-actin staining, fixed and permeabilized cells were incubated with rhodamine phalloidin (Invitrogen) for 10 min. Cells were observed on and pictures were taken using a confocal microscope (Leica SP5).

Luciferase assays

To determine whether miR-194 directly targets the SOCS2 3'UTR, PC3 cells were transfected with miR-194 mimic or negative control. The following day, cells were transfected again with the 500 ng SOCS2 3'UTR construct (75) using Lipofectamine 2000 reagent. After 2 days, luciferase activity was measured using a Dual Luciferase Reporter assay (Promega). Firefly luciferase activity was normalized to Renilla luciferase activity.

Generation of miR-194 over-expressing PC3 and LNCaP cells

Luciferase-tagged PC3 and LNCaP cells were a kind gift from Professor Andreas Evdokiou. The lines were generated using the retroviral expression vector SFG-NES-TGL, which gives rise to a single fusion protein encoding herpes simplex virus thymidine kinase (TK), green fluorescence protein (GFP), and firefly luciferase (Luc), as described previously (76). Lentivirus particles designed to over-express miR-194 were prepared using a standard third generation packaging system in HEK293T/17 cells after transfection of cells with packaging vector and GFP hsa-miR-194-5p miRNA lentivector (Applied Biological Materials Inc., mh11109) or empty vector control (Applied Biological Materials Inc., m003). For viral transduction experiments, luciferase-tagged PC3 and LNCaP cells were seeded at 1.25x107 cells per T75 flask and left overnight to adhere. The next day, cells were transduced with concentrated lentivirus using a MOI of 1 and 6 μg/mL (as final concentration) Polybrene (Sigma) in normal growth media.

Chick chorioallantoic membrane (CAM) assays

CAM assays were approved by the University of Adelaide Animal Ethics Committee (approval number M-2014_079). CAM assays were carried out essentially as described (20), using the *in ovo* method. 5 x 104 PC3 cells per 15 µl of growth media and 8 x 104 LNCaP cells per 15 µl of growth media were mixed with an equal volume of Matrigel and grafted on top of the CAM of day 11 chick embryos. After 3 days, the CAM implants (containing the cell: Matrigel graft) was removed and fixed in 4% formaldehyde and paraffin embedded. Haematoxylin and eosin (H&E) staining and pan-cytokeratin immunohistochemistry were performed as described (20). For quantitative analysis of cancer cell invasion into the mesoderm layer, 8 to 12 CAM images from each embryo (6-8 embryos per treatment) were assessed.

Intravenous experimental metastasis model

Intravenous xenograft experiments were approved by the University of Adelaide Animal Ethics Committee (approval number M-2014-180C). Eight-week old male NOD/SCID mice (Animal Resources Centre, Western Australia) received tail vein injections of 1×106 PC3-194 cells in 200 µl of PBS. Non-invasive, whole-body imaging to monitor luciferase-expressing cells in mice was done at the time of injection and then once every week using the IVIS Lumina XRMS Series III Imaging System (Perkin Elmer). Mice were injected intraperitoneally with 100 µL D-luciferin (Biosynth; Cas # 115144-35-9) solution at 300 mg/kg body weight and then gas-anesthetized with isoflurane. The photon emission transmitted from mice was captured and quantitated by converting to physical units of surface radiance (photons/sec/cm2/sr) using Perkin Elmer Living Image (version 4.5).

Intra-prostatic experimental metastasis model

Intra-prostatic xenograft experiments were approved by the University of Adelaide Animal Ethics Committee (approval number M-2014-180C). Eight-week old male NOD/SCID mice

(Animal Resources Centre, Western Australia) received intra-prostatic injections of 1.5×105 PC3-194 cells in 10 µl of PBS. In vivo imaging was carried out as described above. After sacrificing the animals, organs were removed for *ex vivo* bioluminescence imaging.

Prospective primary prostate cancer cohort

Primary prostate cancer specimens were obtained with written informed consent through the Australian Prostate Cancer BioResource from 44 men who underwent robotic radical prostatectomy at St. Andrew's Hospital (Adelaide, Australia). The study was approved by the University of Adelaide Human Research Ethics Committee (approval number H-2012-016). A subset of these samples (n = 26) were first reported in a previous publication from our group (73); the remainder were collected subsequently. Tissues were homogenized in Qiazol using a Precellys 24 tissue homogenizer (Bertin Technologies) before RNA extraction with miRNeasy mini kits (Qiagen). DNAse treatment was performed using a TurboDNase kit (Ambion) according to the manufacturer's instructions. RNA was quantified using a Nanodrop. Reverse transcription was performed on 400 ng total RNA using the iScript kit (BioRad Laboratories) according to the manufacturer's instructions. Levels of miR-194 and *SOCS2* were not normally distributed, hence Spearman's correlation tests were used to examine relationships between their levels.

Gene set enrichment analysis (GSEA)

GSEA was performed as described previously (73). The GATA2-regulated gene set used in this study was comprised of genes that were down-regulated ($p < 0.001$) in response to GATA knockdown (35).

Measuring levels of miR-194 in serum

Serum total RNA samples from men with metastatic disease have been described previously (77). During this same study, whole blood samples from men with localized prostate cancer were also collected. All samples were collected with institutional approval from the Research Ethics Board of the British Columbia Cancer Agency. Informed consent was obtained from all participating patients and volunteers. Blood was collected in accordance with the National Institute of Cancer standard operating procedures for serum and plasma processing. Total RNA and Taqman qRT-PCR analysis of miR-194 (with a pre-amplification step) was performed as described previously (77).

Statistical analyses

All statistical analyses were carried out using GraphPad Prism (version 5; GraphPad Software, San Diego, CA, USA). Details of statistical tests used are provided in the figure legends. For Kaplan Meier analyses, optimal cutoffs for dichotomizing variables were defined as the point with the most significant (Fisher's exact test) split using Cutoff Finder (78).

FIGURES AND FIGURE LEGENDS

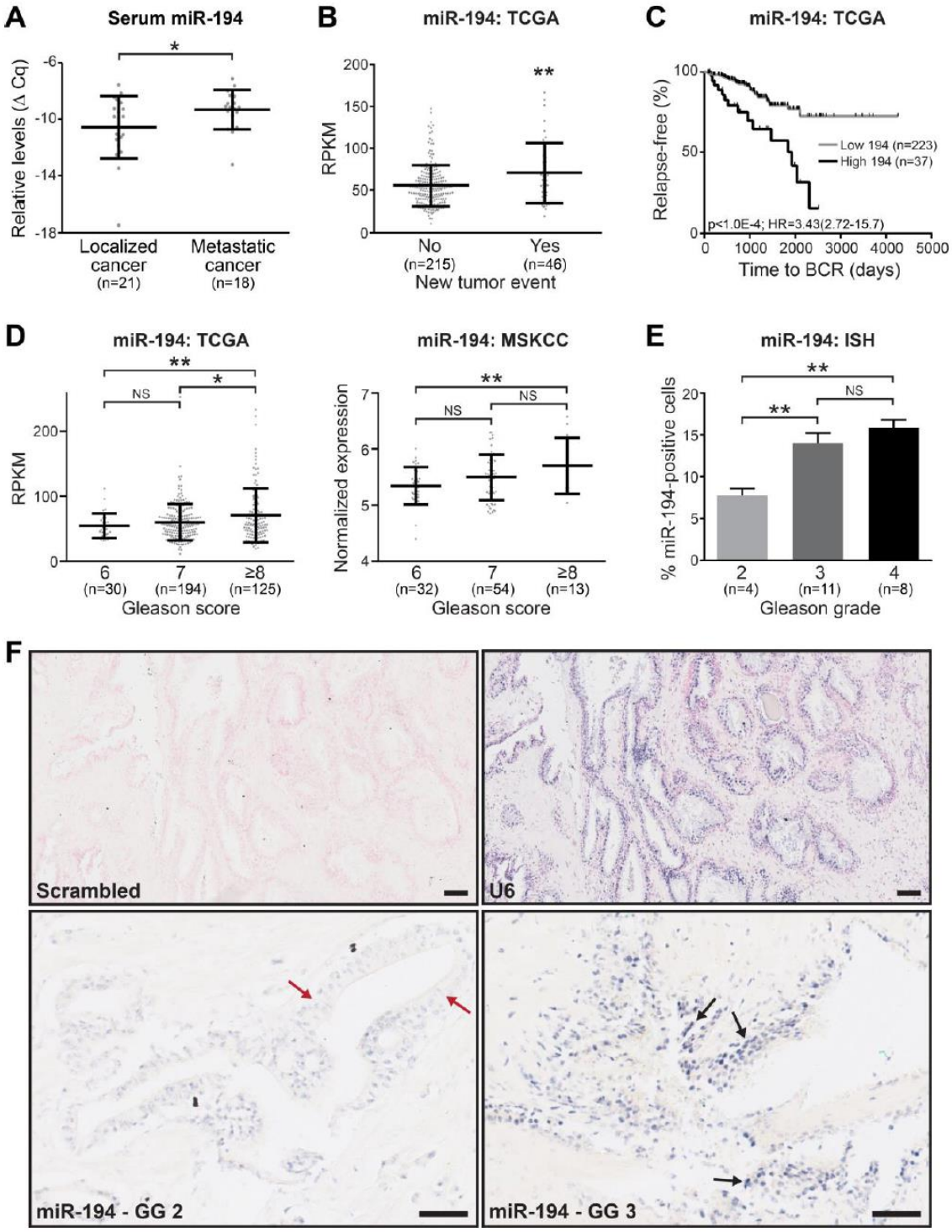

Figure 1. miR-194 is a circulating marker of metastasis and a tissue marker of disease aggressiveness. **(A)** miR-194 is elevated in the serum of patients with metastatic disease. Relative levels (normalized to spiked-in cel-miR-39; Δ Cq = Cq cel-miR-39 – Cq miR-194) of miR-194 in the serum of men with localized (n = 21) versus metastatic (n = 18) disease. Middle line is the mean; lines above and below represent ± standard deviation (SD). *P* value

was calculated using a Mann-Whitney U test (*, $p < 0.05$). **(B)** Expression of miR-194 in primary tumors from patients who experienced a new tumor event or not. Middle line is the mean; lines above and below represent ± standard deviation (SD). *P* value was determined using a an unpaired two-sided *t* test (**, $P < 0.01$). RPKM, reads per kilobase per million mapped reads. **(C)** Kaplan–Meier analysis showing estimated biochemical relapse (BCR)-free probability in patients with high or low levels of miR-194. *P* value was determined using a Log Rank test. **(D)** Expression level of miR-194 in prostate cancer tissues according to increasing Gleason score in the TCGA (18) and MSKCC (16) cohorts. Middle line is the mean; lines above and below represent ± standard deviation (SD). *P* values were determined using unpaired two-sided *t* tests (*, $P < 0.05$; **, $P < 0.01$). **(E)** Expression level of miR-194 in prostate cancer tissues by according to increasing Gleason grade in 23 primary tumors, as estimated using *in situ* hybridization (ISH). Error bars are standard error of the mean (SEM). *P* values were determined using Mann-Whitney U tests (**, $P < 0.01$). **(F)** ISH demonstrates that miR-194 is expressed in prostatic epithelial cells. U6 staining confirmed the preservation of intact small RNAs in the same case, and a scrambled probe demonstrated specificity. Red arrows indicate weak staining in more normal glandular structures; black arrows indicate strong staining in foci of higher tumor grade. Scale bars = 50 μm. Gleason grade, GG.

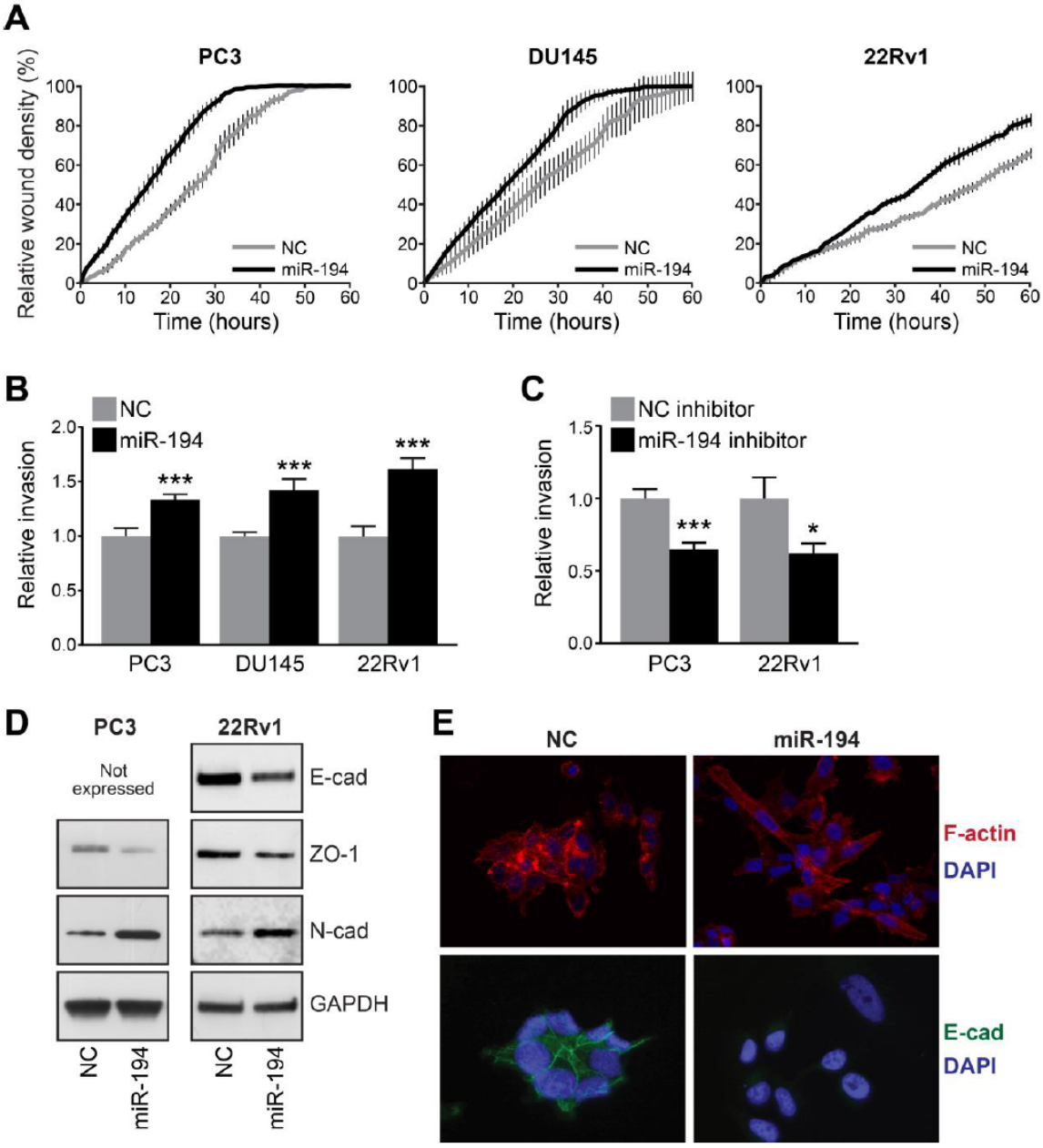

Figure 2. miR-194 enhances metastatic features of prostate cancer cells. **(A)** miR-194 promotes migration of PC3, DU145 and 22Rv1 cell lines. Error bars are ± SEM. **(B-C)** miR-194 promotes invasion of PC3, DU145 and 22Rv1 cells. Values for the negative control (NC) were set to 1, and error bars are SEM. *P* values were determined using unpaired two-sided *t* tests (*, $P < 0.05$; ***, $P < 0.001$). B, cells were transfected with miR-194 mimic or negative control (NC) mimic (B). C, cells were transfected with miR-194 inhibitor or NC inhibitor. Error bars are SEM. **(D)** miR-194 enhances mesenchymal features of prostate cancer cells. The expression of epithelial (E-cad, ZO-1) and mesenchymal (N-cad) markers was examined by Western blotting following transfection of miR-194 or NC mimic in PC3 and 22Rv1 cells. E-cad, E-cadherin; ZO-1, Zona occludens-1; N-cad, N-cadherin. GAPDH was used as a loading control. **(E)** Immunofluorescence analysis of E-cadherin and F-actin expression in 22Rv1 cells transfected with miR-194 or NC mimic. Nuclei were stained with DAPI.

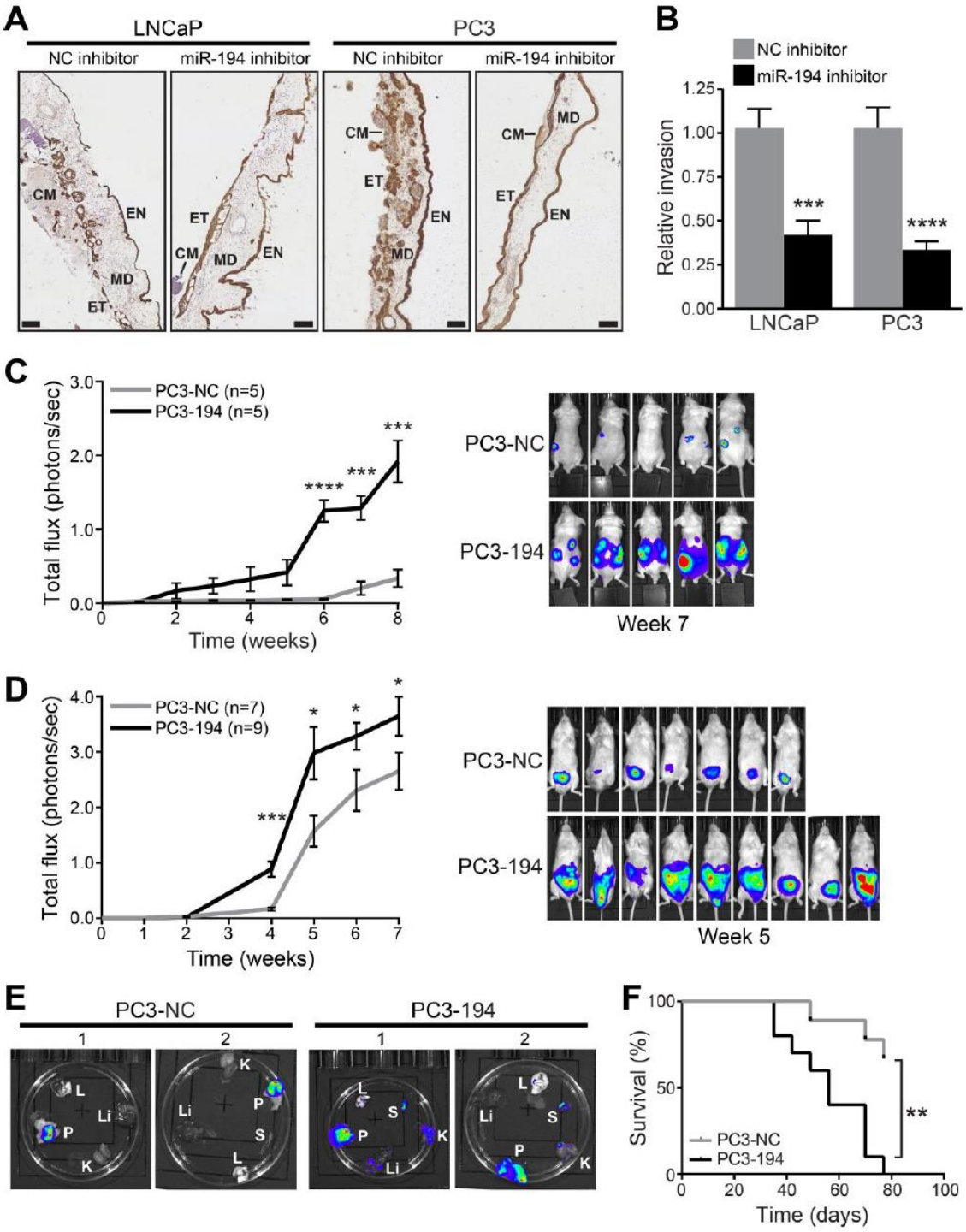

Figure 3. miR-194 promotes invasion and metastasis of prostate cancer *in vivo*. **(A)** Representative immunohistochemical staining of pan-cytokeratin in CAM invasion assays. PC3 and LNCaP cell/Matrigel grafts (CM) were placed on top of the ectoderm (ET) layer and cancer cell invasion into the CAM mesoderm (MD) was assessed in day 14 chick embryos. Endoderm, EN. Scale bars = 100 μm. **(B)** Quantitation of CAM invasion assay data. Data was generated from 48–60 images from at least 6 chicken embryos per treatment. Data represents the mean percentage of images with invasion into the

mesoderm. Error bars are SEM. *P* value was determined using an unpaired two-sided *t* test (***, $P < 0.001$; ****, $P < 0.0001$). **(C)** Over-expression of miR-194 promotes metastasis of PC3 cells in tail vein assays. The graph on left represents luciferase intensity as assessed by whole-animal bioluminescent imaging over time in mice injected with control cells (PC3-NC, n = 5) or miR-194 over-expressing cells (PC3-194, n = 5), as assessed by non-invasive bio-luminescent imaging. Tumor incidence was 100% for both cell lines. Significance of the differences in bioluminescence were assessed using unpaired two-sided *t* tests (***, $P < 0.001$; ****, $P < 0.0001$). Error bars are ± SEM. Right, images of mice at week 7. **(D)** Over-expression of miR-194 promotes growth and metastasis of PC3 intra-prostatic xenografts. The graph on left represents luciferase intensity as assessed by whole-animal bioluminescent imaging over time in mice injected with control cells (PC3-NC, n = 7) or miR-194 over-expressing cells (PC3-194, n = 9), as assessed by non-invasive bio-luminescent imaging. Tumor incidence was 77.8% for PC3-NC (7/9) and 90% (9/10) for PC3-194. Significance of the differences in bioluminescence were assessed using unpaired two-sided *t* tests (*, $P < 0.05$; ***, $P < 0.001$). Error bars are ± SEM. Right, images of mice at week 5. **(E)** Representative bioluminescent images of organs obtained from two PC3-NC and two PC3-194 mice shown in D at time of sacrifice. K, kidney; L, lung; Li, liver, P, prostate primary tumor; S, spleen. **(F)** Kaplan–Meier analysis showing survival of mice with intra-prostatic xenografts. *P* value was determined using a Log Rank test (**, $P < 0.01$).

Figure 4

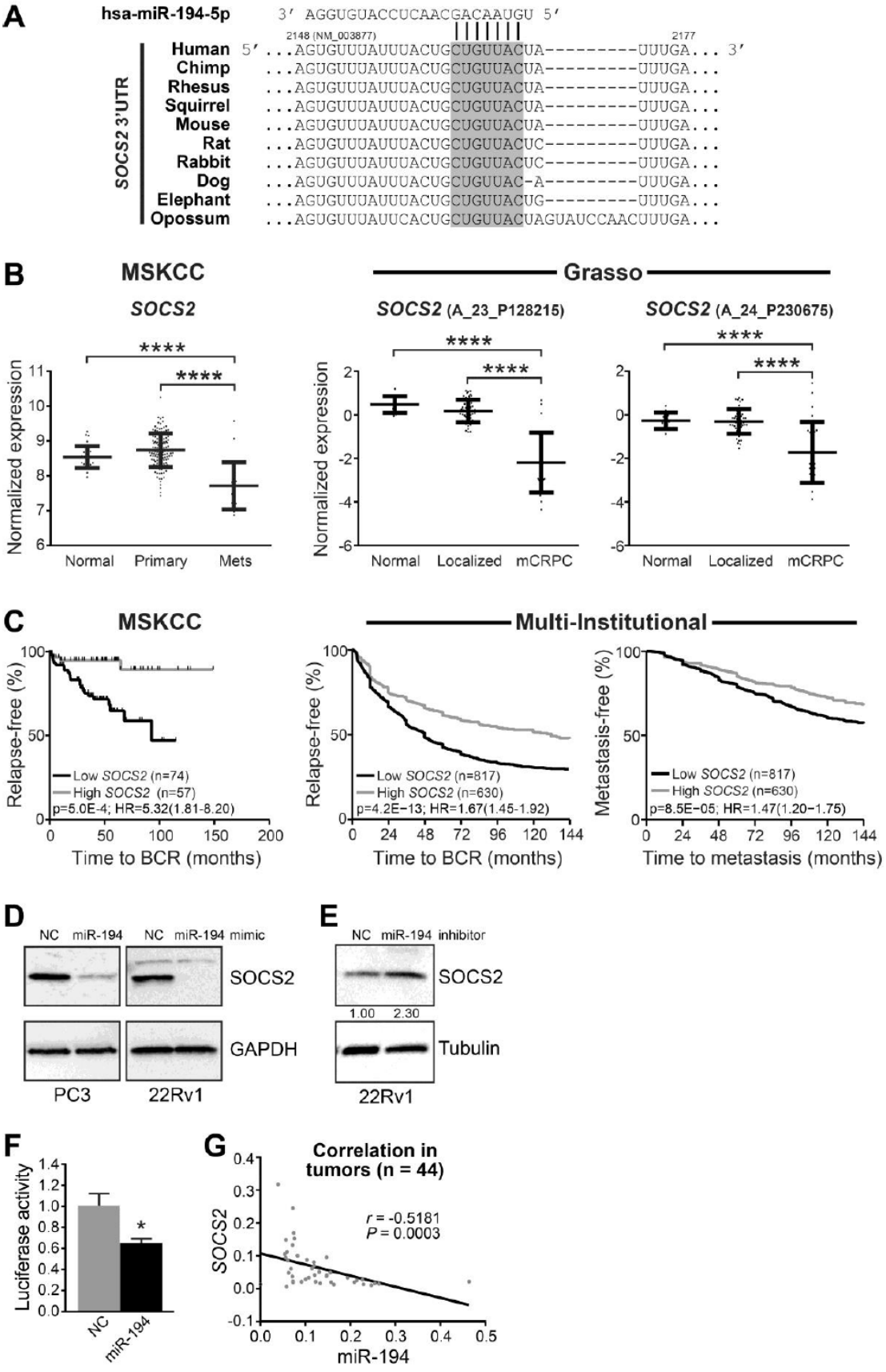
A
hsa-miR-194-5p
3′ AGGUGUACCUCAACGACAAUGU 5′
2148 (NM_003877)
2177
SOCS2 3'UTR
Human 5′...AGUGUUUAUUUACUGCUGUUACUA---------UUUGA... 3′
Chimp ...AGUGUUUAUUUACUGCUGUUACUA---------UUUGA...
Rhesus ...AGUGUUUAUUUACUGCUGUUACUA---------UUUGA...
Squirrel ...AGUGUUUAUUUACUGCUGUUACUA---------UUUGA...
Mouse ...AGUGUUUAUUUACUGCUGUUACUA---------UUUGA...
Rat ...AGUGUUUAUUUACUGCUGUUACUC---------UUUGA...
Rabbit ...AGUGUUUAUUUACUGCUGUUACUC---------UUUGA...
Dog ...AGUGUUUAUUUACUGCUGUUAC-A---------UUUGA...
Elephant ...AGUGUUUAUUUACUGCUGUUACUG---------UUUGA...
Opossum ...AGUGUUUAUUCACUGCUGUUACUAGUAUCCAACUUUGA...
B
MSKCC
Grasso
SOCS2
SOCS2 (A_23_P128215)
SOCS2 (A_24_P230675)
****
Normalized expression
Normal
Primary
Mets
Localized
mCRPC
C
MSKCC
Multi-Institutional
Relapse-free (%)
Low SOCS2 (n=74)
High SOCS2 (n=57)
p=5.0E-4; HR=5.32(1.81-8.20)
Time to BCR (months)
Low SOCS2 (n=817)
High SOCS2 (n=630)
p=4.2E−13; HR=1.67(1.45-1.92)
Metastasis-free (%)
p=8.5E−05; HR=1.47(1.20−1.75)
Time to metastasis (months)
D
NC
miR-194
NC
miR-194 mimic
SOCS2
GAPDH
PC3
22Rv1
E
NC
miR-194 inhibitor
SOCS2
1.00
2.30
Tubulin
22Rv1
F
Luciferase activity
NC
miR-194
G
Correlation in tumors (n = 44)
r = -0.5181
P = 0.0003
SOCS2
miR-194

Figure 4. SOCS2 is a direct target of miR-194. **(A)** Schematic showing conservation of putative miR-194 target site in the 3′ UTR of *SOCS2*. **(B)** Relative expression of *SOCS2* in normal prostate tissue, primary prostate tumours (Primary or Localized) and metastases (Mets or mCRPC). Two different cohorts, Grasso (79) and MSKCC (16), were analyzed. Middle line is the mean; lines above and below represent ± standard deviation (SD). *P* values were determined using unpaired two-sided *t* tests (****, $P < 0.0001$). **(C)** Kaplan-Meier curves showing estimated biochemical relapse (BCR)-free probability in patients with high or low levels of *SOCS2* mRNA in the MSKCC and Multi-Institutional cohorts. *P* values and hazard ratios (HRs) were determined using Log Rank tests. **(D)** Western blot showing SOCS2 levels following transfection with miR-194 mimic or a negative control (NC) in PC3 and 22Rv1 cells. GAPDH was used as a loading control. **(E)** Western blot showing SOCS2 levels following transfection with a miR-194 inhibitor or a negative control (NC) inhibitor in 22Rv1 cells. Tubulin was used as a loading control. Normalized levels of SOCS2 are shown beneath the lanes. **(F)** miR-194 directly targets the *SOCS2* 3'UTR. A Luciferase:SOCS2 3'UTR construct was co-transfected with miR-194 mimic or NC in PC3 cells. Luciferase activity for "NC" was set to 1; bars represent the average of 6 wells per treatment, and error bars are SEM. A *P* value was determined using an unpaired *t* test (*, $P < 0.05$). **(G)** Negative correlation of miR-194 and *SOCS2* in prostate cancer. The graph shows the levels of miR-194 versus *SOCS2* in 44 primary tumors, as determined by qRT-PCR. *SOCS2* was normalized to *GAPDH*, whereas miR-194 was normalized to the reference small RNA U6. *P* and r values were calculated using a Spearman correlation test.

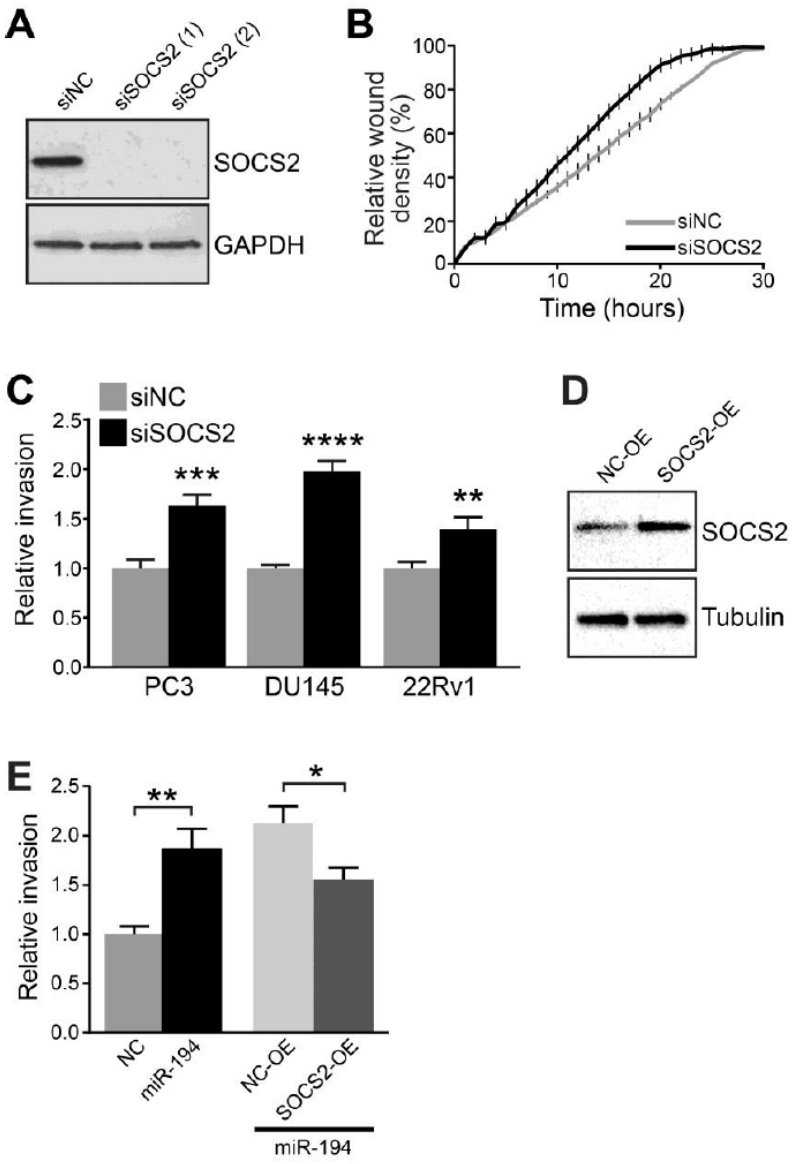

Figure 5. SOCS2 is a biologically relevant target of miR-194 and suppresses metastatic features of prostate cancer cells. **(A)** Western blot showing SOCS2 levels in PC3 cells following transfection with two specific siRNAs (siSOCS2 (1) and siSOCS2 (2)) or a negative control (siNC). GAPDH was used as a loading control. **(B)** Loss of SOCS2 promotes migration of PC3 cells. Error bars are ± SEM. **(C)** Loss of SOCS2 promotes invasion of PC3, DU145 and 22Rv1 cells. *P* values were determined using unpaired two-sided *t* tests (**, $P < 0.01$; ***, $P < 0.001$; ****, $P < 0.0001$). Error bars are SEM. **(D)** Western blot showing SOCS2 levels following transfection with and over-expression construct (SOCS2-OE) or a negative control (NC-OE). **(E)** Over-expression of SOCS2 reverses miR-194-induced invasion in PC3 cells. Error bars are SEM.

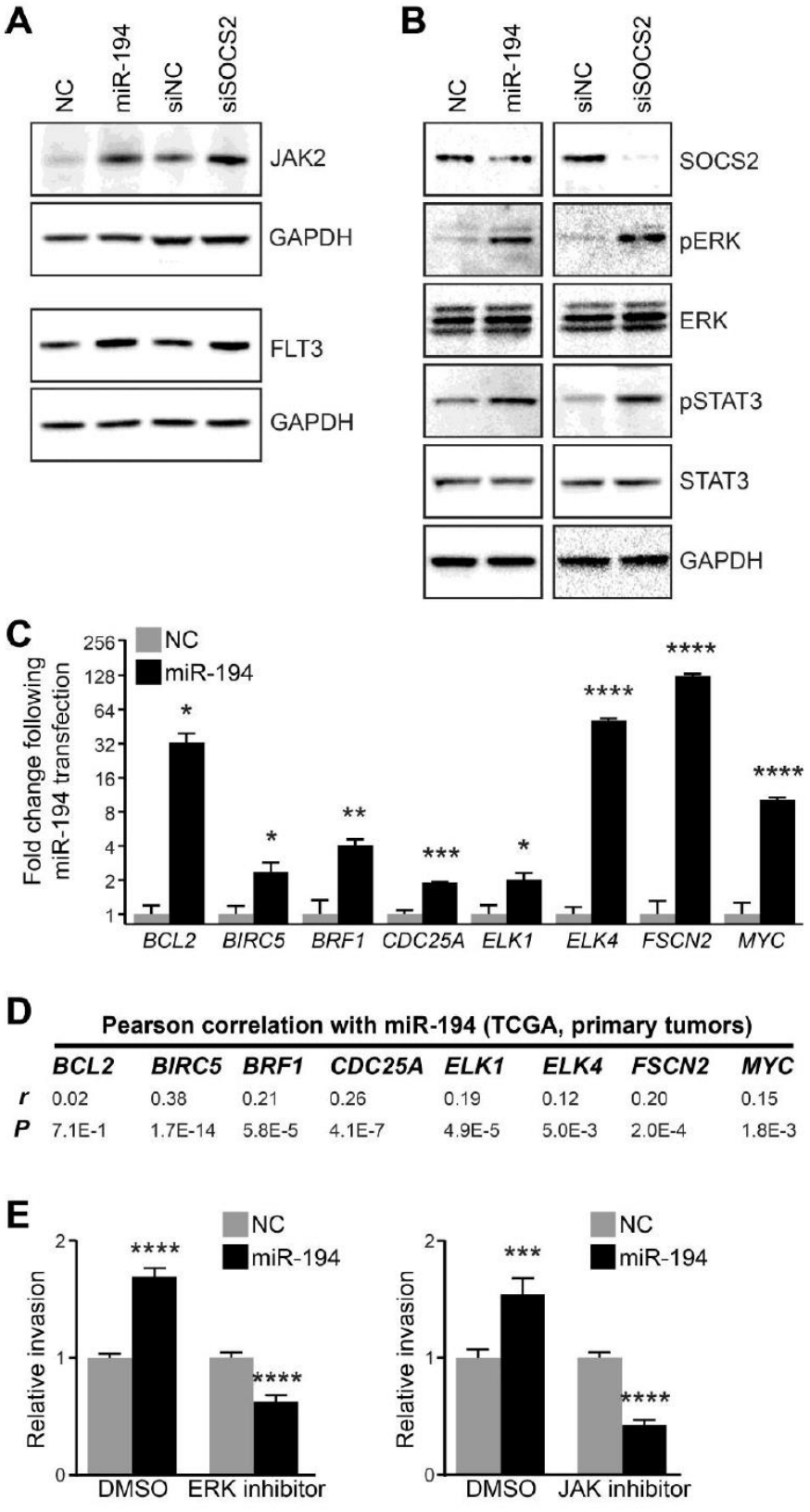

Figure 6. miR-194 activates STAT3 and ERK signalling pathways. **(A)** Western blotting demonstrates that expression of total JAK2 and FLT3 is increased by miR-194 or SOCS2

knockdown in 22Rv1 cells. GAPDH was used as a loading control. **(B)** Western blotting demonstrates that expression of phospho-STAT3 and phospho-ERK is increased by miR-194 or SOCS2 knockdown. GAPDH was used as a loading control. **(C)** Expression of pro-metastasic downstream effectors of STAT3 and ERK signalling are increased in response to miR-194, as revealed by qRT-PCR. Levels of genes were normalized to the *GAPDH*. The control treatment (negative control (NC) mimic) was set to 1. Error bars are SEM. *P* values were determined using unpaired two-sided *t* tests (*, $P < 0.05$; **, $P < 0.01$; ***, $P < 0.001$; ****, $P < 0.0001$). **(D)** Correlation of miR-194 and ERK/STAT3 effector genes in 414 prostate tumors from the TCGA cohort. *P* and r values were calculated using Pearson's correlation tests. **(E)** Inhibition of ERK (with SCH772984; left graph) or JAK (with JAK1 Inhibitor I; right graph) reverses miR-194-mediated invasion in 22Rv1 cells. Error bars are SEM.

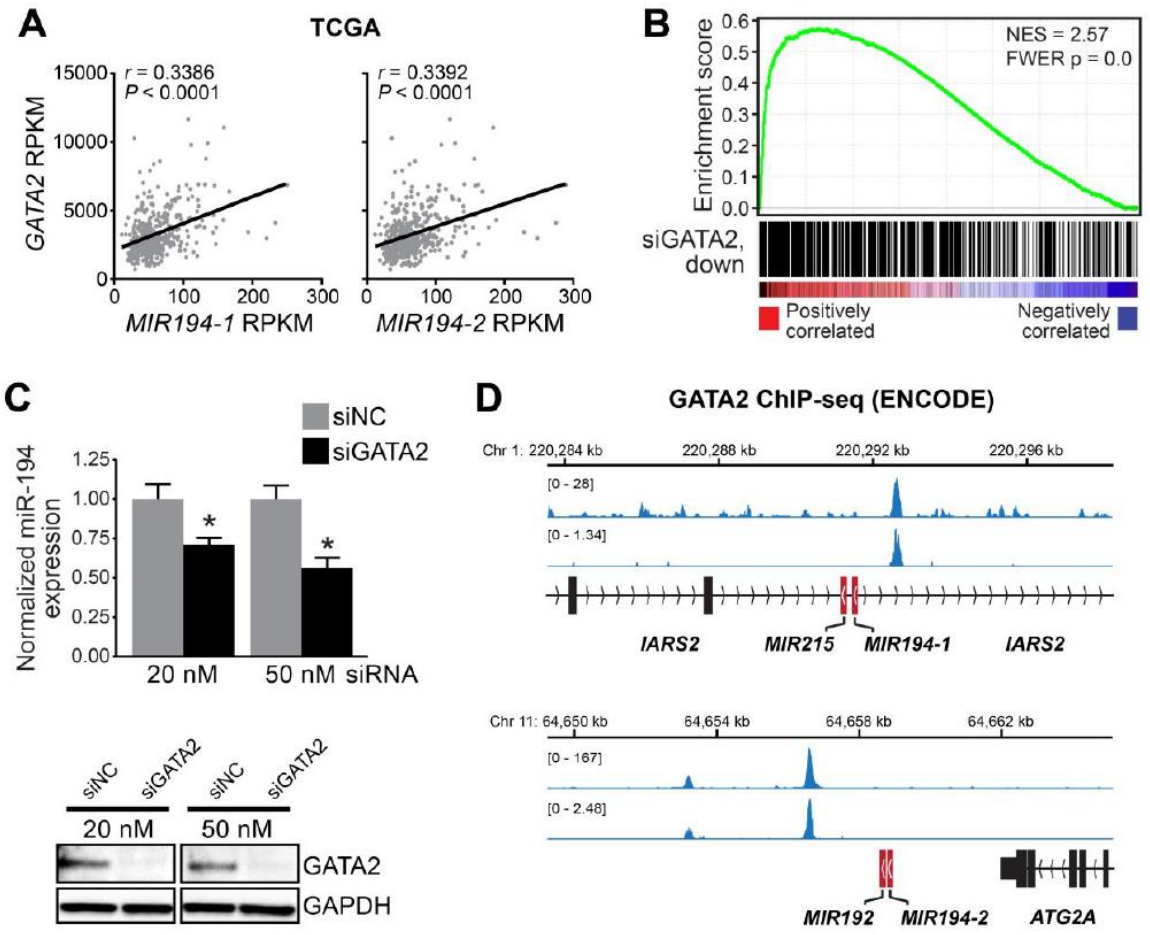

Figure 7. miR-194 is a target of the transcription factor, GATA2. **(A)** Positive correlation of miR-194 and *GATA2* in prostate cancer. The graphs show the levels of the two miR-194-encoding transcripts (*MIR194-1* and *MIR194-2*) versus *GATA2* in 414 tumors from the TCGA cohort. *P* and r values were calculated using Pearson's correlation tests. RPKM, reads per kilobase per million mapped reads. **(B)** Positive association between miR-194 and a signature of GATA2 transcriptional activity (35), as demonstrated by gene set enrichment analysis (GSEA), in the TCGA cohort. **(C)** GATA2 knockdown (siGATA2) causes reduced miR-194 expression in 22Rv1 cells, as determined by qRT-PCR. Two different concentrations of siGATA2 were used in the experiment. Levels of miR-194 were normalized to the reference small RNA U6. *P* value was determined using an unpaired two-sided *t* test (*, $P < 0.05$). Error bars are SEM. Knockdown of GATA2 at the two different siRNA concentrations is shown below; GAPDH is used as a loading control. **(D)** Screenshot (hg19) showing ENCODE ChIP-seq datasets that demonstrate GATA2 binding proximal to the two *MIR194* loci in K562 cells. Two distinct studies are shown; top track is ENCFF000YNN and bottom track is ENCFF000QAU. Arrows indicate direction of transcription.

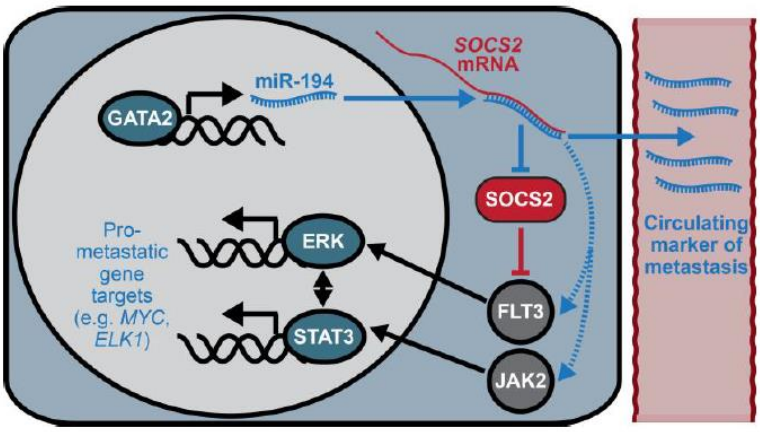

Figure 8. Model of miR-194 regulation and pro-metastatic activity, via SOCS2, in prostate cancer.

Supplementary figures

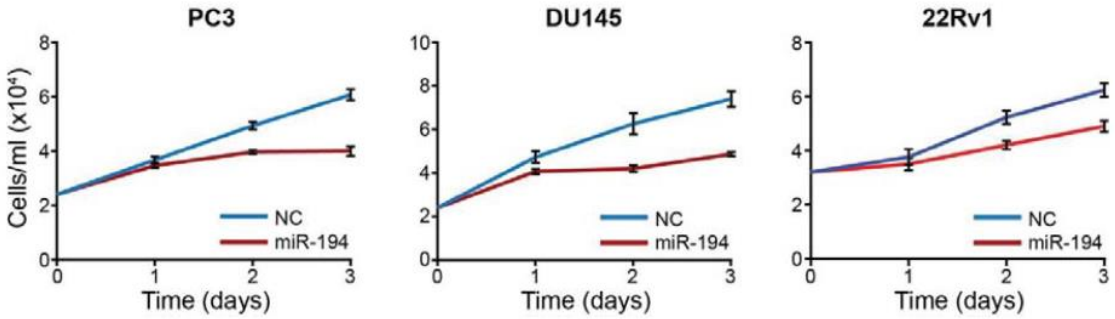

Supplementary figure 1: MiR-194 inhibits growth of prostate cancer cells. Cell lines were transfected with miR-194 mimic or negative control (NC) mimic. Cells were counted using Trypan blue assays at the indicated time points. Error bars are ± SEM.

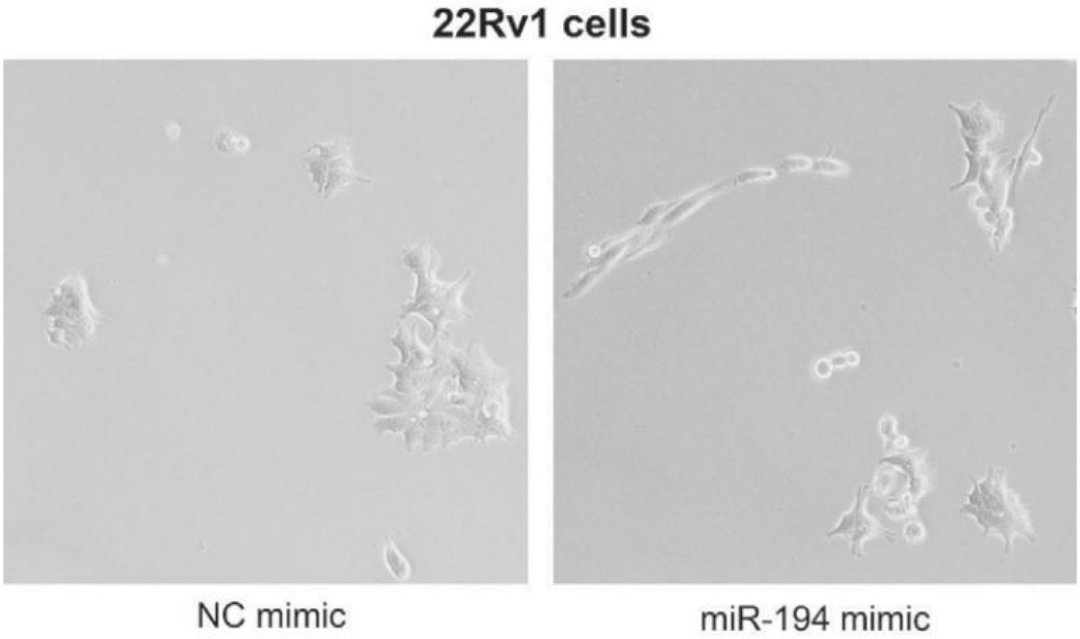

Supplementary figure 2: MiR-194 alters cell morphology. 22Rv1 cells were transfected with miR-194 mimic and negative control (NC) mimic. Representative phase contrast images are shown.

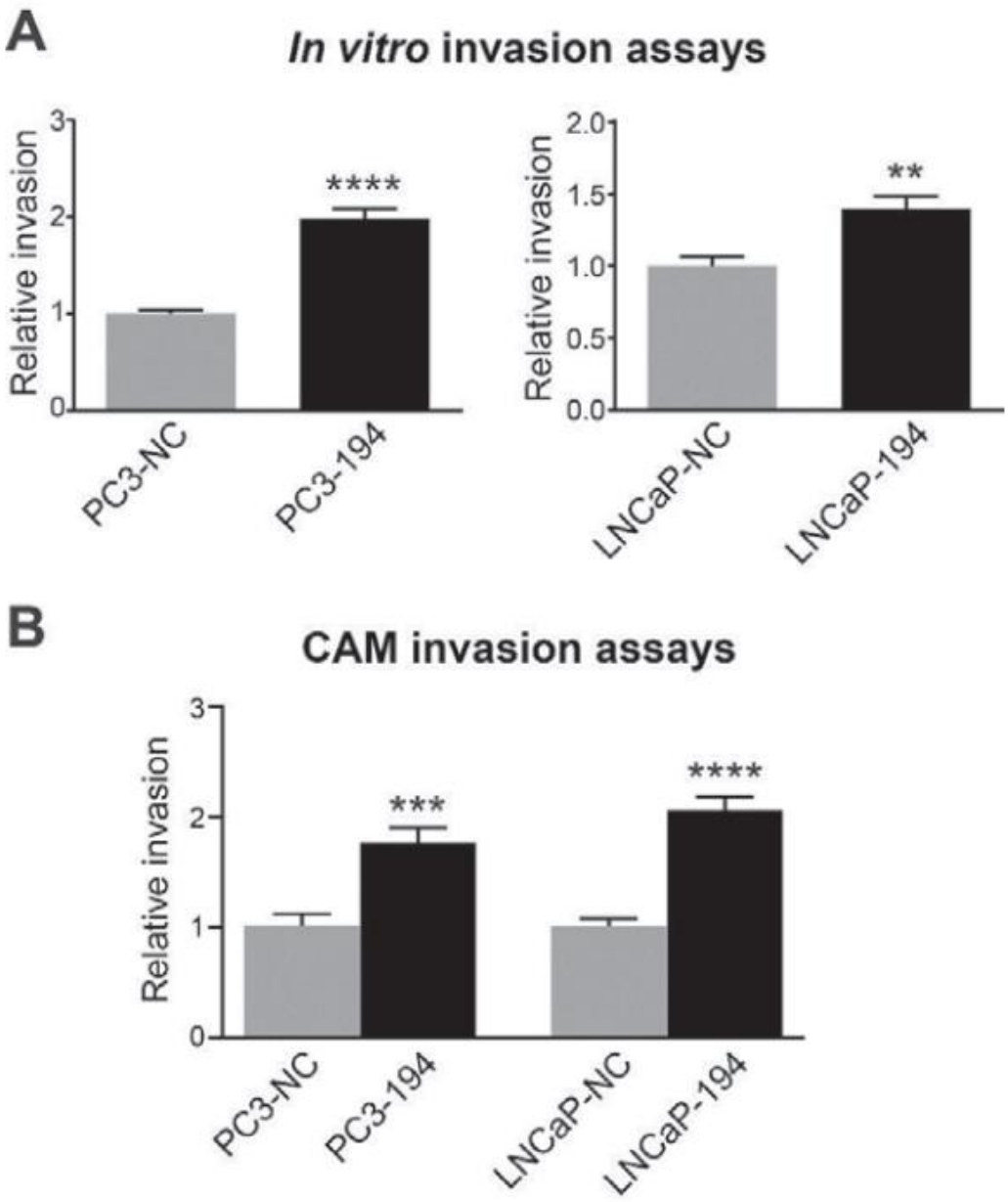

Supplementary figure 3: Stable overexpression of miR-194 promotes cell invasion. (A) *In vitro* invasion assays. Values for the negative control (NC) were set to 1, and error bars are SEM. *P* values were determined using unpaired *t* tests (**, *P* <0.01, ****, *P*<0.0001). (B) CAM invasion assays. Data was generated from 48-60 images from 6 chicken embryos per treatment. Data represents the mean percentage of images with invasion into the mesoderm. Error bars are SEM. *P* values was determined using an unpaired *t* test (***, *P*<0.001, ****, *P*<0.0001)

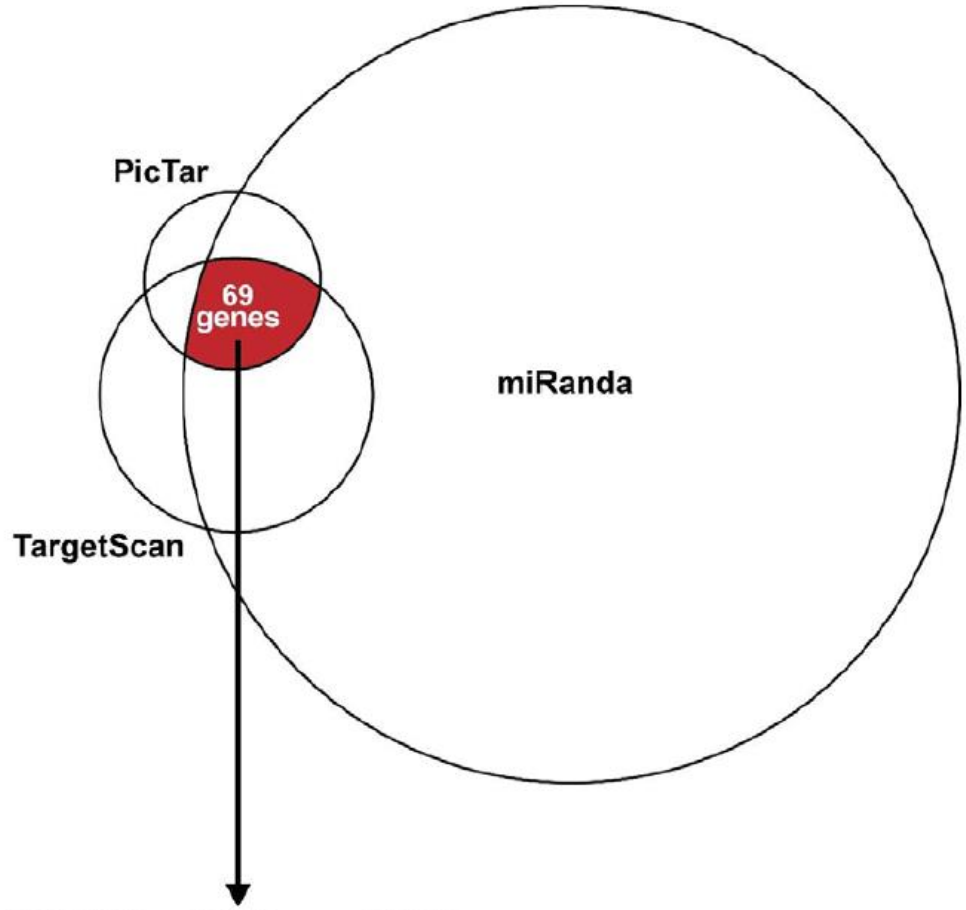

ARHGAP21	GRHL2	RAB6B
ARHGAP24	GRHL3	REV3L
ARID4A	GYG1	RSBN1L
ASAP1	HBEGF	SDAD1
BCKDHA	HNF1B	SDC4
BICD2	HS3ST2	SEPHS1
CAMK2G	ID4	**SOCS2**
CEP350	ITPKB	SP3
CHD4	KLF15	SUFU
CHD6	LHX6	SYVN1
CHD9	LUC7L3	TAF4
CSNK1D	MAP2	TFRC
DCUN1D5	MEIS2	TJAP1
DEPDC1B	MID1IP1	TLN2
DHX15	NAA50	TMEM43
DNMT3A	NFAT5	TRA2B
DUSP9	NUDC	TRIM9
EYA4	PAFAH1B1	TRPS1
FGFR3	PAN3	TSPAN7
FMR1	PAPOLG	UBR3
FOXA1	PFN2	YTHDF1
GJB1	PHF1	ZFAND5
GLIS3	PTPN12	ZFHX4

Supplementary figure 4: Venn diagram showing putative targets of miR-194 from 3 independent prediction algorithms. The 69 targets found by all 3 algorithms are listed.

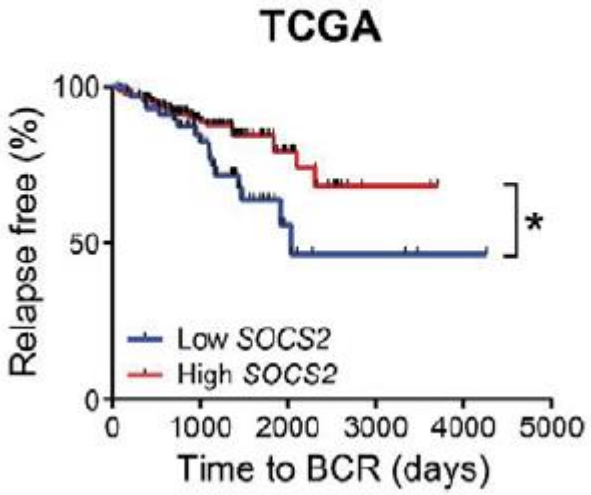

Supplementary figure 5: Kaplan- Meier analysis showing estimated biochemical relapse (BCR) - free probability in patients from the TCGA cohort with high or low levels of *SOCS2 mRNA*. *P* value was determined using a Log Rank test (*, *P*<0.05)

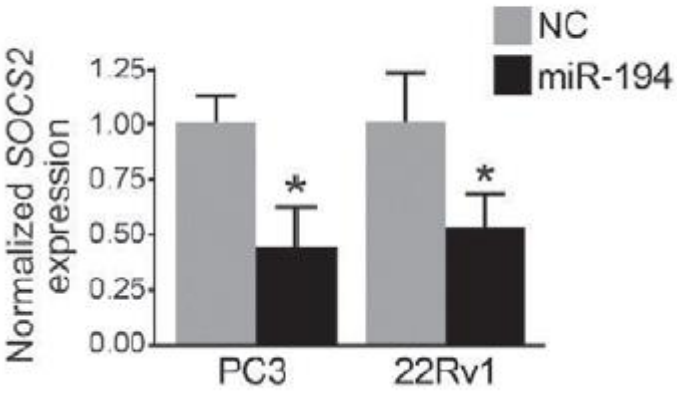

Supplementary figure 6: MiR-194 decreases *SOCS2 mRNA* expression in prostate cancer cells compared to a negative control (NC). Data is normalised to *GAPDH* reference gene. P value was determined using an unpaired two-sided t test (*, *P*<0.05). Error bars are ± SEM.

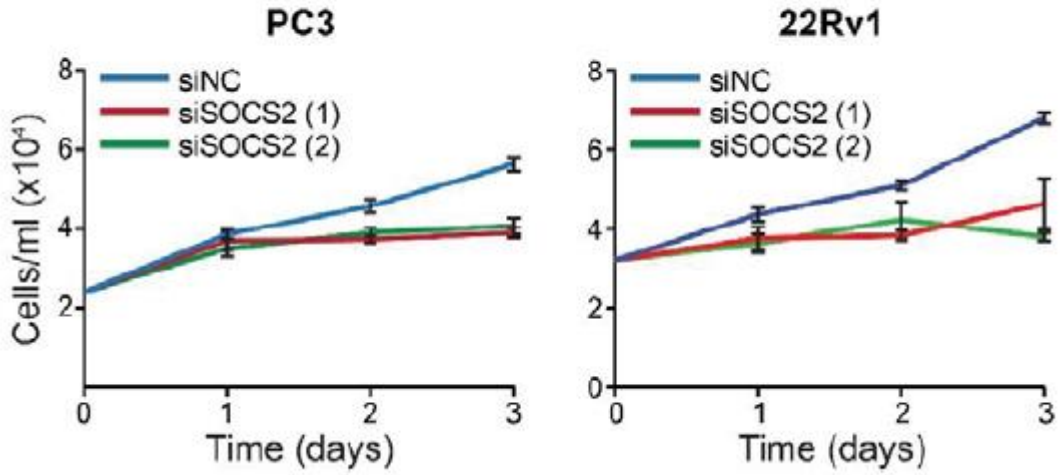

Supplementary figure 7: Knockdown of SOCS2 (siSOCS2) inhibits growth of PC3 and 22Rv1 cells. Cell lines were transfected with two different siRNAs against SOCS2 or a negative (siNC). Cells were counted using Trypan blue assays at the indicated time-points. Error bars are ± SEM.

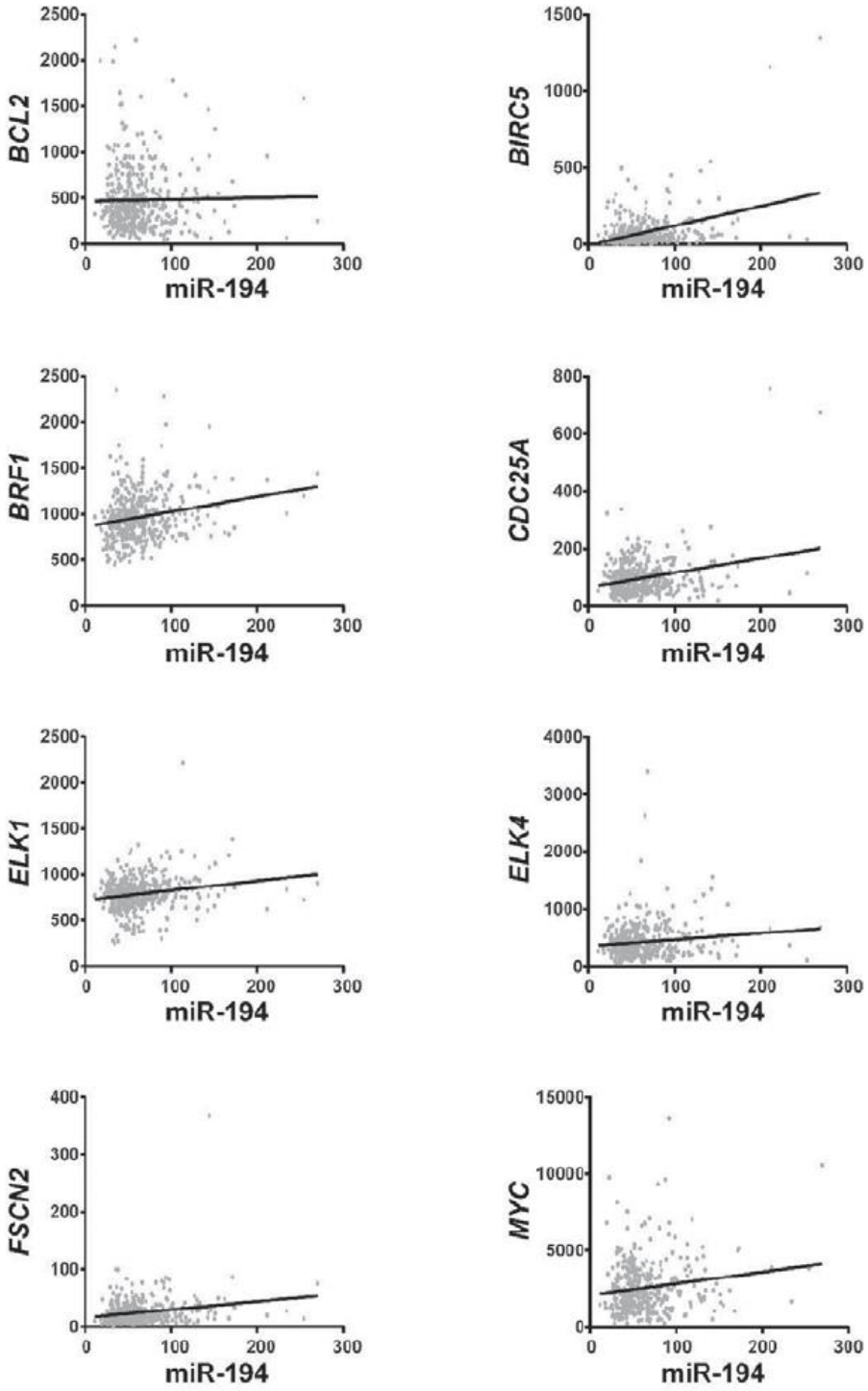

Supplementary figure 8: Plots showing correlation between miR-194 and selected pro-metastatic gene targets of STAT3 and ERK. Data is from TCGA cohort, comprised of 414 tumours.

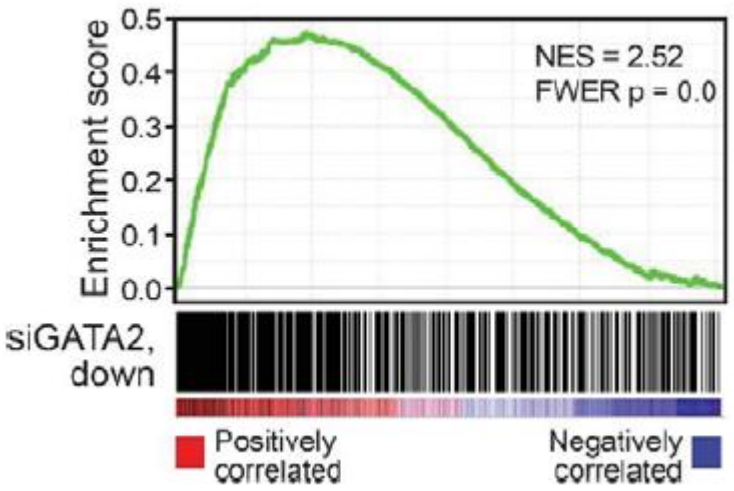

Supplementary figure 9: Positive association between miR-194 and a signature of GATA2 transcriptional activity, as demonstrated by gene set enrichment analysis (GSEA), in the TCGA breast cancer dataset.

References

1. Ferlay J, Soerjomataram I, Dikshit R, Eser S, Mathers C, Rebelo M, Parkin DM, Forman D, and Bray F. Cancer incidence and mortality worldwide: sources, methods and major patterns in GLOBOCAN 2012. *International journal of cancer Journal international du cancer.* 2015;136(5):E359-86.
2. Bray F, Ren JS, Masuyer E, and Ferlay J. Global estimates of cancer prevalence for 27 sites in the adult population in 2008. *International journal of cancer Journal international du cancer.* 2013;132(5):1133-45.
3. Wu JN, Fish KM, Evans CP, Devere White RW, and Dall'Era MA. No improvement noted in overall or cause-specific survival for men presenting with metastatic prostate cancer over a 20-year period. *Cancer.* 2014;120(6):818-23.
4. Jin JK, Dayyani F, and Gallick GE. Steps in prostate cancer progression that lead to bone metastasis. *International journal of cancer Journal international du cancer.* 2011;128(11):2545-61.
5. Santoni M, Piva F, Scarpelli M, Cheng L, Lopez-Beltran A, Massari F, Iacovelli R, Berardi R, Santini D, and Montironi R. The origin of prostate metastases: emerging insights. *Cancer metastasis reviews.* 2015;34(4):765-73.
6. Valastyan S, and Weinberg RA. Tumor metastasis: molecular insights and evolving paradigms. *Cell.* 2011;147(2):275-92.
7. Brodersen P, and Voinnet O. Revisiting the principles of microRNA target recognition and mode of action. *Nat Rev Mol Cell Biol.* 2009;10(2):141-8.
8. Catto JW, Alcaraz A, Bjartell AS, De VWR, Evans CP, Fussel S, Hamdy FC, Kallioniemi O, Mengual L, Schlomm T, et al. MicroRNA in prostate, bladder, and kidney cancer: a systematic review. *European Urology.* 2011;59(5):671-81.
9. Gordanpour A, Nam RK, Sugar L, and Seth A. MicroRNAs in prostate cancer: from biomarkers to molecularly-based therapeutics. *Prostate cancer and prostatic diseases.* 2012;15(4):314-9.
10. Porkka KP, Pfeiffer MJ, Waltering KK, Vessella RL, Tammela TL, and Visakorpi T. MicroRNA expression profiling in prostate cancer. *Cancer Res.* 2007;67(13):6130-5.
11. Ambs S, Prueitt RL, Yi M, Hudson RS, Howe TM, Petrocca F, Wallace TA, Liu CG, Volinia S, Calin GA, et al. Genomic profiling of microRNA and messenger RNA reveals deregulated microRNA expression in prostate cancer. *Cancer Res.* 2008;68(15):6162-70.
12. Schaefer A, Jung M, Mollenkopf HJ, Wagner I, Stephan C, Jentzmik F, Miller K, Lein M, Kristiansen G, and Jung K. Diagnostic and prognostic implications of microRNA profiling in prostate carcinoma. *Int J Cancer.* 2010;126(5):1166-76.
13. Tong AW, Fulgham P, Jay C, Chen P, Khalil I, Liu S, Senzer N, Eklund AC, Han J, and Nemunaitis J. MicroRNA profile analysis of human prostate cancers. *Cancer Gene Ther.* 2009;16(3):206-16.
14. Bouyssou JM, Manier S, Huynh D, Issa S, Roccaro AM, and Ghobrial IM. Regulation of microRNAs in cancer metastasis. *Biochimica et biophysica acta.* 2014;1845(2):255-65.
15. Selth LA, Townley SL, Bert AG, Stricker PD, Sutherland PD, Horvath LG, Goodall GJ, Butler LM, and Tilley WD. Circulating microRNAs predict biochemical recurrence in prostate cancer patients. *British journal of cancer.* 2013;109(3):641-50.
16. Taylor BS, Schultz N, Hieronymus H, Gopalan A, Xiao Y, Carver BS, Arora VK, Kaushik P, Cerami E, Reva B, et al. Integrative genomic profiling of human prostate cancer. *Cancer Cell.* 2010;18(1):11-22.

17. Martens-Uzunova ES, Jalava SE, Dits NF, van Leenders GJ, Moller S, Trapman J, Bangma CH, Litman T, Visakorpi T, and Jenster G. Diagnostic and prognostic signatures from the small non-coding RNA transcriptome in prostate cancer. *Oncogene.* 2012;31(8):978-91.
18. Cancer Genome Atlas Research N. The Molecular Taxonomy of Primary Prostate Cancer. *Cell.* 2015;163(4):1011-25.
19. De Craene B, and Berx G. Regulatory networks defining EMT during cancer initiation and progression. *Nature reviews Cancer.* 2013;13(2):97-110.
20. Lokman NA, Elder AS, Ricciardelli C, and Oehler MK. Chick chorioallantoic membrane (CAM) assay as an in vivo model to study the effect of newly identified molecules on ovarian cancer invasion and metastasis. *Int J Mol Sci.* 2012;13(8):9959-70.
21. Lewis BP, Burge CB, and Bartel DP. Conserved seed pairing, often flanked by adenosines, indicates that thousands of human genes are microRNA targets. *Cell.* 2005;120(1):15-20.
22. Enright AJ, John B, Gaul U, Tuschl T, Sander C, and Marks DS. MicroRNA targets in Drosophila. *Genome Biol.* 2003;5(1):R1.
23. Krek A, Grun D, Poy MN, Wolf R, Rosenberg L, Epstein EJ, MacMenamin P, da Piedade I, Gunsalus KC, Stoffel M, et al. Combinatorial microRNA target predictions. *Nat Genet.* 2005;37(5):495-500.
24. Den RB, Feng FY, Showalter TN, Mishra MV, Trabulsi EJ, Lallas CD, Gomella LG, Kelly WK, Birbe RC, McCue PA, et al. Genomic prostate cancer classifier predicts biochemical failure and metastases in patients after postoperative radiation therapy. *Int J Radiat Oncol Biol Phys.* 2014;89(5):1038-46.
25. Erho N, Crisan A, Vergara IA, Mitra AP, Ghadessi M, Buerki C, Bergstralh EJ, Kollmeyer T, Fink S, Haddad Z, et al. Discovery and validation of a prostate cancer genomic classifier that predicts early metastasis following radical prostatectomy. *PloS one.* 2013;8(6):e66855.
26. Karnes RJ, Bergstralh EJ, Davicioni E, Ghadessi M, Buerki C, Mitra AP, Crisan A, Erho N, Vergara IA, Lam LL, et al. Validation of a genomic classifier that predicts metastasis following radical prostatectomy in an at risk patient population. *J Urol.* 2013;190(6):2047-53.
27. Klein EA, Yousefi K, Haddad Z, Choeurng V, Buerki C, Stephenson AJ, Li J, Kattan MW, Magi-Galluzzi C, and Davicioni E. A genomic classifier improves prediction of metastatic disease within 5 years after surgery in node-negative high-risk prostate cancer patients managed by radical prostatectomy without adjuvant therapy. *Eur Urol.* 2015;67(4):778-86.
28. Prensner JR, Zhao S, Erho N, Schipper M, Iyer MK, Dhanasekaran SM, Magi-Galluzzi C, Mehra R, Sahu A, Siddiqui J, et al. RNA biomarkers associated with metastatic progression in prostate cancer: a multi-institutional high-throughput analysis of SChLAP1. *Lancet Oncol.* 2014;15(13):1469-80.
29. Ross AE, Johnson MH, Yousefi K, Davicioni E, Netto GJ, Marchionni L, Fedor HL, Glavaris S, Choeurng V, Buerki C, et al. Tissue-based Genomics Augments Post-prostatectomy Risk Stratification in a Natural History Cohort of Intermediate- and High-Risk Men. *Eur Urol.* 2016;69(1):157-65.
30. Letellier E, and Haan S. SOCS2: physiological and pathological functions. *Front Biosci (Elite Ed).* 2016;8(189-204.
31. Kazi JU, and Ronnstrand L. Suppressor of cytokine signaling 2 (SOCS2) associates with FLT3 and negatively regulates downstream signaling. *Mol Oncol.* 2013;7(3):693-703.

32. Sen B, Peng S, Woods DM, Wistuba I, Bell D, El-Naggar AK, Lai SY, and Johnson FM. STAT5A-mediated SOCS2 expression regulates Jak2 and STAT3 activity following c-Src inhibition in head and neck squamous carcinoma. *Clin Cancer Res.* 2012;18(1):127-39.
33. Chiang YT, Wang K, Fazli L, Qi RZ, Gleave ME, Collins CC, Gout PW, and Wang Y. GATA2 as a potential metastasis-driving gene in prostate cancer. *Oncotarget.* 2014;5(2):451-61.
34. Vidal SJ, Rodriguez-Bravo V, Quinn SA, Rodriguez-Barrueco R, Lujambio A, Williams E, Sun X, de la Iglesia-Vicente J, Lee A, Readhead B, et al. A targetable GATA2-IGF2 axis confers aggressiveness in lethal prostate cancer. *Cancer Cell.* 2015;27(2):223-39.
35. He B, Lanz RB, Fiskus W, Geng C, Yi P, Hartig SM, Rajapakshe K, Shou J, Wei L, Shah SS, et al. GATA2 facilitates steroid receptor coactivator recruitment to the androgen receptor complex. *Proc Natl Acad Sci U S A.* 2014;111(51):18261-6.
36. Bao C, Li Y, Huan L, Zhang Y, Zhao F, Wang Q, Liang L, Ding J, Liu L, Chen T, et al. NF-kappaB signaling relieves negative regulation by miR-194 in hepatocellular carcinoma by suppressing the transcription factor HNF-1alpha. *Sci Signal.* 2015;8(387):ra75.
37. Chen X, Wang Y, Zang W, Du Y, Li M, and Zhao G. miR-194 targets RBX1 gene to modulate proliferation and migration of gastric cancer cells. *Tumour Biol.* 2015;36(4):2393-401.
38. Dong P, Kaneuchi M, Watari H, Hamada J, Sudo S, Ju J, and Sakuragi N. MicroRNA-194 inhibits epithelial to mesenchymal transition of endometrial cancer cells by targeting oncogene BMI-1. *Mol Cancer.* 2011;10(99.
39. Le XF, Almeida MI, Mao W, Spizzo R, Rossi S, Nicoloso MS, Zhang S, Wu Y, Calin GA, and Bast RC, Jr. Modulation of MicroRNA-194 and cell migration by HER2-targeting trastuzumab in breast cancer. *PloS one.* 2012;7(7):e41170.
40. Li Z, Ying X, Chen H, Ye P, Shen Y, Pan W, and Zhang L. MicroRNA-194 inhibits the epithelial-mesenchymal transition in gastric cancer cells by targeting FoxM1. *Dig Dis Sci.* 2014;59(9):2145-52.
41. Meng Z, Fu X, Chen X, Zeng S, Tian Y, Jove R, Xu R, and Huang W. miR-194 is a marker of hepatic epithelial cells and suppresses metastasis of liver cancer cells in mice. *Hepatology.* 2010;52(6):2148-57.
42. Wang B, Shen ZL, Gao ZD, Zhao G, Wang CY, Yang Y, Zhang JZ, Yan YC, Shen C, Jiang KW, et al. MiR-194, commonly repressed in colorectal cancer, suppresses tumor growth by regulating the MAP4K4/c-Jun/MDM2 signaling pathway. *Cell Cycle.* 2015;14(7):1046-58.
43. Zhao HJ, Ren LL, Wang ZH, Sun TT, Yu YN, Wang YC, Yan TT, Zou W, He J, Zhang Y, et al. MiR-194 deregulation contributes to colorectal carcinogenesis via targeting AKT2 pathway. *Theranostics.* 2014;4(12):1193-208.
44. Han K, Zhao T, Chen X, Bian N, Yang T, Ma Q, Cai C, Fan Q, Zhou Y, and Ma B. microRNA-194 suppresses osteosarcoma cell proliferation and metastasis in vitro and in vivo by targeting CDH2 and IGF1R. *Int J Oncol.* 2014;45(4):1437-49.
45. Khella HW, Bakhet M, Allo G, Jewett MA, Girgis AH, Latif A, Girgis H, Von Both I, Bjarnason GA, and Yousef GM. miR-192, miR-194 and miR-215: a convergent microRNA network suppressing tumor progression in renal cell carcinoma. *Carcinogenesis.* 2013;34(10):2231-9.
46. Song Y, Zhao F, Wang Z, Liu Z, Chiang Y, Xu Y, Gao P, and Xu H. Inverse association between miR-194 expression and tumor invasion in gastric cancer. *Ann Surg Oncol.* 2011;19 Suppl 3(S509-17.

47. Wu X, Liu T, Fang O, Leach LJ, Hu X, and Luo Z. miR-194 suppresses metastasis of non-small cell lung cancer through regulating expression of BMP1 and p27(kip1). *Oncogene.* 2014;33(12):1506-14.
48. Zhang Q, Wei T, Shim K, Wright K, Xu K, Palka-Hamblin HL, Jurkevich A, and Khare S. Atypical role of sprouty in colorectal cancer: sprouty repression inhibits epithelial-mesenchymal transition. *Oncogene.* 2015.
49. Zhang J, Zhao CY, Zhang SH, Yu DH, Chen Y, Liu QH, Shi M, Ni CR, and Zhu MH. Upregulation of miR-194 contributes to tumor growth and progression in pancreatic ductal adenocarcinoma. *Oncol Rep.* 2014;31(3):1157-64.
50. Chung TK, Lau TS, Cheung TH, Yim SF, Lo KW, Siu NS, Chan LK, Yu MY, Kwong J, Doran G, et al. Dysregulation of microRNA-204 mediates migration and invasion of endometrial cancer by regulating FOXC1. *International journal of cancer Journal international du cancer.* 2012;130(5):1036-45.
51. Sundaram P, Hultine S, Smith LM, Dews M, Fox JL, Biyashev D, Schelter JM, Huang Q, Cleary MA, Volpert OV, et al. p53-responsive miR-194 inhibits thrombospondin-1 and promotes angiogenesis in colon cancers. *Cancer Res.* 2011;71(24):7490-501.
52. Mathe EA, Nguyen GH, Bowman ED, Zhao Y, Budhu A, Schetter AJ, Braun R, Reimers M, Kumamoto K, Hughes D, et al. MicroRNA expression in squamous cell carcinoma and adenocarcinoma of the esophagus: associations with survival. *Clin Cancer Res.* 2009;15(19):6192-200.
53. Saad R, Chen Z, Zhu S, Jia P, Zhao Z, Washington MK, Belkhiri A, and El-Rifai W. Deciphering the unique microRNA signature in human esophageal adenocarcinoma. *PloS one.* 2013;8(5):e64463.
54. Slaby O, Srovnal J, Radova L, Gregar J, Juracek J, Luzna P, Svoboda M, Hajduch M, and Ehrmann J. Dynamic changes in microRNA expression profiles reflect progression of Barrett's esophagus to esophageal adenocarcinoma. *Carcinogenesis.* 2015;36(5):521-7.
55. Cabibi D, Caruso S, Bazan V, Castiglia M, Bronte G, Ingrao S, Fanale D, Cangemi A, Calo V, Listi A, et al. Analysis of tissue and circulating microRNA expression during metaplastic transformation of the esophagus. *Oncotarget.* 2016.
56. Kahlert C, Klupp F, Brand K, Lasitschka F, Diederichs S, Kirchberg J, Rahbari N, Dutta S, Bork U, Fritzmann J, et al. Invasion front-specific expression and prognostic significance of microRNA in colorectal liver metastases. *Cancer Sci.* 2011;102(10):1799-807.
57. Zhang C, Shu L, Kim H, Khor TO, Wu R, Li W, and Kong AT. Phenethyl isothiocyanate (PEITC) suppresses prostate cancer cell invasion epigenetically through regulating microRNA-194. *Mol Nutr Food Res.* 2016.
58. Krutzfeldt J, Rosch N, Hausser J, Manoharan M, Zavolan M, and Stoffel M. MicroRNA-194 is a target of transcription factor 1 (Tcf1, HNF1alpha) in adult liver and controls expression of frizzled-6. *Hepatology.* 2012;55(1):98-107.
59. Senanayake U, Das S, Vesely P, Alzoughbi W, Frohlich LF, Chowdhury P, Leuschner I, Hoefler G, and Guertl B. miR-192, miR-194, miR-215, miR-200c and miR-141 are downregulated and their common target ACVR2B is strongly expressed in renal childhood neoplasms. *Carcinogenesis.* 2012;33(5):1014-21.
60. Huang D, He X, Zou J, Guo P, Jiang S, Lv N, Alekseyev Y, Luo L, and Luo Z. Negative regulation of Bmi-1 by AMPK and implication in cancer progression. *Oncotarget.* 2015.

61. Jung KH, McCarthy RL, Zhou C, Uprety N, Barton MC, and Beretta L. MicroRNA-194 Regulates Hepatocytic Differentiation of Progenitor Cells by Targeting YAP1. *Stem Cells*. 2016.
62. Hoefer J, Kern J, Ofer P, Eder IE, Schafer G, Dietrich D, Kristiansen G, Geley S, Rainer J, Gunsilius E, et al. SOCS2 correlates with malignancy and exerts growth-promoting effects in prostate cancer. *Endocrine-related cancer*. 2014;21(2):175-87.
63. Iglesias-Gato D, Chuan YC, Wikstrom P, Augsten S, Jiang N, Niu Y, Seipel A, Danneman D, Vermeij M, Fernandez-Perez L, et al. SOCS2 mediates the cross talk between androgen and growth hormone signaling in prostate cancer. *Carcinogenesis*. 2014;35(1):24-33.
64. Zhu JG, Dai QS, Han ZD, He HC, Mo RJ, Chen G, Chen YF, Wu YD, Yang SB, Jiang FN, et al. Expression of SOCSs in human prostate cancer and their association in prognosis. *Mol Cell Biochem*. 2013;381(1-2):51-9.
65. Wu D, Sunkel B, Chen Z, Liu X, Ye Z, Li Q, Grenade C, Ke J, Zhang C, Chen H, et al. Three-tiered role of the pioneer factor GATA2 in promoting androgen-dependent gene expression in prostate cancer. *Nucleic Acids Res*. 2014;42(6):3607-22.
66. Bishop JL, Thaper D, and Zoubeidi A. The Multifaceted Roles of STAT3 Signaling in the Progression of Prostate Cancer. *Cancers (Basel)*. 2014;6(2):829-59.
67. Rodriguez-Berriguete G, Fraile B, Martinez-Onsurbe P, Olmedilla G, Paniagua R, and Royuela M. MAP Kinases and Prostate Cancer. *J Signal Transduct*. 2012;2012(169170.
68. Foley C, and Mitsiades N. Moving Beyond the Androgen Receptor (AR): Targeting AR-Interacting Proteins to Treat Prostate Cancer. *Horm Cancer*. 2016;7(2):84-103.
69. Stegeman S, Moya L, Selth LA, Spurdle AB, Clements JA, and Batra J. A genetic variant of MDM4 influences regulation by multiple microRNAs in prostate cancer. *Endocrine-related cancer*. 2015;22(2):265-76.
70. Selth LA, Townley S, Gillis JL, Ochnik AM, Murti K, Macfarlane RJ, Chi KN, Marshall VR, Tilley WD, and Butler LM. Discovery of circulating microRNAs associated with human prostate cancer using a mouse model of disease. *Int J Cancer*. 2011;131(3):652-61.
71. Jorgensen S, Baker A, Moller S, and Nielsen BS. Robust one-day in situ hybridization protocol for detection of microRNAs in paraffin samples using LNA probes. *Methods*. 2010;52(4):375-81.
72. Hickey TE, Irvine CM, Dvinge H, Tarulli GA, Hanson AR, Ryan NK, Pickering MA, Birrell SN, Hu DG, Mackenzie PI, et al. Expression of androgen receptor splice variants in clinical breast cancers. *Oncotarget*. 2015.
73. Selth LA, Das R, Townley SL, Coutinho I, Hanson AR, Centenera MM, Stylianou N, Sweeney K, Soekmadji C, Jovanovic L, et al. A ZEB1-miR-375-YAP1 pathway regulates epithelial plasticity in prostate cancer. *Oncogene*. 2016.
74. Moore NL, Buchanan G, Harris JM, Selth LA, Bianco-Miotto T, Hanson AR, Birrell SN, Butler LM, Hickey TE, and Tilley WD. An androgen receptor mutation in the MDA-MB-453 cell line model of molecular apocrine breast cancer compromises receptor activity. *Endocrine-related cancer*. 2012;19(4):599-613.
75. Nishikawa E, Osada H, Okazaki Y, Arima C, Tomida S, Tatematsu Y, Taguchi A, Shimada Y, Yanagisawa K, Yatabe Y, et al. miR-375 is activated by ASH1 and inhibits YAP1 in a lineage-dependent manner in lung cancer. *Cancer Res*. 2011;71(19):6165-73.
76. Zinonos I, Labrinidis A, Lee M, Liapis V, Hay S, Ponomarev V, Diamond P, Findlay DM, Zannettino AC, and Evdokiou A. Anticancer efficacy of Apo2L/TRAIL is

retained in the presence of high and biologically active concentrations of osteoprotegerin in vivo. *J Bone Miner Res.* 2011;26(3):630-43.
77. Selth LA, Townley S, Gillis JL, Ochnik AM, Murti K, Macfarlane RJ, Chi KN, Marshall VR, Tilley WD, and Butler LM. Discovery of circulating microRNAs associated with human prostate cancer using a mouse model of disease. *International journal of cancer Journal international du cancer.* 2012;131(3):652-61.
78. Budczies J, Klauschen F, Sinn BV, Gyorffy B, Schmitt WD, Darb-Esfahani S, and Denkert C. Cutoff Finder: a comprehensive and straightforward Web application enabling rapid biomarker cutoff optimization. *PloS one.* 2012;7(12):e51862.
79. Grasso CS, Wu YM, Robinson DR, Cao X, Dhanasekaran SM, Khan AP, Quist MJ, Jing X, Lonigro RJ, Brenner JC, et al. The mutational landscape of lethal castration-resistant prostate cancer. *Nature.* 2012;487(7406):239-43.

CHAPTER 5: ROLE OF microRNA-375 IN PROSTATE CANCER METASTASIS

"A ZEB1-miR-375-YAP1 pathway regulates epithelial plasticity in prostate cancer"

The following chapter includes a manuscript published in Oncogene, followed by supplementary figures and tables that make up a significant proportion of the work completed as a part of this PhD. A general discussion of this chapter had been included at the end.

Statement of Authorship

Title of Paper	A ZEB1-miR-375-YAP1 pathway regulates epithelial plasticity in prostate cancer
Publication Status	☑ Published ☐ Accepted for Publication ☐ Submitted for Publication ☐ Unpublished and Unsubmitted w ork w ritten in manuscript style
Publication Details	A ZEB1-miR-375-YAP1 pathway regulates epithelial plasticity in prostate cancer. Luke. A Selth, **Rajdeep Das**, Scott L Townley, Isabel Coutinho, Adrienne R Hanson, Margaret Centenera, Nataly Stylianou, Katrina Sweeney, Carolina Soekmadji, Lidija Jovanovic, Colleen C Nelson, Amina Zoubeidi, Lisa M Butler, Gregory J Goodall, Brett G Hollier, Philip A. Gregory, Wayne D Tilley. Oncogene. 2016 Jun 6. doi: 10.1038/onc.2016.185.

Principal Author

Name of Principal Author	Luke A Selth		
Contribution to the Paper	Conceived the project; project supervision; designed the experiments; analysed data; made the figures; and wrote the manuscript		
Signature		Date	27/07/2016

Co-Author Contributions

By signing the Statement of Authorship, each author certifies that:

i. the candidate's stated contribution to the publication is accurate (as detailed above);

ii. permission is granted for the candidate in include the publication in the thesis; and

iii. the sum of all co-author contributions is equal to 100% less the candidate's stated contribution.

Name of Co-Author (Candidate)	Rajdeep Das		
Contribution to the Paper	Performed experiments (cell culture and transfection, RT-qPCR, western blots, cellular migration and invasion assays, chick chorioallantoic membrane assays); co-designed experiments (with Dr Selth); and analysed data		
Certification:	This paper reports on original research I conducted during the period of my Higher Degree by Research candidature and is not subject to any obligations or contractual agreements with a third party that would constrain its inclusion in this thesis.		
Overall percentage (%)	35%		
Signature		Date	27/07/2016

Name of Co-Author	Scott L Townley
Contribution to the Paper	Assisted in cell culture and transfection, ChIP-qPCR, luciferase assay; analysed data
Signature	Date 28/7/16

Name of Co-Author	Isabel Coutinho
Contribution to the Paper	Assisted with Western blotting; analysed data
Signature	Date 28/7/2016

Name of Co-Author	Adrienne R Hanson
Contribution to the Paper	Assisted with Western blotting and qRT-PCR; analysed data
Signature	Date 27-7-16.

Name of Co-Author	Margaret M Centenera
Contribution to the Paper	Provided primary prostate cancer cohort; helped in manuscript evaluation
Signature	Date 27.7.16

Name of Co-Author	Nataly Stylianou
Contribution to the Paper	Generated the stable LNCaP-iZEB1 cell line
Signature	Date 1/8/2016

Name of Co-Author	Katrina Sweeney		
Contribution to the Paper	Generated the stable LNCaP-iZEB1 cell line		
Signature		Date	27/07/2016

Name of Co-Author	Carolina Soekmadji		
Contribution to the Paper	Provided serum samples from men with metastatic prostate cancer (with matched clinical data)		
Signature	I, Dr Luke Selth (first author of the publication and principal supervisor of Rajdeep Das) sign on behalf of Carolina Soekmadji. We tried to contact Carolina several times to get her signature, unfortunately she was not reachable.	Date	14-08-16

Name of Co-Author	Lidija Jovanovic		
Contribution to the Paper	Provided serum samples from men with metastatic prostate cancer (with matched clinical data)		
Signature		Date	1/8/2016

Name of Co-Author	Colleen C Nelson		
Contribution to the Paper	Provided serum samples from men with metastatic prostate cancer (with matched clinical data)		
Signature		Date	28/07/2016

Name of Co-Author	Amina Zoubeidi		
Contribution to the Paper	Assisted in experimental design; provided reagents		
Signature		Date	August 2nd, 2016

Name of Co-Author	Lisa M Butler		
Contribution to the Paper	Analysed data and edited the paper		
Signature		Date	27/7/16

Name of Co-Author	Gregory J Goodall		
Contribution to the Paper	Analysed data and edited the paper		
Signature		Date	27 July 2016

Name of Co-Author	Brett G Hollier		
Contribution to the Paper	Designed experiments; assisted in data analysis; and edited the paper		
Signature		Date	27-7-2016

Name of Co-Author	Philip A. Gregory		
Contribution to the Paper	Designed experiments; assisted in data analysis; and edited the paper		
Signature		Date	27/07/2016

Name of Co-Author	Wayne D Tilley		
Contribution to the Paper	Project supervision; assisted in data analysis and interpretation; manuscript editing		
Signature		Date	27/07/2016

My role in this study

Performed experiments (cell culture and transfection, RT-qPCR, western blots, cellular migration and invasion assays, chick chorioallantoic membrane assays); co-designed experiments with my principal supervisor Dr Luke Selth; and analysed data

Oncogene (2016), 1–11

www.nature.com/onc

ORIGINAL ARTICLE

A ZEB1-miR-375-YAP1 pathway regulates epithelial plasticity in prostate cancer

LA Selth[1,2,3], R Das[1,2,3], SL Townley[1,2,3], I Coutinho[1,2,3], AR Hanson[1,2,3], MM Centenera[2,3,4], N Stylianou[5], K Sweeney[5], C Soekmadji[5], L Jovanovic[5], CC Nelson[5], A Zoubeidi[6], LM Butler[2,3,4], GJ Goodall[3,7,8], BG Hollier[5], PA Gregory[3,7] and WD Tilley[1,2,3]

MicroRNA-375 (miR-375) is frequently elevated in prostate tumors and cell-free fractions of patient blood, but its role in genesis and progression of prostate cancer is poorly understood. In this study, we demonstrated that miR-375 is inversely correlated with epithelial–mesenchymal transition signatures (EMT) in clinical samples and can drive mesenchymal–epithelial transition (MET) in model systems. Indeed, miR-375 potently inhibited invasion and migration of multiple prostate cancer lines. The transcription factor YAP1 was found to be a direct target of miR-375 in prostate cancer. Knockdown of YAP1 phenocopied miR-375 overexpression, and overexpression of YAP1 rescued anti-invasive effects mediated by miR-375. Furthermore, transcription of the miR-375 gene was shown to be directly repressed by the EMT transcription factor, ZEB1. Analysis of multiple patient cohorts provided evidence for this ZEB1-miR-375-YAP1 regulatory circuit in clinical samples. Despite its anti-invasive and anti-EMT capacities, plasma miR-375 was found to be correlated with circulating tumor cells in men with metastatic disease. Collectively, this study provides new insight into the function of miR-375 in prostate cancer, and more broadly identifies a novel pathway controlling epithelial plasticity and tumor cell invasion in this disease.

Oncogene advance online publication, 6 June 2016; doi:10.1038/onc.2016.185

http://www.nature.com/onc/journal/vaop/ncurrent/full/onc2016185a.html

Introduction

Prostate cancer is the second most common solid tumor in men worldwide and, despite significant advances in early diagnosis and management, it remains a leading cause of cancer-related death.[1] The vast majority of these deaths are a consequence of metastasis, which occurs primarily to lymph nodes and bone. Although mortality rates are decreasing overall, for men presenting with *de novo* metastatic prostate cancer there has been no improvement in overall or disease-specific survival in the past 25 years.[2] A better understanding of the pathobiology of prostate cancer metastasis is urgently required to improve patient outcomes.

Metastasis of epithelial-derived cancers, such as prostate cancer, encompasses a complex series of events whereby epithelial tumor cells invade the surrounding stroma, enter blood or lymphatic circulation, arrest at distant anatomic sites, exit the vasculature, and colonize a secondary location through metastatic outgrowth. An emerging paradigm is the importance of epithelial plasticity, defined as flux between epithelial and mesenchymal

states, for successful metastasis.[3] During epithelial–mesenchymal transition (EMT), sessile, structured epithelial cells lose cell-to-cell contacts and gain expression of mesenchymal factors, enabling migration and invasion into surrounding stroma and facilitating traversal of circulatory systems.[4] Thiery postulated more than a decade ago that the reverse process, mesenchymal–epithelial transition (MET), could facilitate successful metastatic colonization of disseminated tumor cells,[5] since redifferentiation to an epithelial state is associated with restoration of proliferative capacity. Although the clinical relevance of MET remains somewhat contentious, recent studies utilizing *in vivo* experimental models have provided strong evidence for its importance during secondary tumor development.[6, 7, 8, 9, 10]

Epithelial plasticity in cancer is primarily triggered by soluble factors secreted from the surrounding stroma that impinge on tumor cell signaling pathways, including TGF-β, Wnt/β-catenin, FGF, EGF and Notch.[4] These pathways in turn converge on central transcriptional mediators of the EMT program, for example members of the Snail, Twist and ZEB families, which orchestrate the changes in cell state.[4] In addition to these transcription factors, more recent work has found that microRNAs (miRNAs, miRs), small, non-coding regulators of gene expression, are critical regulators of epithelial plasticity.[11, 12]

MiR-375 has been described as a robust biomarker of prostate cancer, both within the tumor and in circulation,[13] but its molecular function has remained largely uncharacterized in this disease. Here we demonstrate that miR-375 occupies a nexus between Zinc finger E-box binding homeobox 1 (ZEB1) and Yes-associated protein 1 (YAP1) in a novel pathway that regulates epithelial plasticity and tumor cell invasion in prostate cancer, and provide new insight into the association between circulating miR-375 and metastasis.

Results

MiR-375 is elevated in prostate cancer and associated with an epithelial phenotype

To assess the robustness of the association between miR-375 and prostate cancer, we conducted a meta-analysis of 7 published data sets.[14, 15, 16, 17, 18, 19] In each of the data sets, miR-375 was elevated in malignant compared to normal tissue, with an overall mean increase in expression of 2.4-fold compared with non-malignant tissue (Figure 1a; P=0.003). This meta-analysis demonstrates that elevated miR-375 expression is a common characteristic of prostate cancer.

To elucidate potential functional consequences of elevated miR-375 in prostate cancer, we initially subjected a cohort of 98 primary tumors with matched miRNA:mRNA data[17] to gene set enrichment analysis.[20] As expected, gene sets comprised of predicted miR-375 targets were significantly negatively correlated with miR-375, validating the approach (Supplementary Figure 1). By scanning curated gene sets in the MSigDB collection,[20] we found that genes known to be elevated in prostate cancer were associated with high miR-375 expression, providing additional evidence for its link to this disease (Supplementary Figure 2). Interestingly, we also observed a prominent negative association of miR-375 with several EMT gene sets (Figure 1b and Supplementary Figure 3). To further test its association with epithelial phenotypes, miR-375 expression was examined in 48 cell lines classified as epithelial (*n*=11) or mesenchymal (*n*=37) from the NCI-60 panel, and was found to be significantly higher in epithelial lines (Figure 1c). We expanded on these findings by quantitating miR-375 expression in a panel of prostate cancer cell lines, and found it to be highest in the 22Rv1, VCaP and C4-2B models, which possess epithelial features, and lowest in the PC3 model, which possesses a more mesenchymal phenotype[21] (Figure 1d). Another line with more epithelial features, LNCaP,[22] and DU-145, which has an undefined phenotype according to NCI-60 classification,[21] exhibited intermediate expression of miR-375 (Figure 1d). Collectively, our results indicate that miR-375 is a marker of epithelial differentiation in prostate cancer.

MiR-375 promotes MET of mesenchymal prostate cancer cell lines

A recent report demonstrated a role for miR-375 in reversing EMT-like features associated with tamoxifen resistance in breast cancer cells.[23] Combined with our findings above, we hypothesized that miR-375 may directly inhibit EMT and/or facilitate MET in prostate cancer. To test this idea, we ectopically expressed miR-375 in PC3 cells, which possess a more mesenchymal-like gene expression profile,[21] and found it was sufficient to increase the expression of epithelial markers (*CDH1* (E-cadherin; only at the RNA level, protein was undetectable) and *Zona occludens-1* (ZO-1)) and decrease the expression of mesenchymal markers (*FN1*(Fibronectin) and *VIM* (Vimentin)) (Figures 2a and b). These data indicate that miR-375 can drive an epithelial-like program in PC3 cells.

The capacity of cancer cells to migrate and invade is an important requirement of metastasis, and both of these characteristics are a hallmark of EMT. With this in mind, the effect of miR-375 on migration and invasion of prostate cancer cell lines was assessed. Increasing the levels of miR-375 hampered the invasive (Figure 2c) and migratory (Figure

2d) capacity of PC3 cells, findings that were re-capitulated in DU-145 cells (Figure 2c and Supplementary Figure 4). We also tested the effect of transient overexpression of miR-375 on the invasive capacity of the AR-positive, androgen-independent LNCaP derivative, C4-2B, and observed a similar deficit in invasive and migratory capacity (Figure 2c and Supplementary Figure 4). Collectively, these results indicate that miR-375 can facilitate MET and thereby suppress migration and invasion of prostate cancer cells.

Epithelial differentiation states are often also associated with higher rates of proliferation. However, ectopic expression of miR-375 significantly decreased the viability of PC3, DU145 and C4-2B cells, as well as enhancing cell death in DU145 cells (Figure 2e and Supplementary Figure 4). Growth suppression by miR-375 was only evident after 3 days in PC3 cells, indicating that the repression of prostate cancer cell migration and invasion, which were evident within ~10–15 h, were independent of this anti-proliferative effect.

Since transient overexpression can potentially yield spurious results, we used locked nucleic acid (LNA) inhibitors of miR-375 to further evaluate its function. We focused on the anti-invasive capacity of miR-375 as a biologically relevant readout of its role in prostate cancer cells, and used the C4-2B line, which has relatively high endogenous levels of miR-375, as the model system. As expected, suppression of miR-375 activity with an LNA inhibitor caused C4-2B cells to invade more efficiently through Matrigel (Figure 2f).

We subsequently examined the anti-invasive activity of miR-375 in a more physiologically relevant setting by using chick chorioallantoic membrane (CAM) assays.[24] Invasion of cells through the ectoderm of the CAM into the mesoderm was assessed on day 14 of chick embryo development by cytokeratin (CK) immunohistochemistry and haematoxylin and eosin (H&E) staining. C4-2B cells transfected with negative-control LNA invaded through the ectoderm of the CAM very poorly (Figure 2g, left images). By contrast, transfection of C4-2B cells with the miR-375 LNA inhibitor greatly enhanced their capacity to disrupt the ectodermal layer and invade into the mesoderm (Figure 2g, right images). Quantitation of the CAM assay data are shown in Figure 2h.

MiR-375 targets YAP1 to inhibit EMT in prostate cancer

To identify relevant genes through which miR-375 may exert its ability to suppress EMT and cell growth and maintain epithelial differentiation, we searched the literature and examined lists of predicted targets. MiR-375 is known to target YAP1 in neuroendocrine lung cancer and colorectal cancer.[25, 26] *YAP1* is an oncogene that is amplified in many human malignancies,[27] and encodes a major downstream effector of the Hippo pathway that can promote growth and, in some cases, EMT in cancer model systems.[28, 29] We examined the expression of YAP1 in a panel of prostate cancer cell lines and found that it was highest in the more invasive and/or mesenchymal lines, namely C4-2B, PC3 and DU145 cells, and very low or undetectable in the more epithelial LNCaP, 22Rv1 and VCaP lines (Figure 3a). To determine whether YAP1 may be a relevant target of miR-375 in prostate cancer, we ectopically expressed miR-375 in PC3 and DU145 cells and found that this caused a reduction in YAP1 expression at both the mRNA and protein level (Figure 3b). Conversely, inhibition of miR-375 with an LNA inhibitor resulted in a modest but reproducible increase in YAP1 protein in C4-2B cells (Figure 3c). To confirm that this inverse relationship was a result of direct targeting, miR-375 was co-transfected with a construct containing the *YAP1* 3′-UTR downstream of a constitutively active luciferase reporter gene. As expected, transfection with a miR-375 mimic significantly decreased luciferase expression compared with a negative-control miRNA mimic (Figure 3d). The biological relevance of miR-375 in relation to YAP1 signaling was confirmed by the observation that miR-375 transfection caused decreased activity of a YAP1-responsive promoter (Figure 3e) and reduced expression of a key YAP1 target gene, *Survivin* (Figure 3f).

Having confirmed that YAP1 was a direct target of miR-375 in prostate cancer, we examined its function in prostate cancer cells. YAP1 knockdown decreased the expression of Vim and FN-1 in PC3 cells (Figure 3g), suggesting that it acts to maintain a mesenchymal phenotype. Moreover, loss of YAP1 attenuated the invasion, migration and growth of PC3, DU145 and C4-2B cells (Figures 3h–j; Supplementary Fig. 5), phenocopying miR-375 overexpression.

To further interrogate the relevance of YAP1 as a miR-375 target, we undertook a rescue experiment using a vector expressing the *YAP1* open reading frame (Supplementary Figure 6), which cannot be targeted by miR-375. Importantly, co-expression of three different doses of the YAP1 vector rescued the anti-invasive activity of miR-375 (Figure

3k). Thus, YAP1 is a key downstream target by which miR-375 mediates this tumour suppressive function.

MiR-375 is negatively regulated by ZEB1 during EMT

EMT is controlled primarily by transcription factors of the Snail, Twist and ZEB families. ZEB1 is a key regulator of the expression of epithelial miRNAs, such as miR-200 family members,[30, 31] and acts by binding to E-box-like regulatory elements in gene promoters. Interestingly, the miR-375 promoter also contains E-box-like motifs (Figure 4a) that may be binding sites for ZEB1 in breast cancer,[32]leading us to postulate that miR-375 could be a ZEB1-regulated gene. Supporting this hypothesis, siRNA knockdown of ZEB1 increased the levels of miR-375 in DU-145 cells compared with a control siRNA (Figure 4b). Moreover, ZEB1 knockdown was associated with concomitant loss of YAP1 (Figure 4c). These observations suggest that YAP1 is an indirect target gene of ZEB1 via miR-375.

To determine whether ZEB1 directly binds to the miR-375 gene loci to mediate its transcriptional repression, we conducted chromatin immunoprecipitation (ChIP) assays coupled to qPCR using primers that amplify 4 regions proximal to miR-375 (Figure 4a). We detected significant ZEB1 enrichment at each of the genomic regions, as well as at a positive control locus (the *miR-200b/200a/429* promoter),[33]in DU145 and PC3 cells (Figure 4d). Further supporting our ChIP results, analysis of an ENCODE ChIP-seq data set[34] demonstrated ZEB1 enrichment upstream of the miR-375 gene in HepG2 liver cancer cells (Figure 4e). To confirm that ZEB1 is a direct repressor of the miR-375 gene, we cloned two separate regions (L1, L2) of the miR-375 gene upstream of a luciferase reporter gene (Figure 4a). Following*ZEB1* knockdown, luciferase expression was significantly increased when it was coupled to the L1 and L2 promoter fragments or to a *miR-200b/200a/429* promoter positive control[30] (Figure 4f). Given that both the L1 and L2 fragments were regulated by ZEB1, we speculated that the two E-box-like motifs shared by these DNA sequences (Figure 4a, marked 3 and 4) could be direct target sites for ZEB1. However, reporter constructs with deletion mutations of either of these motifs, separately or together, remained repressed by ZEB1 (Supplementary Figure 7). Collectively, these *in vitro* assays demonstrate that miR-375 is under the direct control of ZEB1 in prostate cancer cells, and that regulatory elements within both the L1 and L2 regions—but likely not the E-box-like motifs 3 and 4—are required for ZEB1 binding and transcriptional regulation.

To further investigate the role of miR-375 and YAP1 in ZEB1-mediated EMT, we transduced LNCaP cells with a doxycycline-inducible form of ZEB1. This model, referred to as LNCaP-iZEB1, underwent a robust EMT within 3 days of doxycycline treatment, evidenced by a more mesenchymal cell morphology with loss of cell–cell contacts (Figure 4g) coupled with decreased epithelial and increased mesenchymal marker expression (Figures 4h and i). Confirming our earlier results, doxycycline treatment led to recruitment of ZEB1 to the miR-375 promoter (Figure 4j) and a concomitant decrease in miR-375 expression (Figure 4k). This finding suggests ZEB1-mediated repression of miR-375 occurs during EMT in prostate cancer cells.

Clinical evidence for a ZEB1-miR-375-YAP1 pathway

To assess the clinical relevance of the ZEB1-miR-375-YAP1 pathway in clinical prostate cancer samples, we examined the relative expression of these factors in a cohort of 26 prospectively collected primary tumors. Supporting the cell line data, negative correlations between the expression levels of miR-375 and both *ZEB1* and*YAP1* were evident, although the miR-375/ZEB1 correlation did not reach statistical significance. By contrast, and supporting the proposed pathway, we found a positive correlation between *ZEB1* and *YAP1* in this cohort (Figure 5a). Importantly, we validated these correlations in two large, publically available data sets from Memorial Sloan-Kettering Cancer Center (Taylor cohort)[17] and The Cancer Genome Atlas (Figure 5b and Supplementary Figure 8). Collectively, these findings suggest that transcriptional downregulation of miR-375 by ZEB1, resulting in de-repression of YAP1, is a pathway that can occur in prostate cancer specimens.

Plasma miR-375 is correlated with circulating tumor cell count

Circulating cell-free miR-375 is a robust biomarker of metastatic prostate cancer,[35,36,37] but our results indicate that miR-375 is a tumor suppressor. To shed further light on this apparent discrepancy, we examined the plasma levels of miR-375 in a contemporary cohort of metastatic castration-resistant prostate cancer (CRPC) patients with known circulating tumor cell (CTC) counts generated by the CellSearch system (Supplementary Table 1). In this cohort, we found that circulating miR-375 was higher in CTC-positive (n=17) versus CTC-negative (n=35) samples (Figure 5c). Indeed, there was a high degree of correlation between these two clinical parameters (all samples: Spearman r=0.5137, P<0.0001), which was particularly evident when considering only the CTC-positive samples (Figure 5d). Thus, while miR-375 acts as a tumor suppressor in prostate

cancer model systems, when it is released into the circulation of men with advanced disease miR-375 may serve as a proxy for CTC numbers.

Discussion

While numerous studies have demonstrated the potential of miR-375 as a tissue and circulating biomarker of prostate cancer, its molecular function has remained largely uncharacterized. In this study, we (1) revealed that miR-375 is a novel repressor of EMT and invasion in prostate cancer, (2) identified YAP1 as a biologically relevant target gene of miR-375 in this process and a potential oncogene in prostate cancer in its own right, (3) revealed a regulatory circuit between ZEB1, miR-375 and YAP1 in prostate cancer model systems that is also evident in clinical samples and (4) demonstrated that circulating miR-375 may be a proxy for CTC count in the blood of men with metastatic CRPC. The ZEB1-miR-375-YAP1 pathway controlling epithelial plasticity and invasion in prostate cancer, characterized herein, is summarized in a model shown in Figure 5e.

Our findings suggest that miR-375 is a potent tumor suppressor by inhibiting EMT, invasion and growth of prostate cancer cells. Given that these traits are generally associated with poor outcome,[38] it is somewhat surprising that levels of circulating miR-375 have been linked to metastasis and disease progression following surgery.[35, 37, 39] Our study has provided insight into this apparent discrepancy by demonstrating that circulating miR-375 is positively correlated with CTC count in men with metastatic CRPC. Interestingly, serum miR-375 levels are also positively correlated with CTC count and a poor prognostic marker in breast cancer patients,[40] suggesting that circulating levels of this miRNA could be a general proxy of CTCs in cancer.

With the tumor suppressive function of miR-375 in mind, we envision at least four non-mutually exclusive explanations for the association between circulating miR-375 and prostate cancer metastasis. First, CTCs may actively release miR-375 to mitigate its repressive effects on growth and EMT, thereby resulting in cells with higher metastatic capacity. Second, despite the apparent tumor suppressive capacity of miR-375 in prostate cancer cell lines and primary tumors, we cannot rule out the possibility that it promotes metastasis and disease progression in CTCs, disseminated tumor cells, micrometastases and/or metastases. In this respect, high circulating levels of miR-375 could be indicative of cancer cells that have undergone or are undergoing MET to facilitate the development of clinical metastasis.[6] Third, recent studies have highlighted the complexity of the

relationship between epithelial plasticity and tumor spread. While early studies indicated that EMT was associated with the acquisition of stemness, tumor-initiating capacity and metastasis,[41] more recent work has indicated that epithelial (or quasi-epithelial) phenotypes are also associated with self-renewal and pluripotency.[7, 9] For example, Celia-Terrassa *et al.*[7] demonstrated that PC3 cells with epithelial features had enhanced self-renewal and pluripotency and greater metastatic capacity than their mesenchymal counterparts, despite the latter being more migratory and invasive *in vitro*. Thus, the epithelial and growth-suppressive phenotype mediated by high levels of miR-375 may, in certain contexts, be associated with the acquisition of metastasis-promoting traits, such as stemness. Finally, our gene set enrichment analysis analysis revealed that miR-375 is positively correlated with androgen signalling in multiple tumor data sets (Supplementary Figure 9). A molecular mechanism that potentially underpins this association was recently elucidated by Chu *et al.*,[42] who demonstrated that the androgen receptor (AR) indirectly promotes miR-375 transcription by suppressing DNA methylation of its promoter. Thus, miR-375 may also serve as a proxy for AR activity and PSA levels, which are themselves prognostic in prostate cancer. It is worth noting that miR-375 could have dichotomous roles as a tumor suppressor and metastamiR in prostate cancer, depending on disease stage, a concept that was also suggested by a paper published during preparation of this manuscript.[43]

In summary, our findings indicate that ZEB1-mediated regulation of miR-375 and its downstream targets, in particular YAP1, influences epithelial plasticity and cell invasion in prostate cancer. This study has implications in terms of utilizing miR-375 as a biomarker and developing novel therapeutic strategies targeting epithelial plasticity in advanced prostate cancer.[3, 44]

Materials and methods

Analysis of miR-375 expression in published data sets – prostate cancer data sets

Data were downloaded from GEO (Ambs, GSE8126; Wach, GSE23022; Schaefer, GSE14857; Lin, GSE36803), ArrayExpress (Martens-Uzunova: E-TABM-794) or The Cancer Genome Atlas data portal. The Taylor data set was downloaded and processed as described previously.[37] *P*-values were determined using unpaired (Ambs, Taylor, Martens, The Cancer Genome Atlas) or paired (Wach, Schaefer, Lin) *t*-tests and the *P*-value for the

'Combined' value was calculated using a one-sample *t*-test, with all contributing data sets/cohorts weighted equally.

NCI60 data sets

Data were downloaded from CellMiner Database Version 1.5 (Blower[45] and Liu[46]) or GEO (Sokilde,[47] GSE26375).

Gene Set Enrichment Analysis (GSEA)

The correlation between expression levels of miR-375 and 19,389 genes was calculated using matched miRNA and mRNA data from 98 prostate tumors in the Taylor cohort.[17] Genes were subsequently ranked according to Pearson correlation coefficient (*r*) value (shown by a heat map), and gene set enrichment analysis (Preranked analysis) was implemented using the Broad Institute's public GenePattern server, using default parameters.

Cell line culture and transfection

PC-3, DU145, C4-2B, LNCaP, VCaP and 22Rv1 human prostate carcinoma cells were obtained from the American Type Culture Collection. All cell lines underwent verification by short-tandem repeat profiling in 2014 by CellBank Australia. PC-3 cells were maintained in RPMI-1640 containing 5% fetal bovine serum. DU145, C4-2B, LNCaP and 22Rv1 cells were cultured in RPMI+10% fetal bovine serum. VCaP cells were maintained in Dulbecco's modified Eagle's medium containing 10% fetal bovine serum, 1% sodium pyruvate, 1% MEM non–essential amino acids and 0.1 nM5α-dihydrotestosterone (DHT; Sigma).

Transfection of miRNA, siRNA, LNA and plasmids

PC3 cells, DU145 and C4-2B cells were transfected with 20 nM miRNA mimics (miR-375 or negative-control mimic; Shanghai GenePharma, Shanghai, China), 20 nMsiRNA (YAP1 siRNA (catalogue number SI02662954) or control siRNA; Qiagen, Valencia, CA, USA), 30 nM siRNA (ZEB1 siRNA pool (catalogue numbers HSS110548, HSS11054 and HSS110550) or control siRNA; Invitrogen, Carlsbad, CA, USA) or 50 nM LNA inhibitor (miR-375 LNA (catalogue number 4101396-102) or control LNA (199006-102); Exiqon, Denmark) using RNAiMAX transfection reagent (Life Technologies, Gaithersburg, MD, USA), according to the manufacturer's instructions. For plasmid transfections, cells were

transfected with Lipofectamine 2000 (Life Technologies), according to the manufacturer's instructions.

Quantitative real-time PCR analysis of miRNA expression

Total RNA was extracted from prostate cancer cells using Trizol essentially as described previously[48] except that the RNA was precipitated with 2.5 volume of ethanol, 10 mM $MgCl_2$, 0.1 volume of 5 M NaCl, and 20 μg of Glyco-Blue (Life Technologies) overnight at −20° C. Levels of miR-375 and U6 small nuclear RNA were measured by qRT-PCR using Taqman assays, following the manufacturer's instructions (Life Technologies). The expression of miR-375 was normalized to U6.

Quantitative real-time PCR analysis of mRNA expression

RNA extraction from cells, using Trizol reagent, and qRT-PCR was done as described previously.[48] *GAPDH* was used for normalization of qRT-PCR data. Primer sequences are available on request.

Western blotting

Protein extraction from cells, using RIPA buffer, and western blotting was done as described previously.[48] Antibodies used in western blotting were: N-cadherin (sc-7939; Santa Cruz Biotechnology, Santa Cruz, CA, USA); Vimentin (ab92547; Abcam, Cambridge, MA, USA); ZO-1 (Santa Cruz, sc-10804); Fibronectin (610077; BD Biosciences, San Jose, CA); E-cadherin (BD Biosciences, 610182); ZEB1 (3396; Cell Signalling Technology, Beverly, MA, USA); EpCAM (2626, Cell Signalling Technology); YAP1 (sc-15407; Santa Cruz); and COXIV (4850, Cell Signalling Technology).

Cell migration and invasion assays

Invasion assays were carried out as described previously.[49] Briefly, 100 μl of diluted Matrigel (diluted 1:1 in cold PBS) was pipetted into each transwell insert (6.5 mm transwell, 8.0-μm pore size) and incubated at 37 °C for 30 min to solidify. Subsequently, the transwell inserts were inverted and 100 μl of PCa cell suspension (1×10^5 cells per ml) transfected with miRNA, siRNA or LNA was pipetted onto the upward-facing microporous membrane. Following cell attachment (4 h at 37 °C), the inserts were placed right side up and 100 μl of fetal bovine serum was added. After 3 days of invasion/growth,

inserts were washed in PBS and cells were fixed with methanol and then stained with propidium idodine. Stained cells were visualized by a confocal microscope (Zeiss LSM 700, Carl Zeiss AG, Oberkochen, Germany) using a × 20 objective. Image J software (US National Institutes of Health, Bethesda, MD, USA) was used to quantify staining. Treatments were done in biological triplicates, and three to four separate regions of each insert were quantified. All experiments were conducted at least twice.

For the rescue experiments shown in Figure 3k, cells were first transfected with miRNA and then with a YAP1 overexpression plasmid (FLAG-tagged YAP1[50]) the following day. These double-transfected cells were then used in invasion assays as described above.

Scratch wound migration assays were performed using an Incucyte (Essen BioScience, Ann Arbor, MI, USA) as described previously.[51] Briefly, following transient transfection of prostate cancer cells with miRNA mimics, siRNAs and appropriate controls in 24-well microplates (Essen Image Lock plates, Essen BioScience), cells were grown to confluence and then a thin 'wound' was introduced by scratching with sterile pipette tips. The microplate was then placed in the Incucyte imaging system to record the migratory ability of the cells into the 'wound' over a period of time. Treatments were done in biological quadruplicates, and 3 separate regions of the scratch was analyzed. All experiments were conducted at least twice.

Growth curves

Growth curves were performed as described previously.[52] Treatments were done in biological triplicates. All experiments were conducted at least twice.

Chick chorioallantoic membrane assays (CAM)

CAM assays were carried out essentially as described,[24] using the *in ovo* method. C4-2B (5×10^4) cells were mixed with Matrigel and grafted on top of the CAM of day 11 chick embryos. Haematoxylin and eosin (H&E) staining and cytokeratin immunohistochemistry were performed as described.[24] For quantitative analysis of cancer cell invasion into the mesoderm layer, 8 to 12 CAM images from each embryo (6 per treatment) were assessed; the graph shown in Figure 2h represents the mean percentage of images with invasion into the mesoderm± s.e.m.

Luciferase assays

To determine whether miR-375 directly targets the YAP1 3′-UTR in prostate cancer cells, PC3 cells were transfected with miR-375 or negative control. The following day, cells were transfected again with a Renilla luciferase (luc) YAP1 3′-UTR construct[25] (a kind gift from Prof Takashi Takahashi) using Lipofectamine 2000 reagent. After 2 days, luciferase activity was measured using a Dual Luciferase Reporter assay (Promega, Madison, WI, USA). Firefly luciferase activity was normalized to Renilla luciferase activity.

To determine whether miR-375 modulates YAP1 activity, we utilized a YAP/TAZ-responsive synthetic promoter driving luciferase expression (8xGTIIC-luciferase).[53]

To assess whether ZEB1 can repress the miR-375 promoter, the L1 and L2 miR-375 promoter regions were cloned into the pGL3 vector. pGL4 constructs containing an alternative promoter region with wildtype or deleted E-box-like motifs have been described previously:[25] the Δ3, Δ4 and Δ3,4 constructs shown in Supplementary Figure 7 correspond to pGL4-ΔE1, pGL4-ΔE2 pGL4-ΔE12 described by Nishikawa and colleagues, respectively. DU145 cells were transfected with either ZEB1 or scrambled siRNA using RNAiMAX transfection reagent. The following day, cells were transfected again with the indicated pGL3 constructs and pRL-CMV (Promega) using Lipofectamine 2000 transfection reagent. After 2 days, luciferase activity was measured using a Dual Luciferase Reporter assay. Firefly luciferase activity was normalized to Renilla luciferase activity. A *miR-200b/200a/429* promoter:luciferase construct[30] was used as a positive control.

Chromatin immunoprecipitation

ChIP assays were performed as described previously[54] using a ZEB1 antibody from Santa Cruz (sc-25388). Two known ZEB1 binding sites from the *miR-200a/b/429*promoter (one just upstream and one just downstream of the transcriptional start site; referred to as -0.124 and 0.180, respectively) were used as positive controls; a site further upstream of the *miR-200a/b/429* promoter (−2.778) was used as negative control.[33]

Prospective primary prostate cancer cohort

Primary prostate cancer specimens were obtained with written informed consent through the Australian Prostate Cancer BioResource from 26 men who underwent robotic radical prostatectomy at St. Andrew's Hospital (Adelaide, Australia). The study was approved by the University of Adelaide Human Research Ethics Committee (HREC). Tissues were homogenized in Qiazol using a Precellys 24 tissue homogenizer (Bertin Technologies, France) before RNA extraction with miRNeasy mini kits (Qiagen, Germany). DNAse treatment was performed using a TurboDNase kit (Ambion, Austin, TX, USA) according to the manufacturer's instructions. RNA was quantified using a Nanodrop. Reverse transcription was performed on 400 ng total RNA using the iScript kit (BioRad Laboratories, Hercules, CA, USA) according to the manufacturer's instructions. Levels of miR-375, *YAP1* and *ZEB1* were not normally distributed, hence Spearman's correlation tests were used to examine relationships between their levels. Levels of miR-375, *YAP1* and *ZEB1* exhibited coefficients of variation of 114%, 43% and 117%, respectively.

Quantitation of circulating miR-375 in men with metastatic prostate cancer

Blood samples from men with metastatic prostate cancer (n=52) were obtained with written informed consent from Princess Alexandra Hospital (Brisbane, Australia), under a protocol approved by the Metro South Health Service District HREC and the Queensland University of Technology HREC. CellSearch analysis was used to count circulating tumor cells from whole blood, as described.[55] To measure levels of miR-375 in matched plasma samples, RNA was extracted and qRT-PCR (with pre-amplification) was carried out as described previously.[39] Levels of miR-375 in the two groups (CTC-negative and CTC-positive) were not normally distributed, hence a two-tailed Mann–Whitney test was used for comparison. Levels of miR-375 exhibited a coefficient of variation of 158% and 178% in the CTC-negative and CTC-positive groups, respectively.

Statistical analyses

All statistical analyses were carried out using GraphPad Prism (version 5; GraphPad Software, San Diego, CA, USA) or MedCalc (version 12; MedCalc Software, Mariakerke, Belgium). Details of statistical tests used are provided in the appropriate methods section or figure legends.

Figures and legends

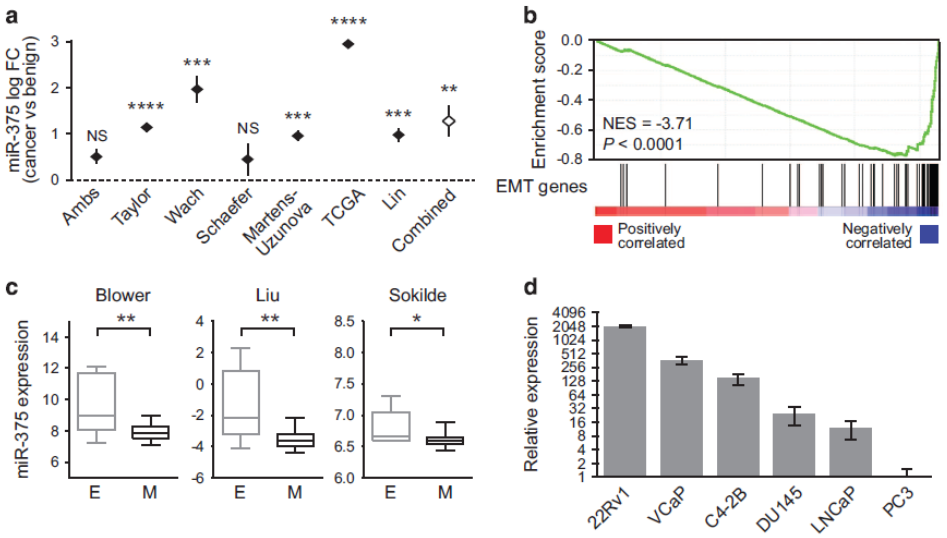

Figure 1. MiR-375 is a marker of epithelial differentiation in prostate cancer. (**a**) Expression of miR-375 expression in published prostate cancer data sets. The filled diamond represents the mean change in expression level (log2 fold-change (FC)) from normal to primary prostate cancer tissue, whereas the vertical line represents ± s.e.m. The open diamond represents the mean change in expression level of miR-375 when all studies are combined. NS, not significant; $^{*}P < 0.05$; $^{**}P < 0.01$; $^{***}P < 0.001$; $^{****}P < 0.0001$. (**b**) Negative association between miR-375 and EMT, as demonstrated by gene set enrichment analysis (GSEA), in the Taylor cohort.[17] (**c**) Boxplots depicting the expression level of miR-375 in epithelial (E, $n = 11$) and mesenchymal (M, $n = 37$) cell lines from the NCI60 panel. *P*-values were determined using unpaired two-sided *t*-tests ($^{*}P < 0.05$; $^{**}P < 0.01$). (**d**) Expression of miR-375 in prostate cancer cell lines (normalized to the reference small RNA U6: $\Delta Cq = Cq\ U6 - Cq$ miR-375). The heavy line is the average of 3 separate samples, with lighter lines representing ± s.e.m.

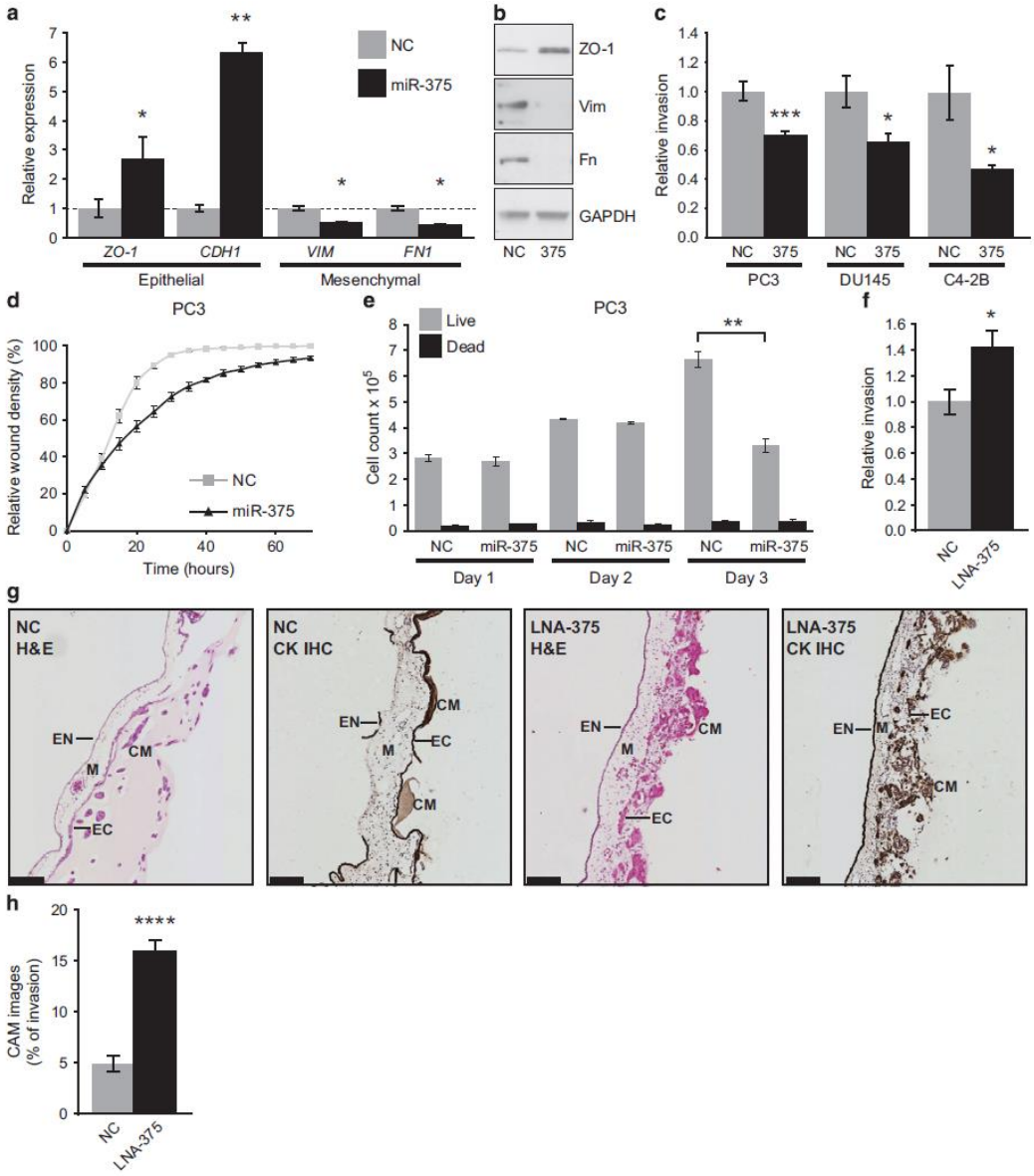

Figure 2. MiR-375 suppresses EMT and invasion of prostate cancer cells. (**a**) MiR-375 inhibits mesenchymal marker expression and promotes epithelial marker expression at the RNA level in PC3 cells compared to a negative control (NC). *CDH1*, E-cadherin; ZO-1, *Zona occludens-1*; *FN1*, Fibronectin; *VIM*, Vimentin. Values for the NC were set to 1, and error bars are ± s.e.m. All the expression data are normalized to the *GAPDH* reference gene. (**b**) MiR-375 ('375') inhibits mesenchymal marker expression (Fn, Vim) and promotes epithelial marker (ZO-1) expression at the protein level in PC3 cells. Zona occludens-1, ZO-1; Fn, Fibronectin; Vim, Vimentin. (**c**) MiR-375 inhibits invasion of PC3, DU145 and C4-2B cells. Values for the NC were set to 1, and error bars are ± s.e.m. *P*-values were determined using unpaired two-sided *t*-tests (**P* < 0.05; ****P* < 0.001). (**d**) MiR-375 inhibits migration of PC3 cells. (**e**) MiR-375 inhibits growth of PC3 cells. Live and dead cells were counted using Trypan blue assays. *P*-values were determined using unpaired two-sided *t*-tests (NS, not significant; ***P* < 0.01). (**f**) MiR-375 LNA inhibitor (LNA-375) enhances the invasive capacity of C4-2B cells. Values for the NC were set to 1, and error bars are ± s.e.m. *P*-value was determined using an unpaired two-sided *t*-test (**P* < 0.05). (**g**) Representative images from CAM invasion assays. C4-2B cancer cell matrigel grafts (CM) were placed on top of the ectoderm (EC) layer and cancer cell invasion into the CAM mesoderm (M) was assessed in day 14 chick embryos. Endoderm, EN. Shown are haematoxylin and eosin (H&E) and cytokeratin (CK) IHC images. Scale bars = 100 µm. (**h**) Quantitation of CAM invasion assay data. Data were generated from 48–60 images from 6 chicken embryos per treatment. Data represent the mean percentage of images with invasion into the mesoderm ± s.e.m. *P*-value was determined using an unpaired two-sided *t*-test (*****P* < 0.0001).

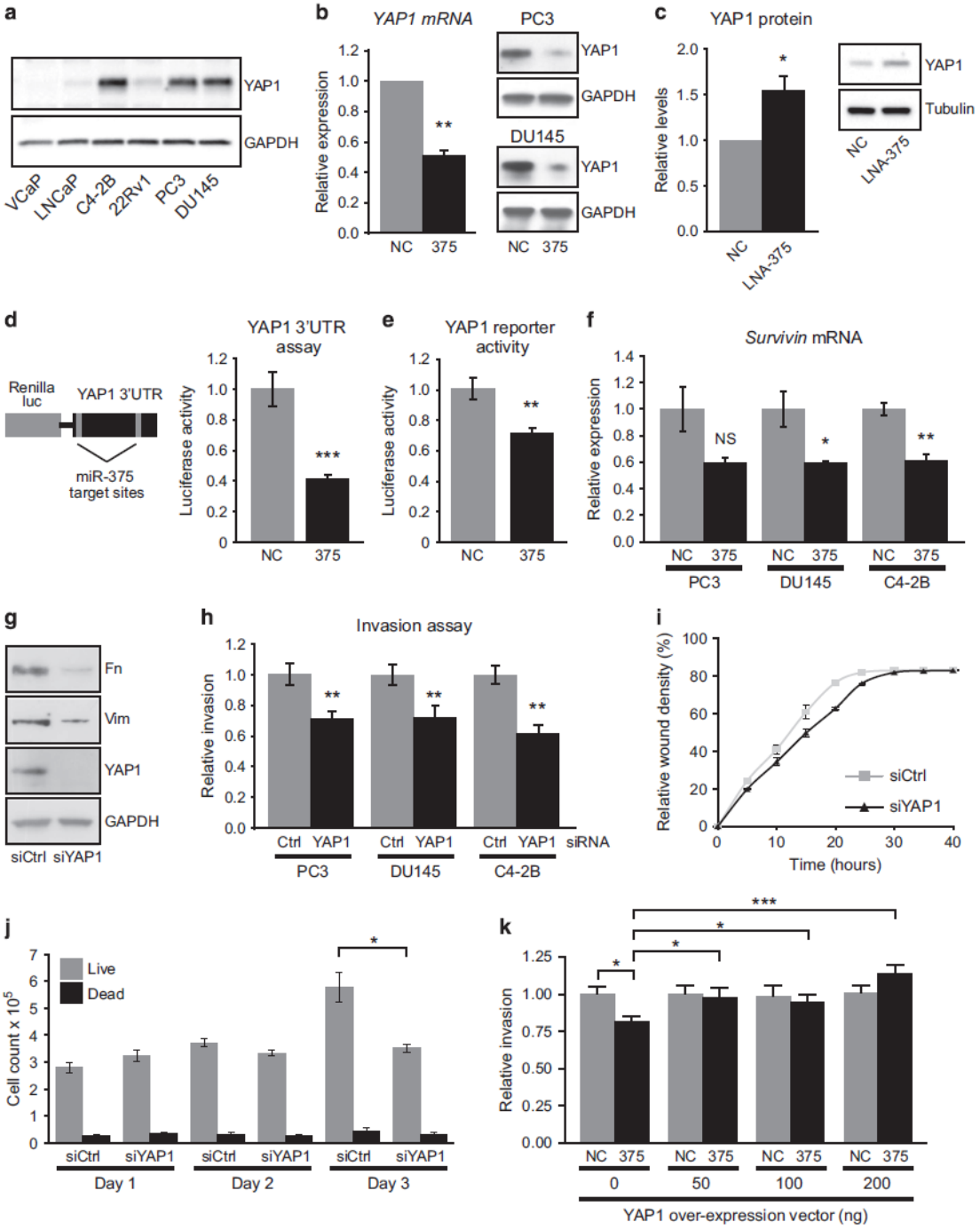

Figure 3. YAP1 is targeted by miR-375 and promotes EMT-like characteristics and invasion of prostate cancer cells. (**a**) Levels of YAP1 protein in a panel of prostate cancer cell lines. (**b**, left) MiR-375 ('375') decreases *YAP1* RNA expression in PC3 cells compared to a negative control (NC). Data are normalized to the *GAPDH* reference gene. (**b**, right) MiR-375 decreases YAP1 protein levels in PC3 and DU145 cells. (**c**) An LNA inhibitor of miR-375 increases YAP1 protein levels in C4-2B cells. The graph on the left shows the average of three independent experiments, in which YAP1 was normalized to tubulin. The western blots on the right are representative images. (**d**) MiR-375 directly targets the YAP1 3′-UTR. Luciferase:YAP1 3′-UTR construct is shown on left. Luciferase activity for 'NC' was set to 1; bars represent the average of 6 wells per treatment, and error bars are ± s.e.m. A *P*-value was determined using an unpaired two-sided *t* test (***$P < 0.001$). (**e**) MiR-375 inhibits transcription from a YAP1 reporter construct. Luciferase activity for NC was set to 1; bars represent the average of 6 wells per treatment, and error bars are ± s.e.m. A *P*-value was determined using an unpaired two-sided *t*-test (**$P < 0.01$). (**f**) MiR-375 reduces expression of the YAP1 target gene, *Survivin*. Data are normalized to the *GAPDH* reference gene. (**g**) YAP1 knockdown decreases the expression of mesenchymal markers in PC3 cells. (**h**) YAP1 knockdown inhibits invasion of PC3, DU145 and C4-2B cells. Values for the NC were set to 1, and error bars are ± s.e.m. *P*-values were determined using unpaired two-sided *t*-tests (**$P < 0.01$). (**i**) YAP1 knockdown inhibits migration of PC3 cells. (**j**) YAP1 knockdown inhibits growth of PC3 cells. Live and dead cells were counted using Trypan blue assays. *P*-values were determined using unpaired two-sided *t*-tests (NS, not significant; *$P < 0.05$). (**k**) Overexpression of YAP1 rescues the anti-invasive activity of miR-375. *P*-values were determined using unpaired two-sided *t*-tests (*$P < 0.05$; ***$P < 0.001$).

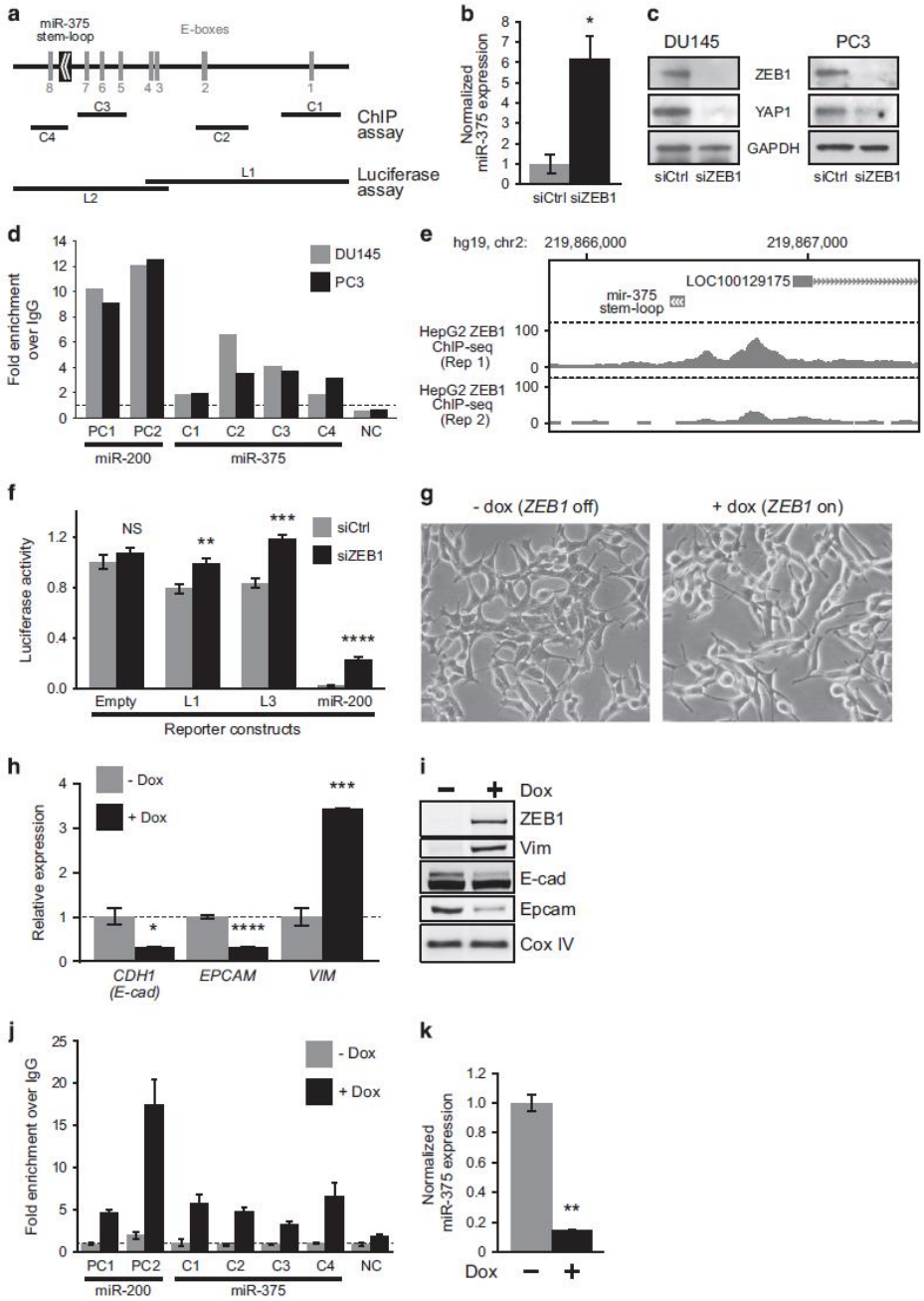

Figure 4. MiR-375 expression is under direct control of the ZEB1 transcription factor. (**a**) Diagram showing the miR-375 gene with upstream and downstream E/Z boxes (E-box-like motifs). Amplicons assessed in the ChIP assay are shown in the middle panel. Cloned fragments of the miR-375 loci used in promoter reporter assays are shown in the bottom panel. (**b**) ZEB1 knockdown causes increased miR-375 expression in DU145 cells. MiR-375 expression was measured by qRT-PCR and normalized to the reference small RNA U6. *P*-value was determined using an unpaired two-sided *t*-test (*$P < 0.05$). (**c**) ZEB1 knockdown causes loss of YAP1 protein. YAP1 levels were measured by western blotting in DU145 (left) and PC3 (right) cells). (**d**) ChIP assay showing ZEB1 binding proximal to the miR-375 gene. The dotted line demarcates no enrichment over an IgG control ChIP. Two known ZEB1 binding sites from the *miR-200a/b/429* promoter were used as positive controls, whereas a site further upstream of the *miR-200a/b/429* promoter (−2.778) was used as negative control (NC). (**e**) UCSC screenshot showing ENCODE ChIP-seq data sets (two biological replicates; GEO sample accession number GSM1010809) that demonstrate ZEB1 binding upstream of the miR-375 gene in HEPG2 cells. Genes in the region (miR-375 and LOC100129175) are shown, with arrows signifying direction of transcription. (**f**) ZEB1 regulates expression of the miR-375 promoter. DU145 cells were transfected with either control (siCtrl) or ZEB1 siRNA (siZEB1) and the indicated pGL3 constructs and luciferase activity measured. A *miR-200b/200a/429* promoter:luciferase construct was used as a positive control. The value for the empty plasmid treated with siCtrl was set to 1. Bars represent the average of 6 wells per treatment, and error bars are ± s.e.m. *P*-values were determined using unpaired two-sided *t*-tests (**$P < 0.01$; ***$P < 0.001$; ****$P < 0.0001$). (**g**) Doxycycline-induced expression of ZEB1 in LNCaP prostate cancer cells induces EMT, as evidenced by a characteristic switch in cell morphology. (**h**) Doxycycline-induced expression of ZEB1 in LNCaP prostate cancer cells induces EMT, as evidenced by changes in gene expression of EMT markers. Levels of E-cadherin (*CDH1*), *EPCAM*, and Vimentin (*VIM*) were measured by qRT-PCR and normalized to the *RPL32* reference gene. The control treatment (- dox) was set to 1. Error bars are ± s.e.m. *P*-values were determined using unpaired two-sided *t*-tests (*$P < 0.05$; **$P < 0.01$; ***$P < 0.001$). (**i**) Doxycycline-induced expression of ZEB1 in LNCaP prostate cancer cells induces EMT, as evidenced by changes in protein expression of EMT markers ZEB1, Vimentin (Vim), E-cadherin (E-cad) and Epcam. CoxIV was used as a loading control. (**j**) ChIP assay showing that ZEB1 is recruited to the miR-375 gene following ZEB1-mediated EMT in LNCaP cells. The dotted line demarcates no enrichment over an IgG control ChIP. Positive (*miR-200a/b/429* promoter) and negative control (NC) binding sites were as in **d**. (**k**) MiR-375 levels decrease in response to ZEB1-mediated EMT in LNCaP cells. The expression of miR-375 was normalized to reference small RNA U6; the control treatment (- dox) was set to 1. Error bars are ± s.e.m. *P*-value was determined using an unpaired two-sided *t*-test (**$P < 0.01$).

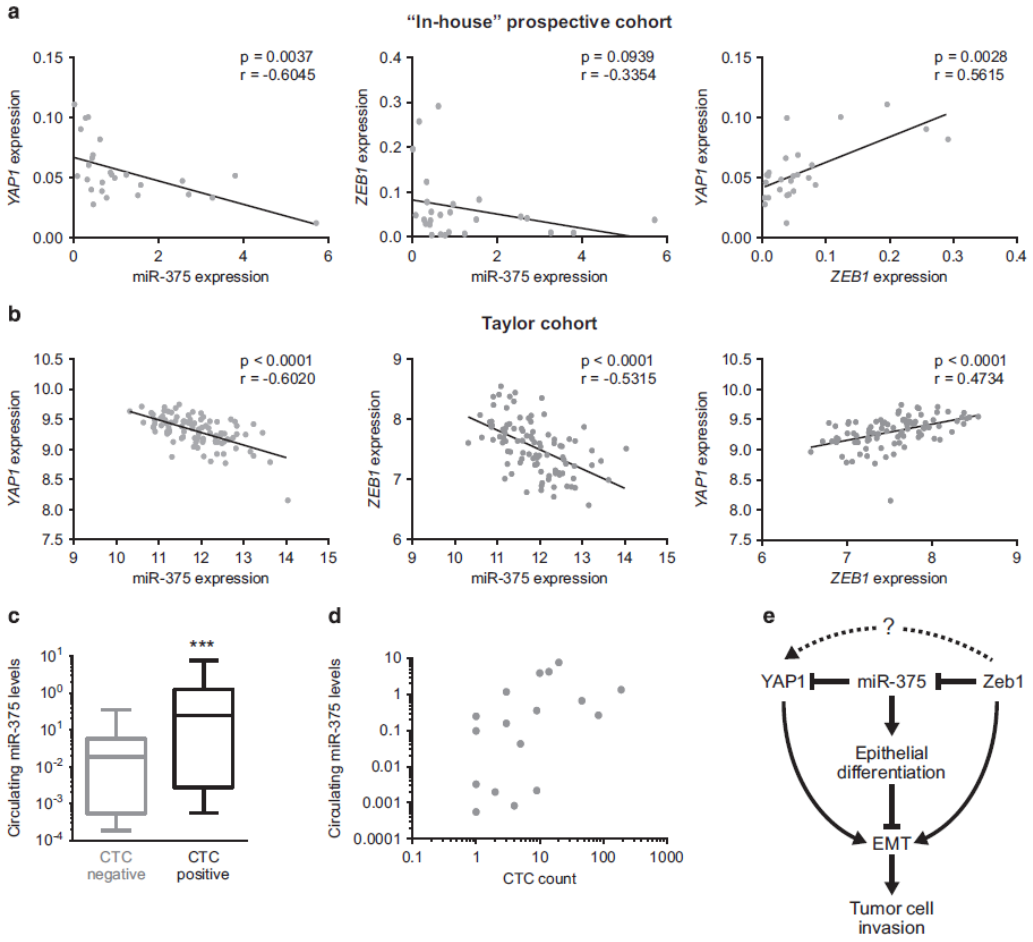

Figure 5. Evidence for a ZEB1-miR-375-YAP1 pathway in clinical samples. (**a, b**) ZEB1 and YAP1 are negatively correlated with miR-375 and positively correlated with each other in two cohorts. (**a**) Graphs show correlations in 26 primary tumors collected prospectively 'in-house'. Gene and miR-375 expression was determined by qRT-PCR; genes were normalized to *GAPDH*, whereas miR-375 was normalized to the reference small RNA U6. *P* and *r* values were calculated using Spearmans's correlation tests. (**b**) Graphs show correlations in 98 tumors from the Taylor data set. *P* and *r* values were calculated using Pearson's correlation tests. (**c**) Circulating miR-375 levels are higher in CTC-positive ($n = 17$) versus CTC-negative ($n = 35$) metastatic CRPC patients. Circulating miR-375 was measured as described in Materials and Methods. *P*-value was determined using a two-tailed Mann–Whitney test (***$P < 0.001$). (**d**) Circulating miR-375 levels are correlated with CTC count in metastatic CRPC patients. (**e**) Model for control of epithelial plasticity in prostate cancer by ZEB1, miR-375 and YAP1. The '?' symbol refers to the fact that we cannot rule out miR-375-independent mechanisms by which ZEB1 drives YAP1 expression.

Supplementary figures and legends

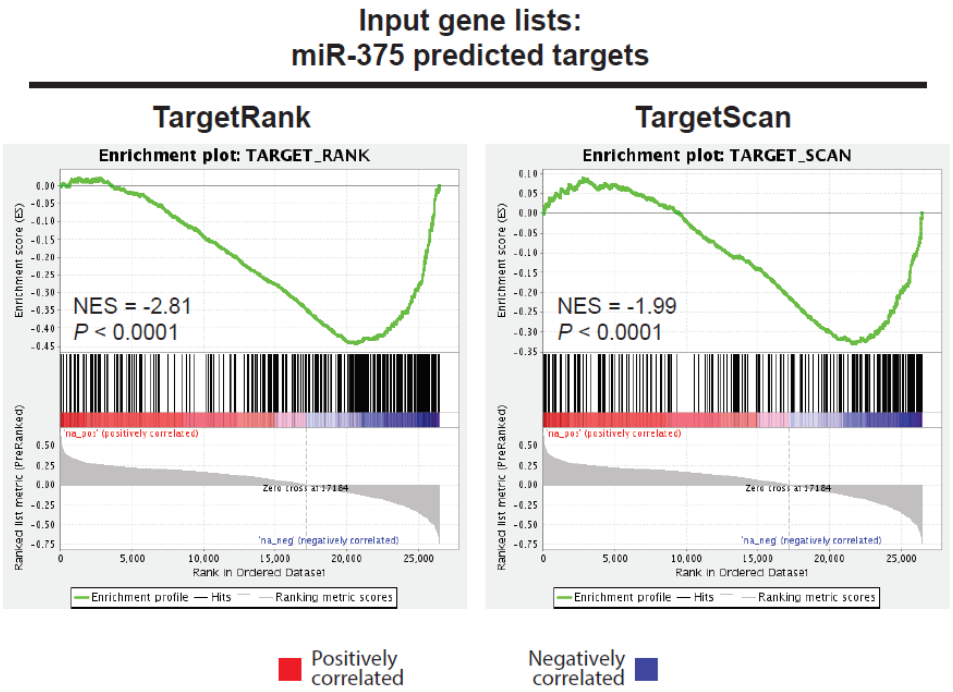

Supplementary Figure 1

Negative correlation between miR-375 and its predicted target genes, as demonstrated by gene set enrichment analysis (GSEA).[1] The correlation between expression levels of miR-375 and 19,389 genes was calculated using matched miRNA and mRNA data from 98 prostate tumors in the Taylor cohort.[2] Genes were subsequently ranked according to Pearson correlation coefficient (r) value (shown by a heat map), and GSEA (Preranked analysis) was implemented using the Broad Institute's public GenePattern server, using default parameters. Lists of predicted miR-375 target genes were downloaded from TargetRank[3] and TargetScan[4] websites. Running enrichment scores are plotted (top graph) and normalized enrichment scores (NES) and *P* values are indicated.

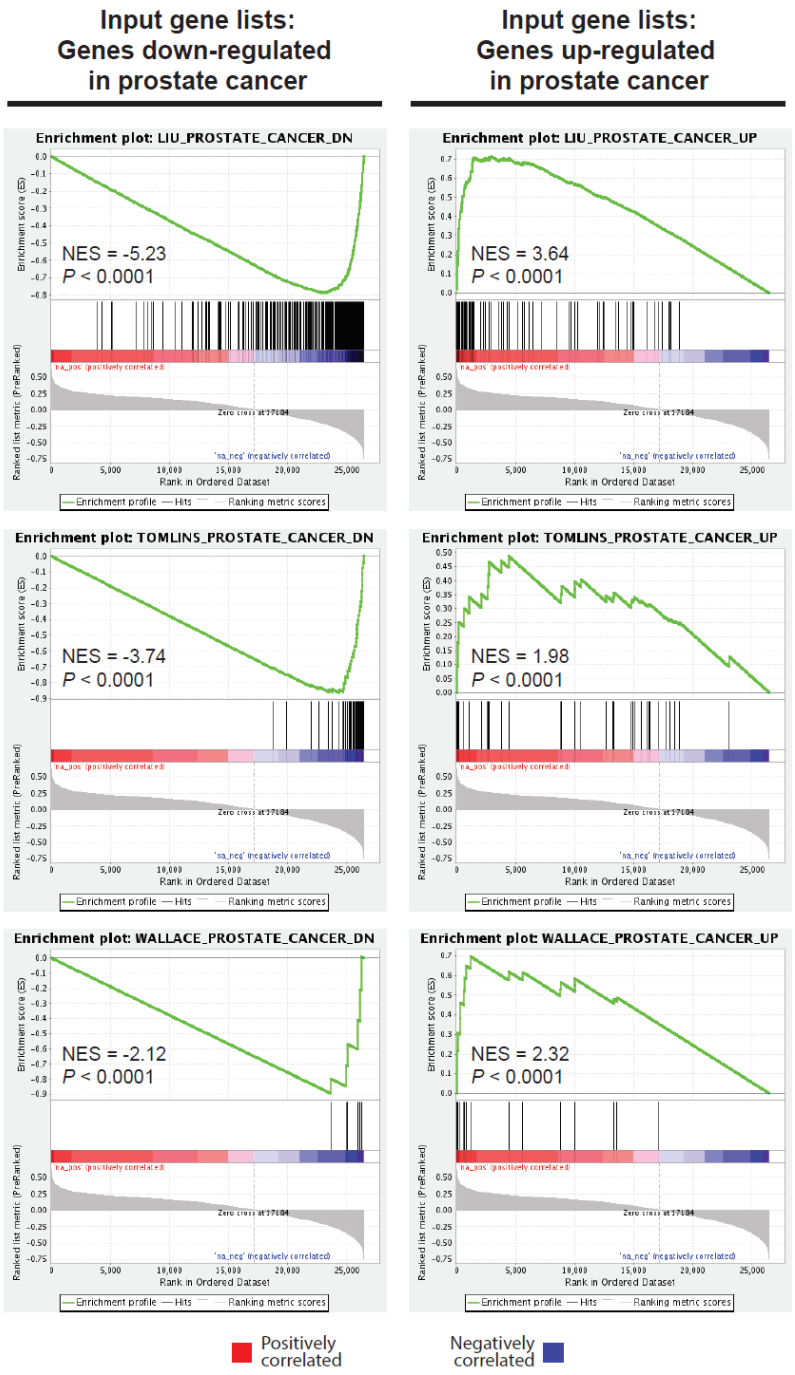

Supplementary Figure 2

Correlation between miR-375 and genes altered in prostate cancer, as demonstrated by GSEA. See Supplementary Figure Legend 1 for more detail on the methodology. The gene sets[5-7] were obtained from MSigDB. Plots on the left are gene sets down-regulated in prostate cancer, which are negatively correlated with miR-375. Plots on the right are gene sets up-regulated in prostate cancer, which are positively correlated with miR-375.

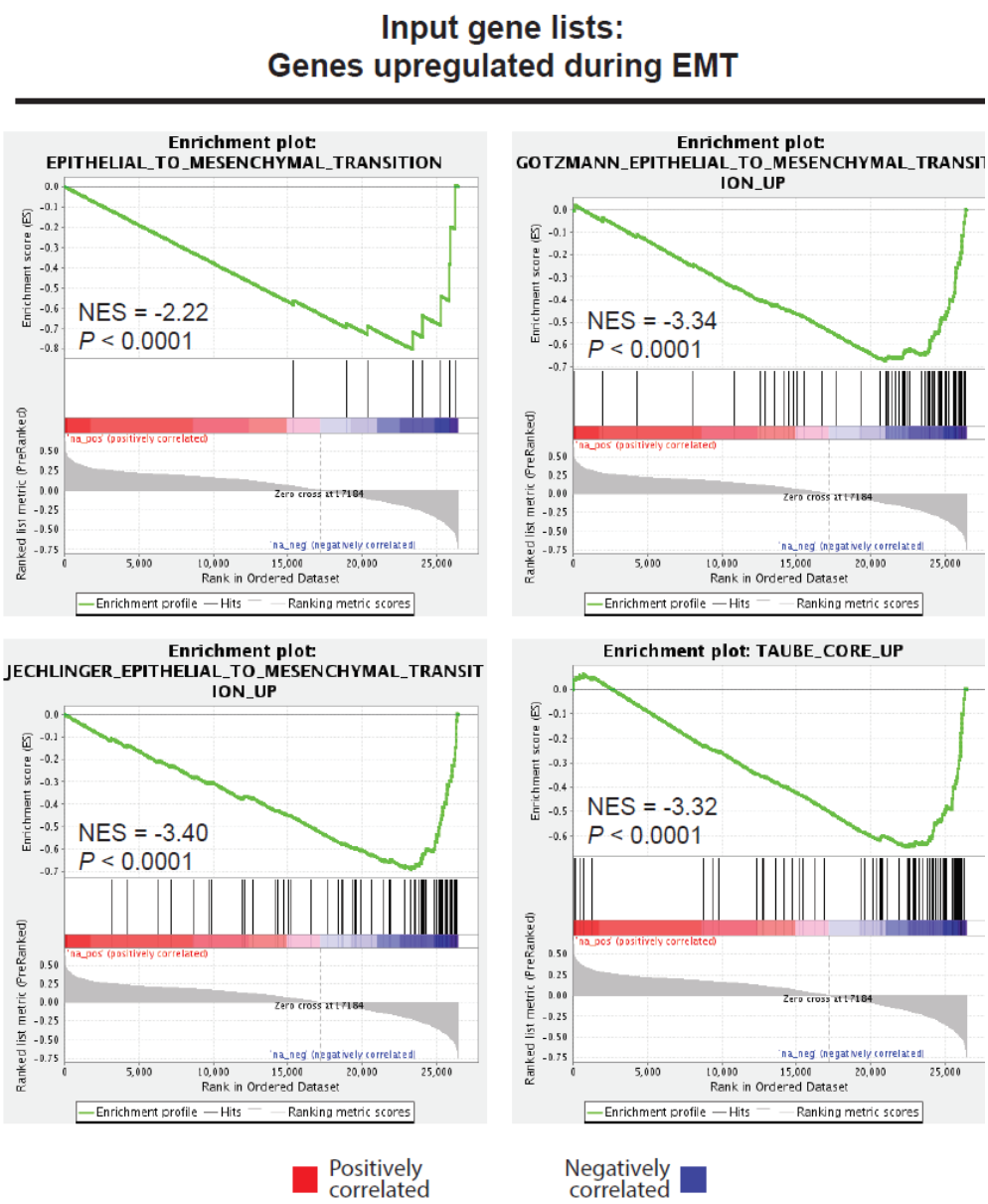

Supplementary Figure 3

Negative correlation between miR-375 and EMT gene sets, as demonstrated by GSEA. See Supplementary Figure Legend 1 for more detail on the methodology. The gene sets[8-10] were obtained from MSigDB.

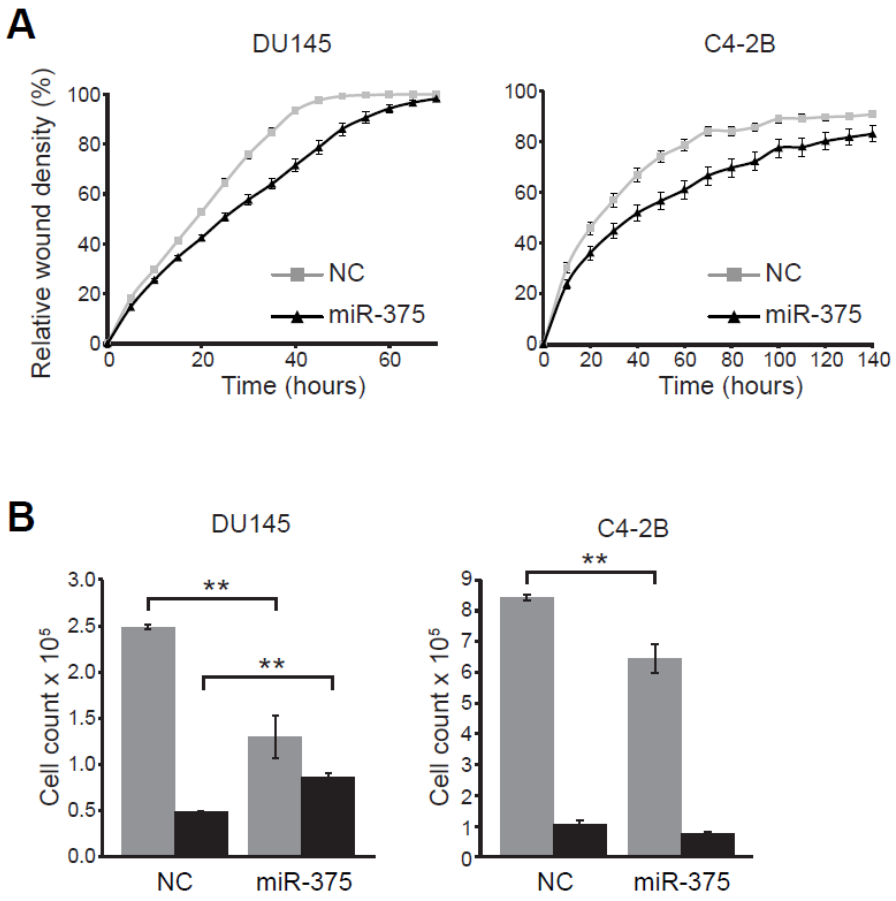

Supplementary Figure 4

(A) MiR-375 inhibits migration of DU145 and C4-2B cells. **(B)** MiR-375 inhibits growth of DU145 and C4-2B cells. Live and dead cells were counted using Trypan blue assays. *P* values were determined using unpaired *t* tests (NS, not significant; **, $P < 0.01$).

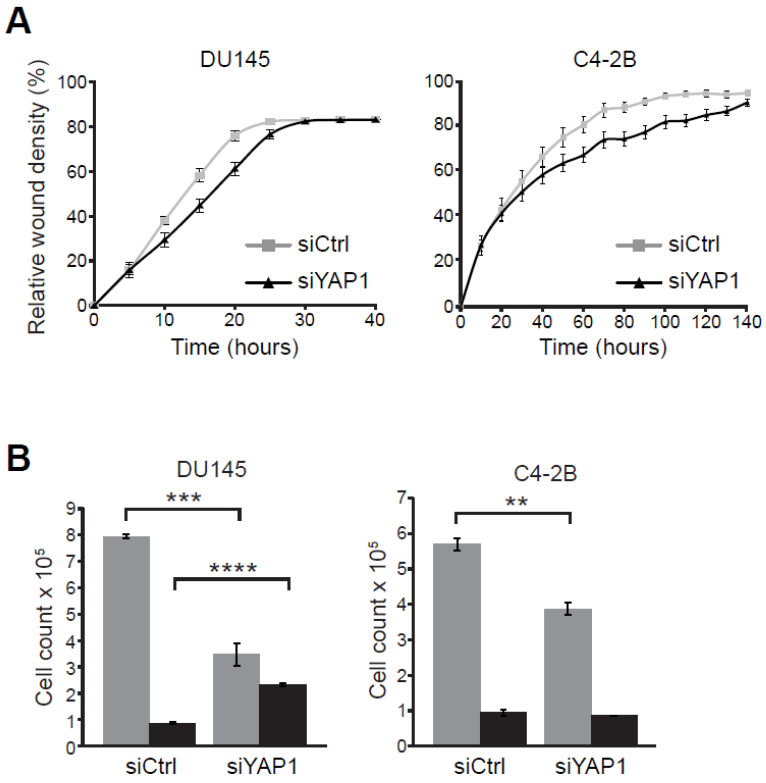

Supplementary Figure 5

(A) Knockdown of YAP1 inhibits migration of DU145 and C4-2B cells. **(B)** Knockdown of YAP1 inhibits growth of DU145 and C4-2B cells. Live and dead cells were counted using Trypan blue assays. *P* values were determined using unpaired *t* tests (**, $P < 0.01$; ***, $P < 0.001$; ****, $P < 0.0001$).

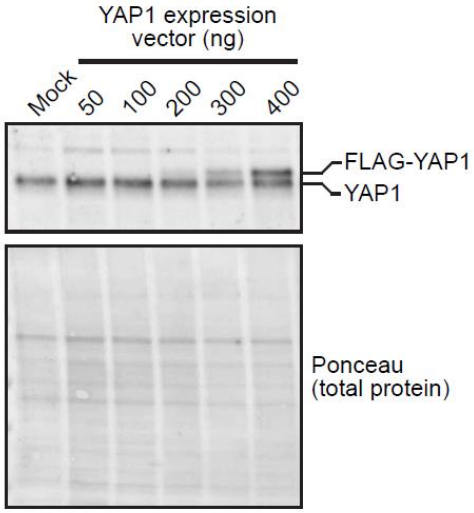

Supplementary Figure 6

Dose-dependent over-expression of FLAG-tagged YAP1 (FLAG-YAP1) in C4-2B cells. Cells were transfected with the indicated amount of expression vector and two days later total protein was assessed by Western blotting using an antibody (sc-15407; Santa Cruz) that detects both the FLAG-tagged form and the endogenous YAP1.

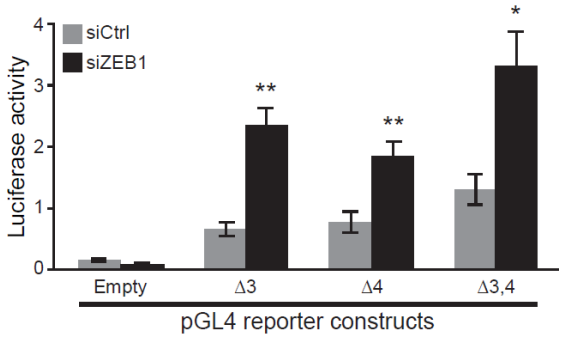

Supplementary Figure 7

Deletion of E-box-like motifs 3 (Δ3), 4 (Δ4) or both (Δ3,4) does not affect ZEB1 regulation of the miR-375 promoter. DU145 cells were transfected with either control (siCtrl) or ZEB1 siRNA (siZEB1) and the indicated pGL4 constructs and luciferase activity measured. Bars represent the average of 6 wells per treatment, and error bars are ± SEM. *P* values were determined using unpaired *t* tests (*, $P < 0.05$; **, $P < 0.01$).

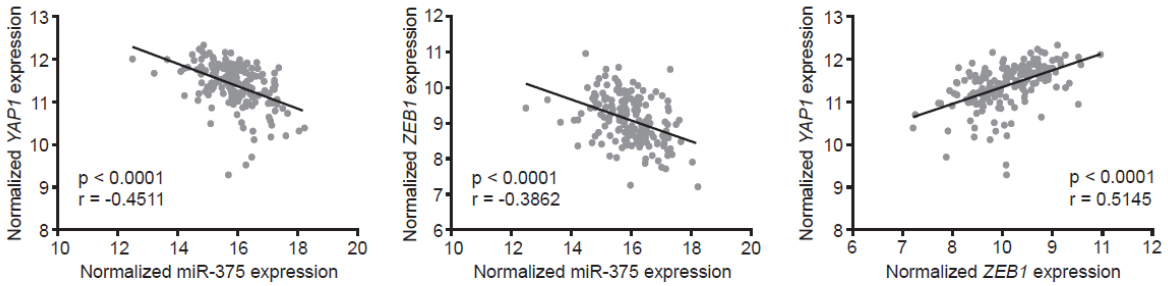

Supplementary Figure 8

ZEB1 and *YAP1* are negatively correlated with miR-375 and positively correlated with each other. Graphs show correlations in 177 tumors from the TCGA dataset; data was obtained from The Cancer Genome Atlas (TCGA) data portal. *P* and r values were calculated using Pearson's tests.

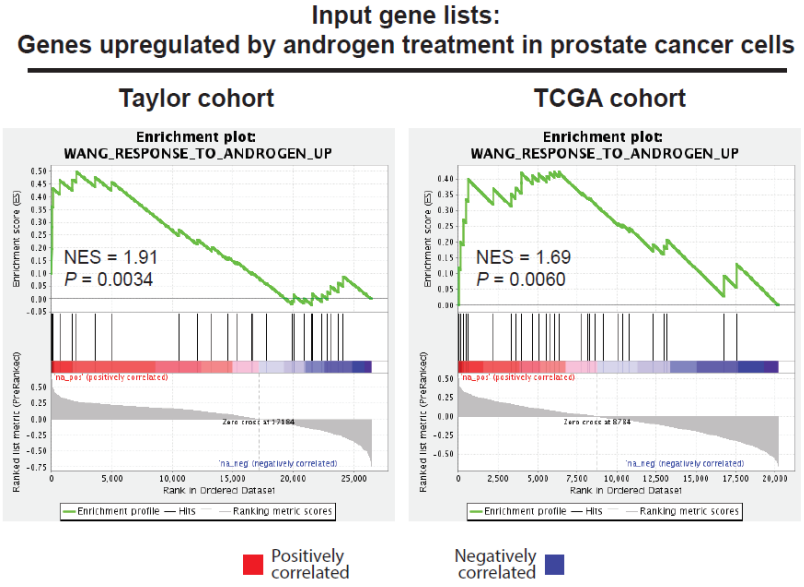

Supplementary Figure 9

miR-375 is positively correlated with an androgen signaling signature[11] in the Taylor (left) and TCGA (right) cohorts. See Supplementary Figure Legend 1 for more detail on the methodology.

Supplementary Table 1. Circulating tumor cell (CTC) counts in a cohort of men with metastatic castration-resistant prostate cancer.

Sample identification	CTC count
001_1	191
001_2	46
001_4	84
002_1	10
002_2	20
003_1	0
003_10	0
003_2	0
003_3	0
003_4	1
003_5	0
003_6	0
003_8	0
003_9	1
004_1	0
004_10	0
004_2	0
004_3	0
004_4	1
004_5	0
004_6	0
004_7	0
004_8	0
004_9	0
005_1	9
005_10	2
005_11	9
005_2	4
005_3	0
005_4	0
005_6	0
005_7	0
005_8	0
006_1	1
006_10	0
006_11	3
006_2	0
006_3	0
006_5	0
006_6	14
006_7	5
006_9	3
007_1	0
007_10	0
007_2	0
007_3	0
007_4	0
007_5	0
007_6	0
007_7	0
007_8	0
007_9	0

References

Quantitation of circulating miR-375 in men with metastatic prostate cancer

Blood samples from men with metastatic prostate cancer ($n = 52$) were obtained with written informed consent from Princess Alexandra Hospital (Brisbane, Australia), under a protocol approved by the Metro South Health Service District HREC and the Queensland University of Technology HREC. CellSearch analysis was used to count circulating tumor cells from whole blood, as described.[55] To measure levels of miR-375 in matched plasma samples, RNA was extracted and qRT-PCR (with pre-amplification) was carried out as described previously.[39] Levels of miR-375 in the two groups (CTC-negative and CTC-positive) were not normally distributed, hence a two-tailed Mann–Whitney test was used for comparison. Levels of miR-375 exhibited a coefficient of variation of 158% and 178% in the CTC-negative and CTC-positive groups, respectively.

Statistical analyses

All statistical analyses were carried out using GraphPad Prism (version 5; GraphPad Software, San Diego, CA, USA) or MedCalc (version 12; MedCalc Software, Mariakerke, Belgium). Details of statistical tests used are provided in the appropriate methods section or figure legends.

CONFLICT OF INTEREST

The authors declare no conflict of interest.

ACKNOWLEDGEMENTS

The YAP1 3′-UTR plasmids were a kind gift from Prof Takashi Takahashi, Nagoya University. The results published here are in part based on the data generated by The Cancer Genome Atlas, established by the National Cancer Institute and the National Human Genome Research Institute, and we are grateful to the specimen donors and relevant research groups associated with this project. We also acknowledge the ENCODE Consortium and the Myers laboratory at the HudsonAlpha Institute for Biotechnology for generating the ZEB1 ChIP-seq data set used in this study. This work was supported by: Young Investigator Awards from the Prostate Cancer Foundation (the Foundation 14 award; LAS) and the Prostate Cancer Foundation of Australia (PCFA)/Movember (YI 0810; LAS, YI 0412; MMC) and grants from PCFA/Movember/Cancer Australia (Grant IDs 1012337 and 1043482; WDT, LAS and LMB) and the National Health and Medical Research Council (Grant ID 1083961). PAG is supported by a Beat Cancer Project fellowship from the Cancer Council of South Australia. BGH is supported by a Queensland government Smart Futures Fund Fellowship. The research programs of LAS, MMC, LMB, CCN, BGH and WDT are supported by the Movember Foundation and the Prostate Cancer Foundation of Australia through Movember Revolutionary Team Awards.

REFERENCES

1 Bray F, Ren JS, Masuyer E, Ferlay J. Global estimates of cancer prevalence for 27 sites in the adult population in 2008. *Int J Cancer* 2013; **132**: 1133–1145.
2 Wu JN, Fish KM, Evans CP, Devere White RW, Dall'Era MA. No improvement noted in overall or cause-specific survival for men presenting with metastatic prostate cancer over a 20-year period. *Cancer* 2014; **120**: 818–823.
3 Das R, Gregory PA, Hollier BG, Tilley WD, Selth LA. Epithelial plasticity in prostate cancer: principles and clinical perspectives. *Trends Mol Med* 2014; **20**: 643–651.
4 De Craene B, Berx G. Regulatory networks defining EMT during cancer initiation and progression. *Nat Rev Cancer* 2013; **13**: 97–110.
5 Thiery JP. Epithelial-mesenchymal transitions in tumour progression. *Nat Rev Cancer* 2002; **2**: 442–454.
6 Banyard J, Chung I, Wilson AM, Vetter G, Le Bechec A, Bielenberg DR *et al.* Regulation of epithelial plasticity by miR-424 and miR-200 in a new prostate cancer metastasis model. *Sci Rep* 2013; **3**: 3151.
7 Celia-Terrassa T, Meca-Cortes O, Mateo F, de Paz AM, Rubio N, Arnal-Estape A *et al.* Epithelial-mesenchymal transition can suppress major attributes of human epithelial tumor-initiating cells. *J Clin Invest* 2012; **122**: 1849–1868.
8 Korpal M, Ell BJ, Buffa FM, Ibrahim T, Blanco MA, Celia-Terrassa T *et al.* Direct targeting of Sec23a by miR-200 s influences cancer cell secretome and promotes metastatic colonization. *Nature medicine* 2011; **17**: 1101–1108.
9 Ocana OH, Corcoles R, Fabra A, Moreno-Bueno G, Acloque H, Vega S *et al.* Metastatic colonization requires the repression of the epithelial-mesenchymal transition inducer Prrx1. *Cancer Cell* 2012; **22**: 709–724.
10 Tsai JH, Donaher JL, Murphy DA, Chau S, Yang J. Spatiotemporal regulation of epithelial-mesenchymal transition is essential for squamous cell carcinoma metastasis. *Cancer Cell* 2012; **22**: 725–736.
11 Gregory PA, Bracken CP, Bert AG, Goodall GJ. MicroRNAs as regulators of epithelial-mesenchymal transition. *Cell cycle* 2008; **7**: 3112–3118.
12 Zhang J, Ma L. MicroRNA control of epithelial-mesenchymal transition and metastasis. *Cancer Metast Rev* 2012; **31**: 653–662.
13 Selth LA, Tilley WD, Butler LM. Circulating microRNAs: macro-utility as markers of prostate cancer? *Endocr Relat Cancer* 2012; **19**: R99–R113.
14 Ambs S, Prueitt RL, Yi M, Hudson RS, Howe TM, Petrocca F *et al.* Genomic profiling of microRNA and messenger RNA reveals deregulated microRNA expression in prostate cancer. *Cancer Res* 2008; **68**: 6162–6170.
15 Martens-Uzunova ES, Jalava SE, Dits NF, van Leenders GJ, Moller S, Trapman J *et al.* Diagnostic and prognostic signatures from the small non-coding RNA transcriptome in prostate cancer. *Oncogene* 2011; **31**: 978–991.
16 Schaefer A, Stephan C, Busch J, Yousef GM, Jung K. Diagnostic, prognostic and therapeutic implications of microRNAs in urologic tumors. *Nat Rev Urol* 2010; **7**: 286–297.
17 Taylor BS, Schultz N, Hieronymus H, Gopalan A, Xiao Y, Carver BS *et al.* Integrative genomic profiling of human prostate cancer. *Cancer Cell* 2010; **18**: 11–22.
18 Wach S, Nolte E, Szczyrba J, Stohr R, Hartmann A, Orntoft T *et al.* MicroRNA profiles of prostate carcinoma detected by multiplatform microRNA screening. *Int J Cancer* 2011; **130**: 611–621.
19 Lin PC, Chiu YL, Banerjee S, Park K, Mosquera JM, Giannopoulou E *et al.* Epigenetic repression of miR-31 disrupts androgen receptor homeostasis and contributes to prostate cancer progression. *Cancer Res* 2013; **73**: 1232–1244.
20 Subramanian A, Tamayo P, Mootha VK, Mukherjee S, Ebert BL, Gillette MA *et al.* Gene set enrichment analysis: a knowledge-based approach for interpreting genome-wide expression profiles. *Proc Natl Acad Sci USA* 2005; **102**: 15545–15550.
21 Kohn KW, Zeeberg BR, Reinhold WC, Sunshine M, Luna A, Pommier Y. Gene expression profiles of the NCI-60 human tumor cell lines define molecular interaction networks governing cell migration processes. *PLoS One* 2012; **7**: e35716.
22 Yuan TC, Veeramani S, Lin FF, Kondrikou D, Zelivianski S, Igawa T *et al.* Androgen deprivation induces human prostate epithelial neuroendocrine differentiation of androgen-sensitive LNCaP cells. *Endocr Relat Cancer* 2006; **13**: 151–167.
23 Ward A, Balwierz A, Zhang JD, Kublbeck M, Pawitan Y, Hielscher T *et al.* Re-expression of microRNA-375 reverses both tamoxifen resistance and accompanying EMT-like properties in breast cancer. *Oncogene* 2012; **32**: 1173–1182.
24 Lokman NA, Elder AS, Ricciardelli C, Oehler MK. Chick chorioallantoic membrane (CAM) assay as an in vivo model to study the effect of newly identified molecules on ovarian cancer invasion and metastasis. *Int J Mol Sci* 2012; **13**: 9959–9970.
25 Nishikawa E, Osada H, Okazaki Y, Arima C, Tomida S, Tatematsu Y *et al.* miR-375 is activated by ASH1 and inhibits YAP1 in a lineage-dependent manner in lung cancer. *Cancer Res* 2011; **71**: 6165–6173.
26 Christensen LL, Holm A, Rantala J, Kallioniemi O, Rasmussen MH, Ostenfeld MS *et al.* Functional screening identifies miRNAs influencing apoptosis and proliferation in colorectal cancer. *PLoS One* 2014; **9**: e96767.
27 Pan D. The hippo signaling pathway in development and cancer. *Dev Cell* 2010; **19**: 491–505.
28 Ota M, Sasaki H. Mammalian Tead proteins regulate cell proliferation and contact inhibition as transcriptional mediators of Hippo signaling. *Development* 2008; **135**: 4059–4069.
29 Shao DD, Xue W, Krall EB, Bhutkar A, Piccioni F, Wang X *et al.* KRAS and YAP1 converge to regulate EMT and tumor survival. *Cell* 2014; **158**: 171–184.
30 Bracken CP, Gregory PA, Kolesnikoff N, Bert AG, Wang J, Shannon MF *et al.* A double-negative feedback loop between ZEB1-SIP1 and the microRNA-200 family regulates epithelial-mesenchymal transition. *Cancer Res* 2008; **68**: 7846–7854.
31 Burk U, Schubert J, Wellner U, Schmalhofer O, Vincan E, Spaderna S *et al.* A reciprocal repression between ZEB1 and members of the miR-200 family promotes EMT and invasion in cancer cells. *EMBO Rep* 2008; **9**: 582–589.
32 de Souza Rocha Simonini P, Breiling A, Gupta N, Malekpour M, Youns M, Omranipour R *et al.* Epigenetically deregulated microRNA-375 is involved in a positive feedback loop with estrogen receptor alpha in breast cancer cells. *Cancer Res* 2010; **70**: 9175–9184.
33 Kolesnikoff N, Attema JL, Roslan S, Bert AG, Schwarz QP, Gregory PA *et al.* Specificity protein 1 (Sp1) maintains basal epithelial expression of the miR-200 family: implications for epithelial-mesenchymal transition. *J Biol Chem* 2014; **289**: 11194–11205.
34 Consortium EP, Bernstein BE, Birney E, Dunham I, Green ED, Gunter C *et al.* An integrated encyclopedia of DNA elements in the human genome. *Nature* 2012; **489**: 57–74.
35 Brase JC, Johannes M, Schlomm T, Falth M, Haese A, Steuber T *et al.* Circulating miRNAs are correlated with tumor progression in prostate cancer. *Int J Cancer* 2011; **128**: 608–616.
36 Bryant RJ, Pawlowski T, Catto JW, Marsden G, Vessella RL, Rhees B *et al.* Changes in circulating microRNA levels associated with prostate cancer. *Br J Cancer* 2012; **106**: 768–774.
37 Selth LA, Townley S, Gillis JL, Ochnik AM, Murti K, Macfarlane RJ *et al.* Discovery of circulating microRNAs associated with human prostate cancer using a mouse model of disease. *Int J Cancer* 2011; **131**: 652–661.

38 Nauseef JT, Henry MD. Epithelial-to-mesenchymal transition in prostate cancer: paradigm or puzzle? *Nat Rev Urol* 2011; **8**: 428–439.
39 Selth LA, Townley SL, Bert AG, Stricker PD, Sutherland PD, Horvath LG *et al.* Circulating microRNAs predict biochemical recurrence in prostate cancer patients. *Br J Cancer* 2013; **109**: 641–650.
40 Madhavan D, Zucknick M, Wallwiener M, Cuk K, Modugno C, Scharpff M *et al.* Circulating miRNAs as surrogate markers for circulating tumor cells and prognostic markers in metastatic breast cancer. *Clin Cancer Res* 2012; **18**: 5972–5982.
41 Mani SA, Guo W, Liao MJ, Eaton EN, Ayyanan A, Zhou AY *et al.* The epithelial-mesenchymal transition generates cells with properties of stem cells. *Cell* 2008; **133**: 704–715.
42 Chu M, Chang Y, Li P, Guo Y, Zhang K, Gao W. Androgen receptor is negatively correlated with the methylation-mediated transcriptional repression of miR-375 in human prostate cancer cells. *Oncol Rep* 2014; **31**: 34–40.
43 Costa-Pinheiro P, Ramalho-Carvalho J, Vieira FQ, Torres-Ferreira J, Oliveira J, Goncalves CS *et al.* MicroRNA-375 plays a dual role in prostate carcinogenesis. *Clin Epigenet* 2015; **7**: 42.
44 Bitting RL, Schaeffer D, Somarelli JA, Garcia-Blanco MA, Armstrong AJ. The role of epithelial plasticity in prostate cancer dissemination and treatment resistance. *Cancer Metast Rev* 2014; **33**: 441–468.
45 Blower PE, Verducci JS, Lin S, Zhou J, Chung JH, Dai Z *et al.* MicroRNA expression profiles for the NCI-60 cancer cell panel. *Mol Cancer Ther* 2007; **6**: 1483–1491.
46 Liu H, D'Andrade P, Fulmer-Smentek S, Lorenzi P, Kohn KW, Weinstein JN *et al.* mRNA and microRNA expression profiles of the NCI-60 integrated with drug activities. *Mol Cancer Ther* 2010; **9**: 1080–1091.
47 Sokilde R, Kaczkowski B, Podolska A, Cirera S, Gorodkin J, Moller S *et al.* Global microRNA analysis of the NCI-60 cancer cell panel. *Mol Cancer Ther* 2011; **10**: 375–384.
48 Moore NL, Buchanan G, Harris JM, Selth LA, Bianco-Miotto T, Hanson AR *et al.* An androgen receptor mutation in the MDA-MB-453 cell line model of molecular apocrine breast cancer compromises receptor activity. *Endocr Relat Cancer* 2012; **19**: 599–613.
49 Yu X, Machesky LM. Cells assemble invadopodia-like structures and invade into matrigel in a matrix metalloprotease dependent manner in the circular invasion assay. *PLoS One* 2012; **7**: e30605.
50 Oka T, Mazack V, Sudol M. Mst2 and Lats kinases regulate apoptotic function of Yes kinase-associated protein (YAP). *J Biol Chem* 2008; **283**: 27534–27546.
51 Neilsen PM, Noll JE, Mattiske S, Bracken CP, Gregory PA, Schulz RB *et al.* Mutant p53 drives invasion in breast tumors through up-regulation of miR-155. *Oncogene* 2013; **32**: 2992–3000.
52 Marrocco DL, Tilley WD, Bianco-Miotto T, Evdokiou A, Scher HI, Rifkind RA *et al.* Suberoylanilide hydroxamic acid (vorinostat) represses androgen receptor expression and acts synergistically with an androgen receptor antagonist to inhibit prostate cancer cell proliferation. *Mol Cancer Ther* 2007; **6**: 51–60.
53 Dupont S, Morsut L, Aragona M, Enzo E, Giulitti S, Cordenonsi M *et al.* Role of YAP/TAZ in mechanotransduction. *Nature* 2011; **474**: 179–183.
54 Schmidt D, Wilson MD, Spyrou C, Brown GD, Hadfield J, Odom DT. ChIP-seq: using high-throughput sequencing to discover protein-DNA interactions. *Methods* 2009; **48**: 240–248.
55 Gasch C, Plummer PN, Jovanovic L, McInnes LM, Wescott D, Saunders CM *et al.* Heterogeneity of miR-10b expression in circulating tumor cells. *Sci Rep* 2015; **5**: 15980.

Supplementary Information accompanies this paper on the *Oncogene* website (http://www.nature.com/onc)

REFERENCES FOR SUPPLEMENTARY DATA

1 Subramanian A, Tamayo P, Mootha VK, Mukherjee S, Ebert BL, Gillette MA *et al*. Gene set enrichment analysis: a knowledge-based approach for interpreting genome-wide expression profiles. Proc Natl Acad Sci U S A 2005; 102: 15545-15550.

2 Taylor BS, Schultz N, Hieronymus H, Gopalan A, Xiao Y, Carver BS *et al*. Integrative genomic profiling of human prostate cancer. Cancer Cell 2010; 18: 11-22.

3 Nielsen CB, Shomron N, Sandberg R, Hornstein E, Kitzman J, Burge CB. Determinants of targeting by endogenous and exogenous microRNAs and siRNAs. RNA 2007; 13: 1894-1910.

4 Lewis BP, Burge CB, Bartel DP. Conserved seed pairing, often flanked by adenosines, indicates that thousands of human genes are microRNA targets. Cell 2005; 120: 15-20.

5 Liu P, Ramachandran S, Ali Seyed M, Scharer CD, Laycock N, Dalton WB *et al*. Sex-determining region Y box 4 is a transforming oncogene in human prostate cancer cells. Cancer Res 2006; 66: 4011-4019.

6 Tomlins SA, Mehra R, Rhodes DR, Cao X, Wang L, Dhanasekaran SM *et al*. Integrative molecular concept modeling of prostate cancer progression. Nature genetics 2007; 39: 41-51.

7 Wallace TA, Prueitt RL, Yi M, Howe TM, Gillespie JW, Yfantis HG *et al*. Tumor immunobiological differences in prostate cancer between African-American and European-American men. Cancer Res 2008; 68: 927-936.

8 Taube JH, Herschkowitz JI, Komurov K, Zhou AY, Gupta S, Yang J *et al*. Core epithelial-to-mesenchymal transition interactome gene-expression signature is associated with claudin-low and metaplastic breast cancer subtypes. Proc Natl Acad Sci U S A 2010; 107: 15449-15454.

9 Gotzmann J, Fischer AN, Zojer M, Mikula M, Proell V, Huber H *et al*. A crucial function of PDGF in TGF-beta-mediated cancer progression of hepatocytes. Oncogene 2006; 25: 3170-3185.

10 Jechlinger M, Grunert S, Tamir IH, Janda E, Ludemann S, Waerner T *et al*. Expression profiling of epithelial plasticity in tumor progression. Oncogene 2003; 22: 7155-7169.

11 Wang G, Jones SJ, Marra MA, Sadar MD. Identification of genes targeted by the androgen and PKA signaling pathways in prostate cancer cells. Oncogene 2006; 25: 7311-7323.

CHAPTER 6: GENERAL DISCUSSION

6.1. General discussion of thesis findings

The broad classes of cellular alterations required for the initiation and progression of cancer have been described (Hanahan and Weinberg 2011) and are composed of changes that drive cell growth, inhibit cell death, and promote metastasis, amongst others. There is compelling evidence that miRNAs are involved in driving and coordinating the expression of these cancer "hallmarks", especially cell migration and invasion, two critical requirements for cancer spread (Bartel 2004, 2009; Bartel and Chen 2004; Iorio and Croce 2009, 2012). However, for most miRNAs, their molecular mechanism of action is largely unknown. Thus, understanding the role of various miRNAs at different stages of prostate cancer progression, along with their expression at those stages, will provide crucial information. This in particularly important knowing the highly heterogeneous nature of prostate cancer (Boyd, et al. 2012). Studies in this thesis have explored the molecular functionality of two miRNAs, miR-194 and miR-375, and provided novel insights into their roles in prostate cancer metastasis.

MiR-194: a new "metastamiR"

Our interest in miR-194 was prompted by a previous study conducted in our laboratory which aimed to identify circulating miRNAs that could be used as prognostic markers for men diagnosed with prostate cancer (Selth et al. 2013). In that study, miR-194 was found to be elevated in serum of men who subsequently experienced disease progression following surgery, suggesting that it could potentially be used to stratify low- and high-risk patients. Further, its expression in tumours was associated with poor patient outcome, and it was elevated in metastases compared to primary tumours and normal prostate tissue. Based on these latter findings, we hypothesized that miR-194 has a direct role in prostate cancer metastasis. Hence, one of my key aims was to determine its function as well as identify its gene targets through which its actions are mediated.

In my PhD studies, I showed miR-194 to be a potent oncogenic miRNA by promoting invasion and migration and EMT in multiple prostate cancer cell lines *in vitro* and metastasis *in vivo*. Further, I identified SOCS2 as a novel, direct and biological relevant target for miR-194. SOCS2 has been found to have tumour suppressive effect on prostate cancer cells (Iglesias-Gato, et al. 2014). In the literature, SOCS2 had been shown to mediate its action by negatively regulating JAK2 and FLT3 and accordingly suppressing

the STAT3 and ERK signalling pathways, two key oncogenic signalling pathways in various cancer, including prostate cancer (Kazi and Ronnstrand 2013; Letellier and Haan 2016; Sen, et al. 2012). I therefore postulated that miR-194 promotes prostate cancer metastasis by upregulating JAK2/STAT3 and FLT3/ERK signalling pathways via SOCS2. Indeed, the results in Chapter 4 confirmed this hypothesis.

In my studies, I also explored what factors regulate miR-194. MicroRNAs are generally transcribed by RNA polymerase II (Pol II), and hence they are regulated by RNA Pol II-associated transcription factors (Cai, et al. 2004; Lee, et al. 2004). For example, transcription factors such as p53, Twist, ZEB1 and ZEB2 and others, positively or negatively regulate miRNA expression (Kim et al. 2009; Krol et al. 2010). By undertaking bioinformatics analysis, we found GATA2, a key transcription factor in prostate cancer, as one of the most highly positively correlated genes to miR-194. This was supported by the decrease in levels of miR-194 in 22Rv1 cells following knockdown of GATA2. A summary of our theory of miR-194 regulation and action as a pro-metastatic miRNA in prostate cancer is shown in Figure 6.1 (this is the same figure from our submitted paper in Chapter 4).

The applicability of GATA2-miR-194-SOCS2 pathway, revealed in this study, to promote prostate cancer metastasis is of considerable interest for the following reasons a) GATA2 is an established pioneer factor for AR-regulated genes in prostate cancer (Chen, et al. 2013; Wu, et al. 2014). Further, a recent study demonstrated a GATA2 dependency of prostate cancer for both chemotherapy resistance and *in vivo* growth (Vidal, et al. 2015). b) In several studies, researchers demonstrated that increased nuclear translocation and phosphorylation of STAT3 are causally related to prostate cancer progression (Civenni, et al. 2016; Moreira, et al. 2015). c) Similar to STAT3, the role of ERK1/2 in prostate cancer as pro-metastasis factor is evident (Jin, et al. 2013; Ma and Wells 2014; Rodriguez-Berriguete, et al. 2012). All in all, these earlier studies along with the findings from my work highlight that miR-194 sits at the centre of key pro-metastatic transcription factors and signalling pathways. Clinical implications of this study are mentioned below.

MiR-375: a potent tumour suppressor miRNA

Similar to miR-194, our interest in miR-375 was triggered by the findings from another previous study conducted in our laboratory, where a mouse model of prostate cancer was

used to identify candidate miRNAs that were elevated in serum compared to healthy control mice (Selth et al. 2012b). In that study, upregulation of miR-141, miR-298, miR-346 and miR-375 were higher in both the mouse model and the serum of men with CRPC compared to controls. Although miR-375 expression levels in body fluids had been previously proposed as diagnostic and prognostic prostate cancer biomarkers, its biological role in prostate carcinogenesis had not been investigated (Cheng, et al. 2013; Huang, et al. 2015; Nguyen et al. 2013). My work demonstrated that miR-375 is a potent tumour suppressor miRNA by inhibiting epithelial mesenchymal transition (EMT), invasion and growth of prostate cancer cells. I further demonstrated that Yes-associated protein (YAP1), a transcriptional coactivator and a potent oncogene itself, is a direct and biological relevant target of miR-375. Again, I explored what factors might regulate miR-375 and found that it is under the direct transcriptional control of the EMT-promoting transcription factor, ZEB1. Figure 6.2 illustrates our concept of miR-375 regulation and action as a potent tumour suppressor miRNA in prostate cancer (previously published; see Chapter 5)

The relevance of ZEB1-miR-375-YAP1 pathway in prostate cancer metastasis is supported by the known roles of ZEB1 and YAP1. ZEB1 is a master regulator of EMT and known to drive cancer metastasis (Drake, et al. 2009; Putzke, et al. 2011). In addition, a recent study demonstrated YAP1 to regulate prostate cancer cell motility, invasion, and castration-resistant growth (Zhang, et al. 2015)

Interestingly, even though we demonstrated anti-invasive and anti-EMT capacities of miR-375, its plasma levels were found to be correlated with circulating tumour cells in men with metastatic prostate cancer. Possibilities for this variation could be a) patients with high circulating level of miR-375 could have CTCs that have undergone or undergoing mesenchymal epithelial transition (MET), a cellular process likely to be important to form metastases efficiently at secondary locations (Gao, et al. 2012). This concept is in agreement with a study that demonstrated that circulating miR-200 family members and miR-375 are surrogate markers for circulating tumour cells in breast cancer and correlated with disease progression and overall survival (Madhavan, et al. 2012). b) The concept of plasticity of EMT has been expanded in recent years with the recognition that cancer cells may undergo partial EMT or MET, and in fact that resulting ‘quasi’ states may be advantageous to metastatic progression. Indeed, cells that have transited fully towards a mesenchymal state are thought to have lost the plasticity required for metastasis

formation (Tsai, et al. 2012). Partial EMT and the resultant quasi-mesenchymal phenotype is often associated with acquisition of stem-ness properties (Mani, et al. 2008). Such cells have been referred to as 'migrating cancer stem cells' and generally possess increased tumour initiation and self-renewal capacity (Brabletz, et al. 2005). Thus, the epithelial and the growth suppressive characteristics mediated by the high levels of miR-375 may be associated with the acquisition of metastasis promoting traits.

Collectively, the studies in this thesis have provided a new insight into the molecular function of these two miRNAs in prostate cancer and have identified two new pathways: metastasis promoting in case of miR-194 and metastasis inhibiting in case of miR-375.

6.2. Clinical implications of my findings

In prostate cancer, more accurate diagnosis and follow-up monitoring after therapies are two of the major challenges for its clinical management. Although prostate-specific antigen (PSA) screening has improved early detection, its levels poorly correlate with tumour aggressiveness or dissemination. Further, there are several studies which demonstrated that PSA levels were not specifically related to the presence of the disease (Roobol and Carlsson 2013). Diagnostic accuracy, in particular in terms of risk stratification, initial staging, active surveillance, and focal therapy, is one of the main issues in this field. Patients undergo repetitive biopsies, which are not only invasive but also indecisive, even when coupled with PSA and digital rectal examination (DRE). Considering these issues, biomarkers that have the capability to identify potentially aggressive tumours at a point when the cancer is still curable while minimizing detection of indolent disease could transform the clinical management of this disease. Moreover, identifying predictive biomarkers for the multitude of new treatment strategies being developed for metastatic prostate cancer is of critical importance (Attard and de Bono 2011).

MiRNAs are attractive molecular biomarker candidates because they can be reproducibly extracted from a wide range of biologic samples and are generally stable and resistant to various storage conditions (Chen, et al. 2008; Fabris, et al. 2016). Furthermore, miRNAs can be easily detected and accurately quantified by a variety of widely used standard techniques, such as qRT-PCR (Selth, et al. 2014). Evidence from the studies provided in this thesis suggest that miR-375 and miR-194 both have the potential to be used as prognostic markers of prostate cancer. In particular, based on the findings, two relevance

can be proposed, a) circulating miR-194 can be used as a marker to detect micrometastases at the time of treatment or predict metastatic recurrence post-treatment. This rationale is supported by our findings that circulating levels of miR-194 were higher in men with metastatic compared with localised disease and that miR-194 was found to be higher in the tumours of men who subsequently experienced a new tumour event, in large independent cohorts. Consequently, it might be suggested that patients with a high miR-194 expression should be considered for adjuvant therapy in order to optimize their prognosis. b) The utility of miR-375 as biomarker could be twofold: first, potentially miR-375 could be used in a test along with PSA and DRE to provide complementary information at the time of diagnosis to whether or not there is an urgency of biopsy for men with elevated serum PSA level. This possibility is based on an earlier study from our group in which small RNA sequencing and qRT-PCR was used to access the potential of seminal fluid miRNAs as diagnostic biomarkers of prostate cancer (Selth et al. 2014). In that study we found that seminal fluid derived miR-375 was at higher levels in men with elevated serum PSA levels and biopsy proven cancer compared with men with elevated PSA levels but no cancer. Second, circulating level of miR-375 could be used as a non-invasive marker for monitoring men in active surveillance. This is in position with the findings from the study in this thesis that plasma levels of miR-375 were found to be correlated with circulating tumour cells in men with metastatic prostate cancer and with the opinion that high circulating level of miR-375 may be associated with acquisition of metastasis promoting traits. Active surveillance, also called expectant management is for men with prostate cancer that involves the postponement of immediate therapy. Active surveillance is an accepted option for the initial management of carefully selected men with localized, well-differentiated prostate cancer thought to be at low-risk for progression (Chen, et al. 2016; Dall'Era, et al. 2012; Thompson, et al. 2007). MiR-375 measurements could be used to determine whether or not to proceed with definitive curative interventions. However, substantial studies with longitudinal follow-up are required to validate our above theorem.

The realization that many miRNAs have crucial roles in basic biological processes and that dysregulation of miRNAs is common in human disease has led to considerable interest in the therapeutic targeting of miRNAs. Fundamental findings from my work reveal that inhibition of miR-194 can significantly block invasion of prostate cancer cells *in vitro* and *in vivo*, and therefore, work in this thesis sets a stage to develop strategies to

target this miRNA to block metastasis. Evidence to date suggests that anti-miR-mediated silencing of miRNAs could be a powerful technology for the treatment of human disease (Cheng, et al. 2015; Stenvang, et al. 2012; Su, et al. 2011). Despite of some obstacles on the way for efficient delivery of anti-miRs, considerable progress in the field has been achieved to improve the target binding affinity and nuclease resistance of anti-miRs for their successful deliver *in vivo*, with prospect to improve in the future (Ben-Shushan, et al. 2014; Li and Rana 2014).

To date, three main approaches have been taken: expression vectors (miRNA sponges), antisense oligonucleotides (ASOs) and small-molecule inhibitors (figure 6.3). Overexpression of mRNAs containing artificial miRNA-binding sites, which acts as decoys or 'sponges', can selectively sequester endogenous miRNAs (Meng, et al. 2007). However, despite the wide use of sponges to investigate miRNA function *in vitro*, their utility *in vivo* has thus far been limited to transgenic animals (Ebert and Sharp 2010). On the other hand, considerable attention has been paid to ASO and small molecule inhibition technologies (Bennett and Swayze 2010; Gumireddy, et al. 2008). ASOs designed to directly target and specifically inhibit miRNA function are also called anti-miRs. Anti-miRs bind with high complementarity to miRNAs, thereby blocking their binding to endogenous mRNA targets. Approaches that are based on small molecules are also being developed to manipulate miRNA expression and function. The modes of action of these small molecules are mainly through transcriptional regulation of targeted miRNAs; more specifically, the molecules are designed to reduce levels of the mature, active form of the miRNA by inhibiting processing of the pri-miRNA.

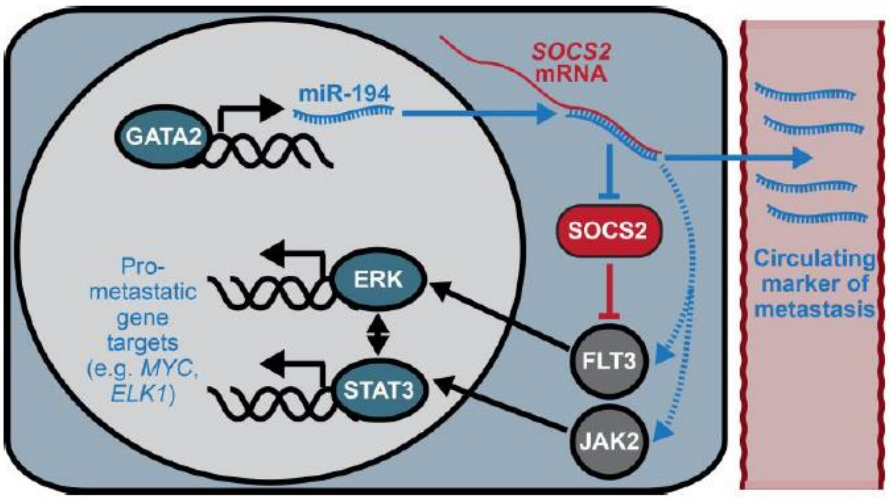

Figure 6.1: Schematic showing regulation and pro-metastatic action of miR-194

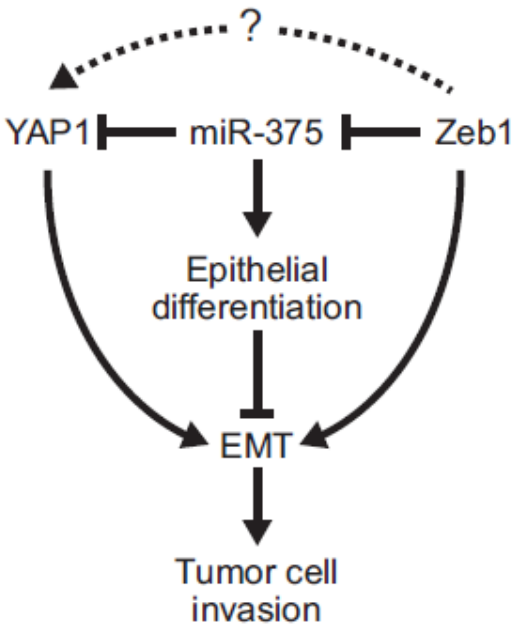

Figure 6.2: Schematic showing regulation and tumour suppressive action of miR-375

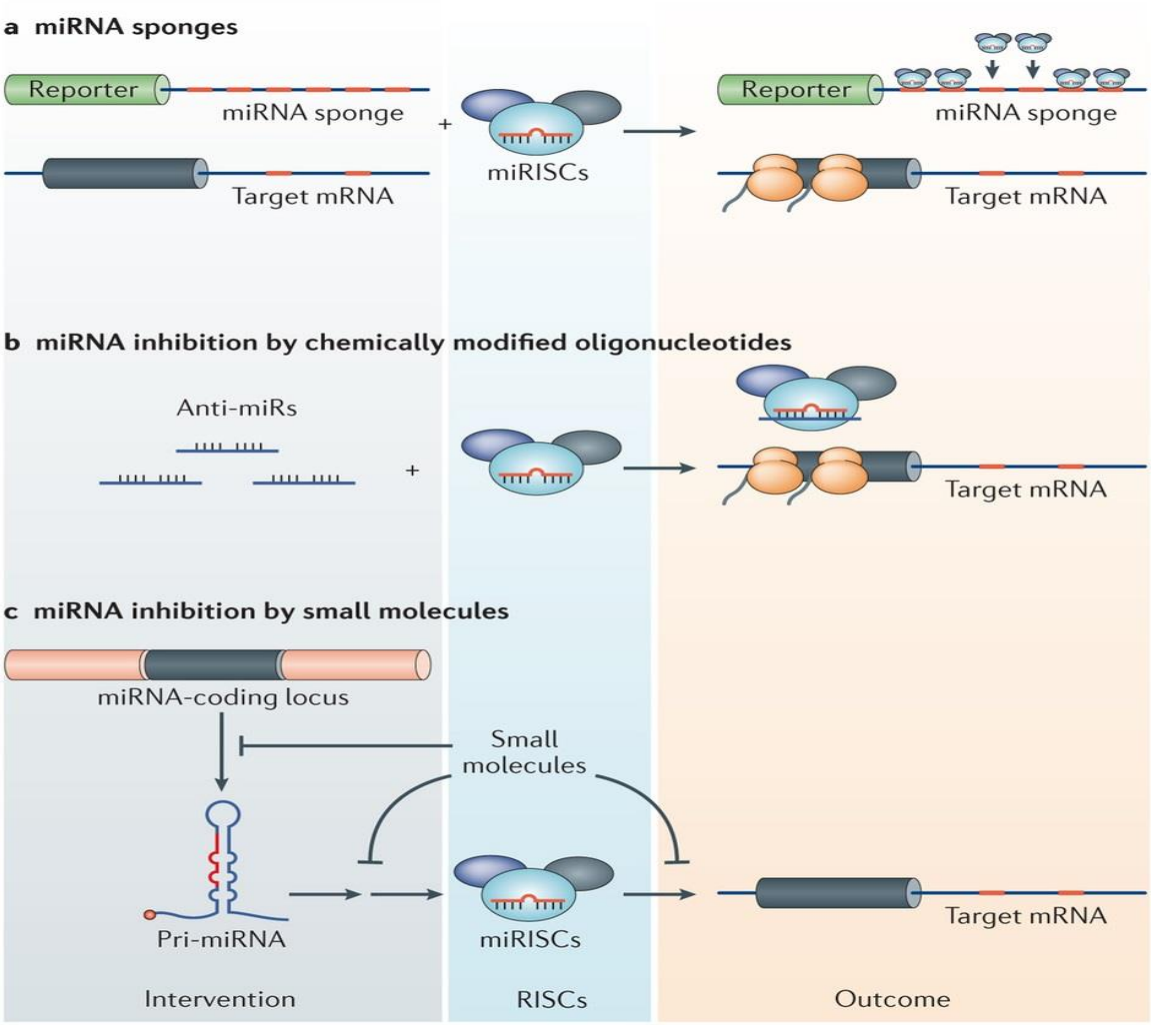

Figure 6.3: miRNA inhibition strategies. Adapted from (Li and Rana 2014)

6.3. Future directions

The canonical way of a miRNA interacting with an mRNA involves base pairing between the 5′ miRNA end (called as 'seed') and a complementary sequence in the target's 3′ untranslated region (3′ UTR). However, studies have demonstrated alternative modes of binding, for example, those involving the 3′ regions of miRNAs (Chi, et al. 2012; Chi, et al. 2009; Xia, et al. 2012). These studies highlight the undiscovered mechanisms of post-transcriptional regulation through miRNAs. More importantly, they also highlight a need for new experimental methods to complement existing computational target prediction methods, where canonical prediction sites are the main focus for miRNA target prediction. The research in this thesis evidently suggest considerable importance of miR-194 and miR-375 in prostate cancer metastasis. Therefore, identifying additional biologically relevant targets of these two miRNAs is essential to unravel the underlying molecular metastatic mechanisms of prostate cancer and to better understand the roles of the two miRNAs within the cellular context. An approach that I propose is to introduce biotinylated microRNA mimics into prostate cancer cells. Studies have exploited this approach to obtain experimental evidence of physical interaction between a specific microRNA of interest and its mRNA targets (Cloonan, et al. 2011; Easow, et al. 2007; Tan and Lieberman 2016). Briefly, biotin-labelled synthetic miRNAs will be transfected to prostate cancer cells to pull-down endogenous mRNA targets. These mRNAs will then be profiled by microarray or RNA-sequencing (figure 6.4). This can also be combined with small RNA sequencing modulation of the miRNA levels. Additionally, proteomics can also be used to identify the role of miRNA-target interaction. A study demonstrated polysome profiling of mRNA species after over-expression of three different miRNA to capture functional mRNA targets by virtue of their reduced occurrence in actively translating poly-ribosomal fractions (Shi, et al. 2010). Therefore, to identify the targets of miR-194 and miR-375 and their effect on the overall proteomic profile of cells, I propose to opt for a proteomic method, like SILAC (stable isotope labelling by amino acids in cell culture) (Baek, et al. 2008; Chen, et al. 2012; Vinther, et al. 2006) following transient modulation of the levels of these two miRNAs, by miRNA mimics or inhibitors.

In the case of metastatic disease, analysis of metastatic tissue can be very informative, but biopsies are highly invasive and complicated procedures and do not always yield tumour material. By contrast, isolation and subsequent characterization of circulating tumour cells

(CTCs) provide an opportunity to bypass the problems associated with obtaining metastatic tissue, serving as a 'liquid biopsy'. To date, there have been many efforts to correlate circulating miRNAs with the number of CTCs, including our previous studies. However, it may be challenging to implement this approach on a broad scale, mainly due to the low number of CTCs in the blood and the issue of leukocyte contamination. Therefore, there is a clear need for an efficient and sensitive method for the detection of miRNA within CTCs. As a prospective investigation to miR-194's and miR-375's in prostate cancer metastasis I propose to integrate *in situ* hybridization (ISH) protocol for detecting miRNAs in single cells with the methodological steps necessary to isolate and identify CTCs from patient blood. A recent study had implemented this approach to detect miR-21 in CTCs (Ortega, et al. 2015). Briefly, CTCs were selected based on cytokeratin (CK) expression and immunocytochemistry and locked-nucleic acid (LNA) probes associated with an enzyme-labelled fluorescence (ELF) signal amplification approach were used to detect miRNA-21 in CTCs (figure 6.5). Thus, this approach can be a potential tool that can be used to monitor prostate cancer patients and determine the efficacy of their treatments.

In order to further clarify the relevance of miR-194 in prostate cancer metastasis, long-term stable silencing of miR-194 should be one of the key future aims. CRISPR/cas9 system is emerging as a novel genome editing tool in biology/medicine research (Chang, et al. 2016). Therefore, applying this technology to silence miR-194 and determine its effect on prostate cancer metastasis will be of considerable interest. Additionally, to determine the therapeutic efficacy of miR-194 in prostate cancer, I propose to perform silencing of miR-194 using anti-miRs *in vivo* using an anti-miR strategy as described in clinical implications section of the general discussion chapter.

6.4. Summary

The possible use of miRNAs in the clinic as biomarkers or therapeutic targets for prostate cancer is based on a growing body of investigations throughout the last decade. The research completed in this thesis provides greater understanding about the role of miR-194 and miR-375 in prostate cancer metastasis. This information could inform the potential application of these miRNAs as biomarkers, and could lead to efforts to target miR-194 to prevent prostate cancer metastasis.

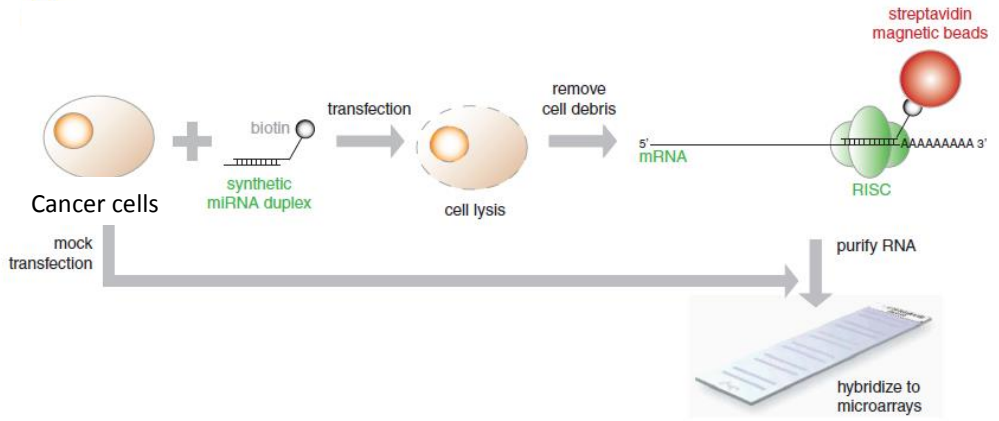

Figure 6.4: Schematic showing the laboratory workflow for the pulldown of mRNA targets of a synthetic biotinylated miRNA (Cloonan et al. 2011)

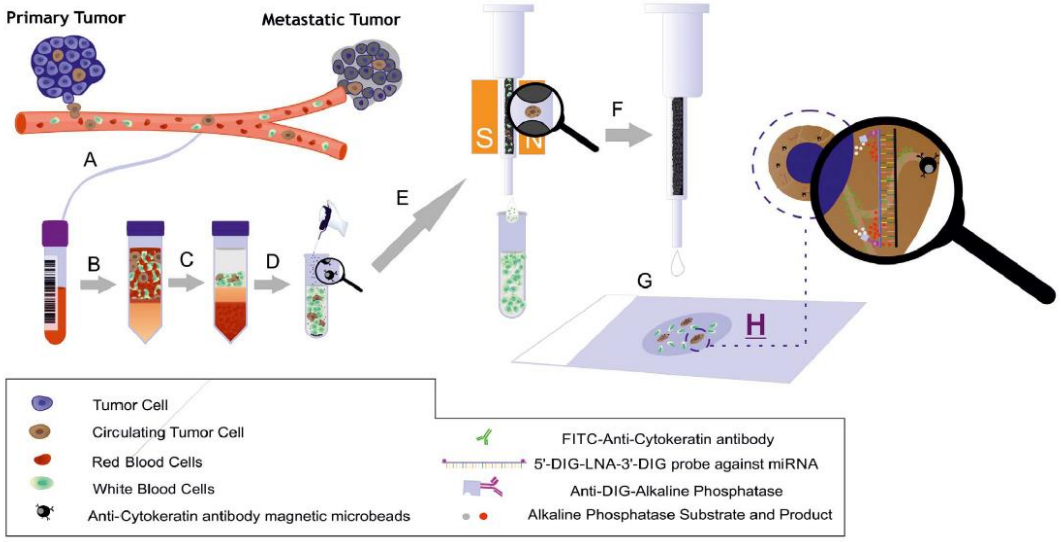

Figure 6.5: Schematic illustration of miR-ISH-CTC (Ortega et al. 2015)

General References

Allegra A, Alonci A, Campo S, Penna G, Petrungaro A, Gerace D & Musolino C 2012 Circulating microRNAs: new biomarkers in diagnosis, prognosis and treatment of cancer (review). *Int J Oncol* **41** 1897-1912.

Andriole GL, Crawford ED, Grubb RL, 3rd, Buys SS, Chia D, Church TR, Fouad MN, Gelmann EP, Kvale PA, Reding DJ, et al. 2009 Mortality results from a randomized prostate-cancer screening trial. *N Engl J Med* **360** 1310-1319.

Andriole GL, Crawford ED, Grubb RL, 3rd, Buys SS, Chia D, Church TR, Fouad MN, Isaacs C, Kvale PA, Reding DJ, et al. 2012 Prostate cancer screening in the randomized Prostate, Lung, Colorectal, and Ovarian Cancer Screening Trial: mortality results after 13 years of follow-up. *J Natl Cancer Inst* **104** 125-132.

ASURAGEN miRInform.

Attar RM, Takimoto CH & Gottardis MM 2009 Castration-resistant prostate cancer: locking up the molecular escape routes. *Clin Cancer Res* **15** 3251-3255.

Attard G & de Bono JS 2011 Translating scientific advancement into clinical benefit for castration-resistant prostate cancer patients. *Clin Cancer Res* **17** 3867-3875.

Baek D, Villen J, Shin C, Camargo FD, Gygi SP & Bartel DP 2008 The impact of microRNAs on protein output. *Nature* **455** 64-71.

Bartel DP 2004 MicroRNAs: genomics, biogenesis, mechanism, and function. *Cell* **116** 281-297.

Bartel DP 2009 MicroRNAs: target recognition and regulatory functions. *Cell* **136** 215-233.

Bartel DP & Chen CZ 2004 Micromanagers of gene expression: the potentially widespread influence of metazoan microRNAs. *Nat Rev Genet* **5** 396-400.

Ben-Shushan D, Markovsky E, Gibori H, Tiram G, Scomparin A & Satchi-Fainaro R 2014 Overcoming obstacles in microRNA delivery towards improved cancer therapy. *Drug Deliv Transl Res* **4** 38-49.

Bennett CF & Swayze EE 2010 RNA targeting therapeutics: molecular mechanisms of antisense oligonucleotides as a therapeutic platform. *Annu Rev Pharmacol Toxicol* **50** 259-293.

Biamonti G, Bonomi S, Gallo S & Ghigna C 2012 Making alternative splicing decisions during epithelial-to-mesenchymal transition (EMT). *Cell Mol Life Sci* **69** 2515-2526.

Boeri M, Pastorino U & Sozzi G 2012 Role of microRNAs in lung cancer: microRNA signatures in cancer prognosis. *Cancer J* **18** 268-274.

Boeri M, Verri C, Conte D, Roz L, Modena P, Facchinetti F, Calabro E, Croce CM, Pastorino U & Sozzi G 2011 MicroRNA signatures in tissues and plasma predict development and prognosis of computed tomography detected lung cancer. *Proc Natl Acad Sci U S A* **108** 3713-3718.

Bonkhoff H & Remberger K 1993 Widespread distribution of nuclear androgen receptors in the basal cell layer of the normal and hyperplastic human prostate. *Virchows Arch A Pathol Anat Histopathol* **422** 35-38.

Bonkhoff H, Stein U & Remberger K 1995 Endocrine-paracrine cell types in the prostate and prostatic adenocarcinoma are postmitotic cells. *Hum Pathol* **26** 167-170.

Boyd LK, Mao X & Lu YJ 2012 The complexity of prostate cancer: genomic alterations and heterogeneity. *Nat Rev Urol* **9** 652-664.

Brabletz T, Jung A, Spaderna S, Hlubek F & Kirchner T 2005 Opinion: migrating cancer stem cells - an integrated concept of malignant tumour progression. *Nat Rev Cancer* **5** 744-749.

Brase JC, Johannes M, Schlomm T, Falth M, Haese A, Steuber T, Beissbarth T, Kuner R & Sultmann H 2011 Circulating miRNAs are correlated with tumor progression in prostate cancer. *Int J Cancer* **128** 608-616.

Braun CJ, Zhang X, Savelyeva I, Wolff S, Moll UM, Schepeler T, Orntoft TF, Andersen CL & Dobbelstein M 2008 p53-Responsive micrornas 192 and 215 are capable of inducing cell cycle arrest. *Cancer Res* **68** 10094-10104.

Brawer MK 2006 Hormonal therapy for prostate cancer. *Rev Urol* **8 Suppl 2** S35-47.

Bryant RJ, Pawlowski T, Catto JW, Marsden G, Vessella RL, Rhees B, Kuslich C, Visakorpi T & Hamdy FC 2012 Changes in circulating microRNA levels associated with prostate cancer. *Br J Cancer* **106** 768-774.
Buscaglia LE & Li Y 2011 Apoptosis and the target genes of microRNA-21. *Chin J Cancer* **30** 371-380.
Cai X, Hagedorn CH & Cullen BR 2004 Human microRNAs are processed from capped, polyadenylated transcripts that can also function as mRNAs. *RNA* **10** 1957-1966.
Calin GA & Croce CM 2006 MicroRNA signatures in human cancers. *Nat Rev Cancer* **6** 857-866.
Cancer AJCo 2010 Cancer staging. edn 7th.
Carthew RW & Sontheimer EJ 2009 Origins and Mechanisms of miRNAs and siRNAs. *Cell* **136** 642-655.
Chaffer CL & Weinberg RA 2011 A perspective on cancer cell metastasis. *Science* **331** 1559-1564.
Chang H, Yi B, Ma R, Zhang X, Zhao H & Xi Y 2016 CRISPR/cas9, a novel genomic tool to knock down microRNA in vitro and in vivo. *Sci Rep* **6** 22312.
Charras G & Paluch E 2008 Blebs lead the way: how to migrate without lamellipodia. *Nat Rev Mol Cell Biol* **9** 730-736.
Chen CY, Chi LM, Chi HC, Tsai MM, Tsai CY, Tseng YH, Lin YH, Chen WJ, Huang YH & Lin KH 2012 Stable isotope labeling with amino acids in cell culture (SILAC)-based quantitative proteomics study of a thyroid hormone-regulated secretome in human hepatoma cells. *Mol Cell Proteomics* **11** M111 011270.
Chen RC, Rumble RB, Loblaw DA, Finelli A, Ehdaie B, Cooperberg MR, Morgan SC, Tyldesley S, Haluschak JJ, Tan W, et al. 2016 Active Surveillance for the Management of Localized Prostate Cancer (Cancer Care Ontario Guideline): American Society of Clinical Oncology Clinical Practice Guideline Endorsement. *J Clin Oncol* **34** 2182-2190.
Chen X, Ba Y, Ma L, Cai X, Yin Y, Wang K, Guo J, Zhang Y, Chen J, Guo X, et al. 2008 Characterization of microRNAs in serum: a novel class of biomarkers for diagnosis of cancer and other diseases. *Cell Res* **18** 997-1006.
Chen Y, Chi P, Rockowitz S, Iaquinta PJ, Shamu T, Shukla S, Gao D, Sirota I, Carver BS, Wongvipat J, et al. 2013 ETS factors reprogram the androgen receptor cistrome and prime prostate tumorigenesis in response to PTEN loss. *Nat Med* **19** 1023-1029.
Cheng CJ, Bahal R, Babar IA, Pincus Z, Barrera F, Liu C, Svoronos A, Braddock DT, Glazer PM, Engelman DM, et al. 2015 MicroRNA silencing for cancer therapy targeted to the tumour microenvironment. *Nature* **518** 107-110.
Cheng HH, Mitchell PS, Kroh EM, Dowell AE, Chery L, Siddiqui J, Nelson PS, Vessella RL, Knudsen BS, Chinnaiyan AM, et al. 2013 Circulating microRNA profiling identifies a subset of metastatic prostate cancer patients with evidence of cancer-associated hypoxia. *PLoS One* **8** e69239.
Chi SW, Hannon GJ & Darnell RB 2012 An alternative mode of microRNA target recognition. *Nat Struct Mol Biol* **19** 321-327.
Chi SW, Zang JB, Mele A & Darnell RB 2009 Argonaute HITS-CLIP decodes microRNA-mRNA interaction maps. *Nature* **460** 479-486.
Chiang Y, Song Y, Wang Z, Liu Z, Gao P, Liang J, Zhu J, Xing C & Xu H 2012 microRNA-192, -194 and -215 are frequently downregulated in colorectal cancer. *Exp Ther Med* **3** 560-566.
Chim SS, Shing TK, Hung EC, Leung TY, Lau TK, Chiu RW & Lo YM 2008 Detection and characterization of placental microRNAs in maternal plasma. *Clin Chem* **54** 482-490.
Chou R, Croswell JM, Dana T, Bougatsos C, Blazina I, Fu R, Gleitsmann K, Koenig HC, Lam C, Maltz A, et al. 2011a Screening for prostate cancer: a review of the evidence for the U.S. Preventive Services Task Force. *Ann Intern Med* **155** 762-771.
Chou R, Dana T, Bougatsos C, Fu R, Blazina I, Gleitsmann K & Rugge JB 2011b In *Treatments for Localized Prostate Cancer: Systematic Review to Update the 2002 U.S. Preventive Services Task Force Recommendation*. Rockville (MD).
Chung LW 1995 The role of stromal-epithelial interaction in normal and malignant growth. *Cancer Surv* **23** 33-42.

Civenni G, Longoni N, Costales P, Dallavalle C, Garcia Inclan C, Albino D, Nunez LE, Moris F, Carbone GM & Catapano CV 2016 EC-70124, a Novel Glycosylated Indolocarbazole Multikinase Inhibitor, Reverts Tumorigenic and Stem Cell Properties in Prostate Cancer by Inhibiting STAT3 and NF-kappaB. *Mol Cancer Ther* **15** 806-818.
Cloonan N, Wani S, Xu Q, Gu J, Lea K, Heater S, Barbacioru C, Steptoe AL, Martin HC, Nourbakhsh E, et al. 2011 MicroRNAs and their isomiRs function cooperatively to target common biological pathways. *Genome Biol* **12** R126.
Cohen RJ, Shannon BA, Phillips M, Moorin RE, Wheeler TM & Garrett KL 2008 Central zone carcinoma of the prostate gland: a distinct tumor type with poor prognostic features. *J Urol* **179** 1762-1767; discussion 1767.
Collins AT & Maitland NJ 2006 Prostate cancer stem cells. *Eur J Cancer* **42** 1213-1218.
Crawford ED, Grubb R, 3rd, Black A, Andriole GL, Jr., Chen MH, Izmirlian G, Berg CD & D'Amico AV 2011 Comorbidity and mortality results from a randomized prostate cancer screening trial. *J Clin Oncol* **29** 355-361.
Culig Z, Hobisch A, Cronauer MV, Radmayr C, Hittmair A, Zhang J, Thurnher M, Bartsch G & Klocker H 1996 Regulation of prostatic growth and function by peptide growth factors. *Prostate* **28** 392-405.
Dall'Era MA, Albertsen PC, Bangma C, Carroll PR, Carter HB, Cooperberg MR, Freedland SJ, Klotz LH, Parker C & Soloway MS 2012 Active surveillance for prostate cancer: a systematic review of the literature. *Eur Urol* **62** 976-983.
Davies JA 1996 Mesenchyme to epithelium transition during development of the mammalian kidney tubule. *Acta Anat (Basel)* **156** 187-201.
Davis BN & Hata A 2009 Regulation of MicroRNA Biogenesis: A miRiad of mechanisms. *Cell Commun Signal* **7** 18.
De Marzo AM, Platz EA, Sutcliffe S, Xu J, Gronberg H, Drake CG, Nakai Y, Isaacs WB & Nelson WG 2007 Inflammation in prostate carcinogenesis. *Nat Rev Cancer* **7** 256-269.
de Souza Rocha Simonini P, Breiling A, Gupta N, Malekpour M, Youns M, Omranipour R, Malekpour F, Volinia S, Croce CM, Najmabadi H, et al. 2010 Epigenetically deregulated microRNA-375 is involved in a positive feedback loop with estrogen receptor alpha in breast cancer cells. *Cancer Res* **70** 9175-9184.
Denys B, El Housni H, Nollet F, Verhasselt B & Philippe J 2010 A real-time polymerase chain reaction assay for rapid, sensitive, and specific quantification of the JAK2V617F mutation using a locked nucleic acid-modified oligonucleotide. *J Mol Diagn* **12** 512-519.
Ding L, Xu Y, Zhang W, Deng Y, Si M, Du Y, Yao H, Liu X, Ke Y, Si J, et al. 2010 MiR-375 frequently downregulated in gastric cancer inhibits cell proliferation by targeting JAK2. *Cell Res* **20** 784-793.
Dong P, Kaneuchi M, Watari H, Hamada J, Sudo S, Ju J & Sakuragi N 2011 MicroRNA-194 inhibits epithelial to mesenchymal transition of endometrial cancer cells by targeting oncogene BMI-1. *Mol Cancer* **10** 99.
Drake JM, Strohbehn G, Bair TB, Moreland JG & Henry MD 2009 ZEB1 enhances transendothelial migration and represses the epithelial phenotype of prostate cancer cells. *Mol Biol Cell* **20** 2207-2217.
Dumortier O, Hinault C & Van Obberghen E 2013 MicroRNAs and Metabolism Crosstalk in Energy Homeostasis. *Cell Metab*.
Easow G, Teleman AA & Cohen SM 2007 Isolation of microRNA targets by miRNP immunopurification. *RNA* **13** 1198-1204.
Ebert MS & Sharp PA 2010 MicroRNA sponges: progress and possibilities. *RNA* **16** 2043-2050.
Edlund M, Sung SY & Chung LW 2004 Modulation of prostate cancer growth in bone microenvironments. *J Cell Biochem* **91** 686-705.
Eis PS, Tam W, Sun L, Chadburn A, Li Z, Gomez MF, Lund E & Dahlberg JE 2005 Accumulation of miR-155 and BIC RNA in human B cell lymphomas. *Proc Natl Acad Sci U S A* **102** 3627-3632.
Esquela-Kerscher A & Slack FJ 2006 Oncomirs - microRNAs with a role in cancer. *Nat Rev Cancer* **6** 259-269.

Fabris L, Ceder Y, Chinnaiyan AM, Jenster GW, Sorensen KD, Tomlins S, Visakorpi T & Calin GA 2016 The Potential of MicroRNAs as Prostate Cancer Biomarkers. *Eur Urol* **70** 312-322.
Fackler OT & Grosse R 2008 Cell motility through plasma membrane blebbing. *J Cell Biol* **181** 879-884.
Fiore R, Khudayberdiev S, Saba R & Schratt G 2011 MicroRNA function in the nervous system. *Prog Mol Biol Transl Sci* **102** 47-100.
Friedman RC, Farh KK, Burge CB & Bartel DP 2009 Most mammalian mRNAs are conserved targets of microRNAs. *Genome Res* **19** 92-105.
Gandellini P, Folini M, Longoni N, Pennati M, Binda M, Colecchia M, Salvioni R, Supino R, Moretti R, Limonta P, et al. 2009 miR-205 Exerts tumor-suppressive functions in human prostate through down-regulation of protein kinase Cepsilon. *Cancer Res* **69** 2287-2295.
Gandellini P, Profumo V, Casamichele A, Fenderico N, Borrelli S, Petrovich G, Santilli G, Callari M, Colecchia M, Pozzi S, et al. 2012 miR-205 regulates basement membrane deposition in human prostate: implications for cancer development. *Cell Death Differ* **19** 1750-1760.
Gao D, Vahdat LT, Wong S, Chang JC & Mittal V 2012 Microenvironmental regulation of epithelial-mesenchymal transitions in cancer. *Cancer Res* **72** 4883-4889.
Gerharz M, Baranowsky A, Siebolts U, Eming S, Nischt R, Krieg T & Wickenhauser C 2007 Morphometric analysis of murine skin wound healing: standardization of experimental procedures and impact of an advanced multitissue array technique. *Wound Repair Regen* **15** 105-112.
Gordetsky J & Epstein J 2016 Grading of prostatic adenocarcinoma: current state and prognostic implications. *Diagn Pathol* **11** 25.
Gregory PA, Bert AG, Paterson EL, Barry SC, Tsykin A, Farshid G, Vadas MA, Khew-Goodall Y & Goodall GJ 2008 The miR-200 family and miR-205 regulate epithelial to mesenchymal transition by targeting ZEB1 and SIP1. *Nat Cell Biol* **10** 593-601.
Grinnell F 2003 Fibroblast biology in three-dimensional collagen matrices. *Trends Cell Biol* **13** 264-269.
Grueter CE, van Rooij E, Johnson BA, DeLeon SM, Sutherland LB, Qi X, Gautron L, Elmquist JK, Bassel-Duby R & Olson EN 2012 A cardiac microRNA governs systemic energy homeostasis by regulation of MED13. *Cell* **149** 671-683.
Gumireddy K, Young DD, Xiong X, Hogenesch JB, Huang Q & Deiters A 2008 Small-molecule inhibitors of microrna miR-21 function. *Angew Chem Int Ed Engl* **47** 7482-7484.
Gupta GP & Massague J 2006 Cancer metastasis: building a framework. *Cell* **127** 679-695.
Hagman Z, Haflidadottir BS, Ceder JA, Larne O, Bjartell A, Lilja H, Edsjo A & Ceder Y 2013 miR-205 negatively regulates the androgen receptor and is associated with adverse outcome of prostate cancer patients. *Br J Cancer* **108** 1668-1676.
Hanahan D & Weinberg RA 2011 Hallmarks of cancer: the next generation. *Cell* **144** 646-674.
Harris WP, Mostaghel EA, Nelson PS & Montgomery B 2009 Androgen deprivation therapy: progress in understanding mechanisms of resistance and optimizing androgen depletion. *Nat Clin Pract Urol* **6** 76-85.
Haseen F, Murray LJ, Cardwell CR, O'Sullivan JM & Cantwell MM 2010 The effect of androgen deprivation therapy on body composition in men with prostate cancer: systematic review and meta-analysis. *J Cancer Surviv* **4** 128-139.
Hay ED 2005 The mesenchymal cell, its role in the embryo, and the remarkable signaling mechanisms that create it. *Dev Dyn* **233** 706-720.
Hayashita Y, Osada H, Tatematsu Y, Yamada H, Yanagisawa K, Tomida S, Yatabe Y, Kawahara K, Sekido Y & Takahashi T 2005 A polycistronic microRNA cluster, miR-17-92, is overexpressed in human lung cancers and enhances cell proliferation. *Cancer Res* **65** 9628-9632.
He H, Jazdzewski K, Li W, Liyanarachchi S, Nagy R, Volinia S, Calin GA, Liu CG, Franssila K, Suster S, et al. 2005a The role of microRNA genes in papillary thyroid carcinoma. *Proc Natl Acad Sci U S A* **102** 19075-19080.

He L, Thomson JM, Hemann MT, Hernando-Monge E, Mu D, Goodson S, Powers S, Cordon-Cardo C, Lowe SW, Hannon GJ, et al. 2005b A microRNA polycistron as a potential human oncogene. *Nature* **435** 828-833.
Heidenreich A, Bellmunt J, Bolla M, Joniau S, Mason M, Matveev V, Mottet N, Schmid HP, van der Kwast T, Wiegel T, et al. 2011a [EAU guidelines on prostate cancer. Part I: screening, diagnosis, and treatment of clinically localised disease]. *Actas Urol Esp* **35** 501-514.
Heidenreich A, Bellmunt J, Bolla M, Joniau S, Mason M, Matveev V, Mottet N, Schmid HP, van der Kwast T, Wiegel T, et al. 2011b EAU guidelines on prostate cancer. Part 1: screening, diagnosis, and treatment of clinically localised disease. *Eur Urol* **59** 61-71.
Heinlein CA & Chang C 2004 Androgen receptor in prostate cancer. *Endocr Rev* **25** 276-308.
Hibio N, Hino K, Shimizu E, Nagata Y & Ui-Tei K 2012 Stability of miRNA 5'terminal and seed regions is correlated with experimentally observed miRNA-mediated silencing efficacy. *Sci Rep* **2** 996.
Hill L, Browne G & Tulchinsky E 2013 ZEB/miR-200 feedback loop: at the crossroads of signal transduction in cancer. *Int J Cancer* **132** 745-754.
Huang X, Yuan T, Liang M, Du M, Xia S, Dittmar R, Wang D, See W, Costello BA, Quevedo F, et al. 2015 Exosomal miR-1290 and miR-375 as prognostic markers in castration-resistant prostate cancer. *Eur Urol* **67** 33-41.
Hugo H, Ackland ML, Blick T, Lawrence MG, Clements JA, Williams ED & Thompson EW 2007 Epithelial--mesenchymal and mesenchymal--epithelial transitions in carcinoma progression. *J Cell Physiol* **213** 374-383.
Hui AB, Lenarduzzi M, Krushel T, Waldron L, Pintilie M, Shi W, Perez-Ordonez B, Jurisica I, O'Sullivan B, Waldron J, et al. 2010 Comprehensive MicroRNA profiling for head and neck squamous cell carcinomas. *Clin Cancer Res* **16** 1129-1139.
Hurteau GJ, Carlson JA, Spivack SD & Brock GJ 2007 Overexpression of the microRNA hsa-miR-200c leads to reduced expression of transcription factor 8 and increased expression of E-cadherin. *Cancer Res* **67** 7972-7976.
Iglesias-Gato D, Chuan YC, Wikstrom P, Augsten S, Jiang N, Niu Y, Seipel A, Danneman D, Vermeij M, Fernandez-Perez L, et al. 2014 SOCS2 mediates the cross talk between androgen and growth hormone signaling in prostate cancer. *Carcinogenesis* **35** 24-33.
Iorio MV & Croce CM 2009 MicroRNAs in cancer: small molecules with a huge impact. *J Clin Oncol* **27** 5848-5856.
Iorio MV & Croce CM 2012 MicroRNA dysregulation in cancer: diagnostics, monitoring and therapeutics. A comprehensive review. *EMBO Mol Med* **4** 143-159.
Iorio MV, Ferracin M, Liu CG, Veronese A, Spizzo R, Sabbioni S, Magri E, Pedriali M, Fabbri M, Campiglio M, et al. 2005 MicroRNA gene expression deregulation in human breast cancer. *Cancer Res* **65** 7065-7070.
Isaacs JT 1999 The biology of hormone refractory prostate cancer. Why does it develop? *Urol Clin North Am* **26** 263-273.
Jin F, Irshad S, Yu W, Belakavadi M, Chekmareva M, Ittmann MM, Abate-Shen C & Fondell JD 2013 ERK and AKT signaling drive MED1 overexpression in prostate cancer in association with elevated proliferation and tumorigenicity. *Mol Cancer Res* **11** 736-747.
Johnson CD, Esquela-Kerscher A, Stefani G, Byrom M, Kelnar K, Ovcharenko D, Wilson M, Wang X, Shelton J, Shingara J, et al. 2007 The let-7 microRNA represses cell proliferation pathways in human cells. *Cancer Res* **67** 7713-7722.
Johnson SM, Grosshans H, Shingara J, Byrom M, Jarvis R, Cheng A, Labourier E, Reinert KL, Brown D & Slack FJ 2005 RAS is regulated by the let-7 microRNA family. *Cell* **120** 635-647.
Jorgensen S, Baker A, Moller S & Nielsen BS 2010 Robust one-day in situ hybridization protocol for detection of microRNAs in paraffin samples using LNA probes. *Methods* **52** 375-381.
Kalluri R & Neilson EG 2003 Epithelial-mesenchymal transition and its implications for fibrosis. *J Clin Invest* **112** 1776-1784.

Kalluri R & Weinberg RA 2009 The basics of epithelial-mesenchymal transition. *J Clin Invest* **119** 1420-1428.
Karantanos T, Corn PG & Thompson TC 2013 Prostate cancer progression after androgen deprivation therapy: mechanisms of castrate resistance and novel therapeutic approaches. *Oncogene*.
Kazi JU & Ronnstrand L 2013 Suppressor of cytokine signaling 2 (SOCS2) associates with FLT3 and negatively regulates downstream signaling. *Mol Oncol* **7** 693-703.
Kim SJ, Uehara H, Yazici S, He J, Langley RR, Mathew P, Fan D & Fidler IJ 2005 Modulation of bone microenvironment with zoledronate enhances the therapeutic effects of STI571 and paclitaxel against experimental bone metastasis of human prostate cancer. *Cancer Res* **65** 3707-3715.
Kim VN, Han J & Siomi MC 2009 Biogenesis of small RNAs in animals. *Nat Rev Mol Cell Biol* **10** 126-139.
Kloosterman WP, Wienholds E, de Bruijn E, Kauppinen S & Plasterk RH 2006 In situ detection of miRNAs in animal embryos using LNA-modified oligonucleotide probes. *Nat Methods* **3** 27-29.
Klymkowsky MW & Savagner P 2009 Epithelial-mesenchymal transition: a cancer researcher's conceptual friend and foe. *Am J Pathol* **174** 1588-1593.
Kohli M & Tindall DJ 2010 New developments in the medical management of prostate cancer. *Mayo Clin Proc* **85** 77-86.
Korpal M & Kang Y 2008 The emerging role of miR-200 family of microRNAs in epithelial-mesenchymal transition and cancer metastasis. *RNA Biol* **5** 115-119.
Krieg M, Weisser H & Tunn S 1995 Potential activities of androgen metabolizing enzymes in human prostate. *J Steroid Biochem Mol Biol* **53** 395-400.
Krol J, Loedige I & Filipowicz W 2010 The widespread regulation of microRNA biogenesis, function and decay. *Nat Rev Genet* **11** 597-610.
Kumar VL & Majumder PK 1995 Prostate gland: structure, functions and regulation. *Int Urol Nephrol* **27** 231-243.
Kurita T, Wang YZ, Donjacour AA, Zhao C, Lydon JP, O'Malley BW, Isaacs JT, Dahiya R & Cunha GR 2001 Paracrine regulation of apoptosis by steroid hormones in the male and female reproductive system. *Cell Death Differ* **8** 192-200.
Kyprianou N & Isaacs JT 1988 Activation of programmed cell death in the rat ventral prostate after castration. *Endocrinology* **122** 552-562.
Lajer CB, Nielsen FC, Friis-Hansen L, Norrild B, Borup R, Garnaes E, Rossing M, Specht L, Therkildsen MH, Nauntofte B, et al. 2011 Different miRNA signatures of oral and pharyngeal squamous cell carcinomas: a prospective translational study. *Br J Cancer* **104** 830-840.
Lawrie CH, Gal S, Dunlop HM, Pushkaran B, Liggins AP, Pulford K, Banham AH, Pezzella F, Boultwood J, Wainscoat JS, et al. 2008 Detection of elevated levels of tumour-associated microRNAs in serum of patients with diffuse large B-cell lymphoma. *Br J Haematol* **141** 672-675.
Le XF, Almeida MI, Mao W, Spizzo R, Rossi S, Nicoloso MS, Zhang S, Wu Y, Calin GA & Bast RC, Jr. 2012 Modulation of MicroRNA-194 and cell migration by HER2-targeting trastuzumab in breast cancer. *PLoS One* **7** e41170.
Leach DA, Need EF, Toivanen R, Trotta AP, Palethorpe HM, Tamblyn DJ, Kopsaftis T, England GM, Smith E, Drew PA, et al. 2015 Erratum: Stromal androgen receptor regulates the composition of the microenvironment to influence prostate cancer outcome. *Oncotarget* **6** 36923.
Lee Y, Kim M, Han J, Yeom KH, Lee S, Baek SH & Kim VN 2004 MicroRNA genes are transcribed by RNA polymerase II. *EMBO J* **23** 4051-4060.
Lee YS & Dutta A 2007 The tumor suppressor microRNA let-7 represses the HMGA2 oncogene. *Genes Dev* **21** 1025-1030.
Letellier E & Haan S 2016 SOCS2: physiological and pathological functions. *Front Biosci (Elite Ed)* **8** 189-204.
Li LM, Hu ZB, Zhou ZX, Chen X, Liu FY, Zhang JF, Shen HB, Zhang CY & Zen K 2010 Serum microRNA profiles serve as novel biomarkers for HBV infection and diagnosis of HBV-positive hepatocarcinoma. *Cancer Res* **70** 9798-9807.

Li Y, Wang F, Xu J, Ye F, Shen Y, Zhou J, Lu W, Wan X, Ma D & Xie X 2011 Progressive miRNA expression profiles in cervical carcinogenesis and identification of HPV-related target genes for miR-29. *J Pathol* **224** 484-495.
Li Z & Rana TM 2014 Therapeutic targeting of microRNAs: current status and future challenges. *Nat Rev Drug Discov* **13** 622-638.
Lim J & Thiery JP 2012 Epithelial-mesenchymal transitions: insights from development. *Development* **139** 3471-3486.
Lissbrant IF, Lissbrant E, Damber JE & Bergh A 2001 Blood vessels are regulators of growth, diagnostic markers and therapeutic targets in prostate cancer. *Scand J Urol Nephrol* **35** 437-452.
Loda M, Fogt F, French FS, Posner M, Cukor B, Aretz HT & Alsaigh N 1994 Androgen receptor immunohistochemistry on paraffin-embedded tissue. *Mod Pathol* **7** 388-391.
Lu J, Getz G, Miska EA, Alvarez-Saavedra E, Lamb J, Peck D, Sweet-Cordero A, Ebert BL, Mak RH, Ferrando AA, et al. 2005 MicroRNA expression profiles classify human cancers. *Nature* **435** 834-838.
Ma B & Wells A 2014 The mitogen-activated protein (MAP) kinases p38 and extracellular signal-regulated kinase (ERK) are involved in hepatocyte-mediated phenotypic switching in prostate cancer cells. *J Biol Chem* **289** 11153-11161.
Ma R, Jiang T & Kang X 2012 Circulating microRNAs in cancer: origin, function and application. *J Exp Clin Cancer Res* **31** 38.
Madhavan D, Zucknick M, Wallwiener M, Cuk K, Modugno C, Scharpff M, Schott S, Heil J, Turchinovich A, Yang R, et al. 2012 Circulating miRNAs as surrogate markers for circulating tumor cells and prognostic markers in metastatic breast cancer. *Clin Cancer Res* **18** 5972-5982.
Maitland NJ, Bryce SD, Stower MJ & Collins AT 2006 Prostate cancer stem cells: a target for new therapies. *Ernst Schering Found Symp Proc* 155-179.
Majid S, Dar AA, Saini S, Yamamura S, Hirata H, Tanaka Y, Deng G & Dahiya R 2010 MicroRNA-205-directed transcriptional activation of tumor suppressor genes in prostate cancer. *Cancer* **116** 5637-5649.
Mani SA, Guo W, Liao MJ, Eaton EN, Ayyanan A, Zhou AY, Brooks M, Reinhard F, Zhang CC, Shipitsin M, et al. 2008 The epithelial-mesenchymal transition generates cells with properties of stem cells. *Cell* **133** 704-715.
Maygarden SJ & Pruthi R 2005 Gleason grading and volume estimation in prostate needle biopsy specimens: evolving issues. *Am J Clin Pathol* **123 Suppl** S58-66.
Mazar J, DeBlasio D, Govindarajan SS, Zhang S & Perera RJ 2011 Epigenetic regulation of microRNA-375 and its role in melanoma development in humans. *FEBS Lett* **585** 2467-2476.
McNeal JE 1981 The zonal anatomy of the prostate. *Prostate* **2** 35-49.
McNeal JE, Redwine EA, Freiha FS & Stamey TA 1988 Zonal distribution of prostatic adenocarcinoma. Correlation with histologic pattern and direction of spread. *Am J Surg Pathol* **12** 897-906.
Medh RD & Thompson EB 2000 Hormonal regulation of physiological cell turnover and apoptosis. *Cell Tissue Res* **301** 101-124.
Mees ST, Mardin WA, Wendel C, Baeumer N, Willscher E, Senninger N, Schleicher C, Colombo-Benkmann M & Haier J 2010 EP300--a miRNA-regulated metastasis suppressor gene in ductal adenocarcinomas of the pancreas. *Int J Cancer* **126** 114-124.
Meng F, Henson R, Wehbe-Janek H, Ghoshal K, Jacob ST & Patel T 2007 MicroRNA-21 regulates expression of the PTEN tumor suppressor gene in human hepatocellular cancer. *Gastroenterology* **133** 647-658.
Meng Z, Fu X, Chen X, Zeng S, Tian Y, Jove R, Xu R & Huang W 2010 miR-194 is a marker of hepatic epithelial cells and suppresses metastasis of liver cancer cells in mice. *Hepatology* **52** 2148-2157.
Micalizzi DS & Ford HL 2009 Epithelial-mesenchymal transition in development and cancer. *Future Oncol* **5** 1129-1143.
Michael MZ, SM OC, van Holst Pellekaan NG, Young GP & James RJ 2003 Reduced accumulation of specific microRNAs in colorectal neoplasia. *Mol Cancer Res* **1** 882-891.

Miller KD, Siegel RL, Lin CC, Mariotto AB, Kramer JL, Rowland JH, Stein KD, Alteri R & Jemal A 2016 Cancer treatment and survivorship statistics, 2016. *CA Cancer J Clin*.
MiRNATherapeutics MiRNA Therapeutics.
Mitchell PS, Parkin RK, Kroh EM, Fritz BR, Wyman SK, Pogosova-Agadjanyan EL, Peterson A, Noteboom J, O'Briant KC, Allen A, et al. 2008 Circulating microRNAs as stable blood-based markers for cancer detection. *Proc Natl Acad Sci U S A* **105** 10513-10518.
Mo MH, Chen L, Fu Y, Wang W & Fu SW 2012 Cell-free Circulating miRNA Biomarkers in Cancer. *J Cancer* **3** 432-448.
Moreira D, Zhang Q, Hossain DM, Nechaev S, Li H, Kowolik CM, D'Apuzzo M, Forman S, Jones J, Pal SK, et al. 2015 TLR9 signaling through NF-kappaB/RELA and STAT3 promotes tumor-propagating potential of prostate cancer cells. *Oncotarget* **6** 17302-17313.
Mottet N, Bellmunt J, Bolla M, Joniau S, Mason M, Matveev V, Schmid HP, van der Kwast T, Wiegel T, Zattoni F, et al. 2011 [EAU guidelines on prostate cancer. Part II: treatment of advanced, relapsing, and castration-resistant prostate cancer]. *Actas Urol Esp* **35** 565-579.
Murakami Y, Yasuda T, Saigo K, Urashima T, Toyoda H, Okanoue T & Shimotohno K 2006 Comprehensive analysis of microRNA expression patterns in hepatocellular carcinoma and non-tumorous tissues. *Oncogene* **25** 2537-2545.
Nguyen DX, Bos PD & Massague J 2009 Metastasis: from dissemination to organ-specific colonization. *Nat Rev Cancer* **9** 274-284.
Nguyen DX & Massague J 2007 Genetic determinants of cancer metastasis. *Nat Rev Genet* **8** 341-352.
Nguyen HC, Xie W, Yang M, Hsieh CL, Drouin S, Lee GS & Kantoff PW 2013 Expression differences of circulating microRNAs in metastatic castration resistant prostate cancer and low-risk, localized prostate cancer. *Prostate* **73** 346-354.
Obeid JP, Zafar N & El Hokayem J 2016 Steroid Hormone Receptor Coregulators in Endocrine Cancers. *IUBMB Life* **68** 504-515.
Ortega FG, Lorente JA, Garcia Puche JL, Ruiz MP, Sanchez-Martin RM, de Miguel-Perez D, Diaz-Mochon JJ & Serrano MJ 2015 miRNA in situ hybridization in circulating tumor cells--MishCTC. *Sci Rep* **5** 9207.
Paranjape T, Slack FJ & Weidhaas JB 2009 MicroRNAs: tools for cancer diagnostics. *Gut* **58** 1546-1554.
Park SM, Gaur AB, Lengyel E & Peter ME 2008 The miR-200 family determines the epithelial phenotype of cancer cells by targeting the E-cadherin repressors ZEB1 and ZEB2. *Genes Dev* **22** 894-907.
Peng X, Guo W, Liu T, Wang X, Tu X, Xiong D, Chen S, Lai Y, Du H, Chen G, et al. 2011 Identification of miRs-143 and -145 that is associated with bone metastasis of prostate cancer and involved in the regulation of EMT. *PLoS One* **6** e20341.
Pierorazio PM, Walsh PC, Partin AW & Epstein JI 2013 Prognostic Gleason grade grouping: data based on the modified Gleason scoring system. *BJU Int* **111** 753-760.
Podgorski I, Linebaugh BE, Sameni M, Jedeszko C, Bhagat S, Cher ML & Sloane BF 2005 Bone microenvironment modulates expression and activity of cathepsin B in prostate cancer. *Neoplasia* **7** 207-223.
Porkka KP, Pfeiffer MJ, Waltering KK, Vessella RL, Tammela TL & Visakorpi T 2007 MicroRNA expression profiling in prostate cancer. *Cancer Res* **67** 6130-6135.
Potosky AL, Reeve BB, Clegg LX, Hoffman RM, Stephenson RA, Albertsen PC, Gilliland FD & Stanford JL 2002 Quality of life following localized prostate cancer treated initially with androgen deprivation therapy or no therapy. *J Natl Cancer Inst* **94** 430-437.
Prins GS, Birch L & Greene GL 1991 Androgen receptor localization in different cell types of the adult rat prostate. *Endocrinology* **129** 3187-3199.
Putzke AP, Ventura AP, Bailey AM, Akture C, Opoku-Ansah J, Celiktas M, Hwang MS, Darling DS, Coleman IM, Nelson PS, et al. 2011 Metastatic progression of prostate cancer and e-cadherin regulation by zeb1 and SRC family kinases. *Am J Pathol* **179** 400-410.

Rodriguez-Berriguete G, Fraile B, Martinez-Onsurbe P, Olmedilla G, Paniagua R & Royuela M 2012 MAP Kinases and Prostate Cancer. *J Signal Transduct* **2012** 169170.
Roobol MJ & Carlsson SV 2013 Risk stratification in prostate cancer screening. *Nat Rev Urol* **10** 38-48.
Roodman GD 2004 Mechanisms of bone metastasis. *N Engl J Med* **350** 1655-1664.
Ryan BM, Robles AI & Harris CC 2010 Genetic variation in microRNA networks: the implications for cancer research. *Nat Rev Cancer* **10** 389-402.
Sar M, Lubahn DB, French FS & Wilson EM 1990 Immunohistochemical localization of the androgen receptor in rat and human tissues. *Endocrinology* **127** 3180-3186.
Schaefer A, Jung M, Mollenkopf HJ, Wagner I, Stephan C, Jentzmik F, Miller K, Lein M, Kristiansen G & Jung K 2010 Diagnostic and prognostic implications of microRNA profiling in prostate carcinoma. *Int J Cancer* **126** 1166-1176.
Schroder FH, Hugosson J, Roobol MJ, Tammela TL, Ciatto S, Nelen V, Kwiatkowski M, Lujan M, Lilja H, Zappa M, et al. 2009 Screening and prostate-cancer mortality in a randomized European study. *N Engl J Med* **360** 1320-1328.
Scott RW, Crighton D & Olson MF 2011 Modeling and imaging 3-dimensional collective cell invasion. *J Vis Exp*.
Selbach M, Schwanhausser B, Thierfelder N, Fang Z, Khanin R & Rajewsky N 2008 Widespread changes in protein synthesis induced by microRNAs. *Nature* **455** 58-63.
Selth LA, Roberts MJ, Chow CW, Marshall VR, Doi SA, Vincent AD, Butler LM, Lavin MF, Tilley WD & Gardiner RA 2014 Human seminal fluid as a source of prostate cancer-specific microRNA biomarkers. *Endocr Relat Cancer* **21** L17-21.
Selth LA, Tilley WD & Butler LM 2012a Circulating microRNAs: macro-utility as markers of prostate cancer? *Endocr Relat Cancer* **19** R99-R113.
Selth LA, Townley S, Gillis JL, Ochnik AM, Murti K, Macfarlane RJ, Chi KN, Marshall VR, Tilley WD & Butler LM 2012b Discovery of circulating microRNAs associated with human prostate cancer using a mouse model of disease. *Int J Cancer* **131** 652-661.
Selth LA, Townley SL, Bert AG, Stricker PD, Sutherland PD, Horvath LG, Goodall GJ, Butler LM & Tilley WD 2013 Circulating microRNAs predict biochemical recurrence in prostate cancer patients. *Br J Cancer* **109** 641-650.
Sen B, Peng S, Woods DM, Wistuba I, Bell D, El-Naggar AK, Lai SY & Johnson FM 2012 STAT5A-mediated SOCS2 expression regulates Jak2 and STAT3 activity following c-Src inhibition in head and neck squamous carcinoma. *Clin Cancer Res* **18** 127-139.
Senanayake U, Das S, Vesely P, Alzoughbi W, Frohlich LF, Chowdhury P, Leuschner I, Hoefler G & Guertl B 2012 miR-192, miR-194, miR-215, miR-200c and miR-141 are downregulated and their common target ACVR2B is strongly expressed in renal childhood neoplasms. *Carcinogenesis* **33** 1014-1021.
Shah RB 2009 Current perspectives on the Gleason grading of prostate cancer. *Arch Pathol Lab Med* **133** 1810-1816.
Shi M, Liu D, Duan H, Shen B & Guo N 2010 Metastasis-related miRNAs, active players in breast cancer invasion, and metastasis. *Cancer Metastasis Rev* **29** 785-799.
Shook D & Keller R 2003 Mechanisms, mechanics and function of epithelial-mesenchymal transitions in early development. *Mech Dev* **120** 1351-1383.
Siegel RL, Miller KD & Jemal A 2016 Cancer statistics, 2016. *CA Cancer J Clin* **66** 7-30.
Sita-Lumsden A, Dart DA, Waxman J & Bevan CL 2013 Circulating microRNAs as potential new biomarkers for prostate cancer. *Br J Cancer* **108** 1925-1930.
Steeg PS 2006 Tumor metastasis: mechanistic insights and clinical challenges. *Nat Med* **12** 895-904.
Stenvang J, Petri A, Lindow M, Obad S & Kauppinen S 2012 Inhibition of microRNA function by antimiR oligonucleotides. *Silence* **3** 1.
Su J, Baigude H, McCarroll J & Rana TM 2011 Silencing microRNA by interfering nanoparticles in mice. *Nucleic Acids Res* **39** e38.

Sun S, Sprenger CC, Vessella RL, Haugk K, Soriano K, Mostaghel EA, Page ST, Coleman IM, Nguyen HM, Sun H, et al. 2010 Castration resistance in human prostate cancer is conferred by a frequently occurring androgen receptor splice variant. *J Clin Invest* **120** 2715-2730.
Szczyrba J, Loprich E, Wach S, Jung V, Unteregger G, Barth S, Grobholz R, Wieland W, Stohr R, Hartmann A, et al. 2010 The microRNA profile of prostate carcinoma obtained by deep sequencing. *Mol Cancer Res* **8** 529-538.
Takamizawa J, Konishi H, Yanagisawa K, Tomida S, Osada H, Endoh H, Harano T, Yatabe Y, Nagino M, Nimura Y, et al. 2004 Reduced expression of the let-7 microRNAs in human lung cancers in association with shortened postoperative survival. *Cancer Res* **64** 3753-3756.
Tan SM & Lieberman J 2016 Capture and Identification of miRNA Targets by Biotin Pulldown and RNA-seq. *Methods Mol Biol* **1358** 211-228.
Taylor LG, Canfield SE & Du XL 2009 Review of major adverse effects of androgen-deprivation therapy in men with prostate cancer. *Cancer* **115** 2388-2399.
Thompson I, Thrasher JB, Aus G, Burnett AL, Canby-Hagino ED, Cookson MS, D'Amico AV, Dmochowski RR, Eton DT, Forman JD, et al. 2007 Guideline for the management of clinically localized prostate cancer: 2007 update. *J Urol* **177** 2106-2131.
Tolstrup N, Nielsen PS, Kolberg JG, Frankel AM, Vissing H & Kauppinen S 2003 OligoDesign: Optimal design of LNA (locked nucleic acid) oligonucleotide capture probes for gene expression profiling. *Nucleic Acids Res* **31** 3758-3762.
Tomankova T, Petrek M & Kriegova E 2010 Involvement of microRNAs in physiological and pathological processes in the lung. *Respir Res* **11** 159.
Tong AW, Fulgham P, Jay C, Chen P, Khalil I, Liu S, Senzer N, Eklund AC, Han J & Nemunaitis J 2009 MicroRNA profile analysis of human prostate cancers. *Cancer Gene Ther* **16** 206-216.
Trang P, Medina PP, Wiggins JF, Ruffino L, Kelnar K, Omotola M, Homer R, Brown D, Bader AG, Weidhaas JB, et al. 2010 Regression of murine lung tumors by the let-7 microRNA. *Oncogene* **29** 1580-1587.
Tsai JH, Donaher JL, Murphy DA, Chau S & Yang J 2012 Spatiotemporal regulation of epithelial-mesenchymal transition is essential for squamous cell carcinoma metastasis. *Cancer Cell* **22** 725-736.
Tsukamoto Y, Nakada C, Noguchi T, Tanigawa M, Nguyen LT, Uchida T, Hijiya N, Matsuura K, Fujioka T, Seto M, et al. 2010 MicroRNA-375 is downregulated in gastric carcinomas and regulates cell survival by targeting PDK1 and 14-3-3zeta. *Cancer Res* **70** 2339-2349.
Tucci P, Agostini M, Grespi F, Markert EK, Terrinoni A, Vousden KH, Muller PA, Dotsch V, Kehrloesser S, Sayan BS, et al. 2012 Loss of p63 and its microRNA-205 target results in enhanced cell migration and metastasis in prostate cancer. *Proc Natl Acad Sci U S A* **109** 15312-15317.
Turley EA, Veiseh M, Radisky DC & Bissell MJ 2008 Mechanisms of disease: epithelial-mesenchymal transition--does cellular plasticity fuel neoplastic progression? *Nat Clin Pract Oncol* **5** 280-290.
Valladares-Ayerbes M, Reboredo M, Medina-Villaamil V, Iglesias-Diaz P, Lorenzo-Patino MJ, Haz M, Santamarina I, Blanco M, Fernandez-Tajes J, Quindos M, et al. 2012 Circulating miR-200c as a diagnostic and prognostic biomarker for gastric cancer. *J Transl Med* **10** 186.
Vargas HA, Akin O, Franiel T, Goldman DA, Udo K, Touijer KA, Reuter VE & Hricak H 2012 Normal central zone of the prostate and central zone involvement by prostate cancer: clinical and MR imaging implications. *Radiology* **262** 894-902.
Verze P, Cai T & Lorenzetti S 2016 The role of the prostate in male fertility, health and disease. *Nat Rev Urol*.
Vidal SJ, Rodriguez-Bravo V, Quinn SA, Rodriguez-Barrueco R, Lujambio A, Williams E, Sun X, de la Iglesia-Vicente J, Lee A, Readhead B, et al. 2015 A targetable GATA2-IGF2 axis confers aggressiveness in lethal prostate cancer. *Cancer Cell* **27** 223-239.
Vinther J, Hedegaard MM, Gardner PP, Andersen JS & Arctander P 2006 Identification of miRNA targets with stable isotope labeling by amino acids in cell culture. *Nucleic Acids Res* **34** e107.

Volinia S, Calin GA, Liu CG, Ambs S, Cimmino A, Petrocca F, Visone R, Iorio M, Roldo C, Ferracin M, et al. 2006 A microRNA expression signature of human solid tumors defines cancer gene targets. *Proc Natl Acad Sci U S A* **103** 2257-2261.
Wijnhoven BP, Hussey DJ, Watson DI, Tsykin A, Smith CM, Michael MZ & South Australian Oesophageal Research G 2010 MicroRNA profiling of Barrett's oesophagus and oesophageal adenocarcinoma. *Br J Surg* **97** 853-861.
Wikstrom P, Lissbrant IF, Stattin P, Egevad L & Bergh A 2002 Endoglin (CD105) is expressed on immature blood vessels and is a marker for survival in prostate cancer. *Prostate* **51** 268-275.
Winter J, Jung S, Keller S, Gregory RI & Diederichs S 2009 Many roads to maturity: microRNA biogenesis pathways and their regulation. *Nat Cell Biol* **11** 228-234.
Witkos TM, Koscianska E & Krzyzosiak WJ 2011 Practical Aspects of microRNA Target Prediction. *Curr Mol Med* **11** 93-109.
Wittmann J & Jack HM 2010 Serum microRNAs as powerful cancer biomarkers. *Biochim Biophys Acta* **1806** 200-207.
Wu D, Sunkel B, Chen Z, Liu X, Ye Z, Li Q, Grenade C, Ke J, Zhang C, Chen H, et al. 2014 Three-tiered role of the pioneer factor GATA2 in promoting androgen-dependent gene expression in prostate cancer. *Nucleic Acids Res* **42** 3607-3622.
Xia Z, Clark P, Huynh T, Loher P, Zhao Y, Chen HW, Ren P, Rigoutsos I & Zhou R 2012 Molecular dynamics simulations of Ago silencing complexes reveal a large repertoire of admissible 'seed-less' targets. *Sci Rep* **2** 569.
Yanaihara N, Caplen N, Bowman E, Seike M, Kumamoto K, Yi M, Stephens RM, Okamoto A, Yokota J, Tanaka T, et al. 2006 Unique microRNA molecular profiles in lung cancer diagnosis and prognosis. *Cancer Cell* **9** 189-198.
Yang J, Mani SA, Donaher JL, Ramaswamy S, Itzykson RA, Come C, Savagner P, Gitelman I, Richardson A & Weinberg RA 2004 Twist, a master regulator of morphogenesis, plays an essential role in tumor metastasis. *Cell* **117** 927-939.
Yang Q, Fung KM, Day WV, Kropp BP & Lin HK 2005 Androgen receptor signaling is required for androgen-sensitive human prostate cancer cell proliferation and survival. *Cancer Cell Int* **5** 8.
Yu L, Todd NW, Xing L, Xie Y, Zhang H, Liu Z, Fang H, Zhang J, Katz RL & Jiang F 2010 Early detection of lung adenocarcinoma in sputum by a panel of microRNA markers. *Int J Cancer* **127** 2870-2878.
Yu X & Machesky LM 2012 Cells assemble invadopodia-like structures and invade into matrigel in a matrix metalloprotease dependent manner in the circular invasion assay. *PLoS One* **7** e30605.
Zhang B, Pan X, Cobb GP & Anderson TA 2007 microRNAs as oncogenes and tumor suppressors. *Dev Biol* **302** 1-12.
Zhang L, Yang S, Chen X, Stauffer S, Yu F, Lele SM, Fu K, Datta K, Palermo N, Chen Y, et al. 2015 The hippo pathway effector YAP regulates motility, invasion, and castration-resistant growth of prostate cancer cells. *Mol Cell Biol* **35** 1350-1362.
Zhou J, Song S, Cen J, Zhu D, Li D & Zhang Z 2012 MicroRNA-375 is downregulated in pancreatic cancer and inhibits cell proliferation in vitro. *Oncol Res* **20** 197-203.